ECCO Version 4: Second Release

G. Forget[1], J.-M. Campin[1], P. Heimbach[1,2,3], C. N. Hill[1], R. M. Ponte[4], and C. Wunsch[5]

[1] Dept. of Earth, Atmospheric and Planetary Sciences, Massachusetts Institute of Technology, Cambridge MA 02139 USA; [2] Institute for Computational Engineering and Sciences, The University of Texas at Austin, Austin, TX 78712, USA; [3] Jackson School of Geosciences, The University of Texas at Austin, Austin, TX 78712, USA; [4] Atmospheric and Environmental Research, Inc., Lexington MA 02421 USA; [5] Dept. of Earth and Planetary Sciences, Harvard University, Cambridge, MA 02139 USA

March 31, 2016

The purpose of this note is twofold: (1) document the second release of ECCO version 4 state estimates (ECCO v4-r2); (2) provide a citable identifier to distinguish it from the previous release (ECCO v4-r1; Forget et al 2015).

Access ECCO v4-r2: online access is free and unrestricted via `http://ecco-group.org/` ; at the time of writing the ECCO v4-r2 files are accessed via `ftp://mit.ecco-group.org/ecco_for_las/version_4/release2/` and `http://mit.ecco-group.org/opendap/ecco_for_las/version_4/release2/contents.html`

Software Used for ECCO v4-r2: the state estimate output files (provided online) and its depiction (provided below) were produced using the 'checkpoint64u' versions of the general circulation model (MITgcm and ECCO v4 settings) and Matlab analysis toolboxes (gcmfaces and MITprof).

Solution History: the 1992-2011 solution documented here (ECCO v4-r2) is a minor update to the original ECCO v4 solution documented by Forget et al 2015 (ECCO v4-r1). As compared with ECCO v4-r1 (see Forget et al 2015 for details and notations) ECCO v4-r2 benefits from a few additional corrections in the model settings:

1. Inclusion of geothermal heating at the sea floor in MITgcm and ECCO v4 settings.
2. Inclusion of $\mathcal{K}_{gm}$ and $\mathcal{K}_{\sigma}$ interpolation to C-grid velocity points in MITgcm and ECCO v4 settings.
3. Re-inclusion of targeted bottom viscosity in ECCO v4 settings.
4. Re-inclusion of estimated wind stress adjustments over 2000-2011 in ECCO v4 settings.
5. Re-adjustment of ECCO v4 global mean precipitation (homogeneously) to match the AVISO global mean sea level time series (`http://www.aviso.altimetry.fr/`).

Contents Included Below: the gcmfaces 'standard analysis' (introduced in Forget et al. 2015) appended below for ECCO v4-r2 depicts routinely monitored characteristics of ECCO solutions. It allows for direct comparison with the published ECCO v4-r1 standard analysis (doi:10.5194/gmd-8-3071-2015-supplement).

References: Forget, G., J.-M. Campin, P. Heimbach, C. N. Hill, R. M. Ponte, and C. Wunsch, 2015: ECCO version 4: an integrated framework for non-linear inverse modeling and global ocean state estimation. Geoscientific Model Development, 8, 3071-3104, doi:10.5194/gmd-8-3071-2015 (`http://www.geosci-model-dev.net/8/3071/2015/`)

Contact Us: ecco-support@mit.edu (`http://mailman.mit.edu/mailman/listinfo/ecco-support`)

Table of contents

fit to in situ data

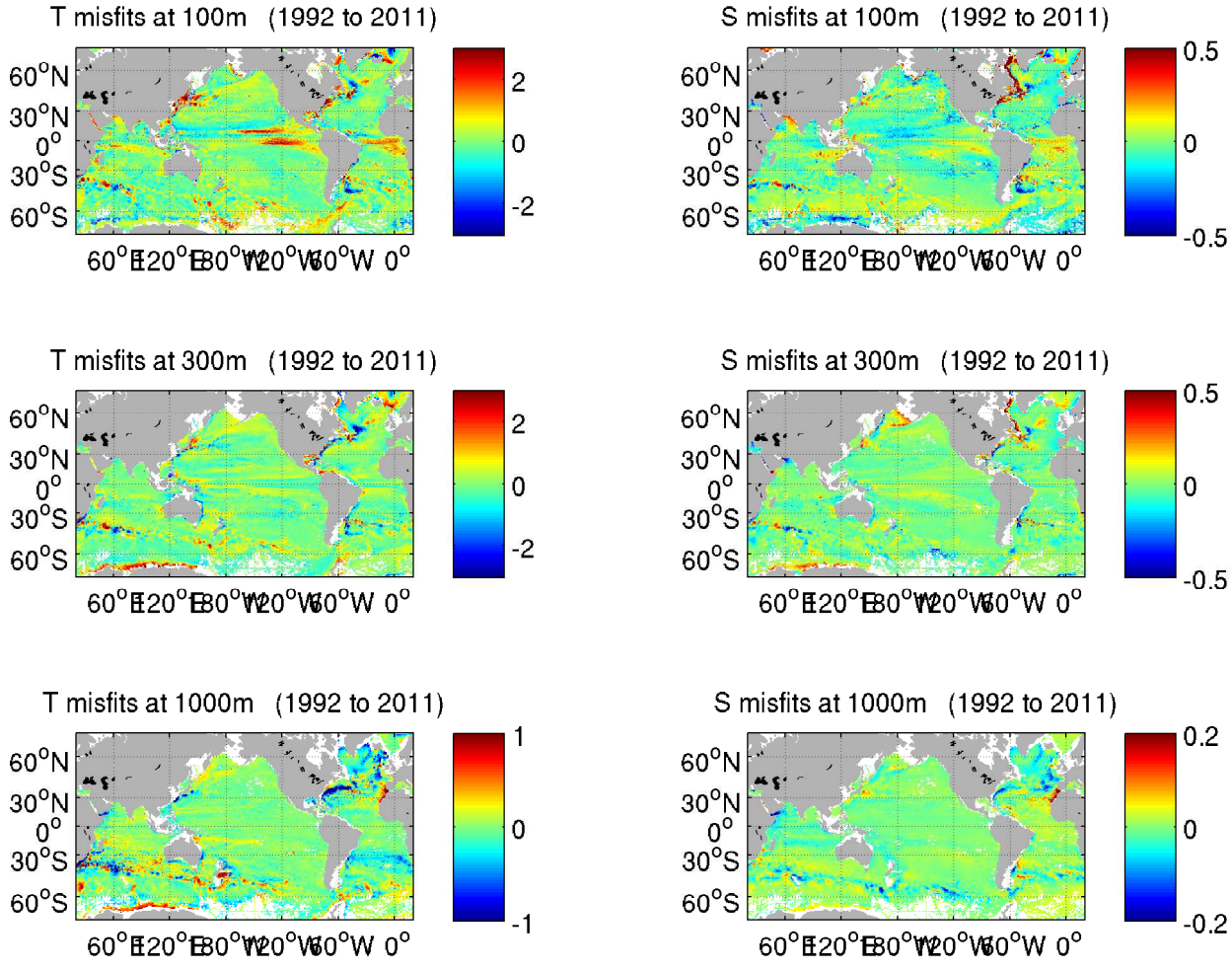

Figure : Time mean misfit (model-data) for in situ profiles, at various depths (rows), for T (left; in K) and S (right; in psu).

fit to in situ data

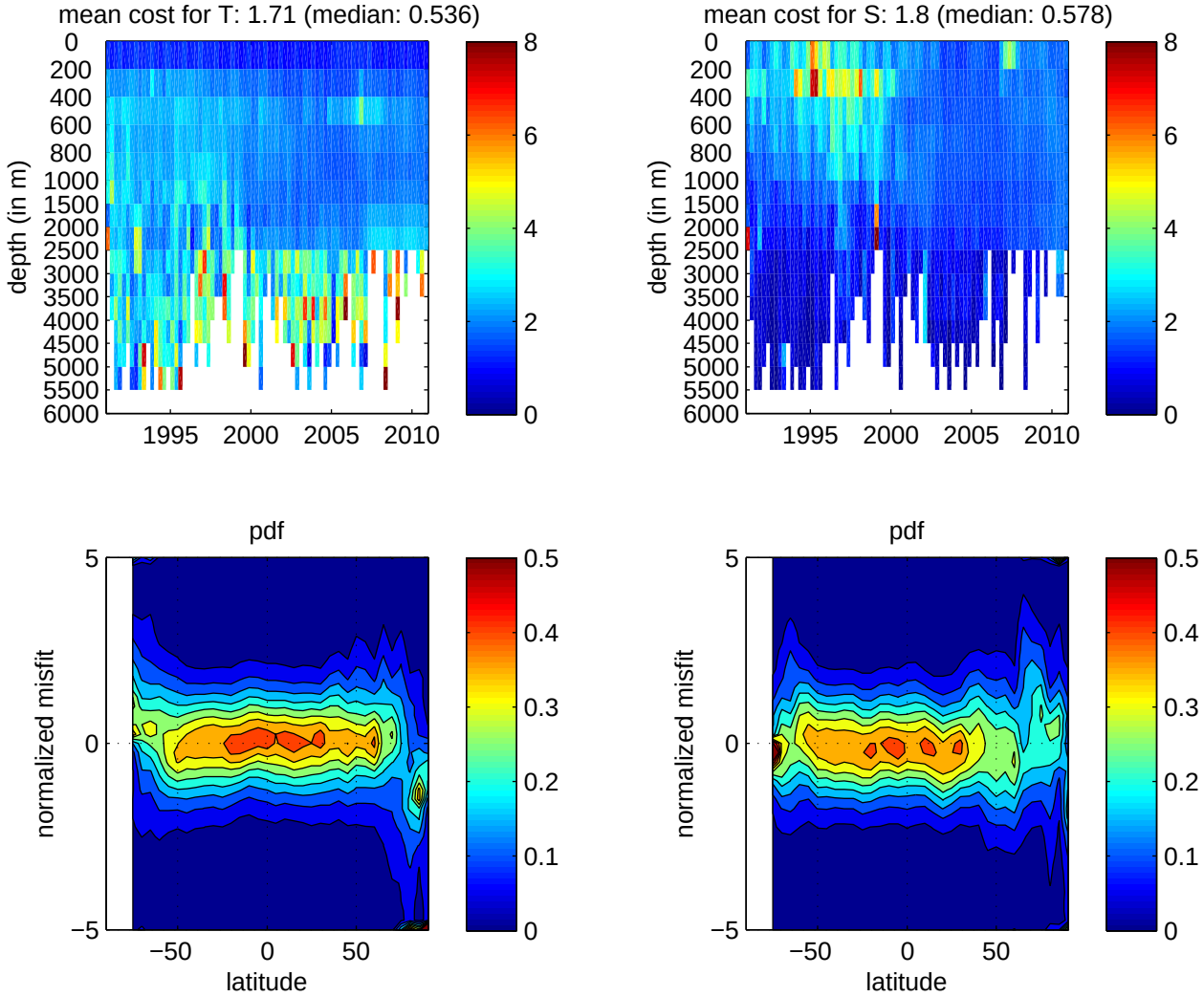

Figure : Cost function (top) for in situ profiles, as a function of depth and time. Distribution of normalized misfits (bottom) as a function of latitude. For T (left) and S (right).

fit to in situ data

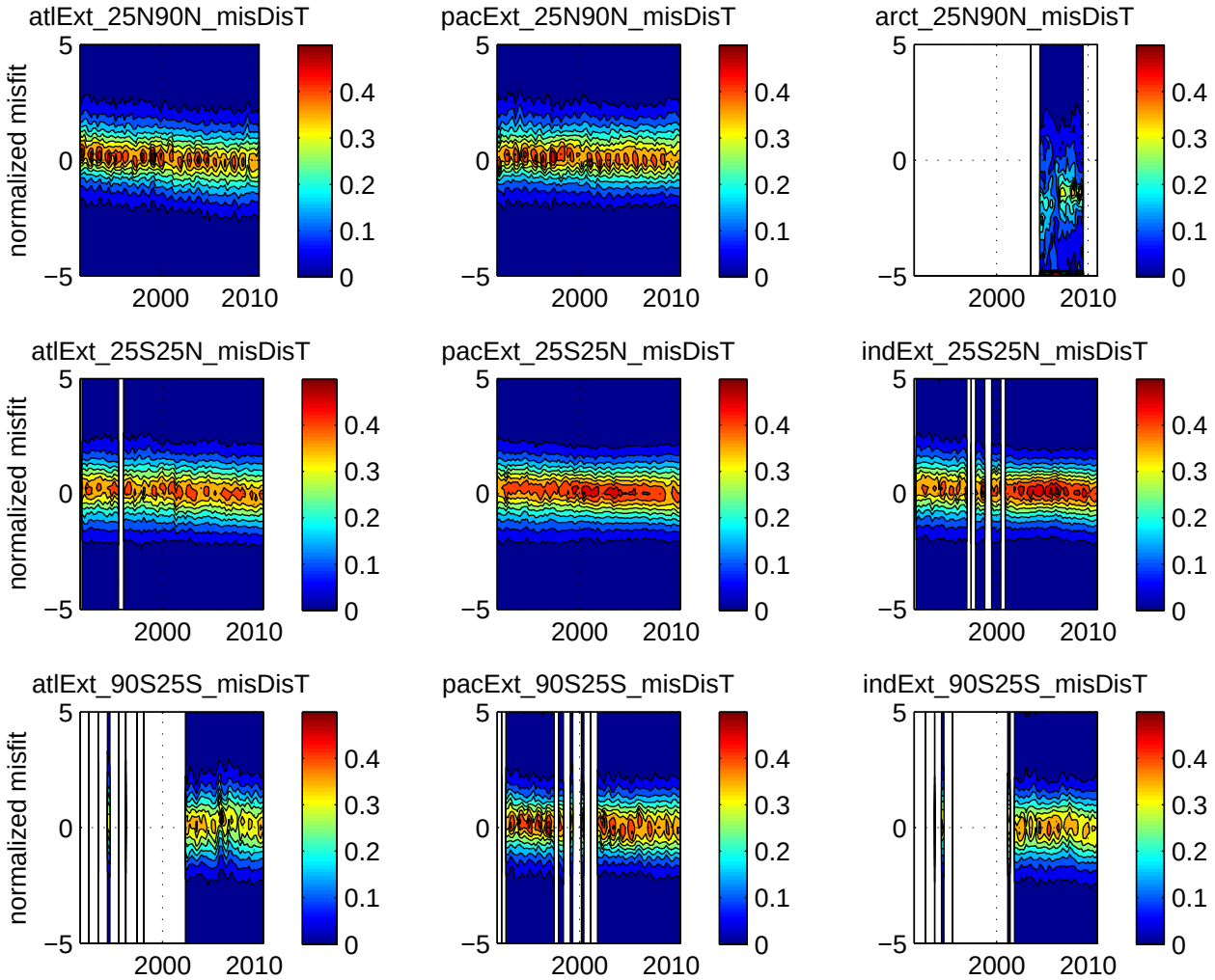

Figure : Distribution of normalized misfits per basin (panel) as a function of latitude, for T

fit to in situ data

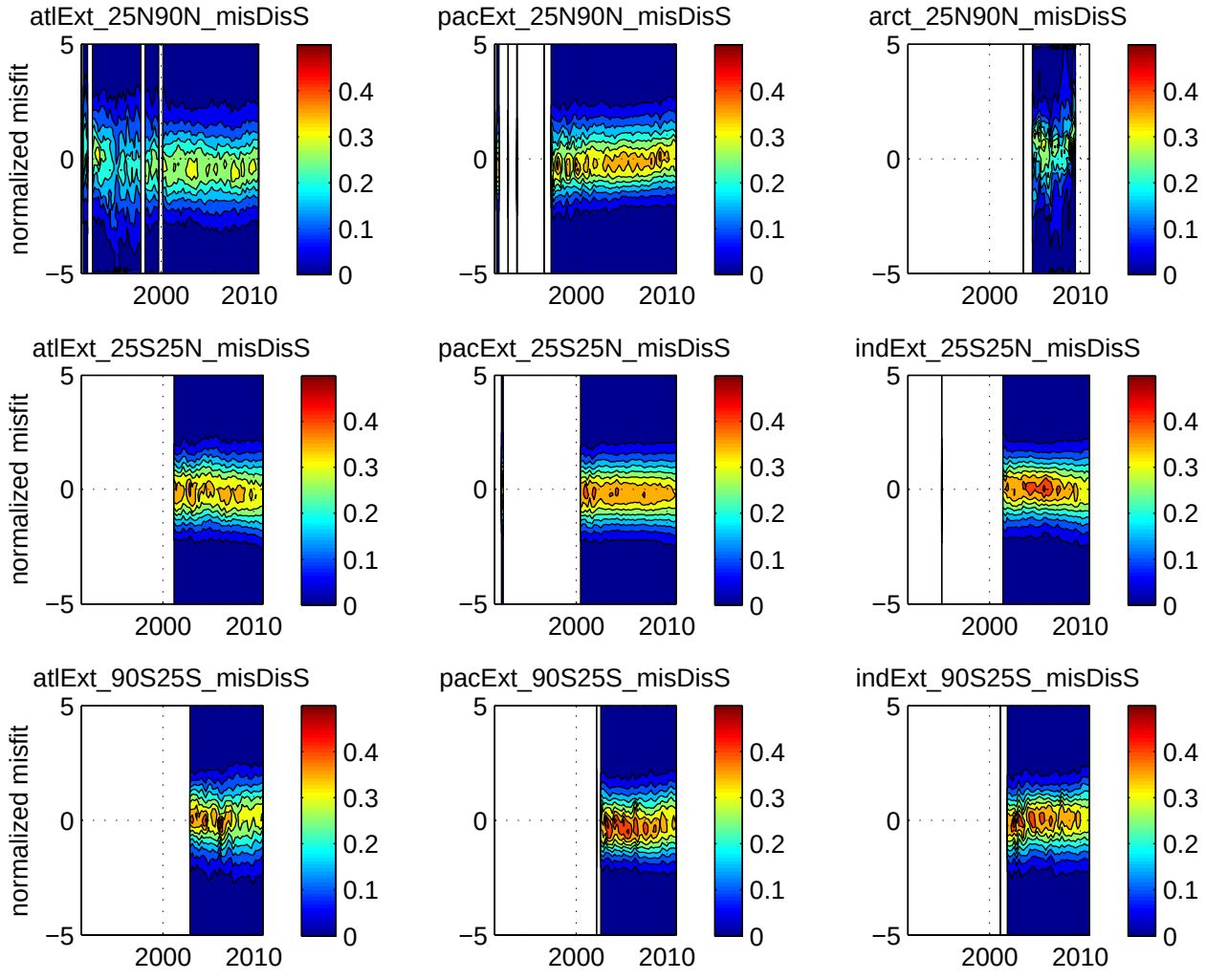

Figure : Distribution of normalized misfits per basin (panel) as a function of latitude, for S

fit to altimeter data (RADS)

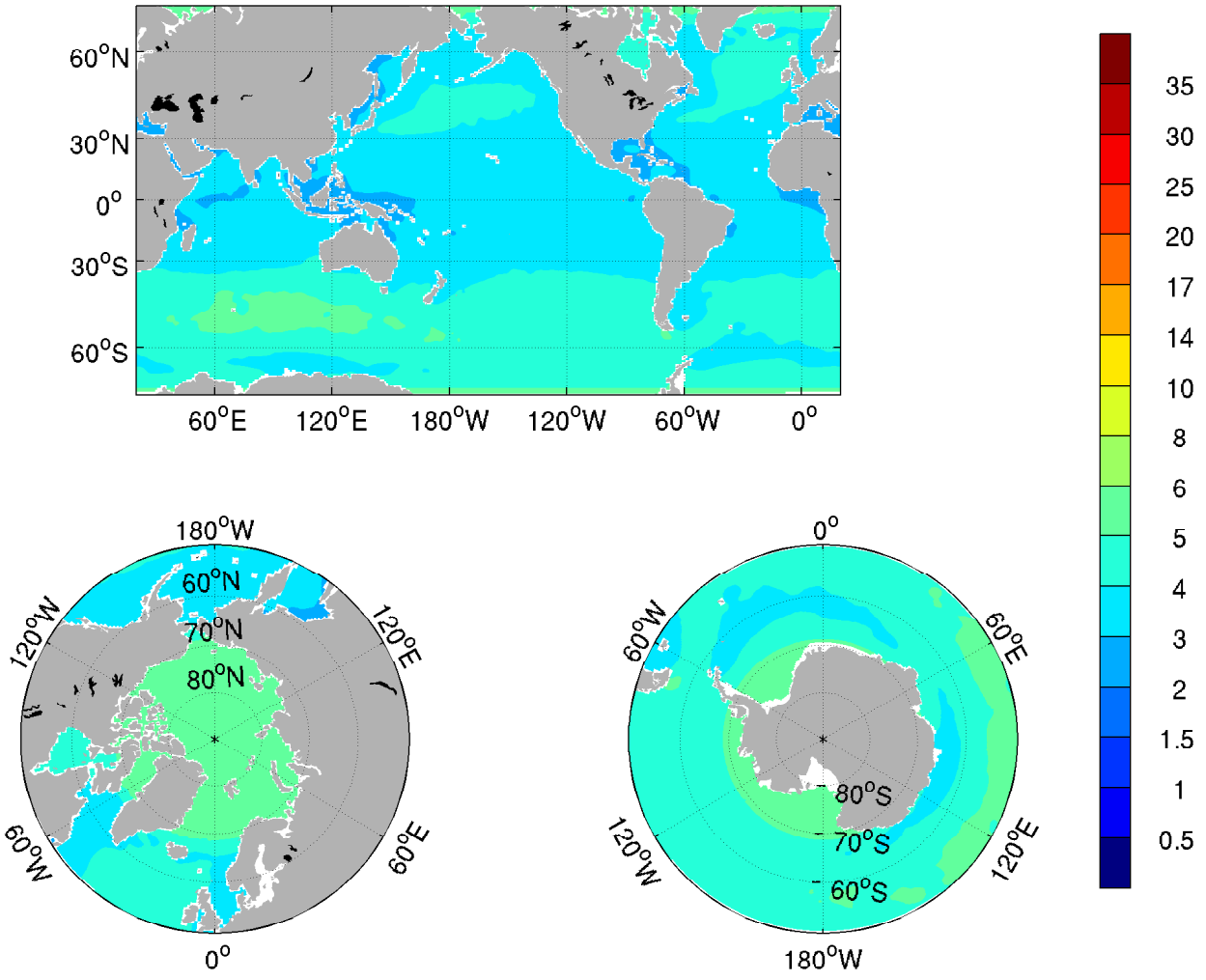

Figure : mean dynamic topography prior uncertainty (cm)

fit to altimeter data (RADS)

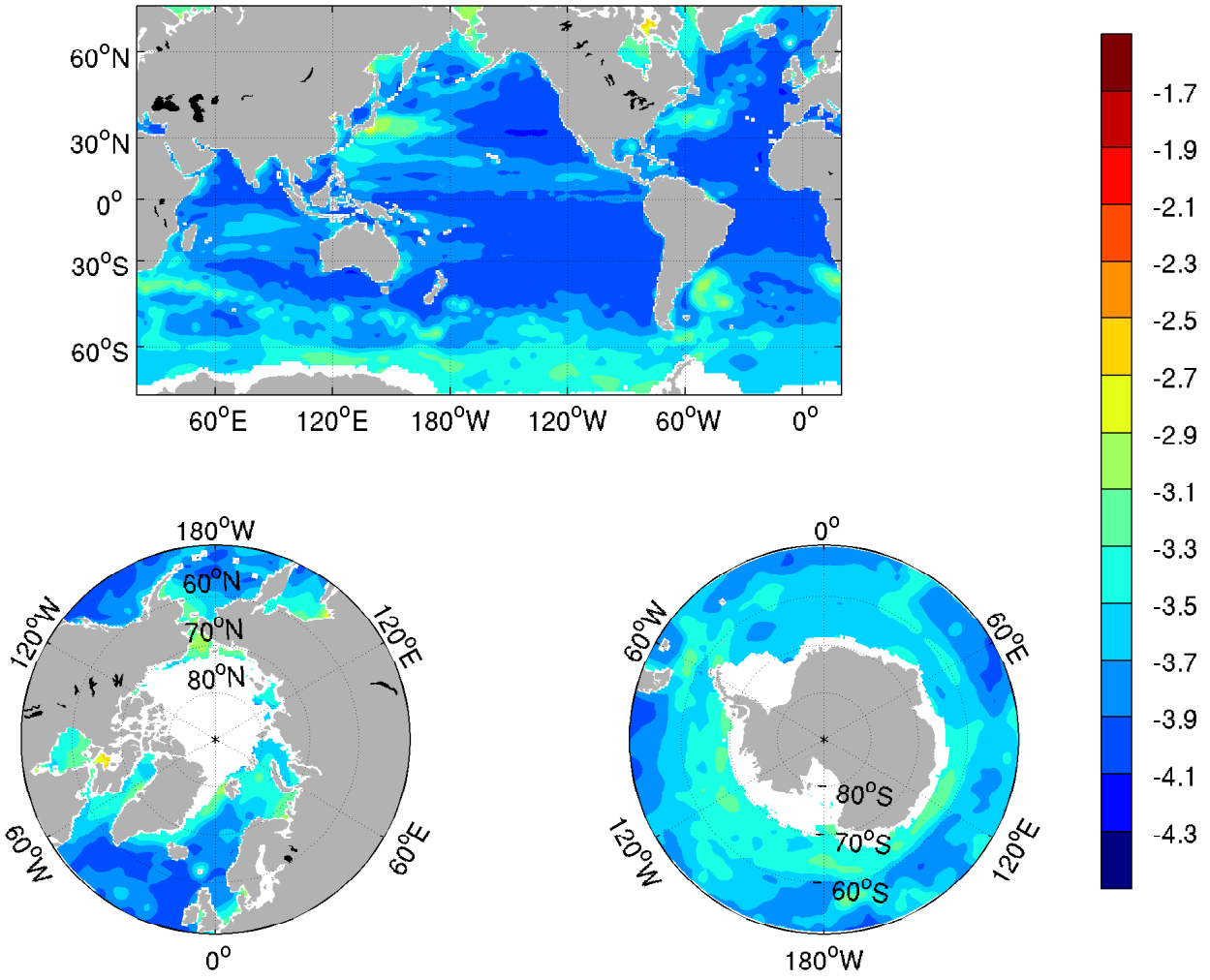

Figure : log(prior error variance) – sea level anomaly (m^2) – large space/time scales

fit to altimeter data (RADS)

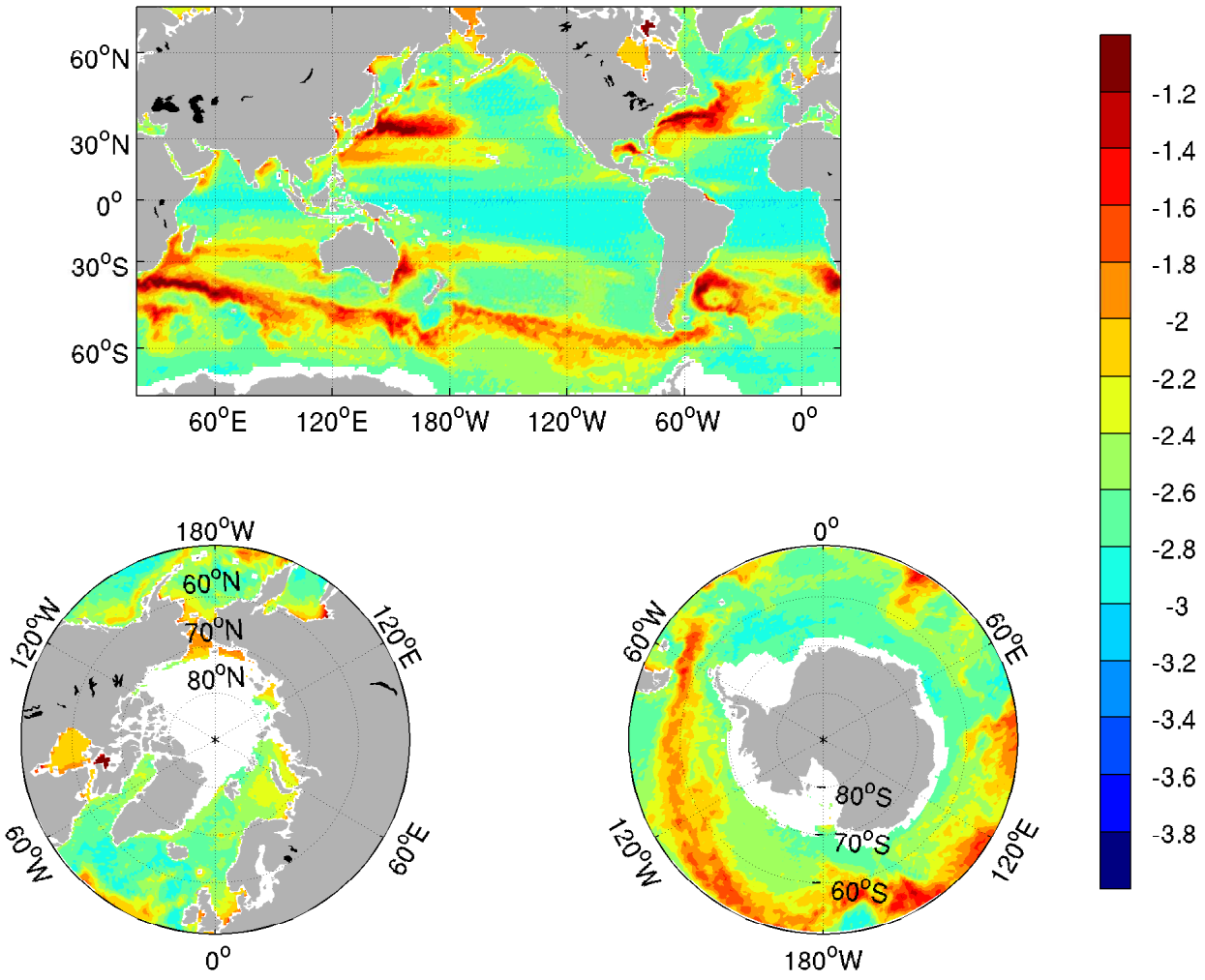

Figure : log(prior error variance) – sea level anomaly (m^2) – pointwise

fit to altimeter data (RADS)

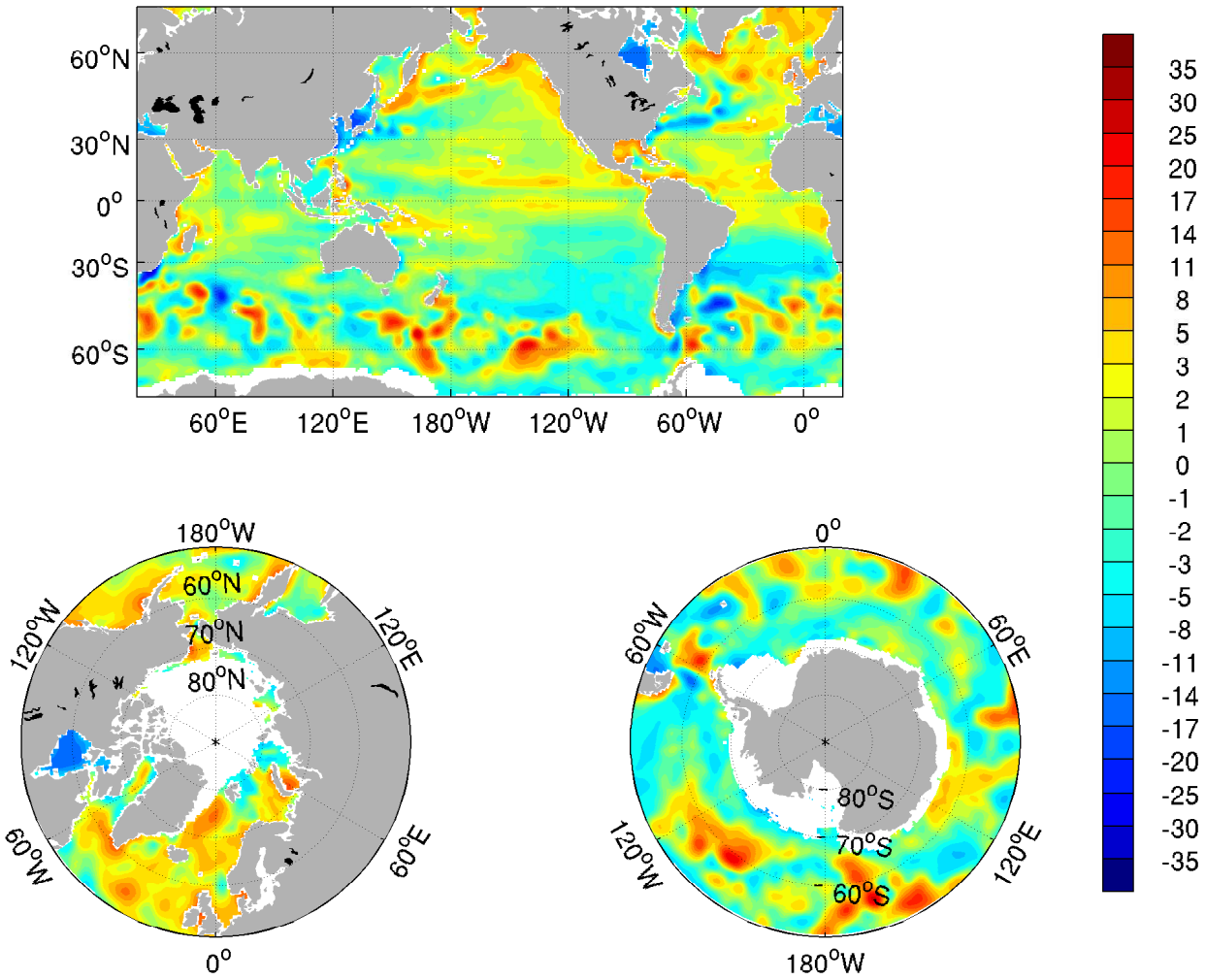

Figure : mean dynamic topography misfit (cm)

fit to altimeter data (RADS)

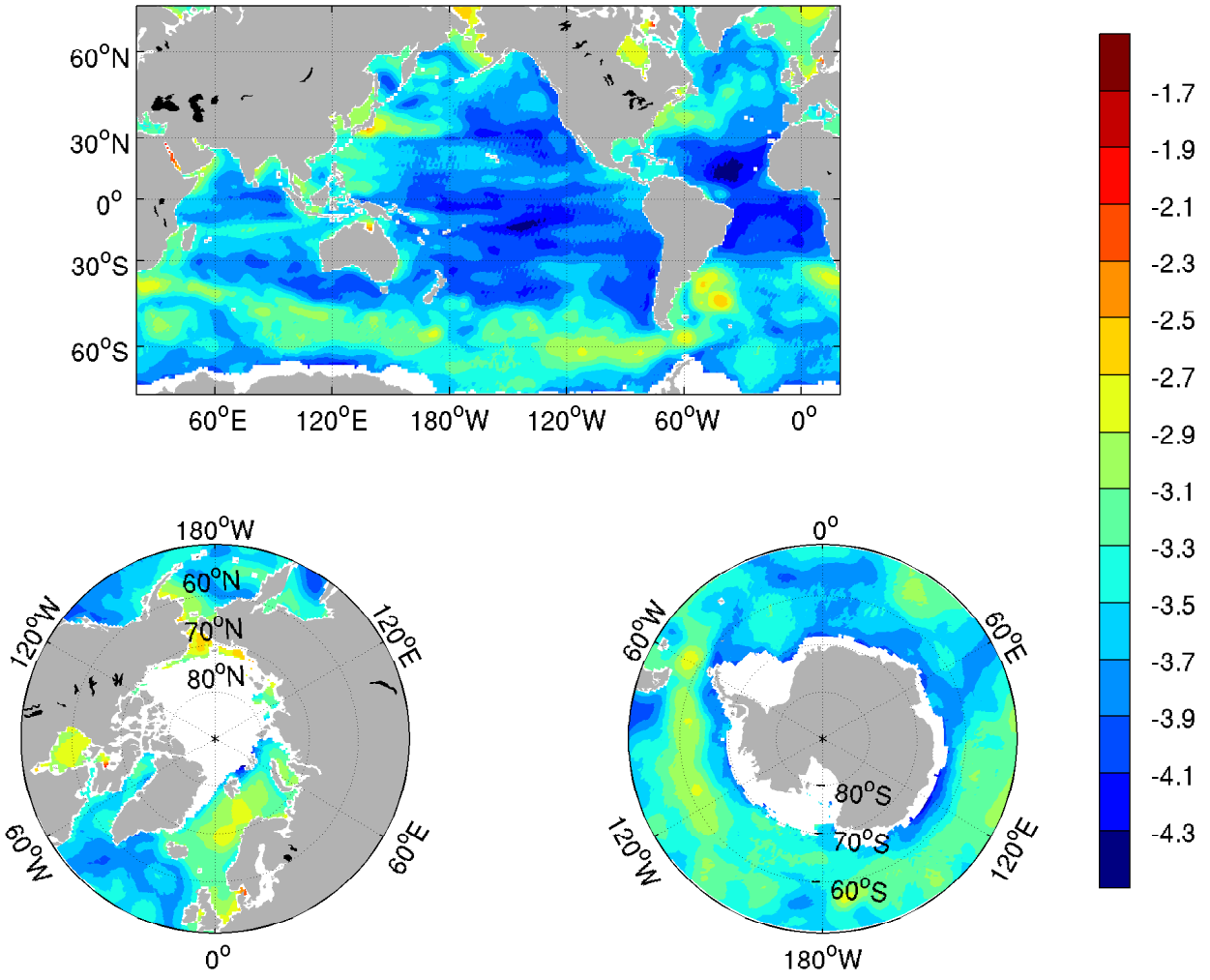

Figure : modeled-observed log(variance) – sea level anomaly (m^2) – large space/time scales

fit to altimeter data (RADS)

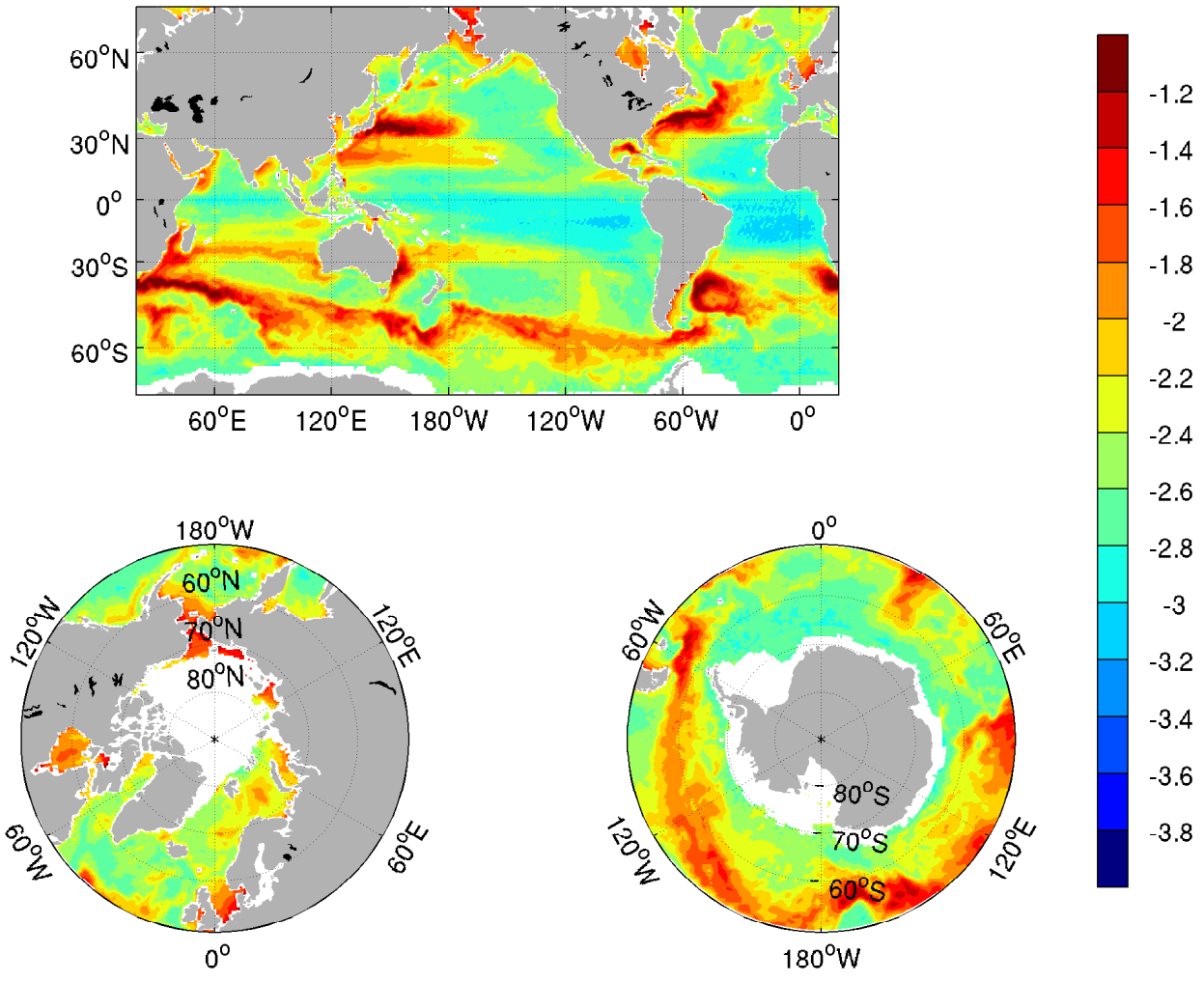

Figure : modeled-observed log(variance) – sea level anomaly (m^2) – pointwise

fit to altimeter data (RADS)

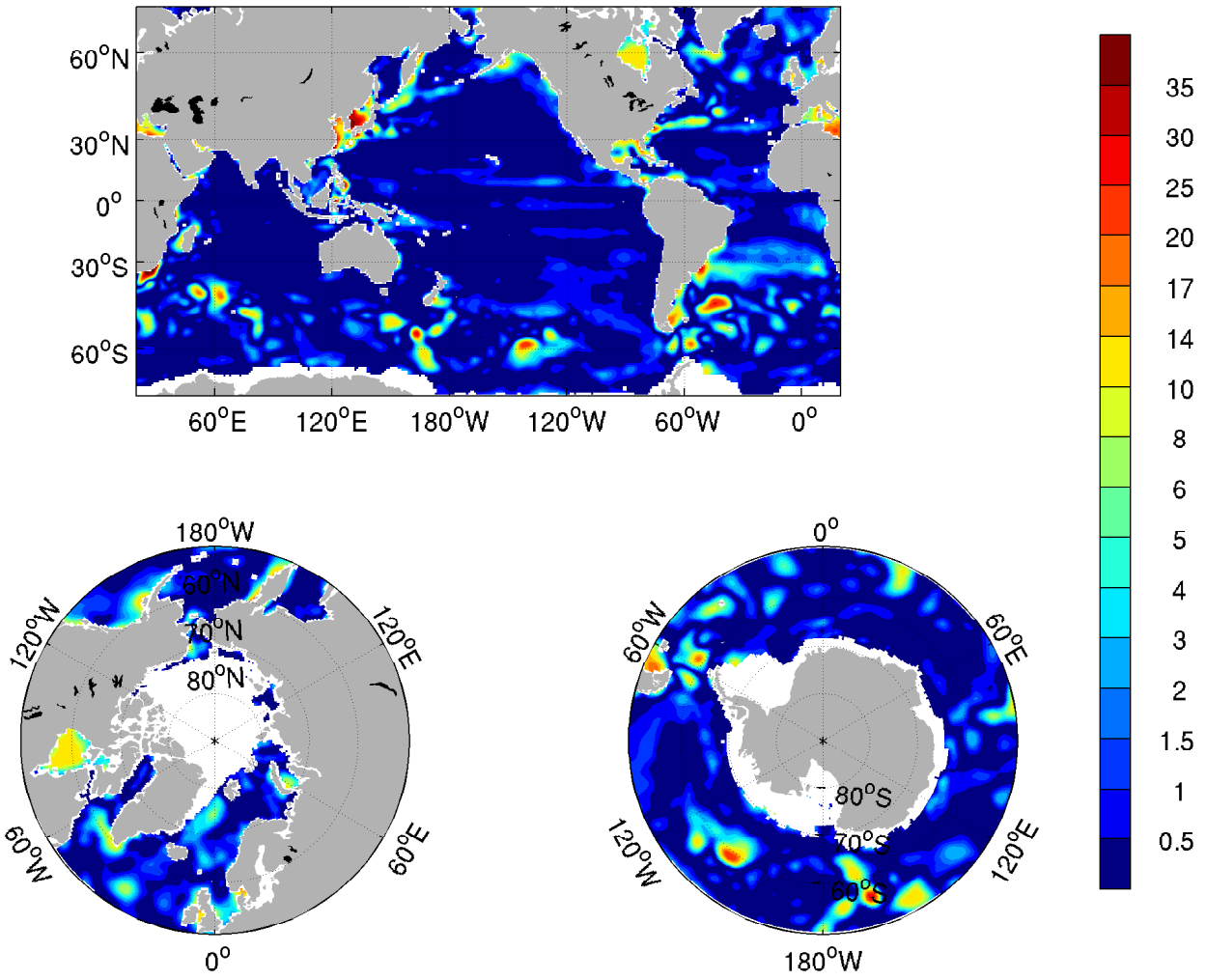

Figure : modeled-observed cost – mean dynamic topography

fit to altimeter data (RADS)

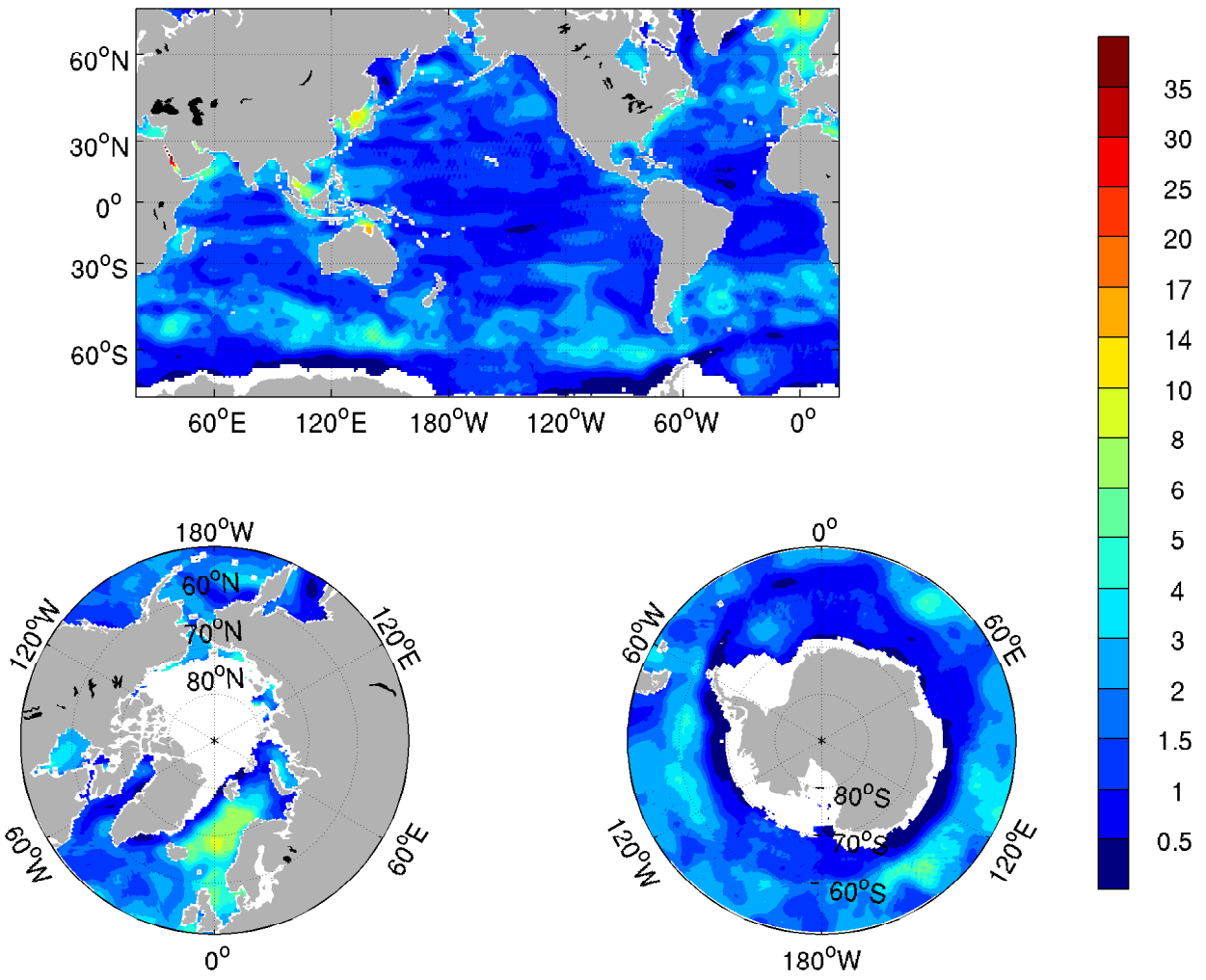

Figure : modeled-observed cost – sea level anomaly – large space/time scales

fit to altimeter data (RADS)

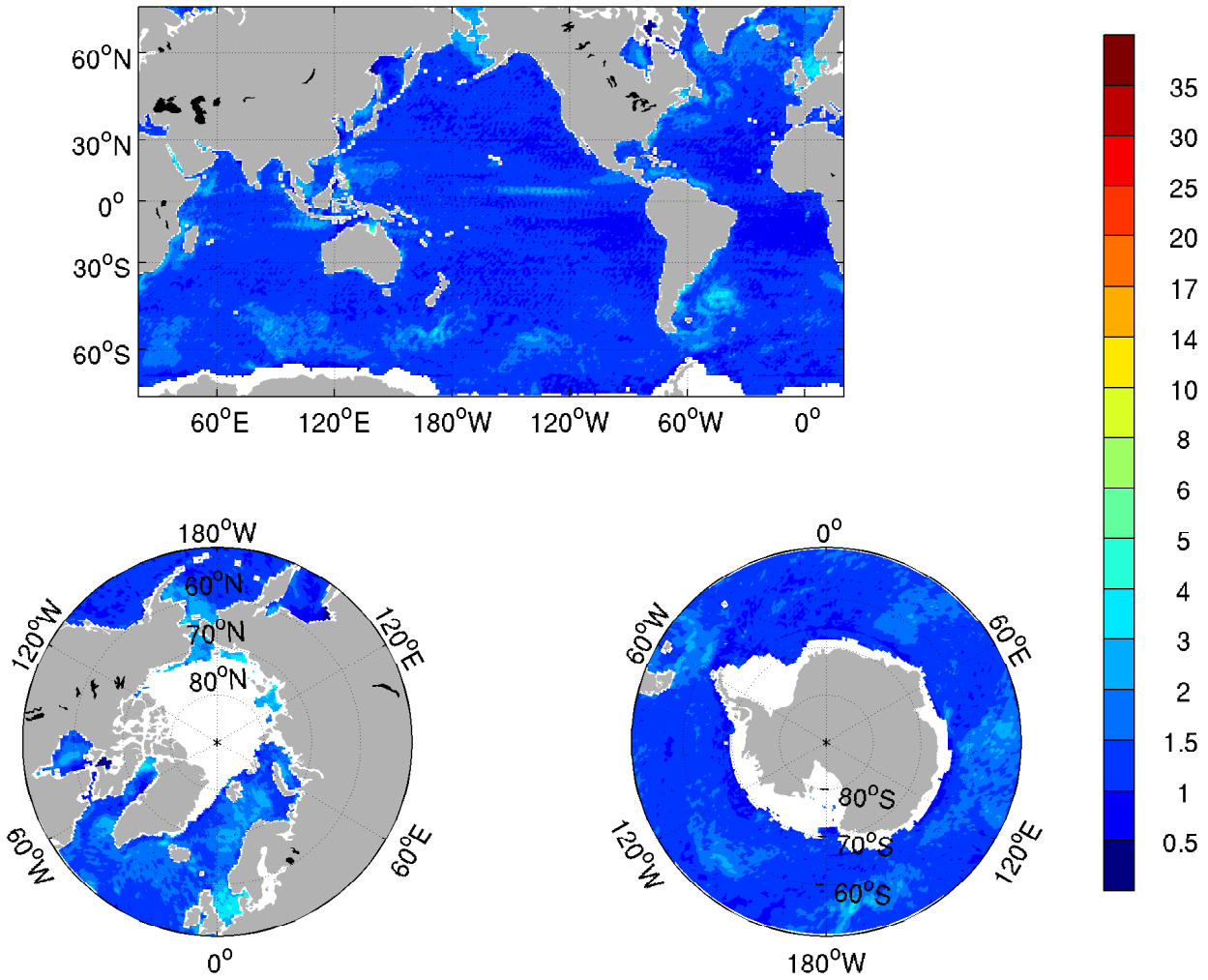

Figure : modeled-observed cost – sea level anomaly – pointwise

fit to altimeter data (RADS)

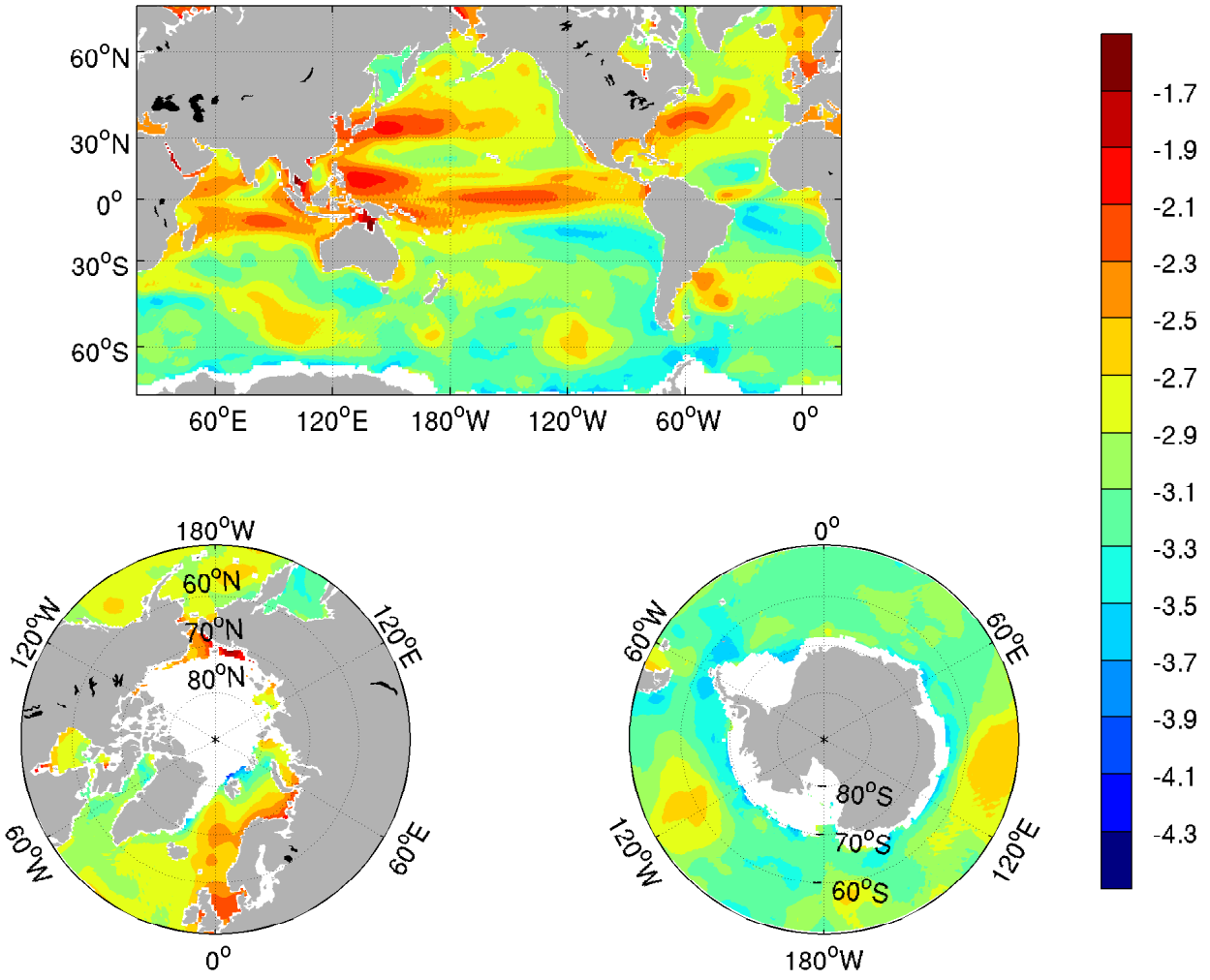

Figure : observed log(variance) – sea level anomaly (m^2) – large space/time scales

fit to altimeter data (RADS)

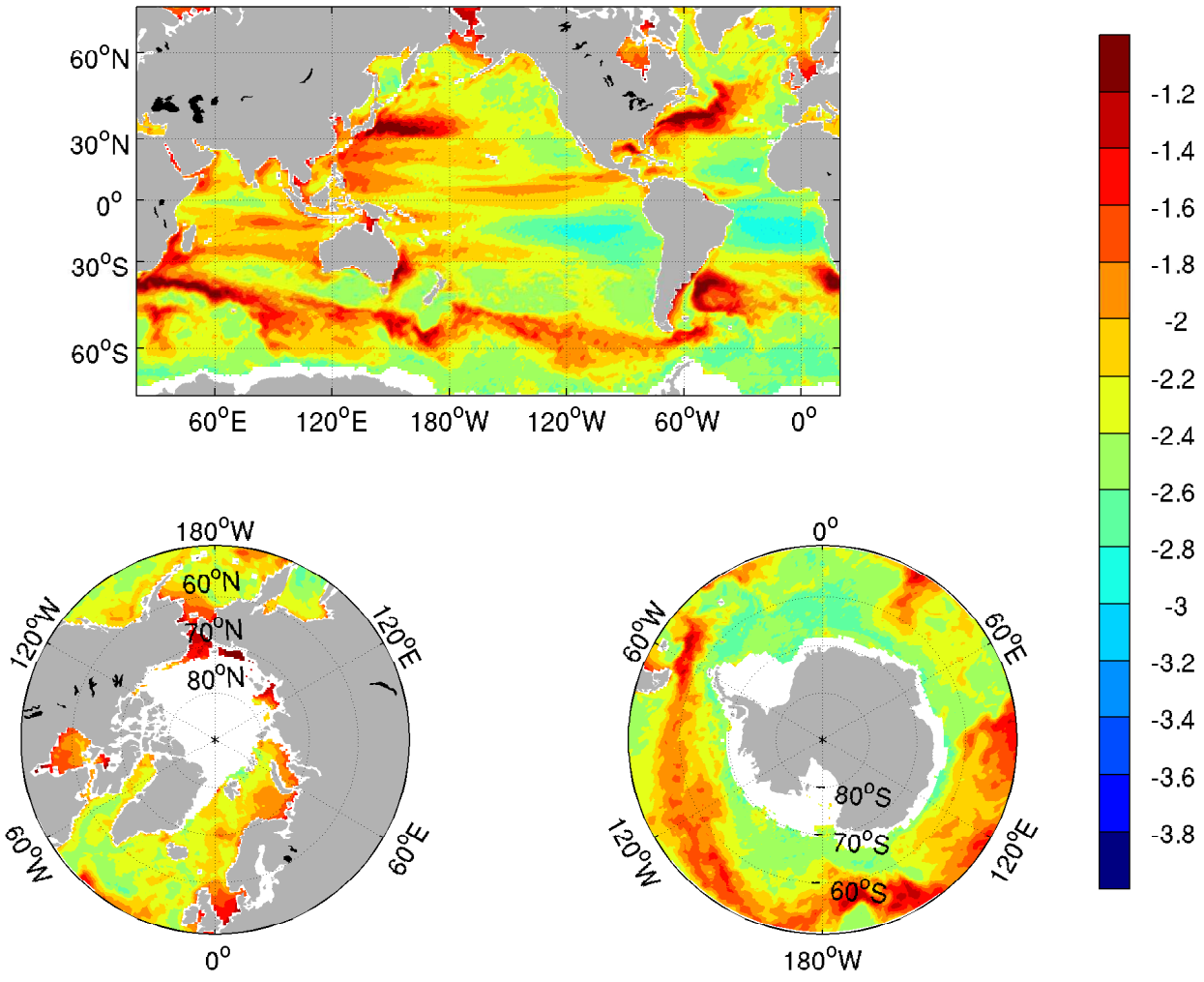

Figure : observed log(variance) – sea level anomaly (m^2) – pointwise

fit to altimeter data (RADS)

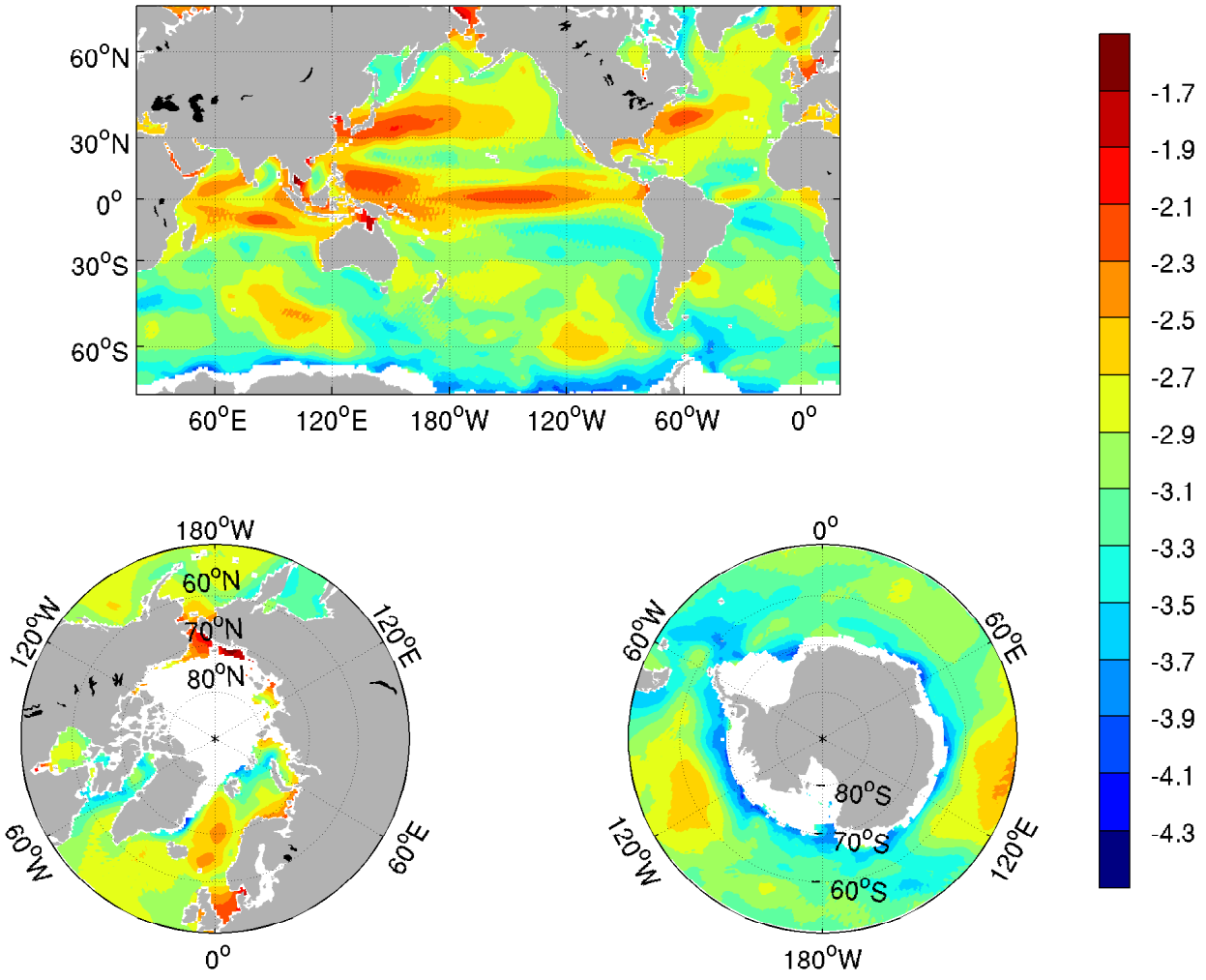

Figure : modeled log(variance) – sea level anomaly (m^2) – large space/time scales

fit to altimeter data (RADS)

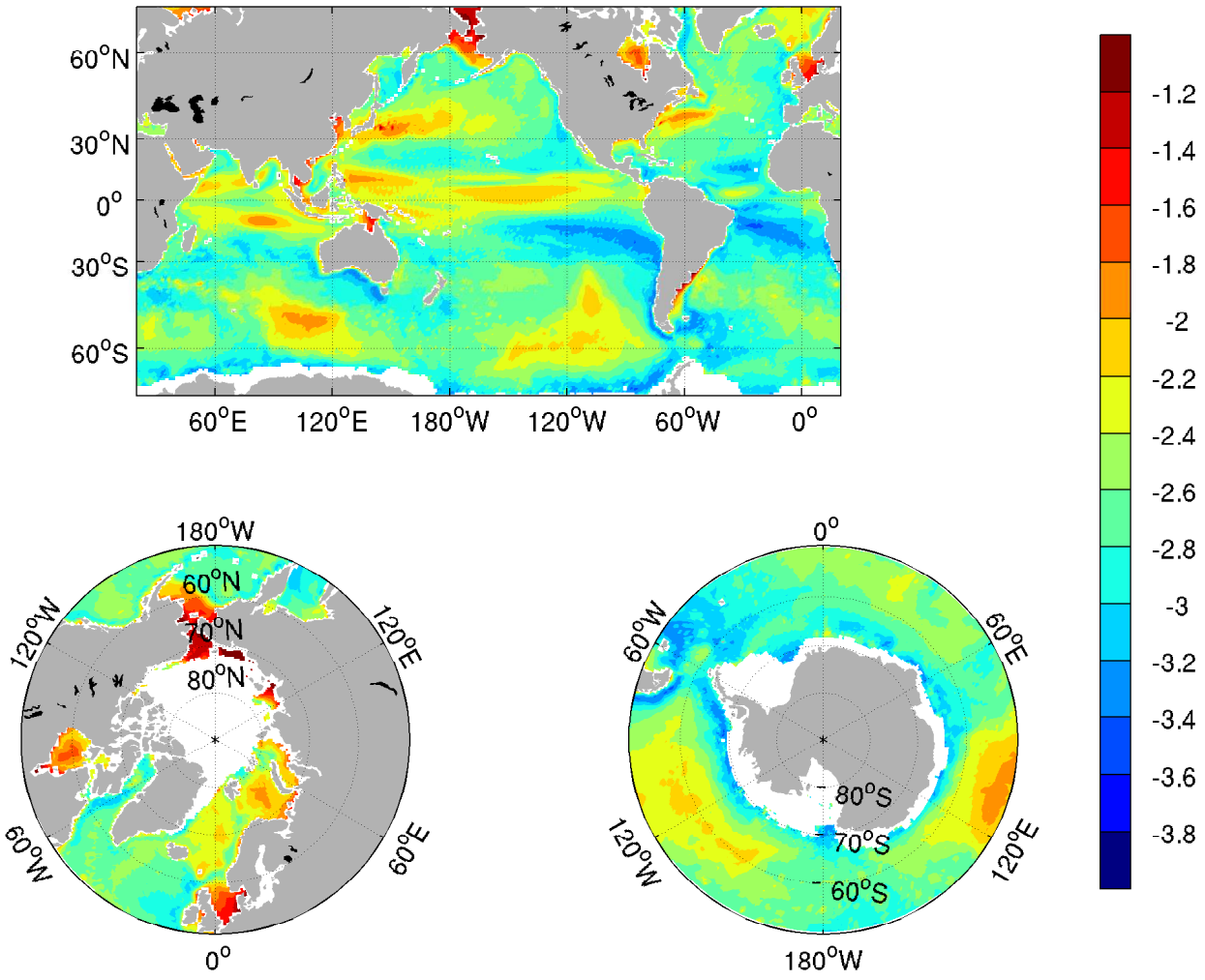

Figure : modeled log(variance) – sea level anomaly (m^2) – pointwise

fit to sst data

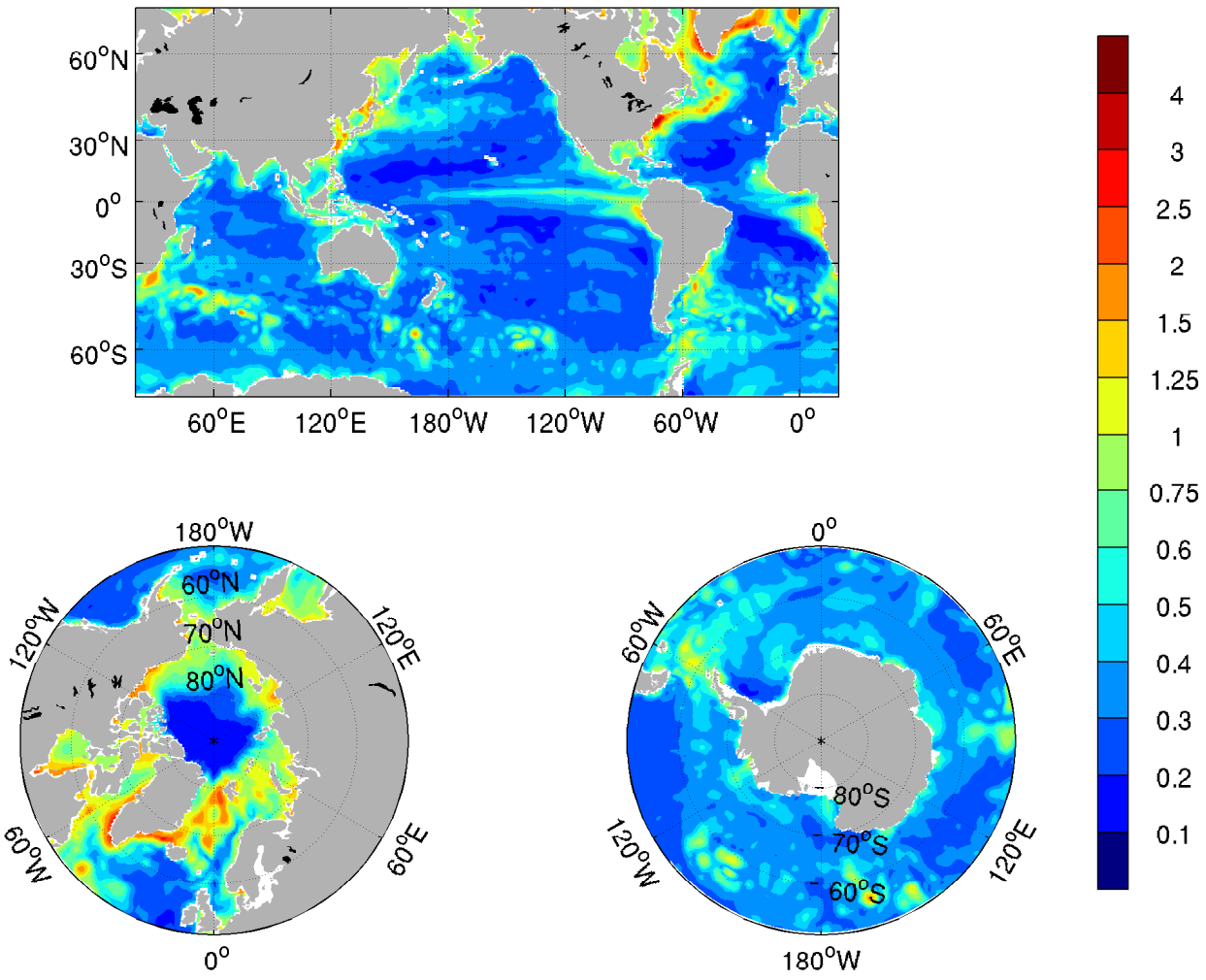

Figure : modeled-Reynolds rms – sea surface temperature (K)

fit to sst data

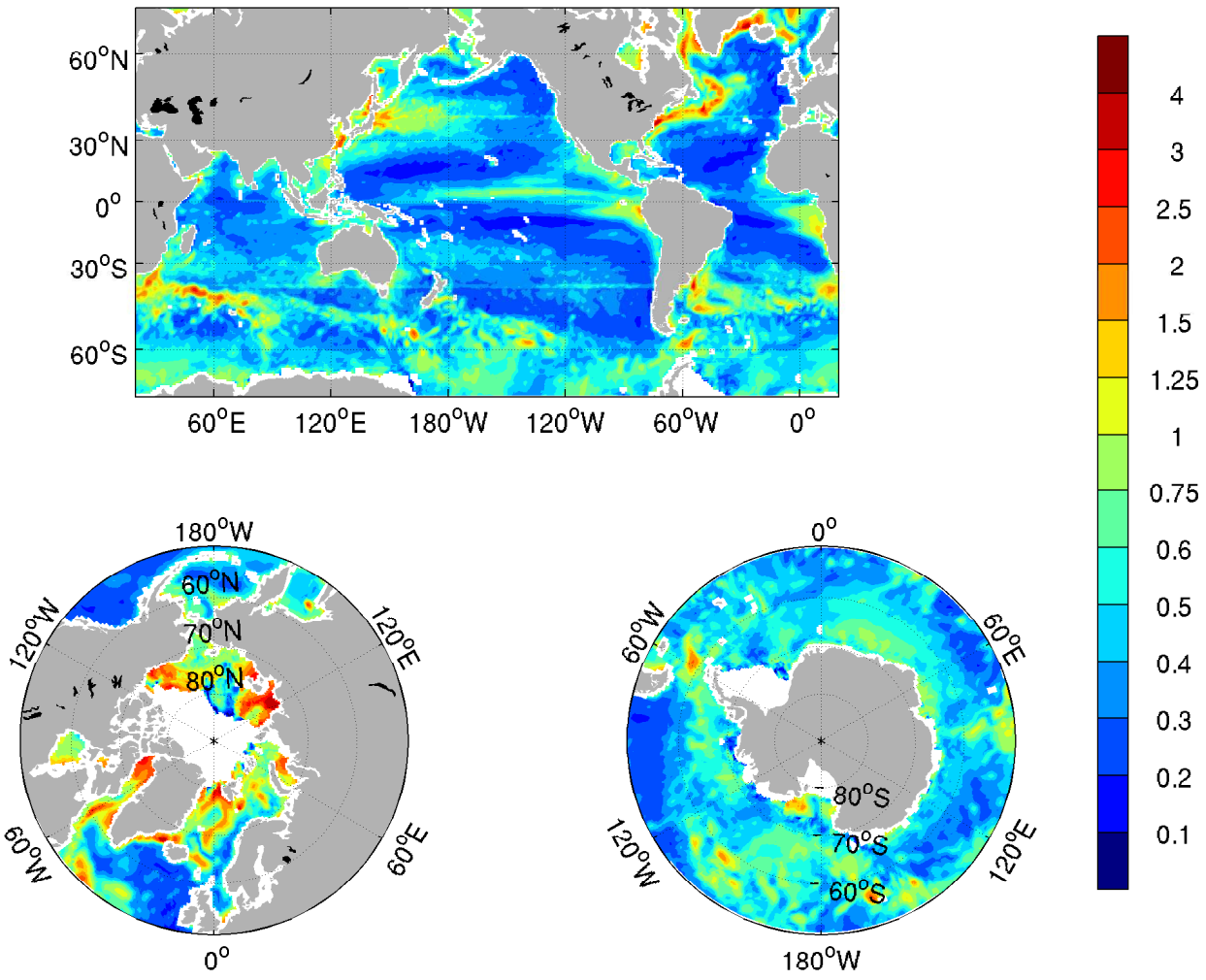

Figure : modeled-REMSS rms – sea surface temperature (K)

fit to sst data

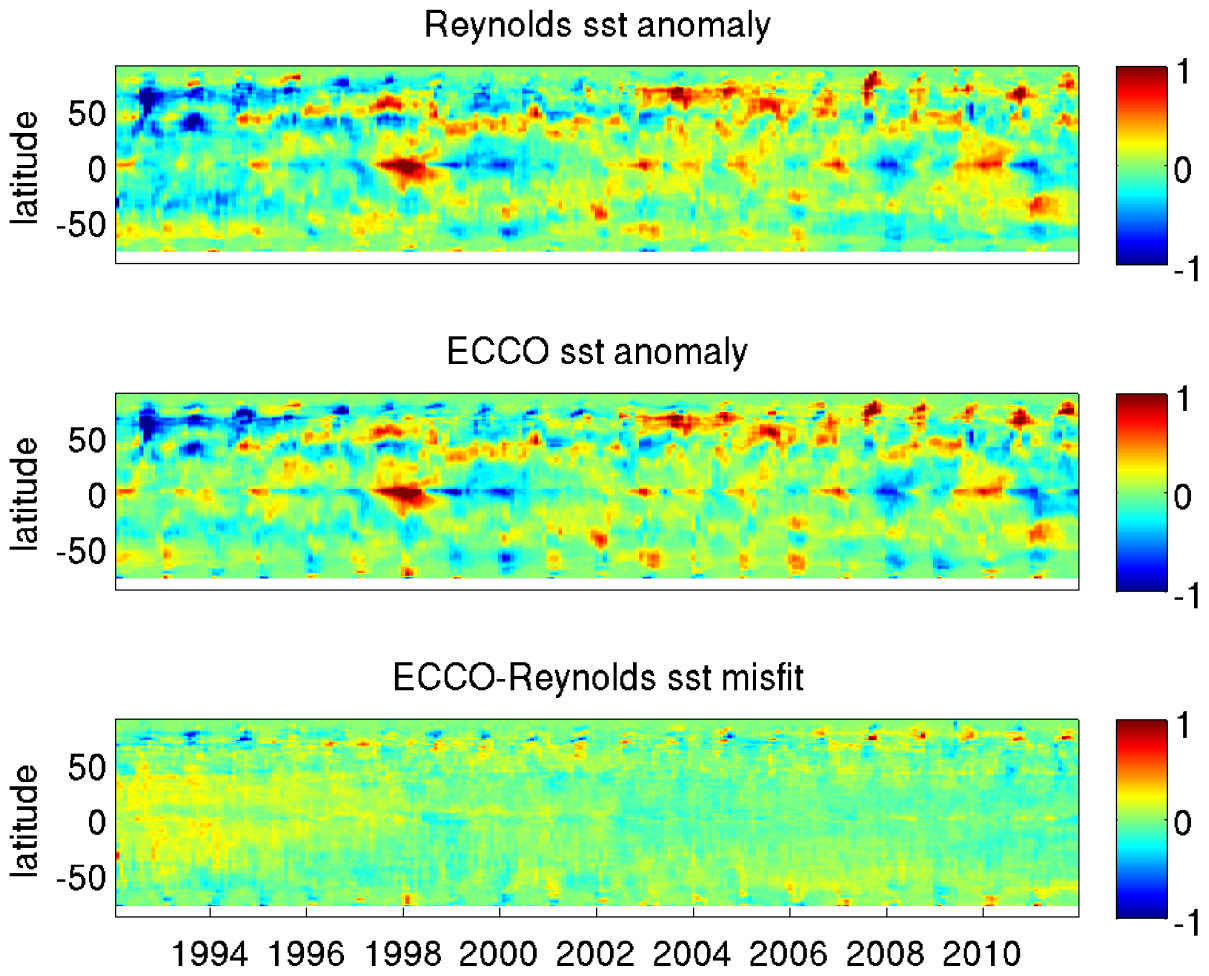

Figure : ECCO and Reynolds zonal mean sst anomalies (K)

fit to sst data

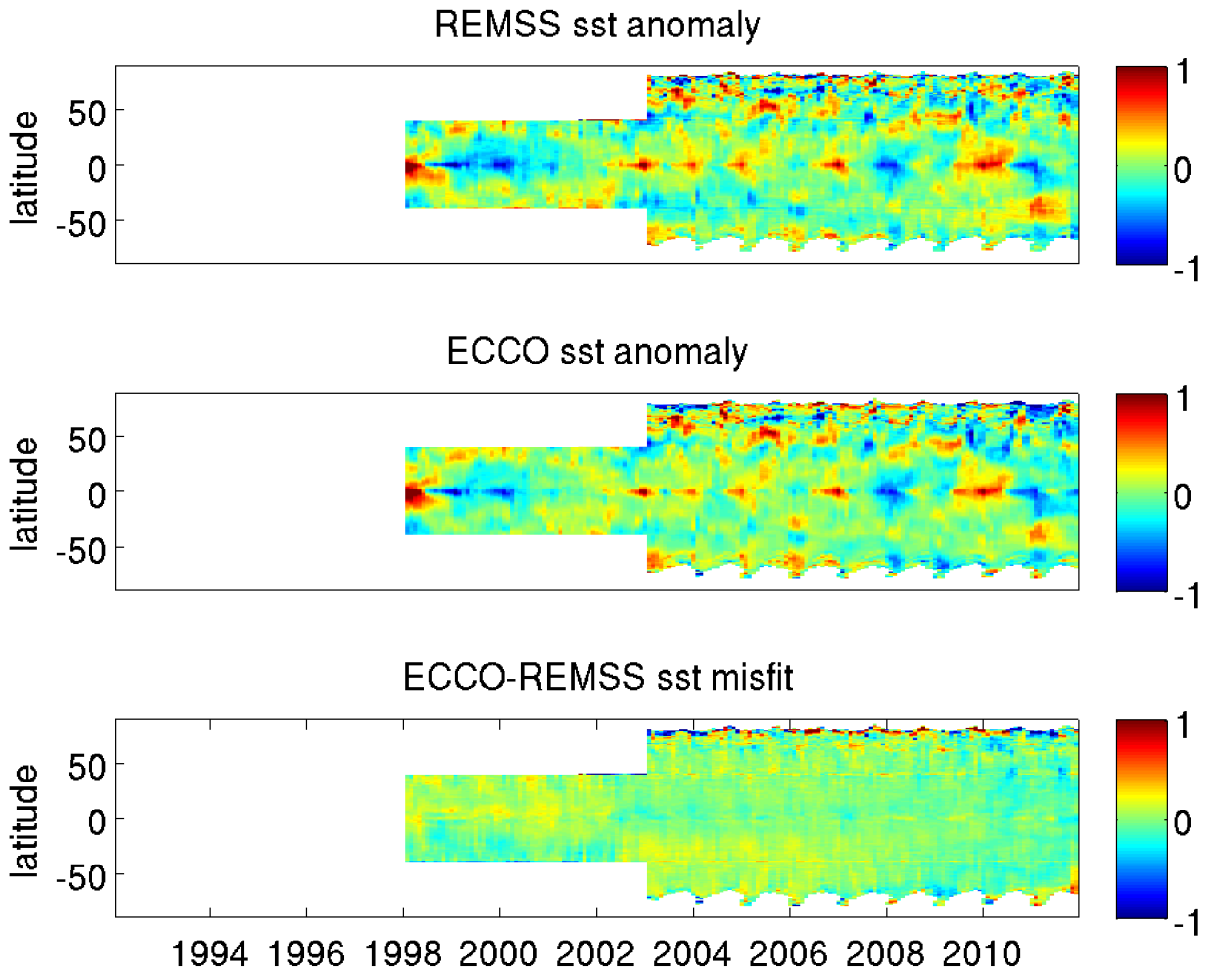

Figure : ECCO and REMSS zonal mean sst anomalies (K)

fit to seaice data

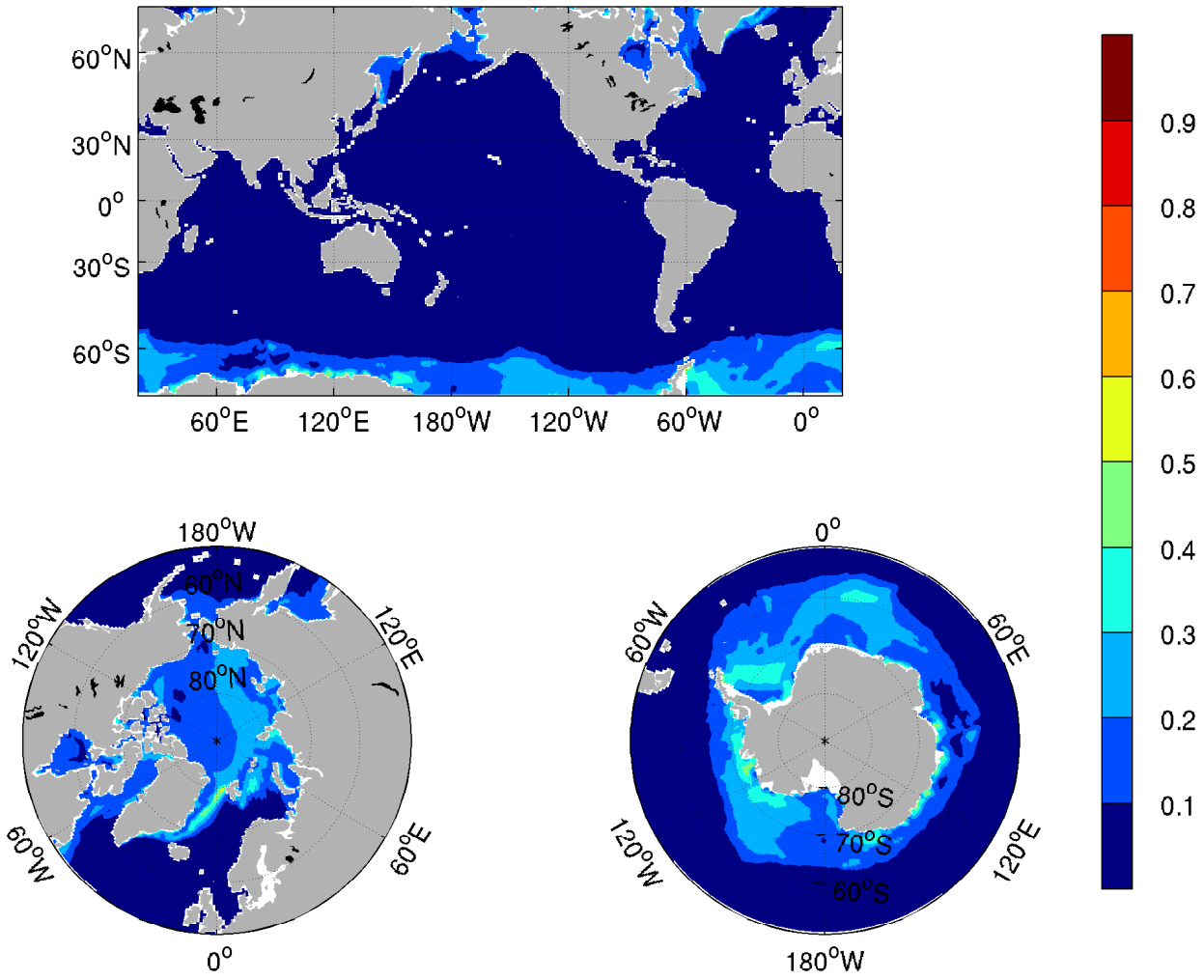

Figure : modeled-observed rms – sea ice concentration

fit to seaice data

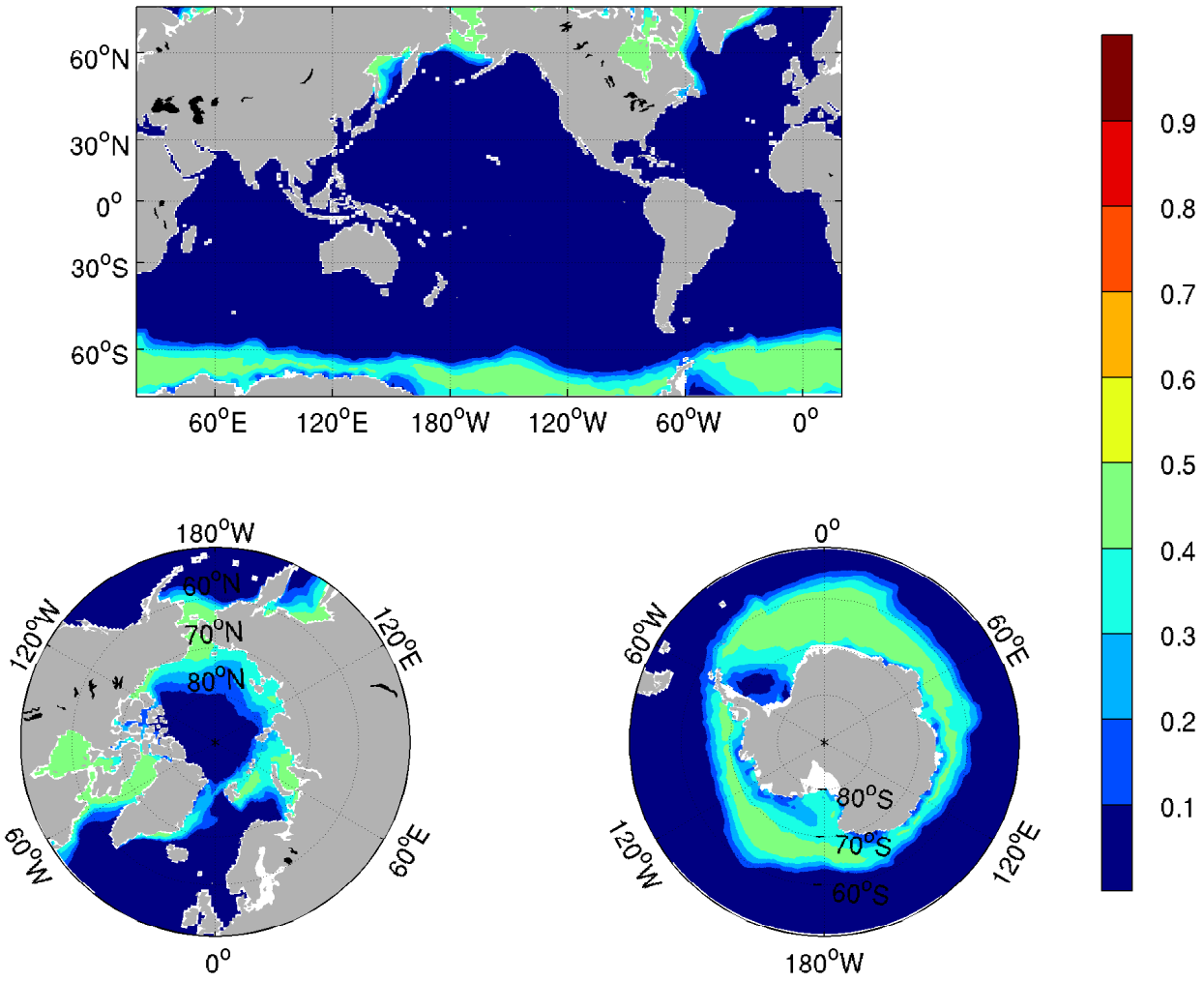

Figure : observed std – sea ice concentration

fit to seaice data

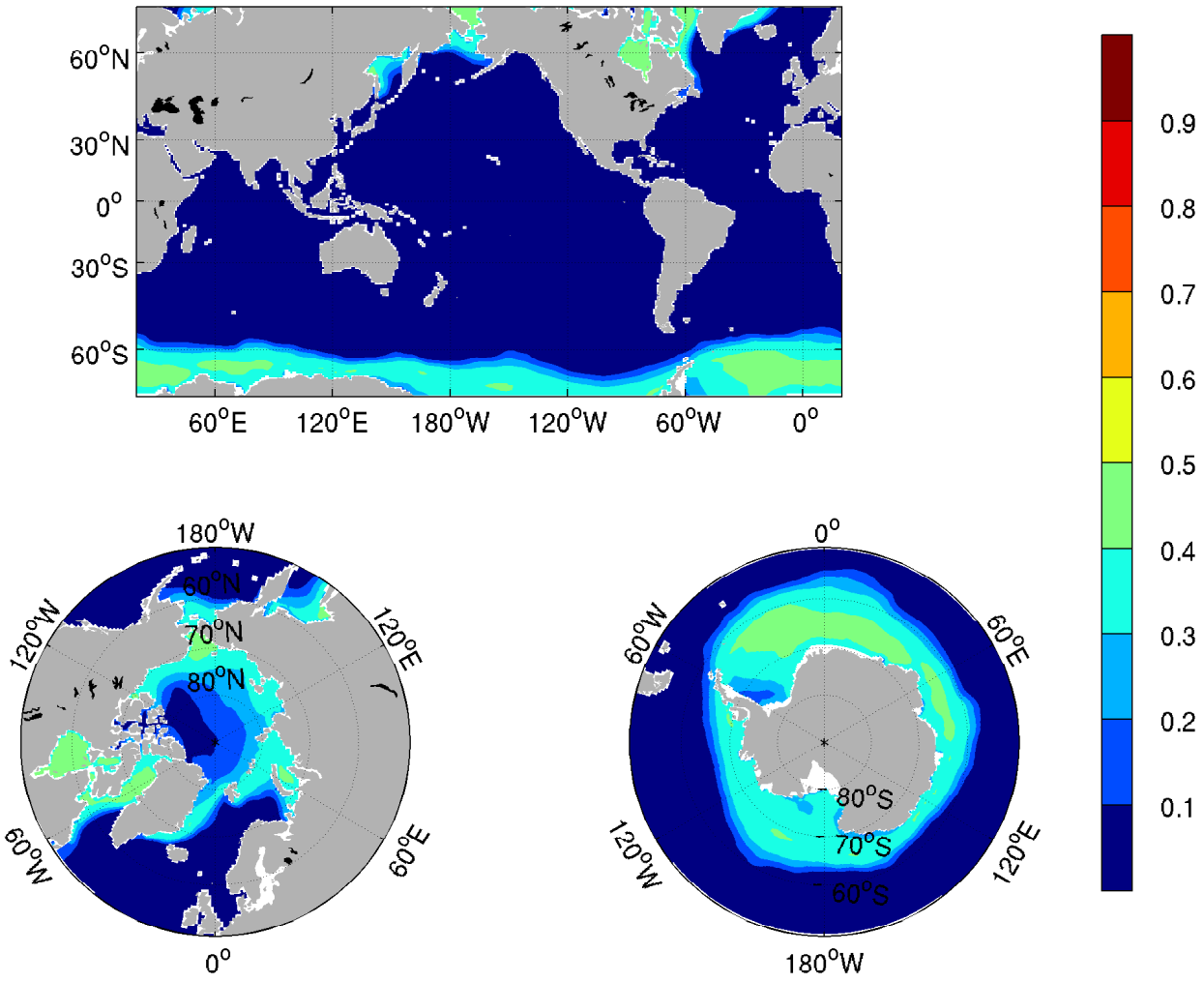

Figure : modelled std – sea ice concentration

fit to seaice data

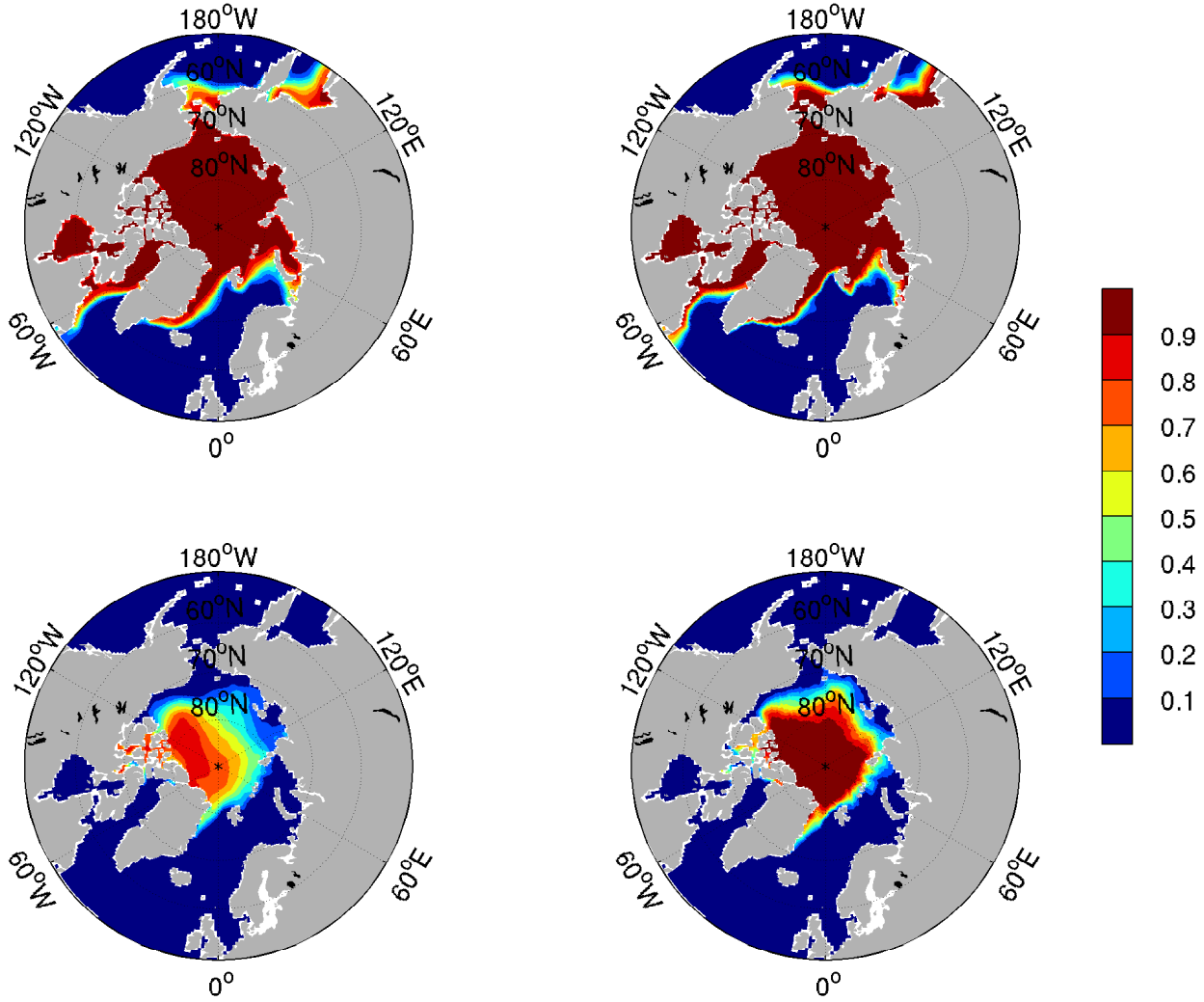

Figure : ECCO (left) and NSIDC (right, gsfc bootstrap) ice concentration in March (top) and September (bottom).

fit to seaice data

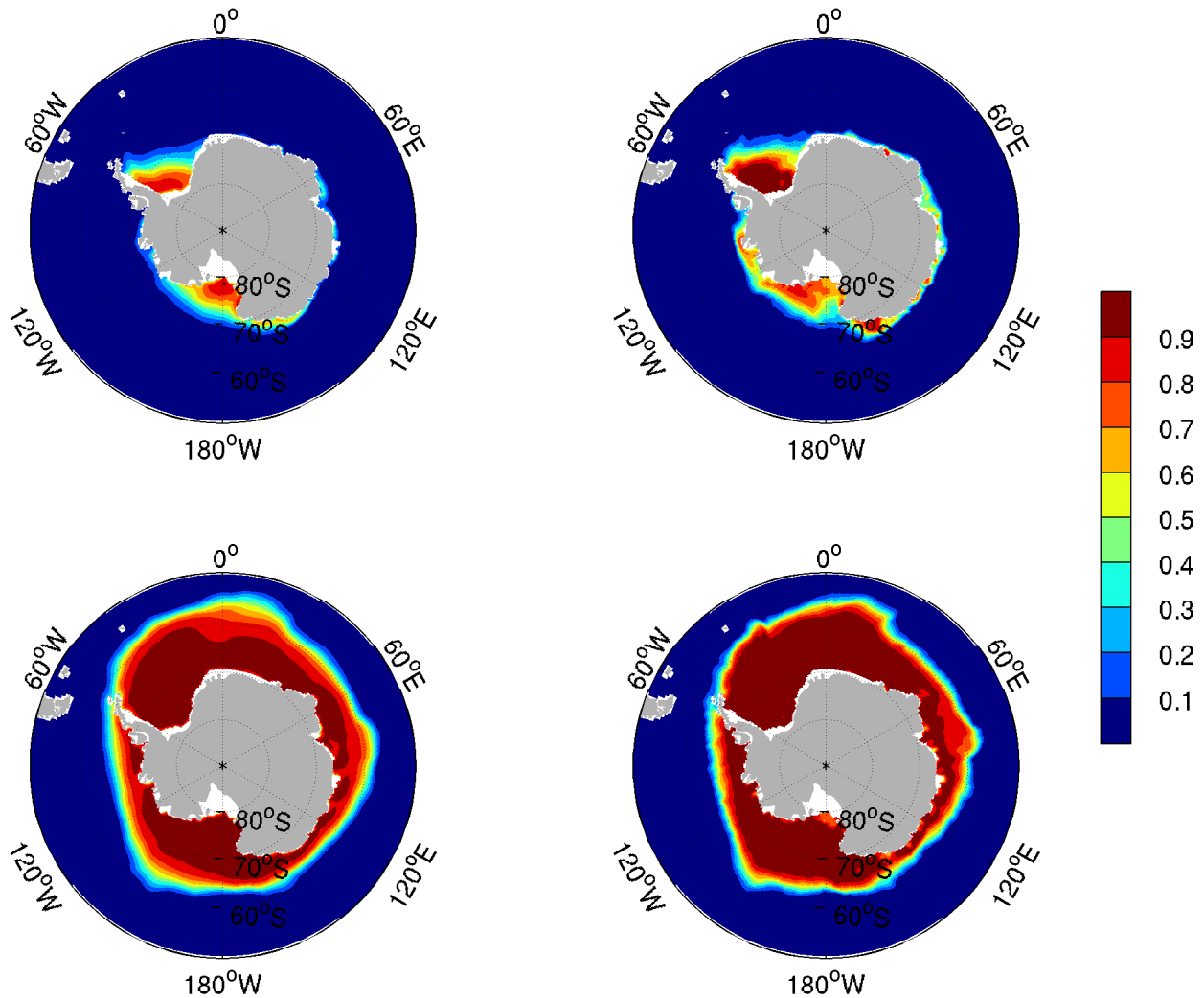

Figure : ECCO (left) and NSIDC (right, gsfc bootstrap) ice concentration in March (top) and September (bottom).

fit to seaice data

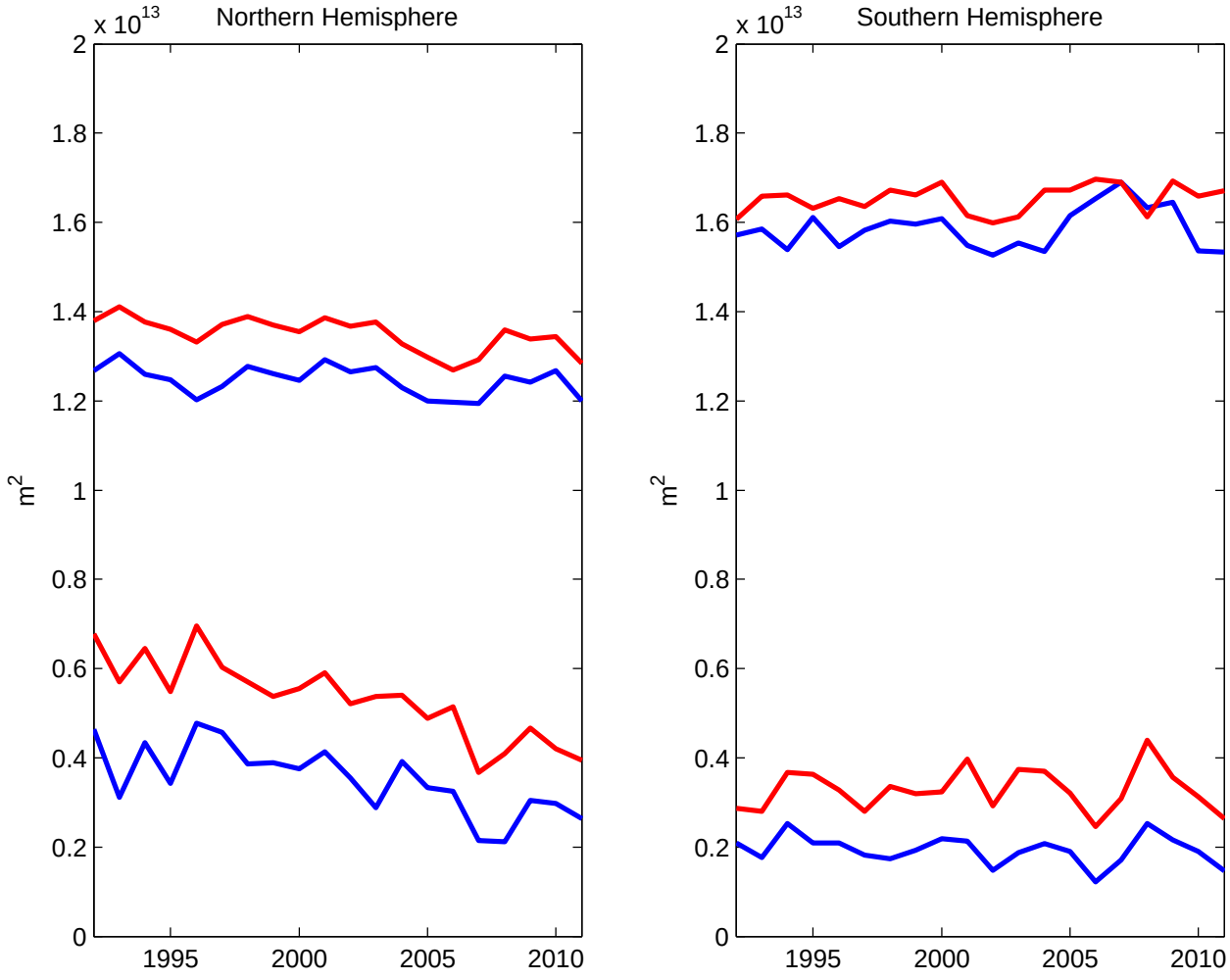

Figure : ECCO (blue) and NSIDC (red, gsfc bootstrap) ice concentration in March and September in Northern Hemisphere (left) and Southern Hemisphere (right)

fit to seaice data

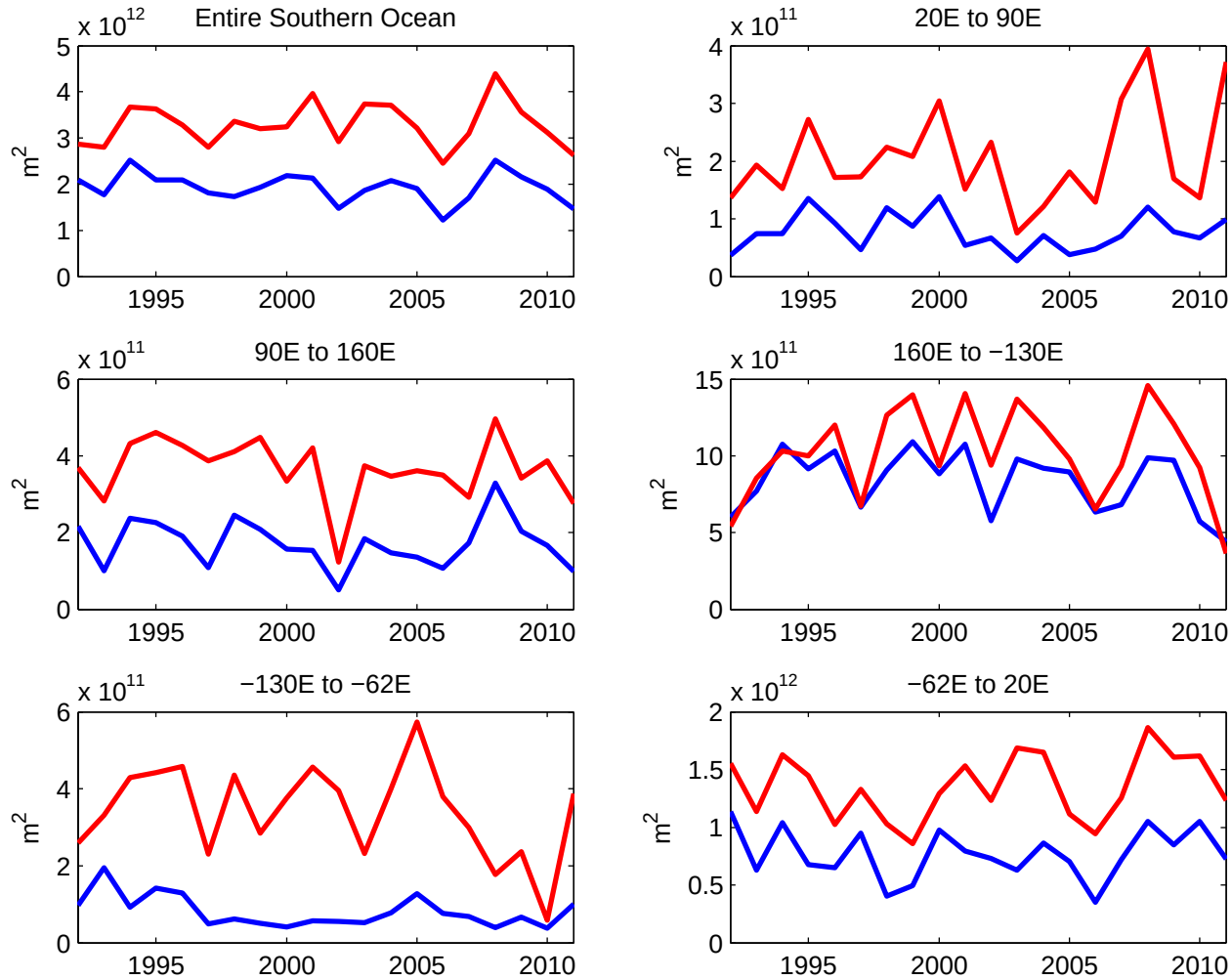

Figure : ECCO (blue) and NSIDC (red, gsfc bootstrap) ice concentration in March per Southern Ocean sector

fit to seaice data

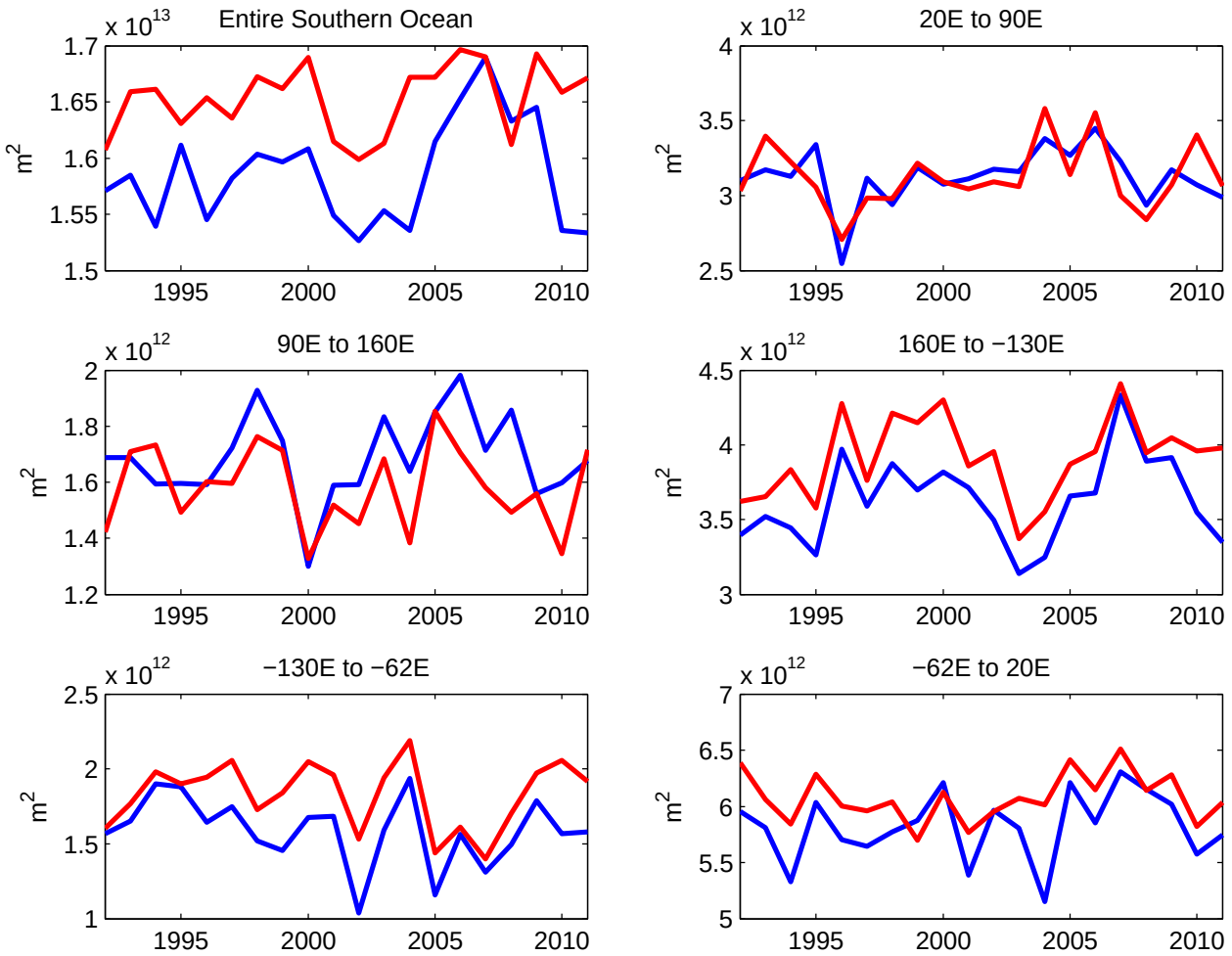

Figure : ECCO (blue) and NSIDC (red, gsfc bootstrap) ice concentration in September per Southern Ocean sector

barotropic streamfunction

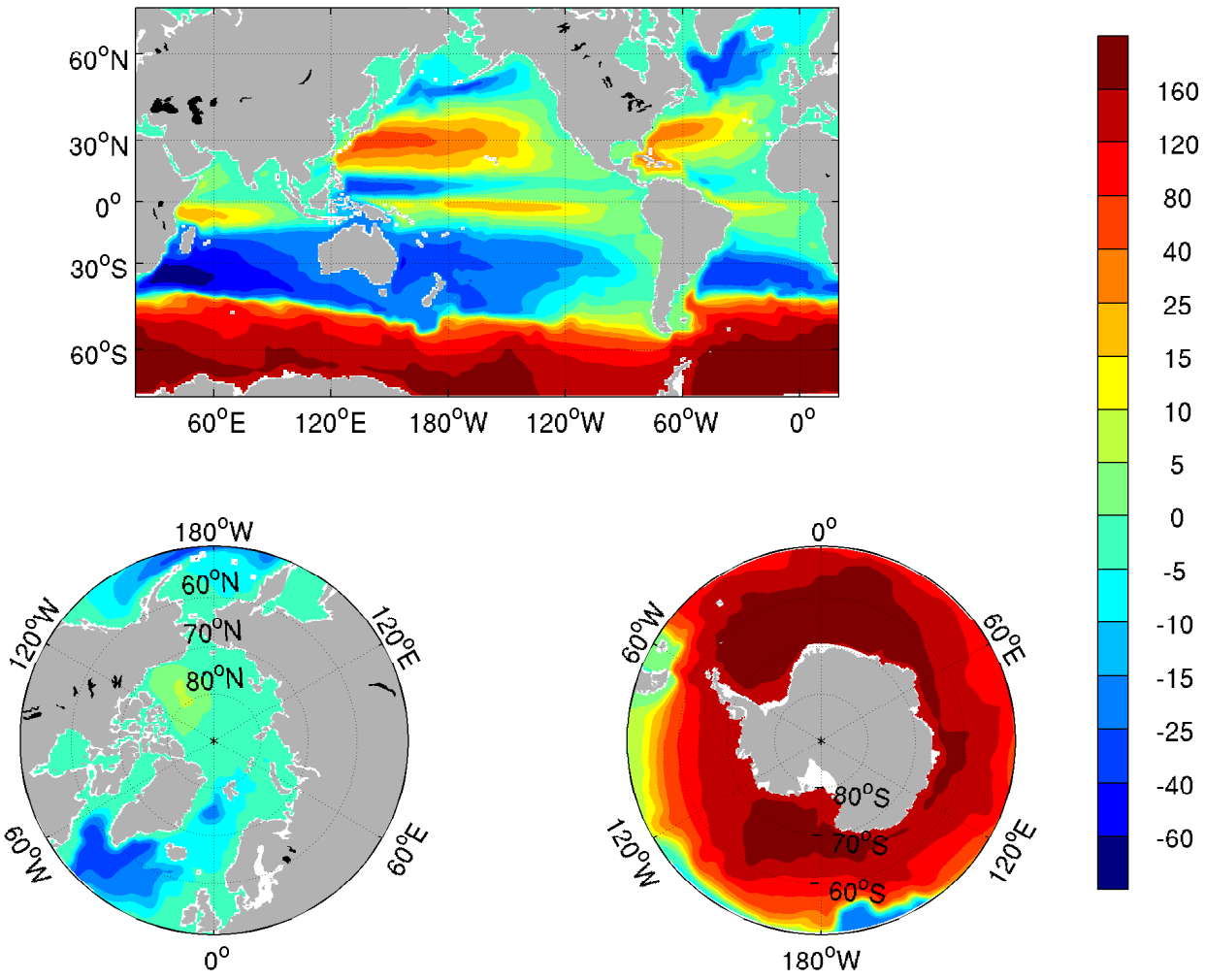

Figure : 1992-2011 mean – barotropic streamfunction (Sv)

barotropic streamfunction

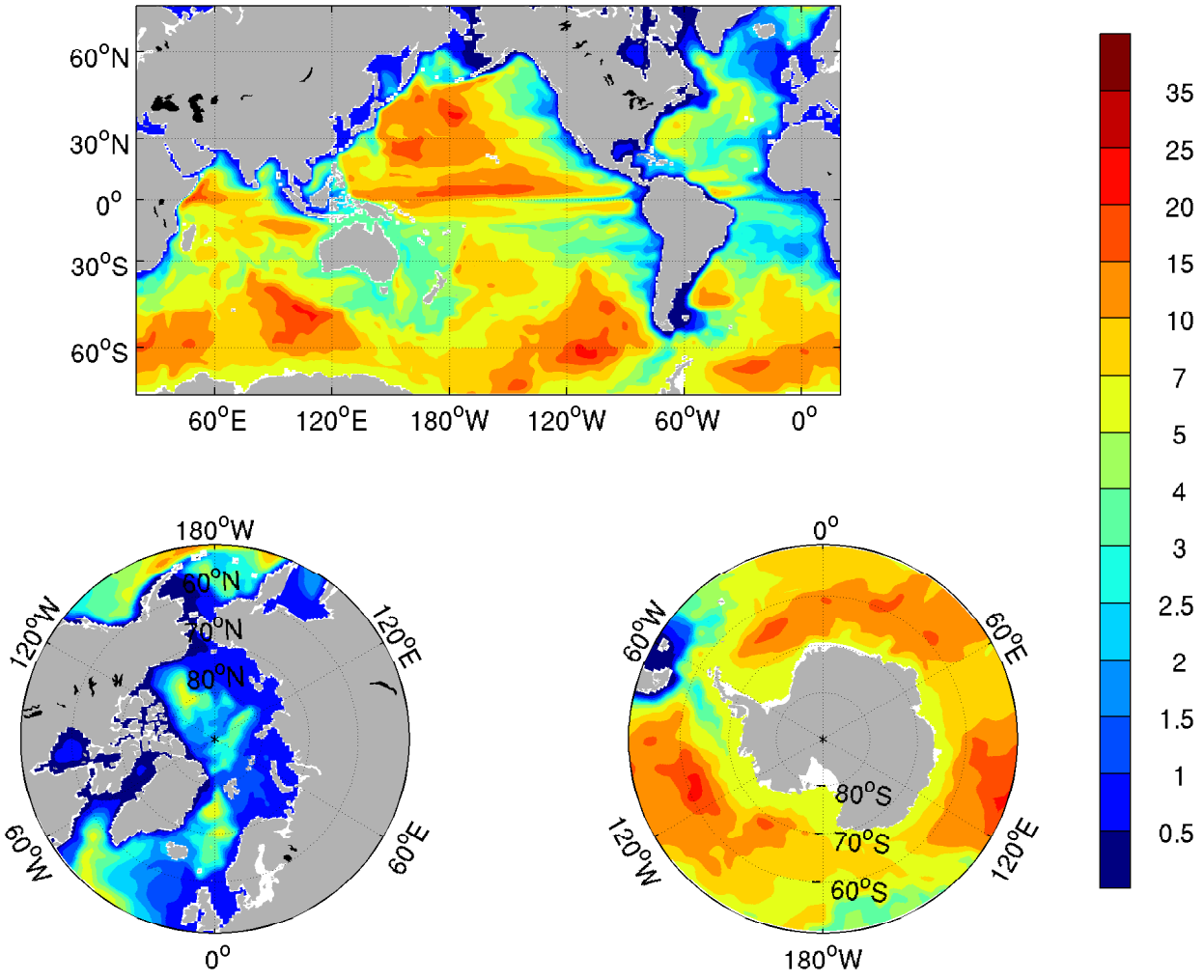

Figure : 1992-2011 standard deviation – barotropic streamfunction (Sv)

meridional streamfunction

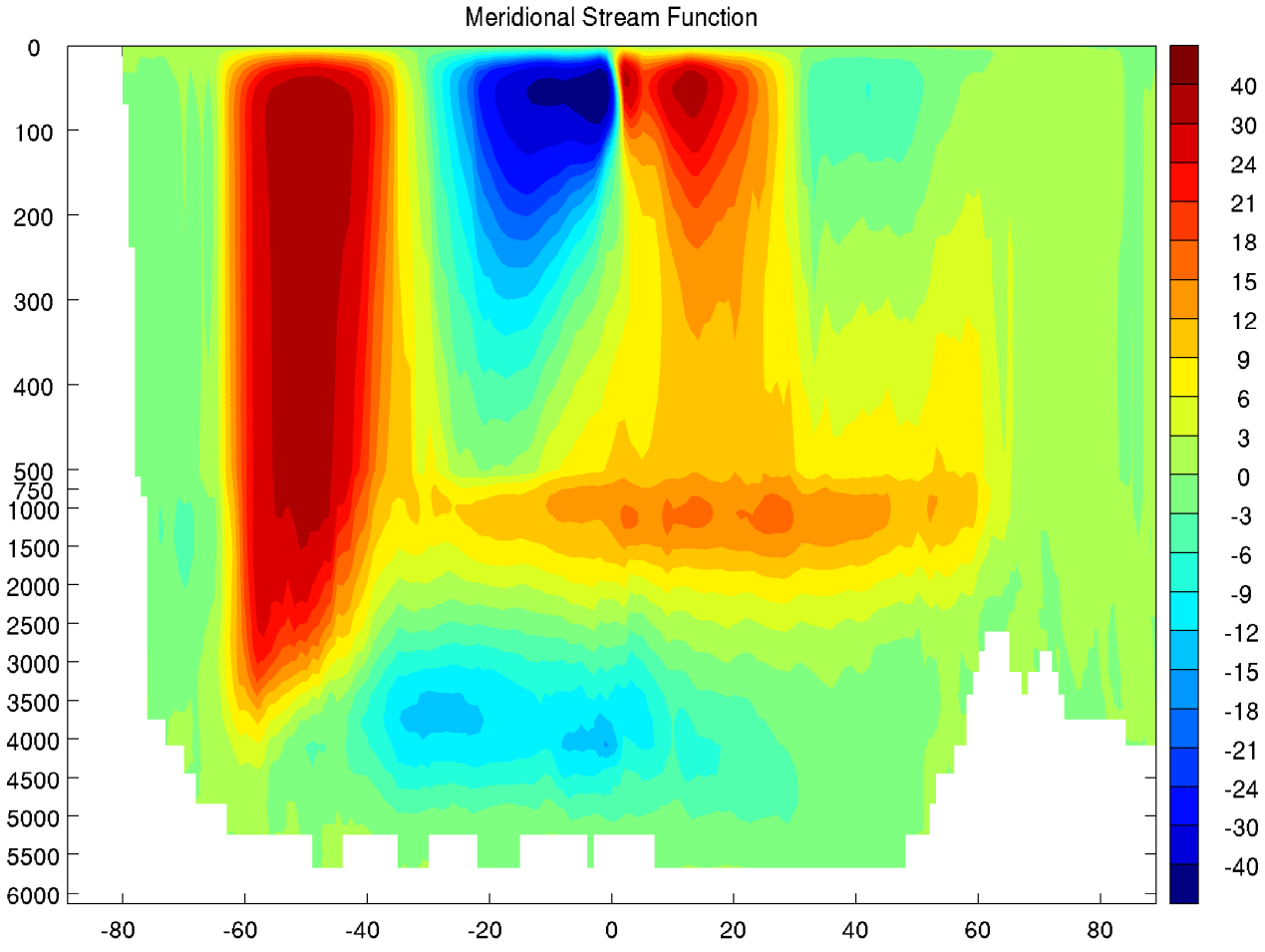

Figure : 1992-2011 mean – overturning streamfunction (Sv)

meridional streamfunction

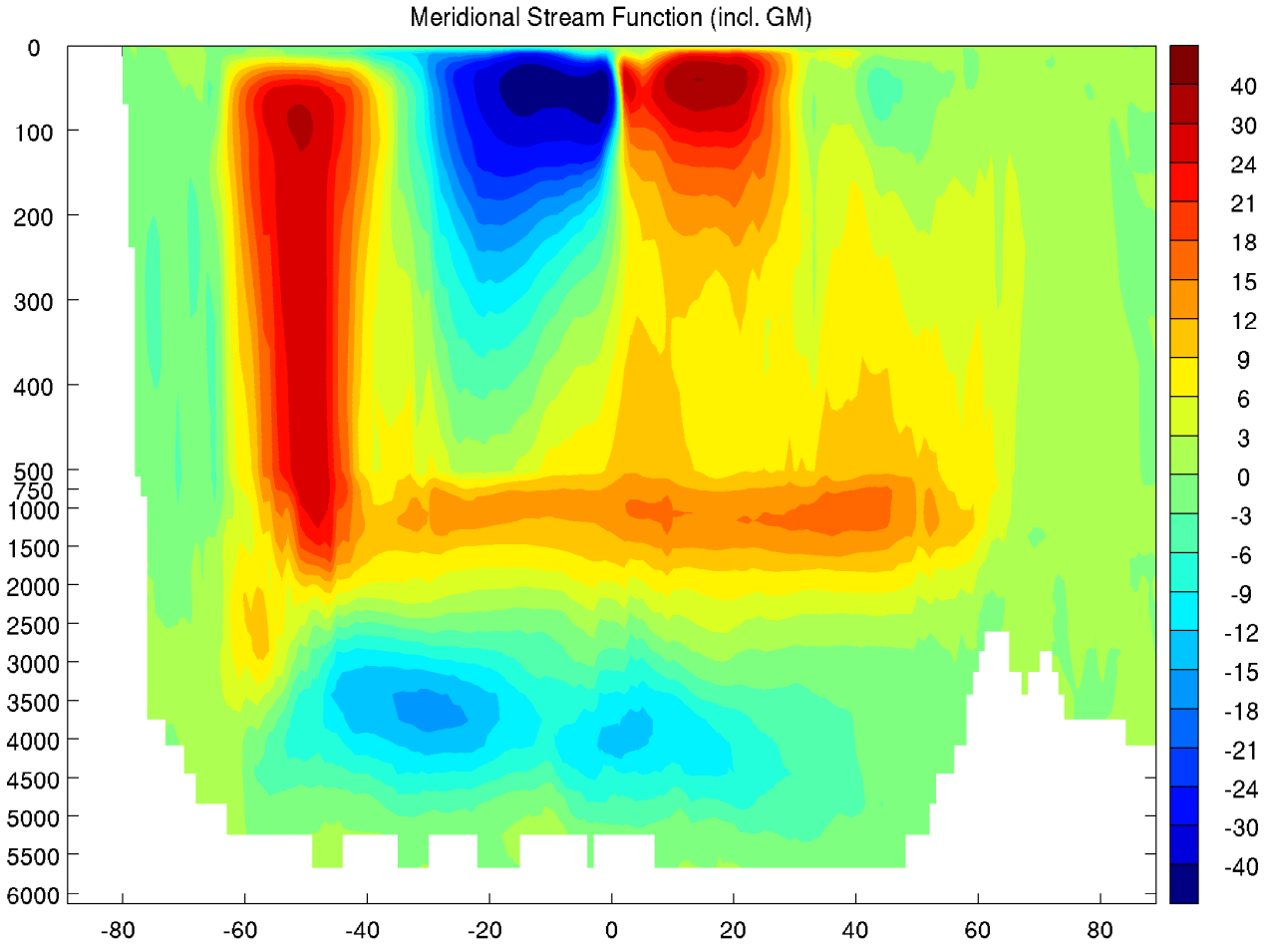

Figure : 1992-2011 mean – overturning streamfunction incl. GM (Sv)

meridional streamfunction

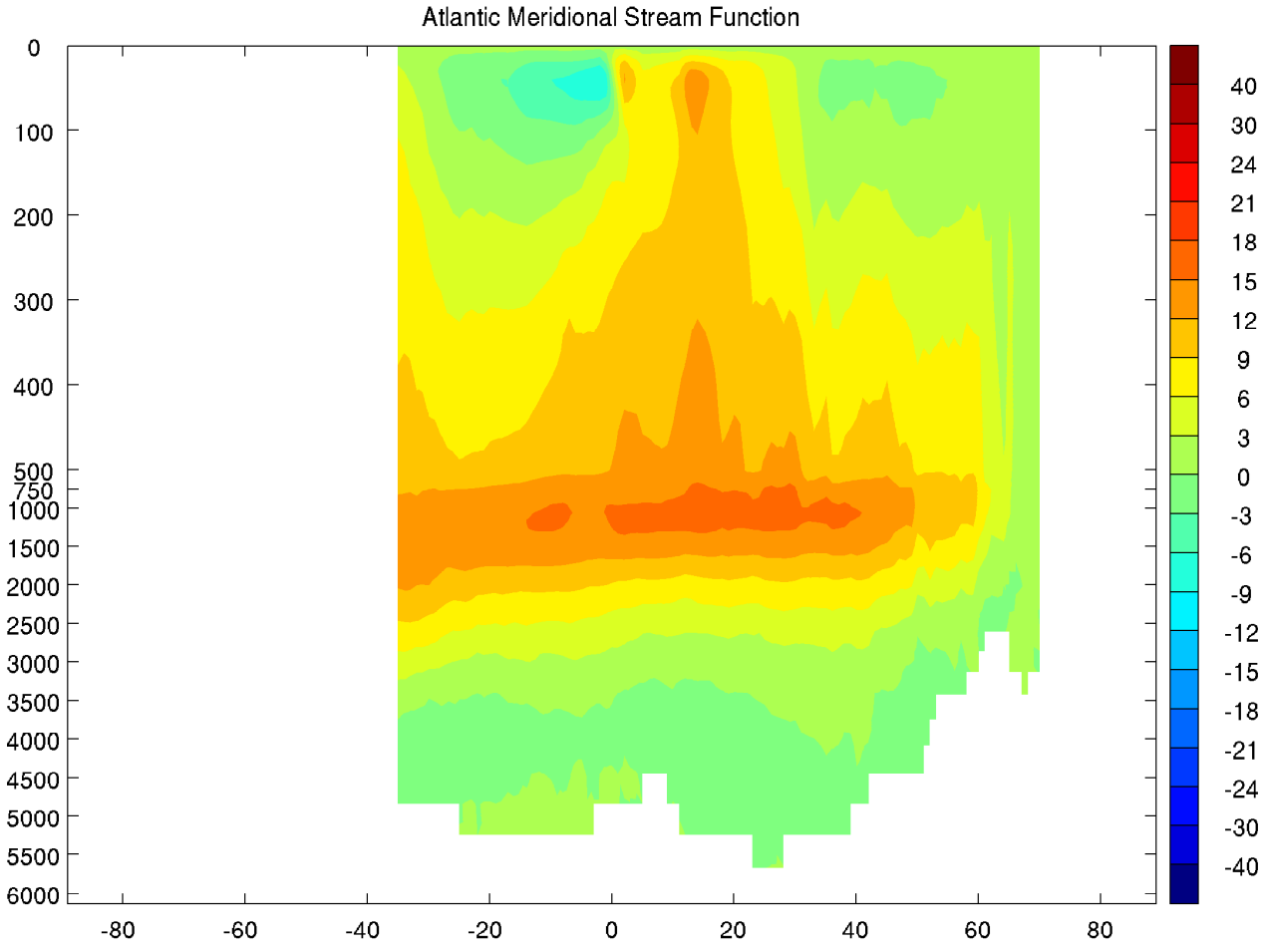

Figure : 1992-2011 mean – Atlantic overturning streamfunction (Sv)

meridional streamfunction

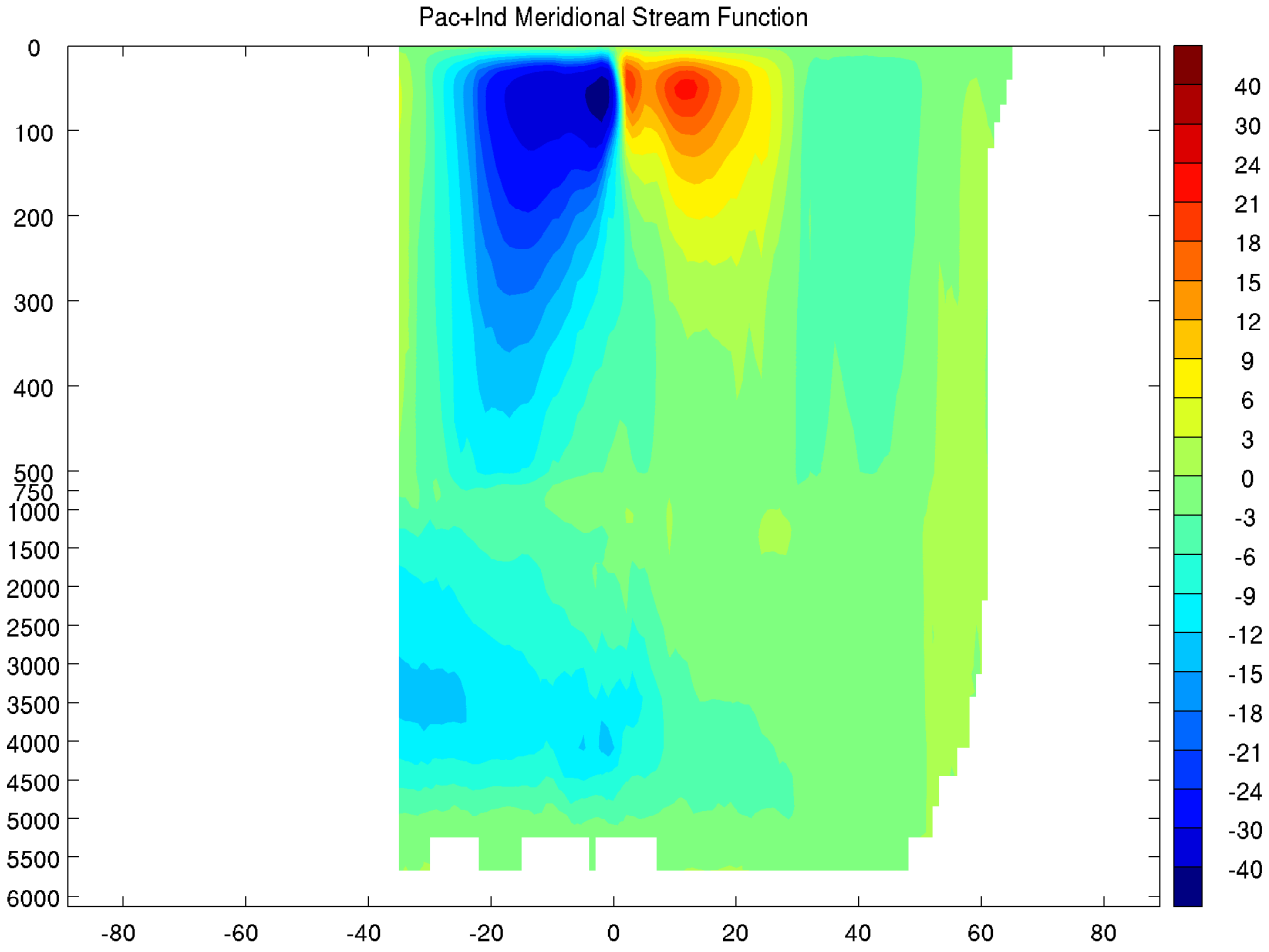

Figure : 1992-2011 mean – Pac+Ind overturning streamfunction (Sv)

meridional streamfunction

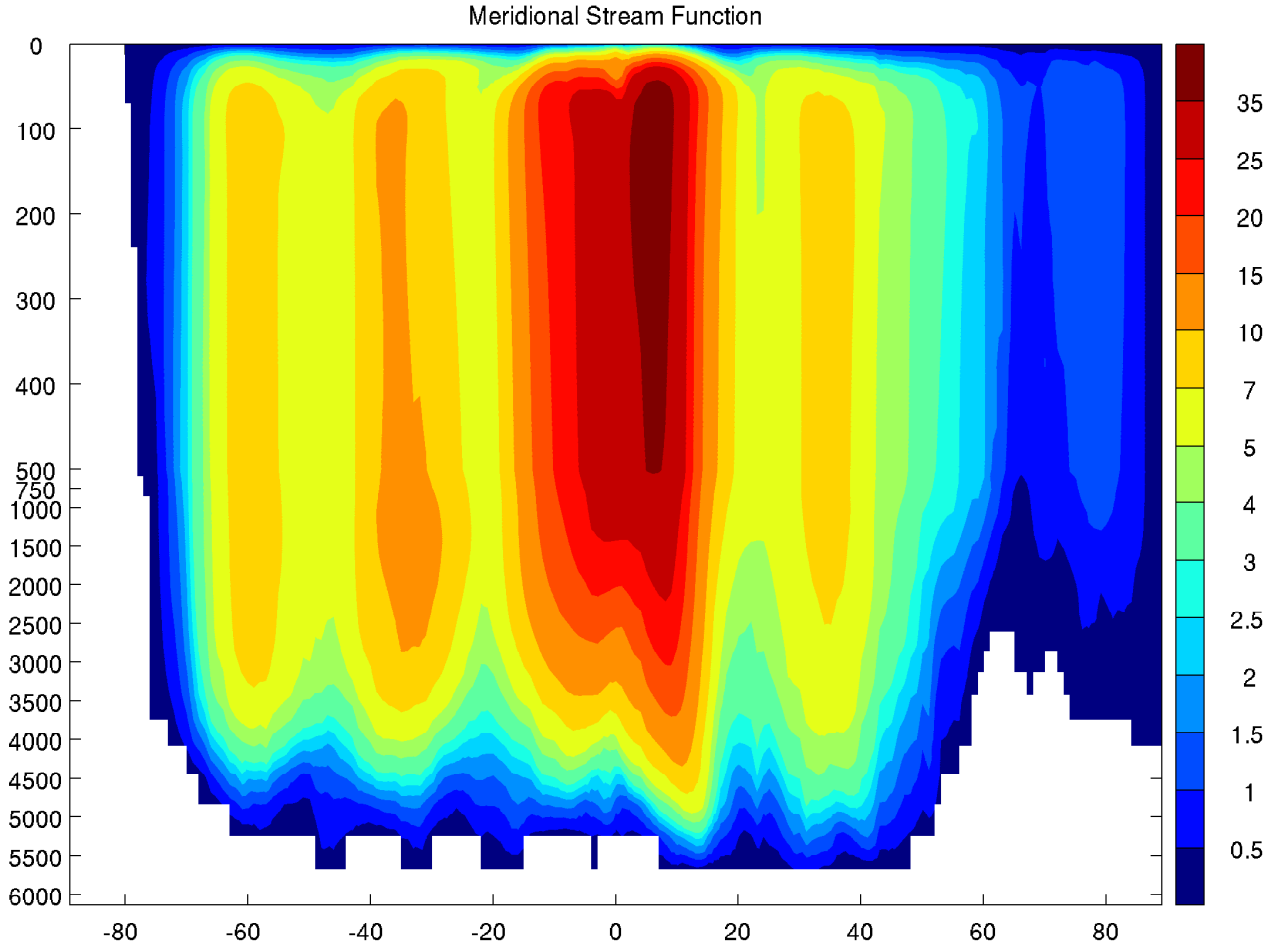

Figure : 1992-2011 standard deviation – overturning streamfunction (Sv)

meridional streamfunction

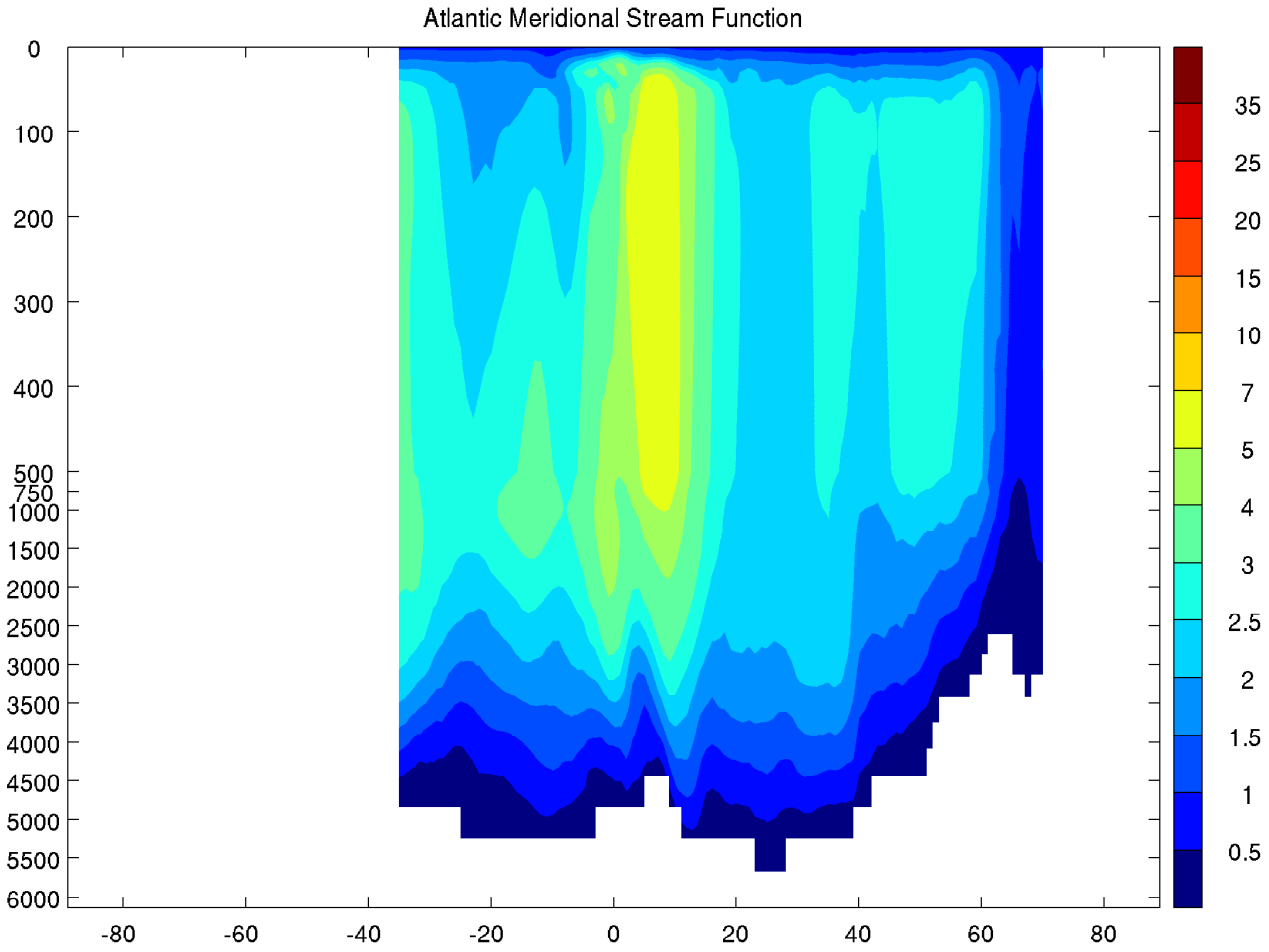

Figure : 1992-2011 standard deviation – Atlantic overturning streamfunction (Sv)

meridional streamfunction (time series)

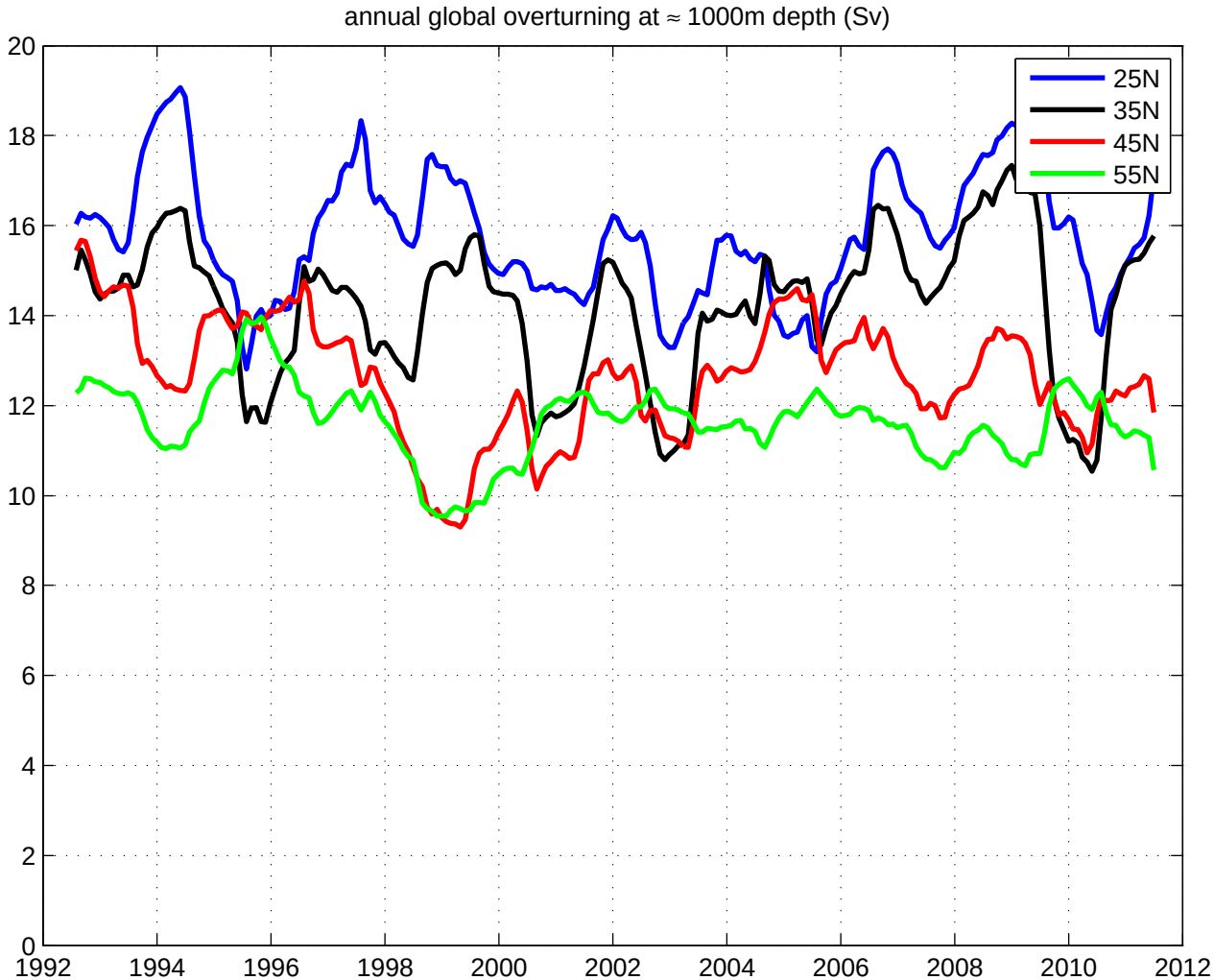

Figure : annual global overturning at select latitudes at $\approx$ 1000m depth

meridional streamfunction (time series)

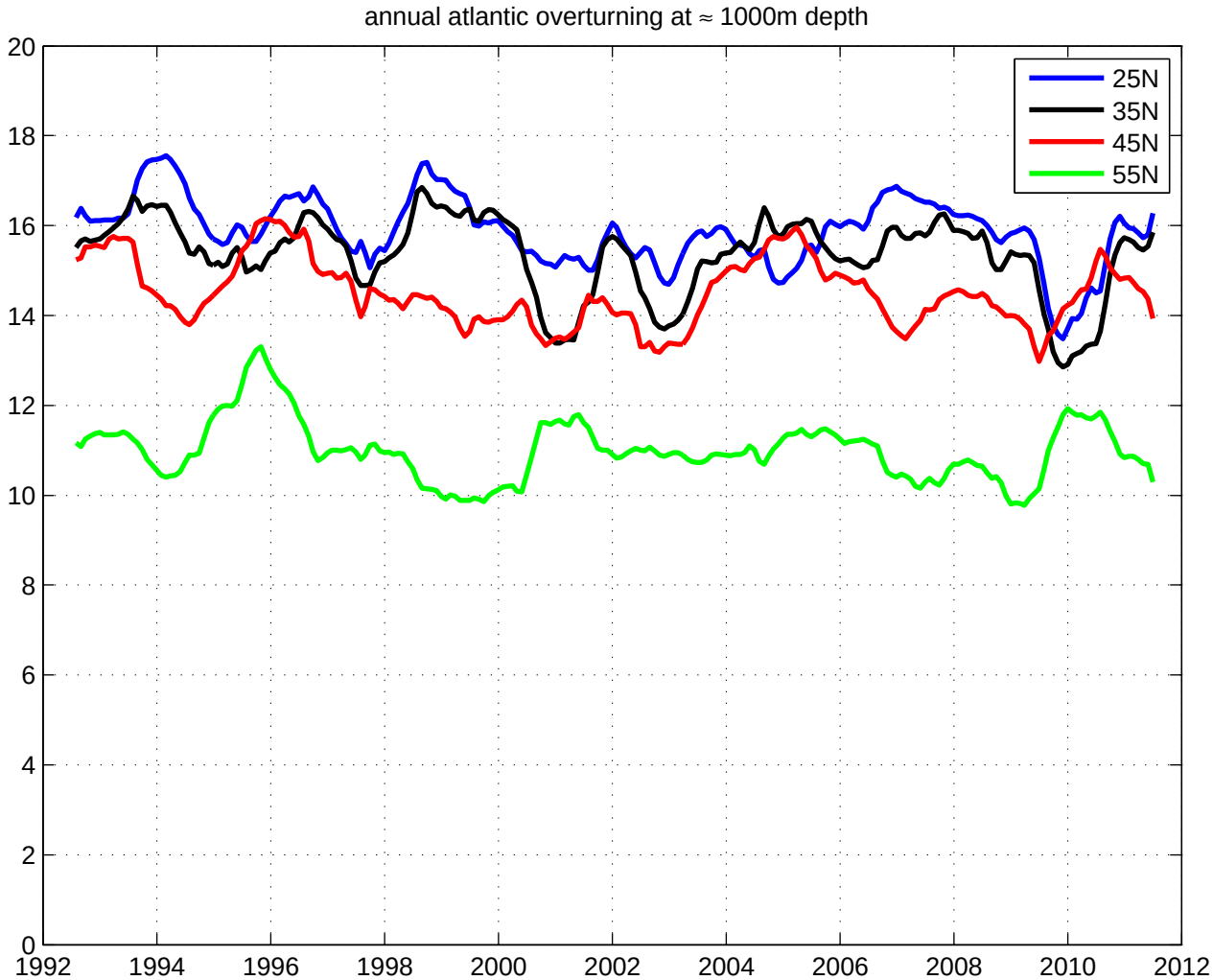

Figure : annual Atlantic overturning at select latitudes at ≈ 1000m depth (Sv)

meridional heat transport

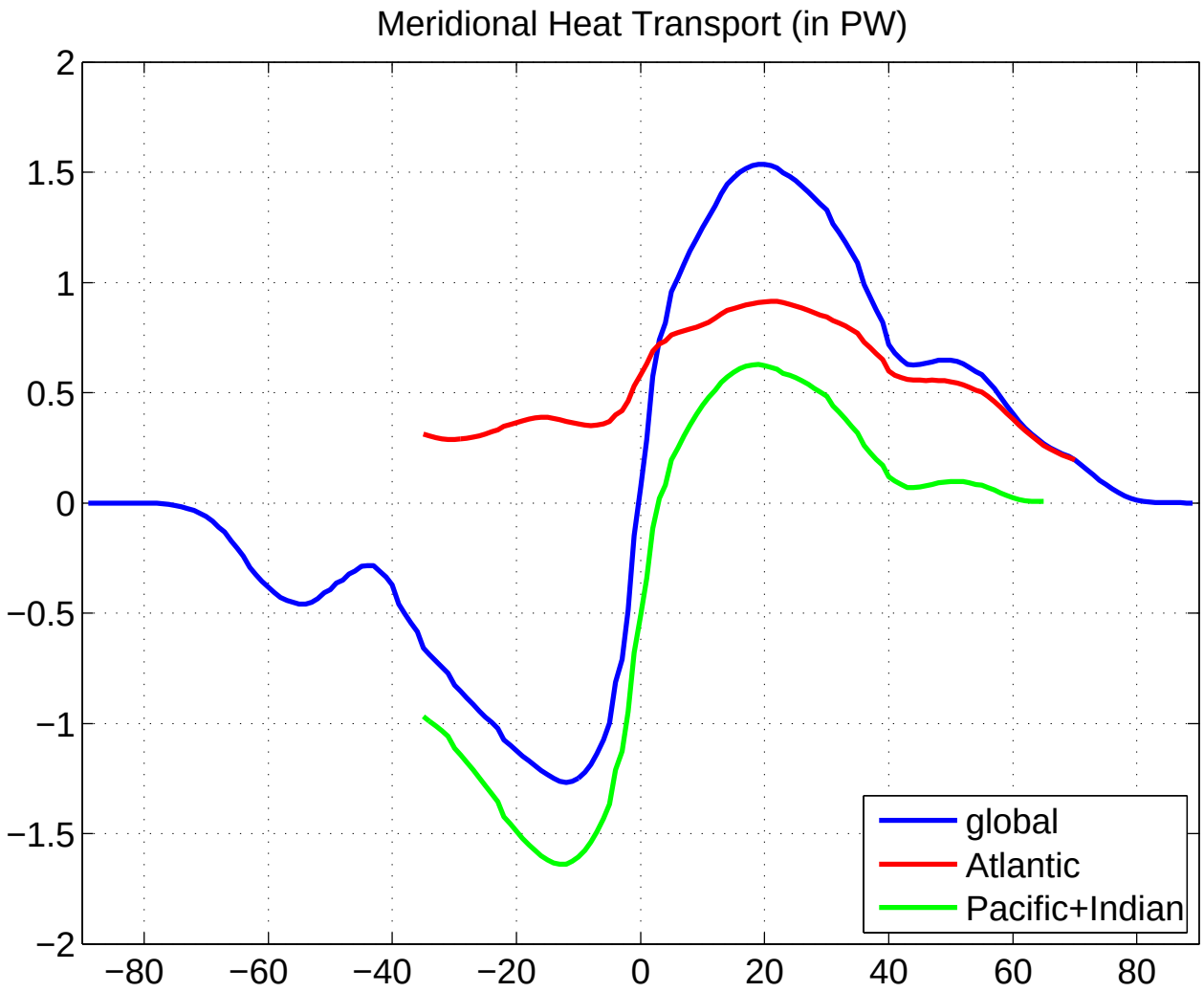

Figure : 1992-2011 mean – meridional heat transport (PW)

meridional heat transport

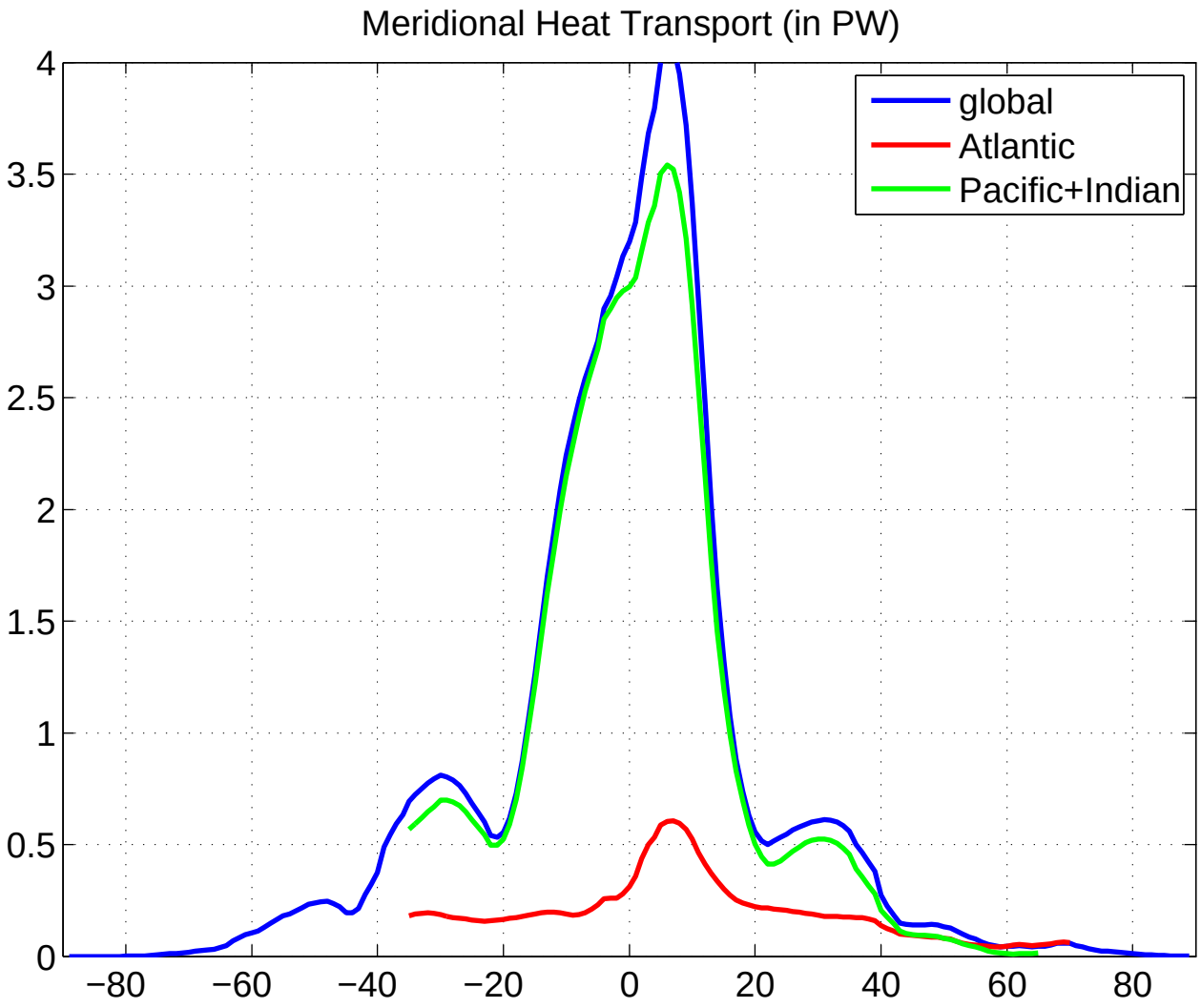

Figure : 1992-2011 standard deviation – meridional heat transport (PW)

meridional freshwater transport

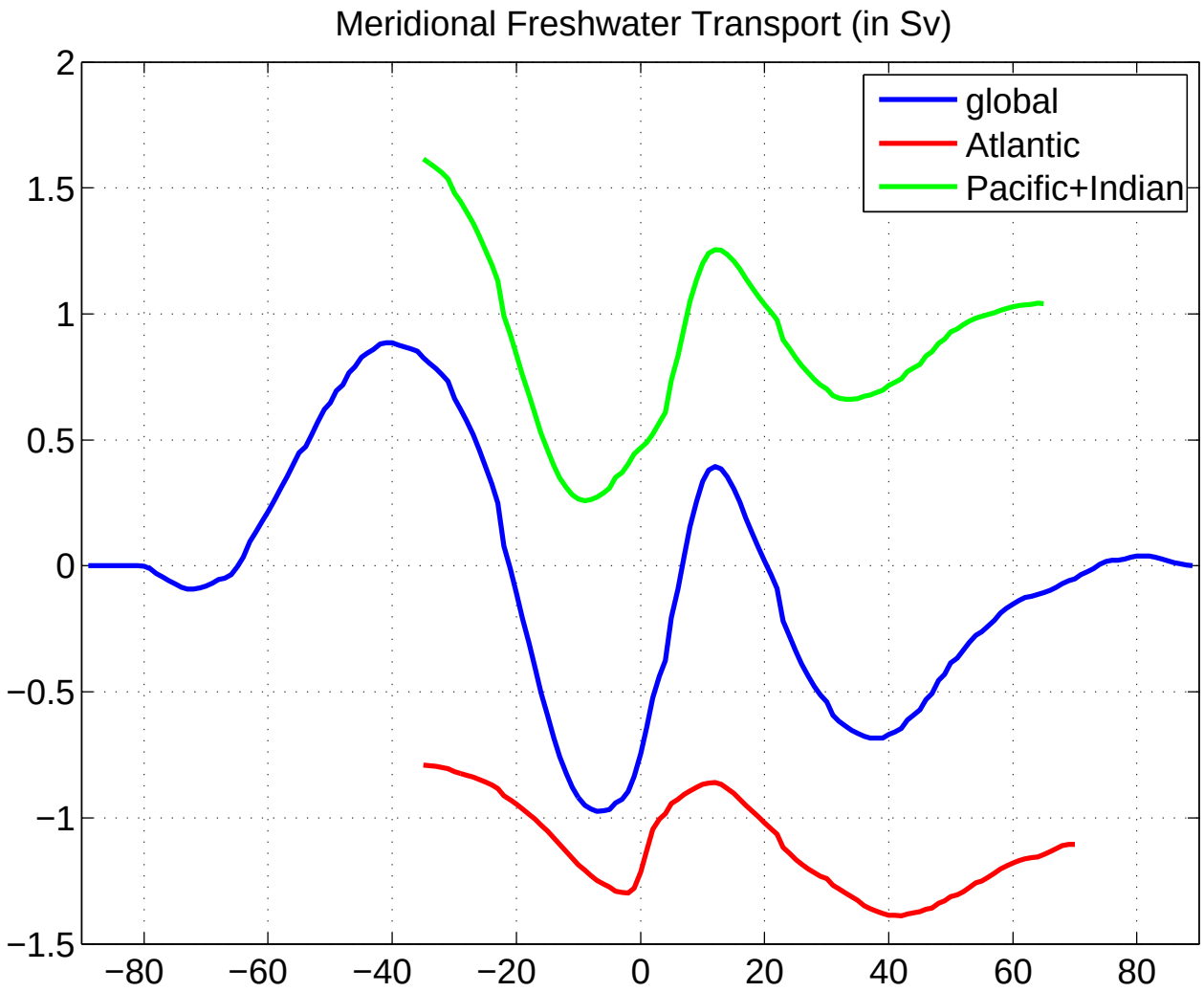

Figure : 1992-2011 mean – meridional freshwater transport (Sv)

meridional freshwater transport

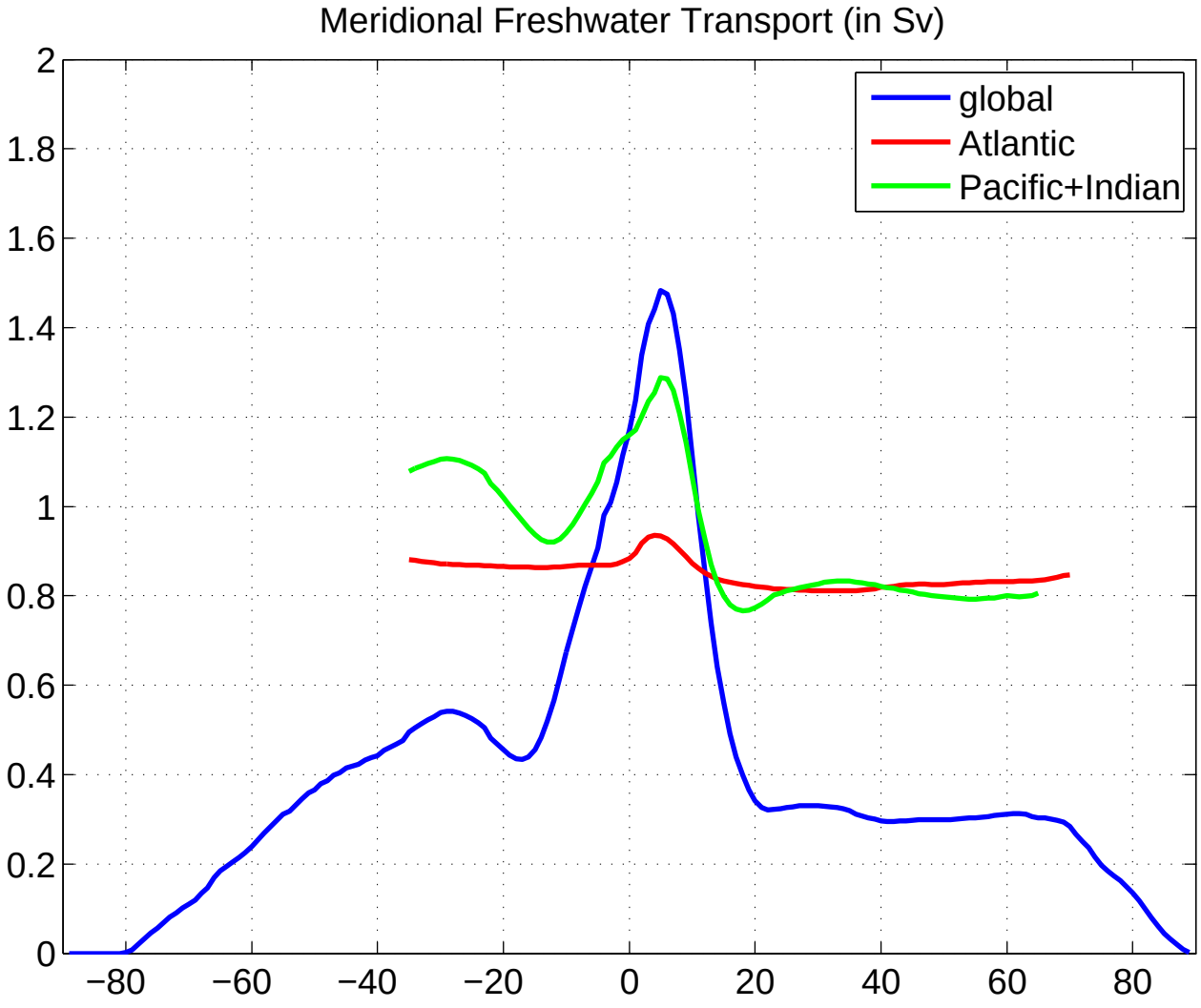

Figure : 1992-2011 standard deviation – meridional freshwater transport (Sv)

meridional salt transport

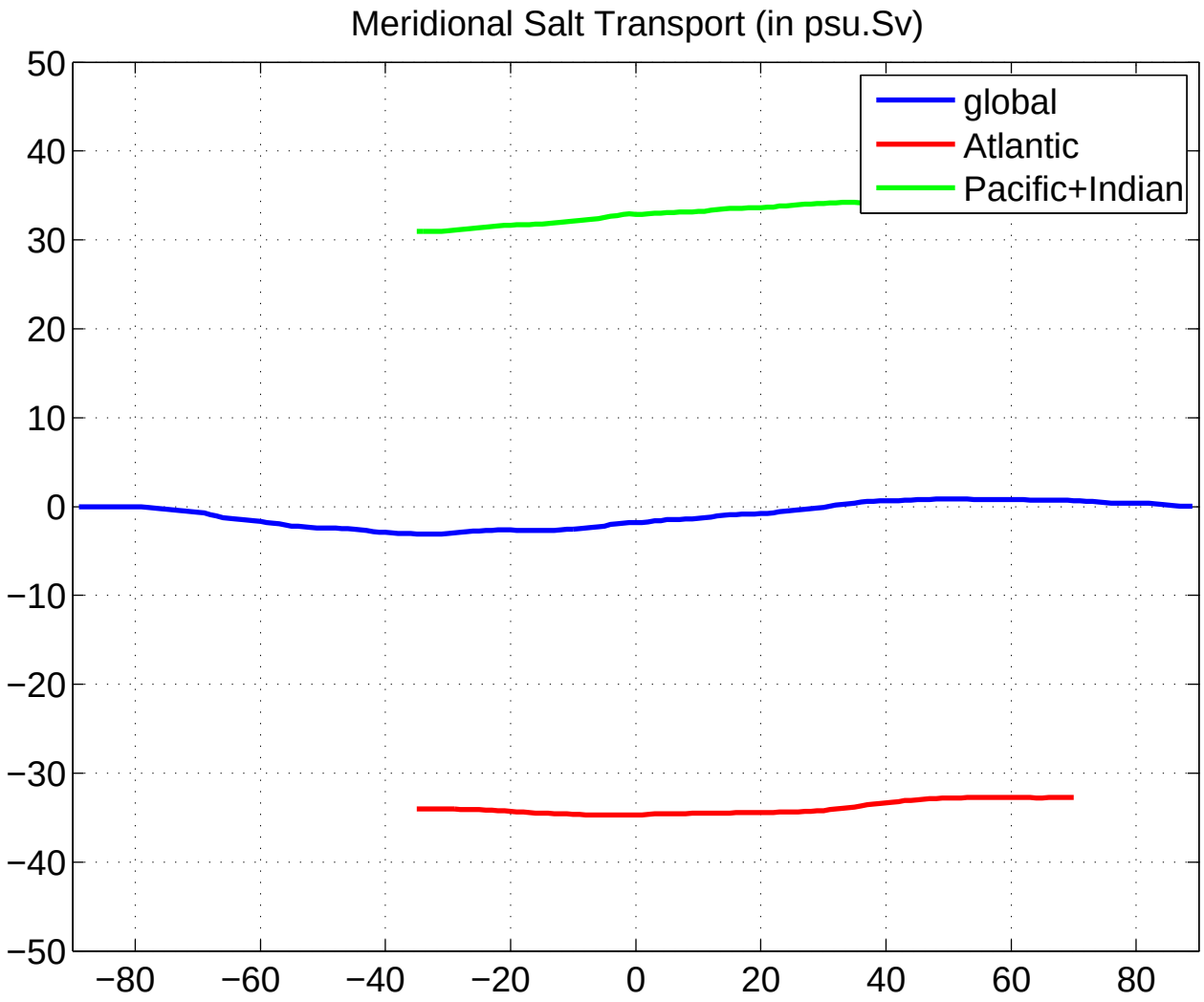

Figure : 1992-2011 mean – meridional salt transport (psu.Sv)

meridional salt transport

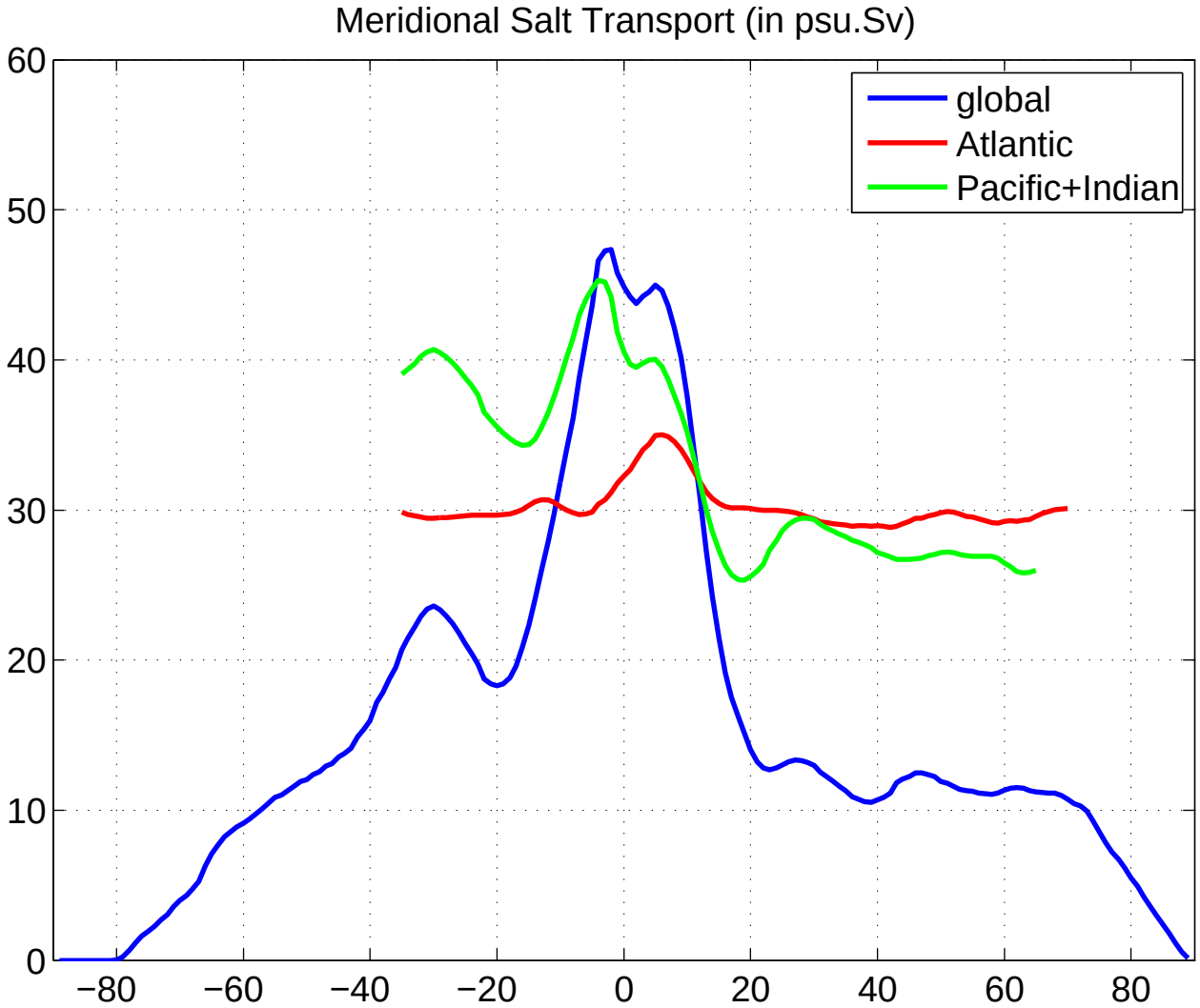

Figure : 1992-2011 standard deviation – meridional salt transport (psu.Sv)

meridional transports (time series)

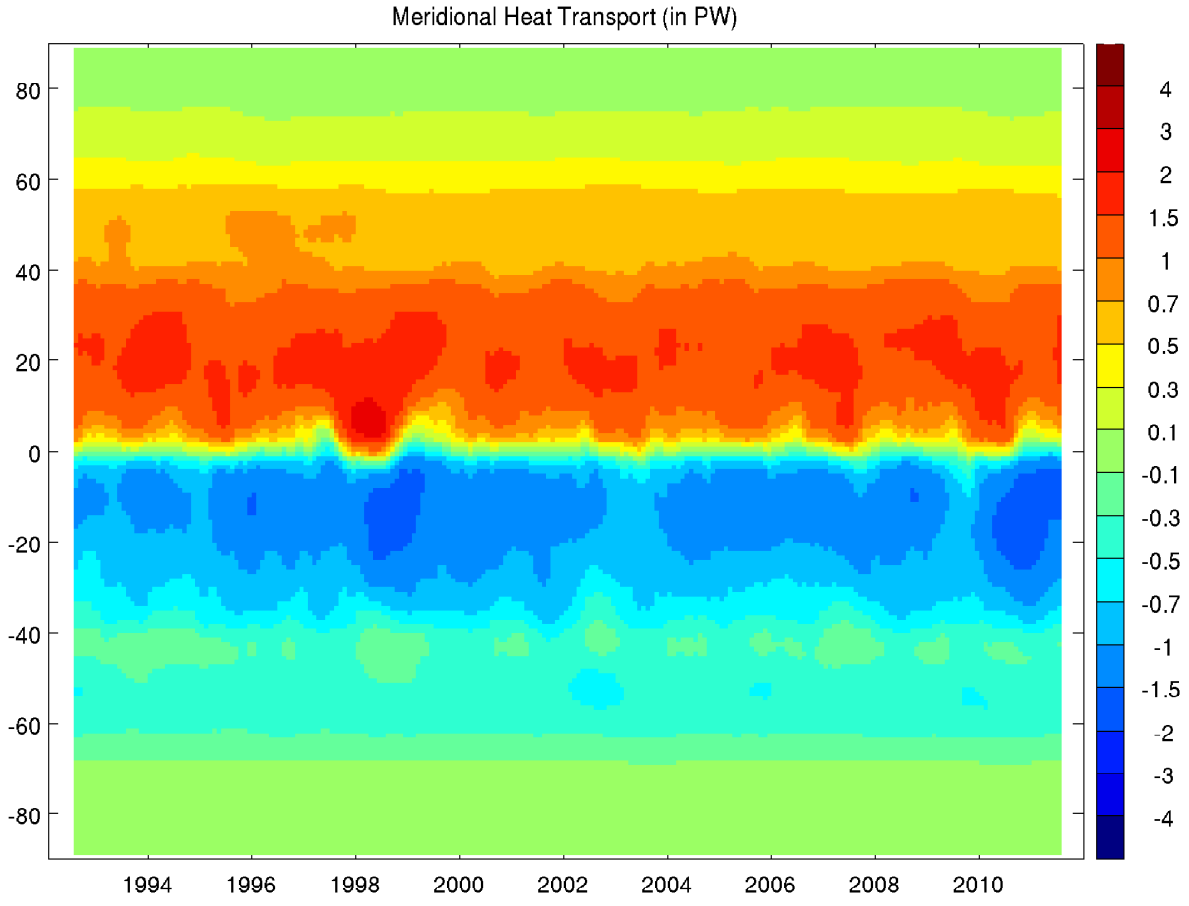

Figure : meridional heat transport (PW, annual mean)

meridional transports (time series)

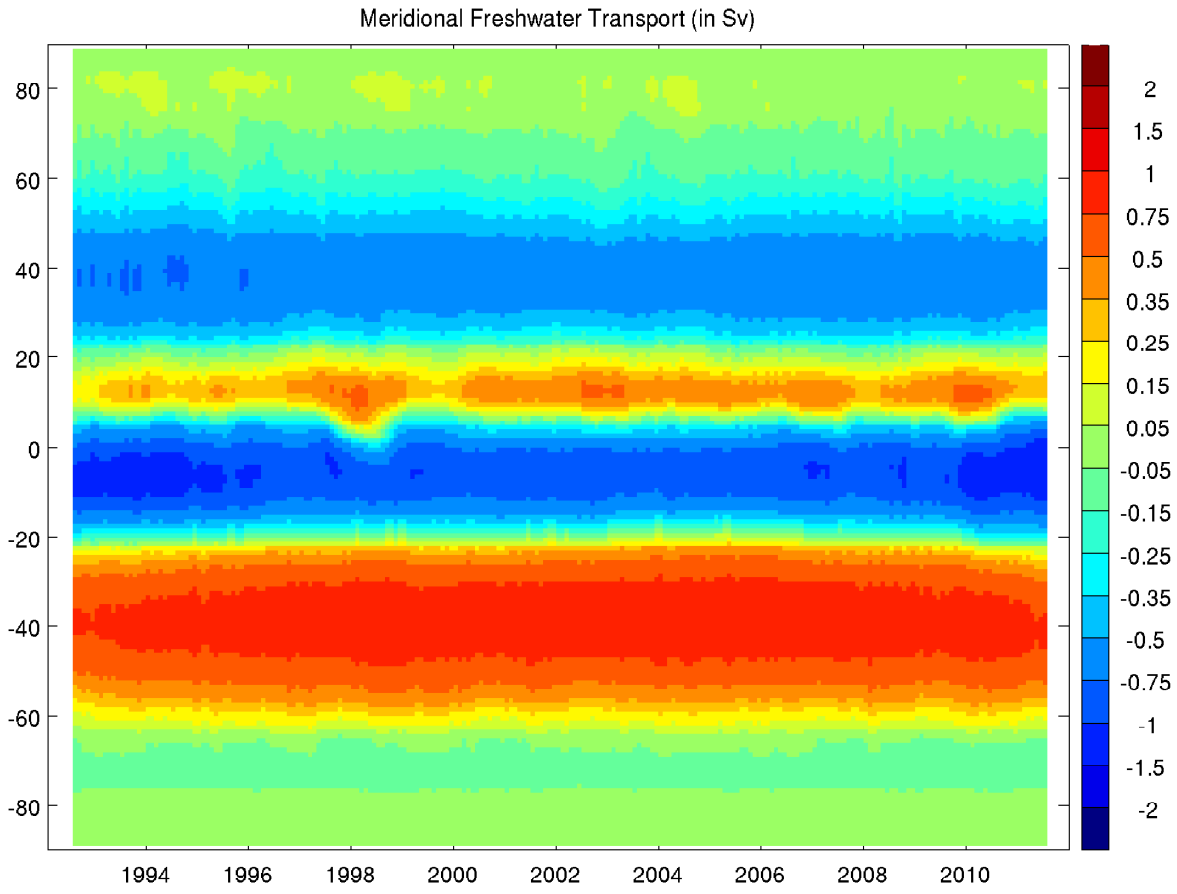

Figure : meridional freshwater transport (Sv, annual mean)

meridional transports (time series)

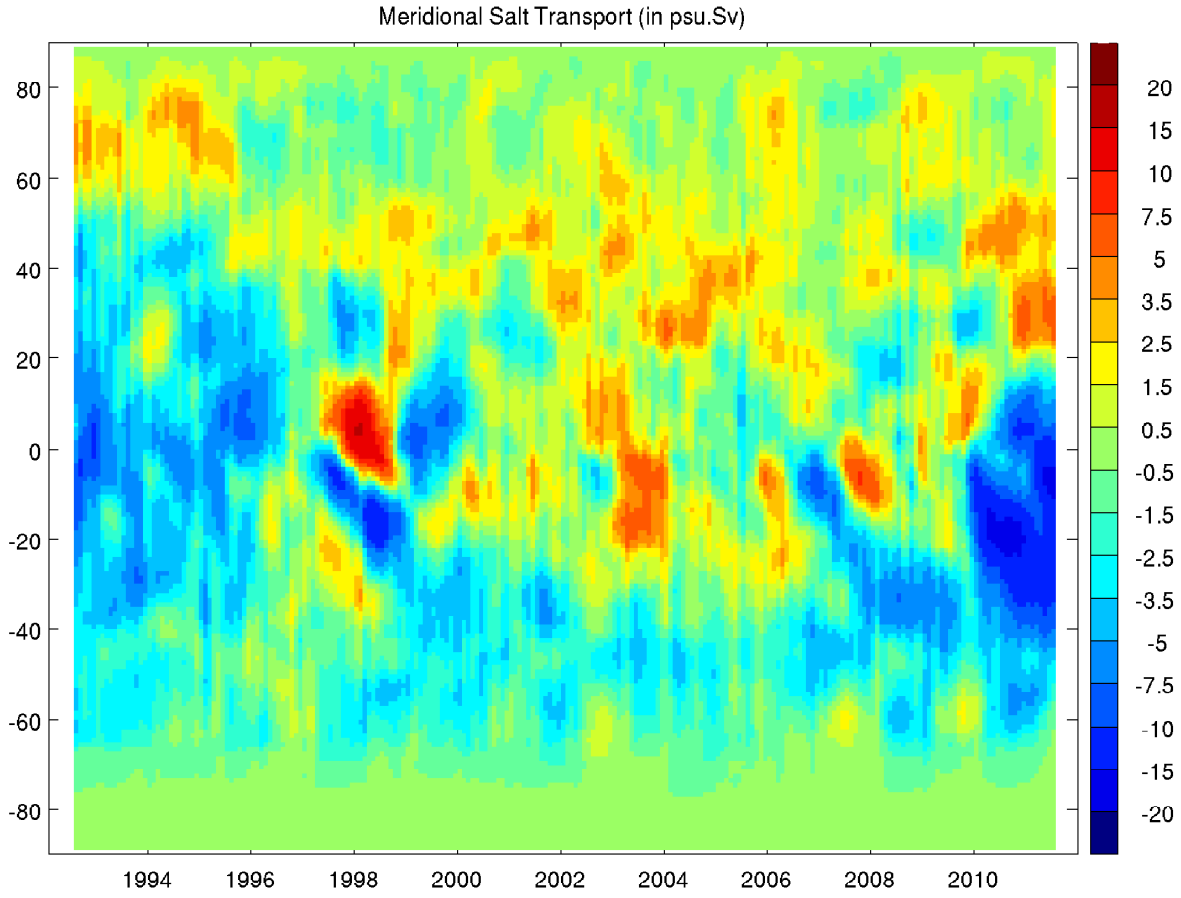

Figure : meridional salt transport (psu.Sv, annual mean)

transects transport

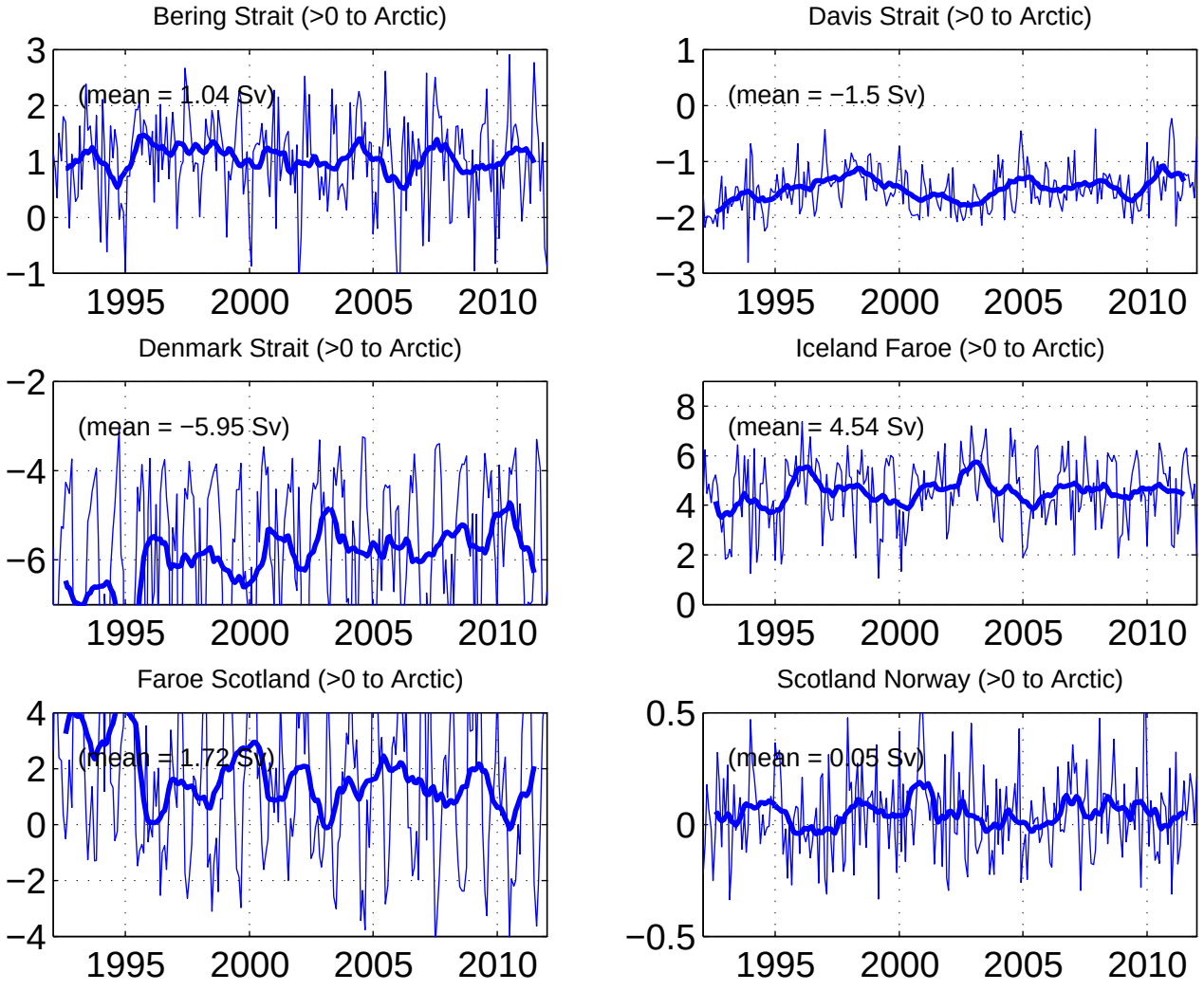

Figure : volume transports entering the Arctic (Sv, annual mean)

transects transport

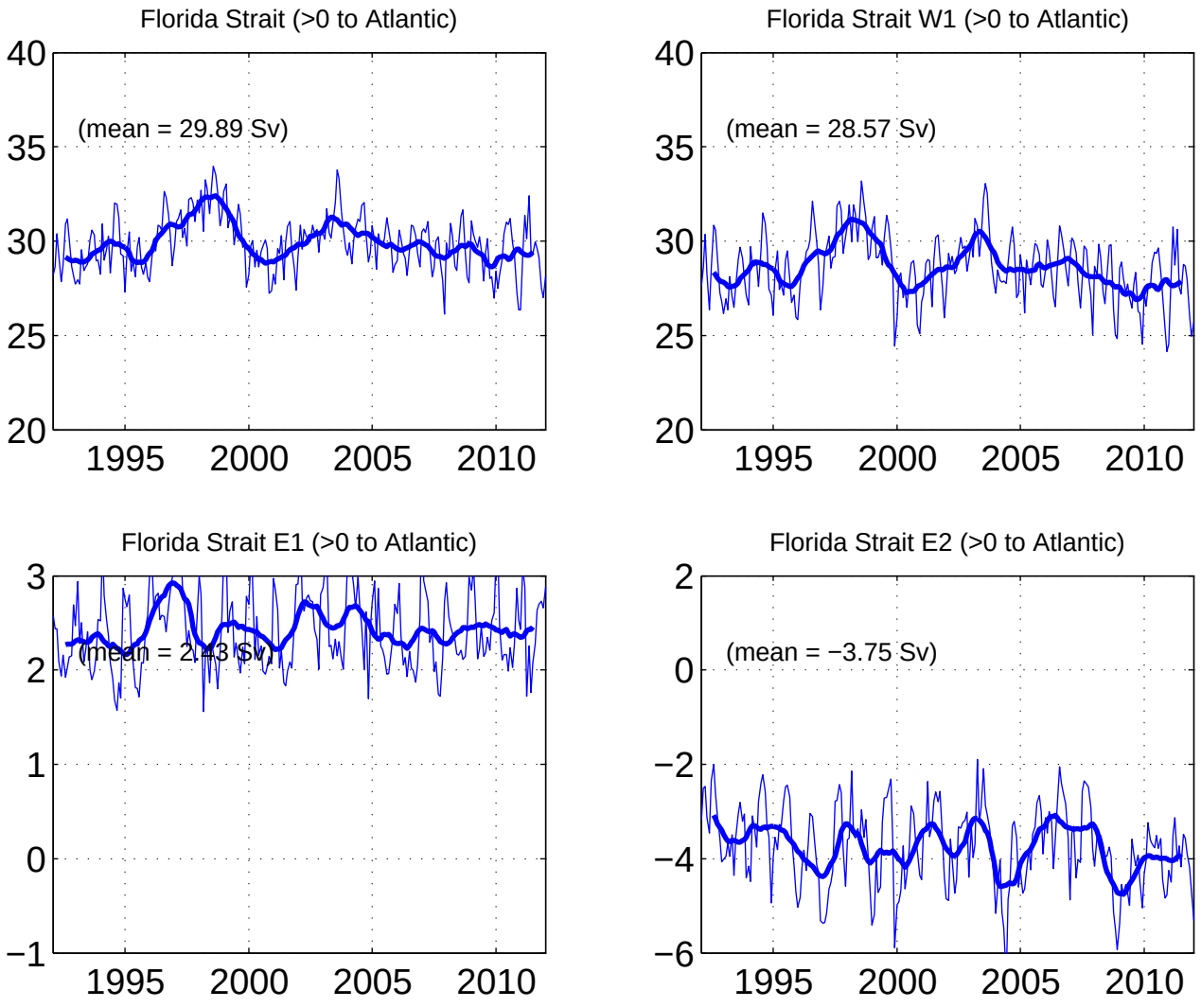

Figure : volume transports entering the Atlantic (Sv, annual mean)

transects transport

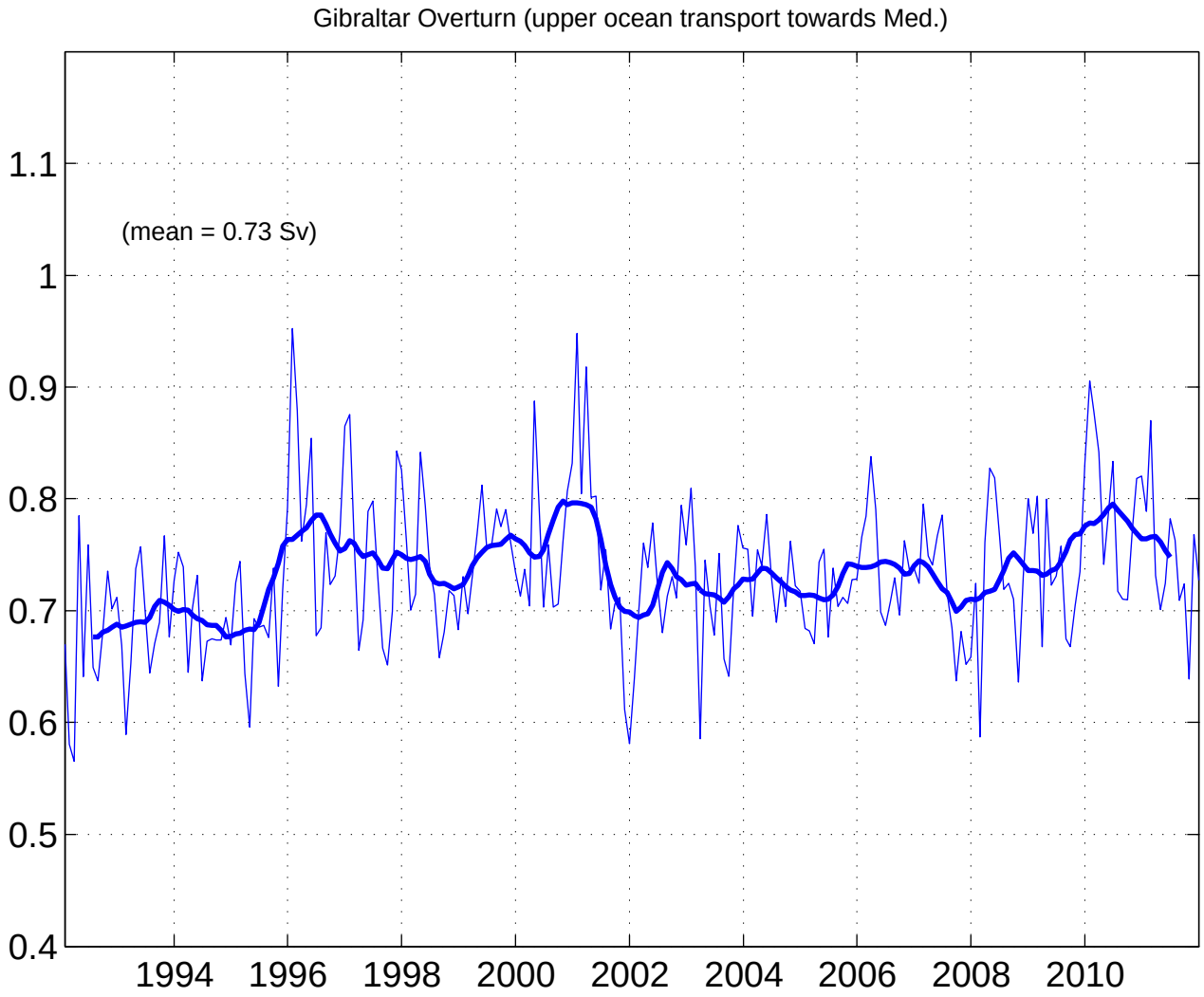

Figure : Gibraltar Overturn (Sv, annual mean)

transects transport

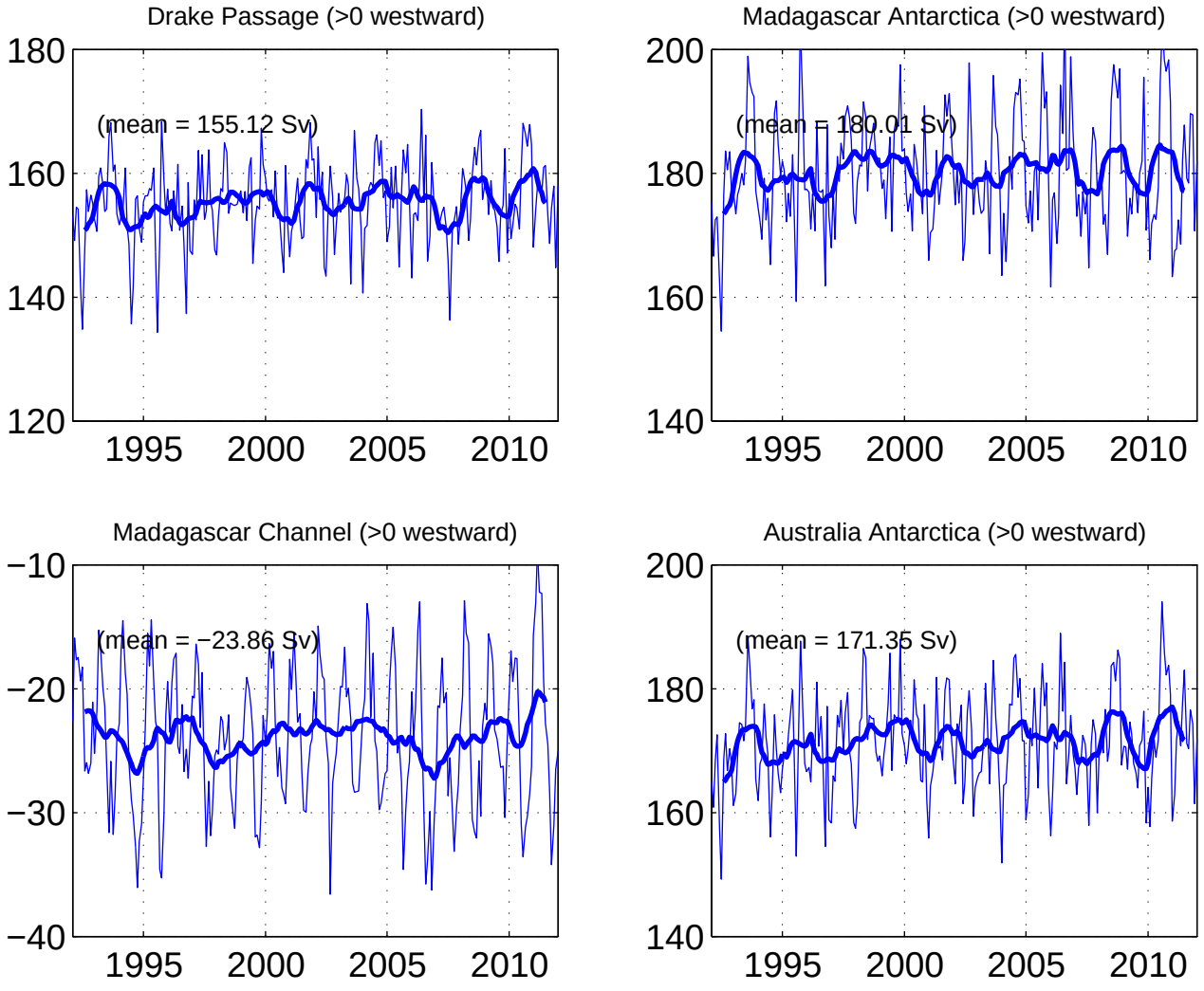

Figure : ACC volume transports (Sv, annual mean)

transects transport

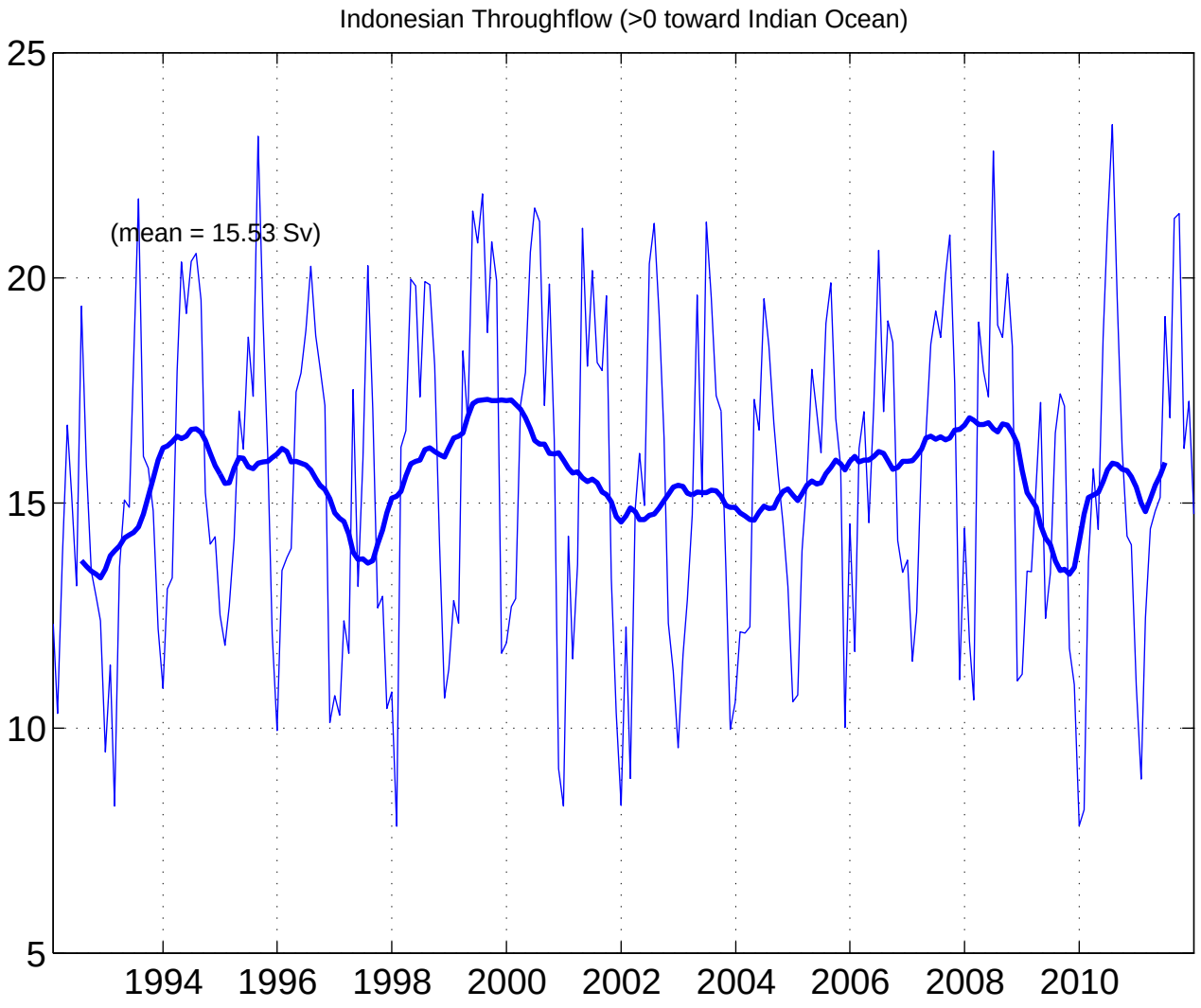

Figure : Indonesian Throughflow (Sv, annual mean)

sea surface height

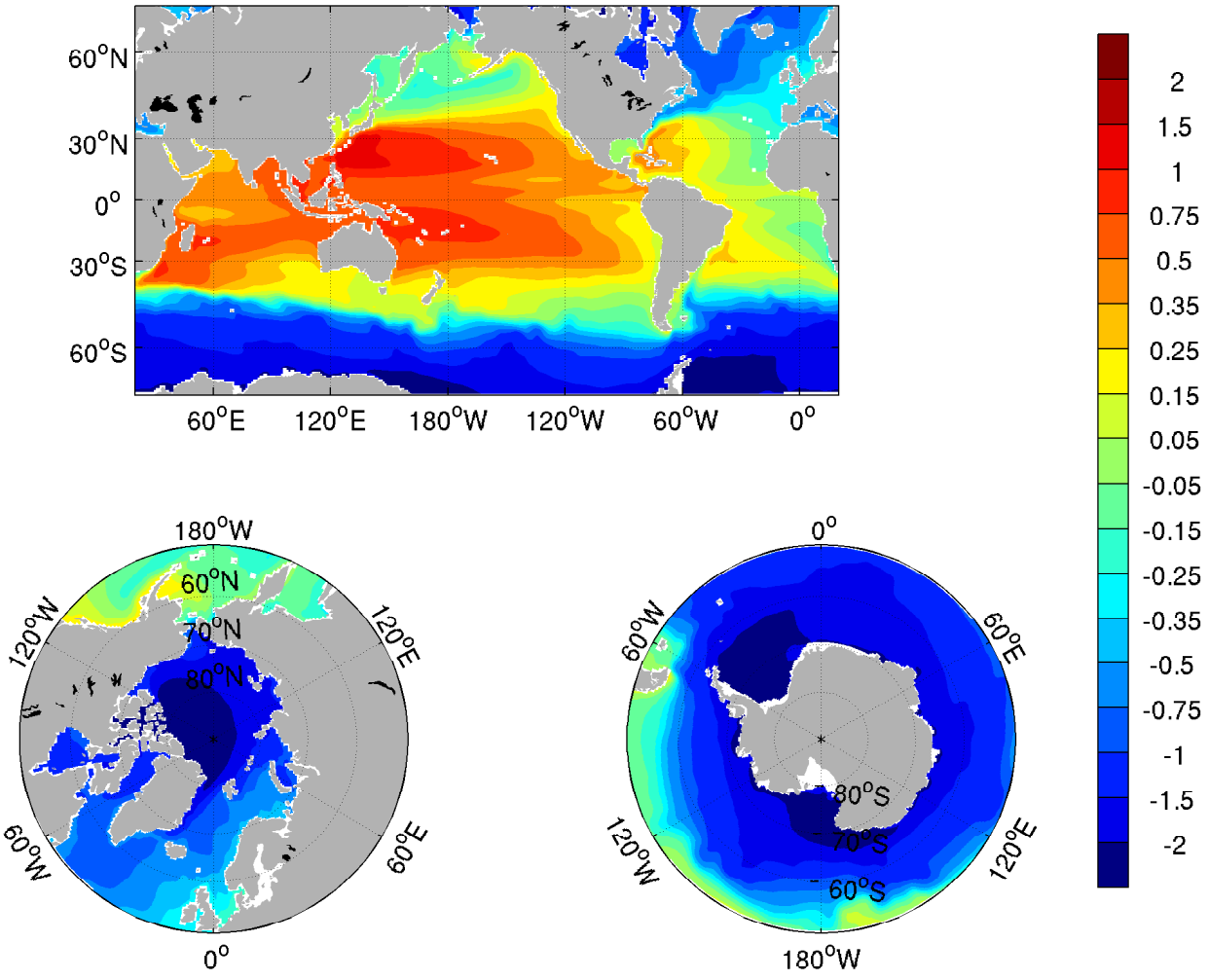

Figure : 1992-2011 mean – sea surface height (EXCLUDING ice, in m)

sea surface height

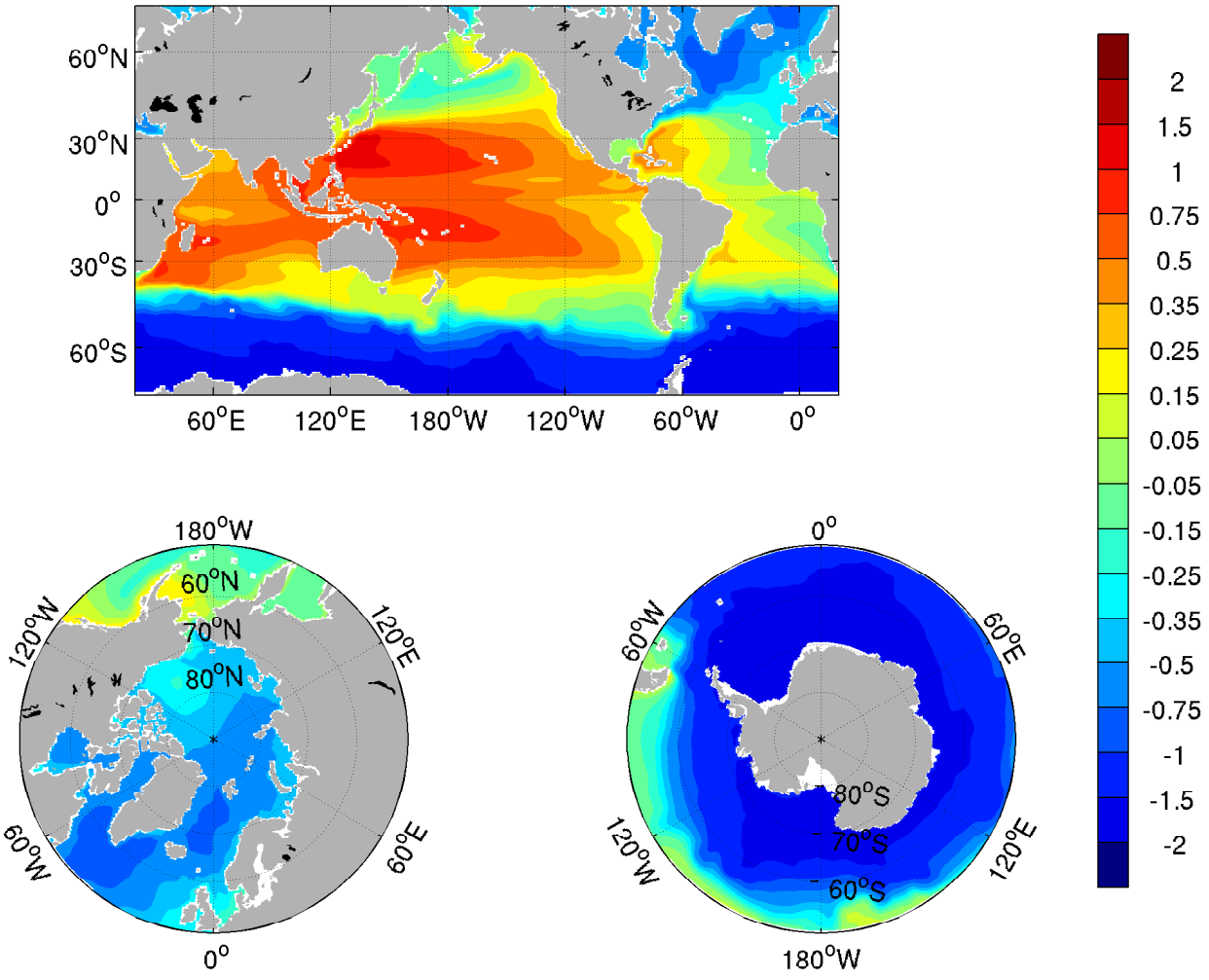

Figure : 1992-2011 mean – sea surface height (INCLUDING ice, in m)

sea surface height

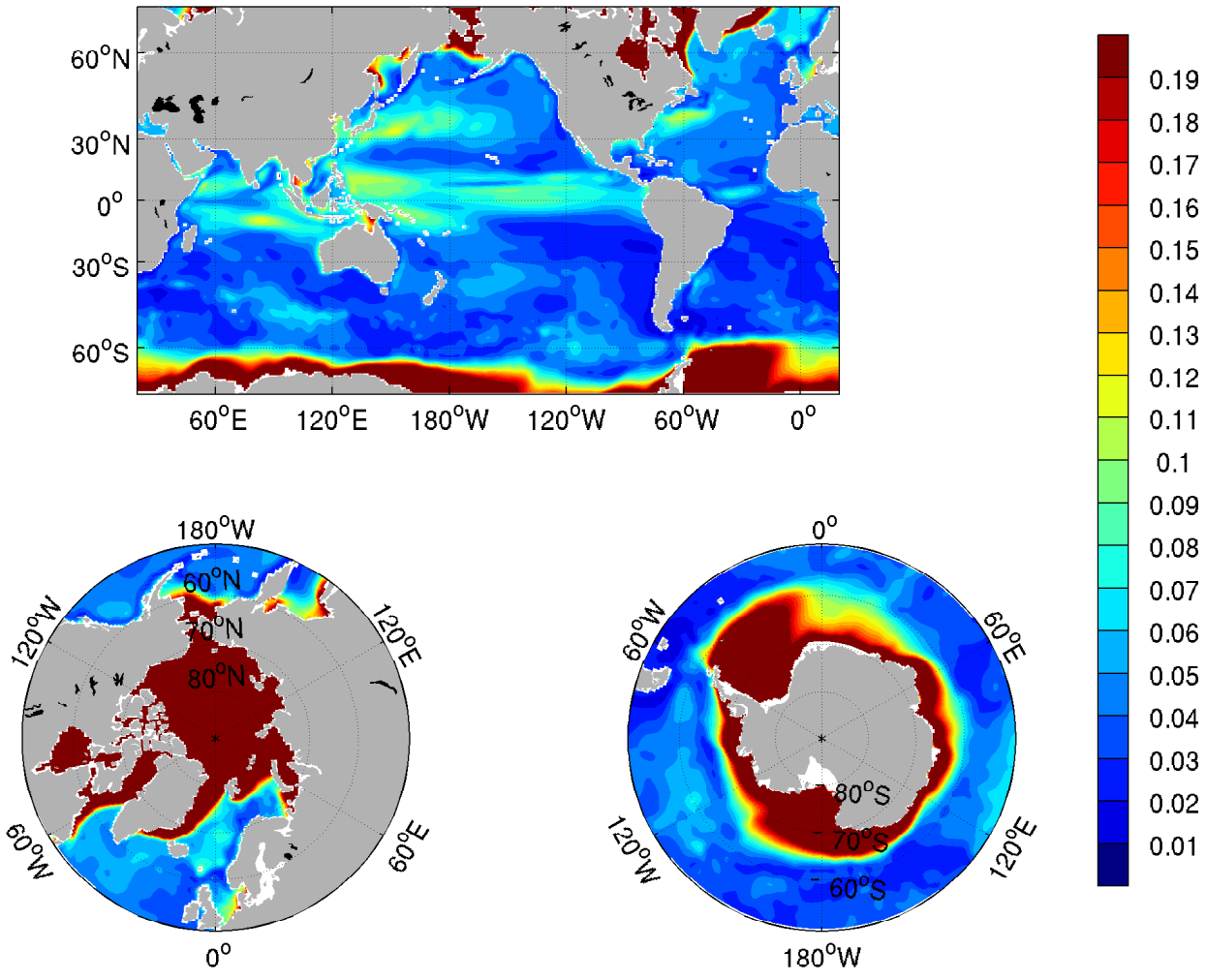

Figure : 1992-2011 standard deviation – sea surface height (EXCLUDING ice, in m)

sea surface height

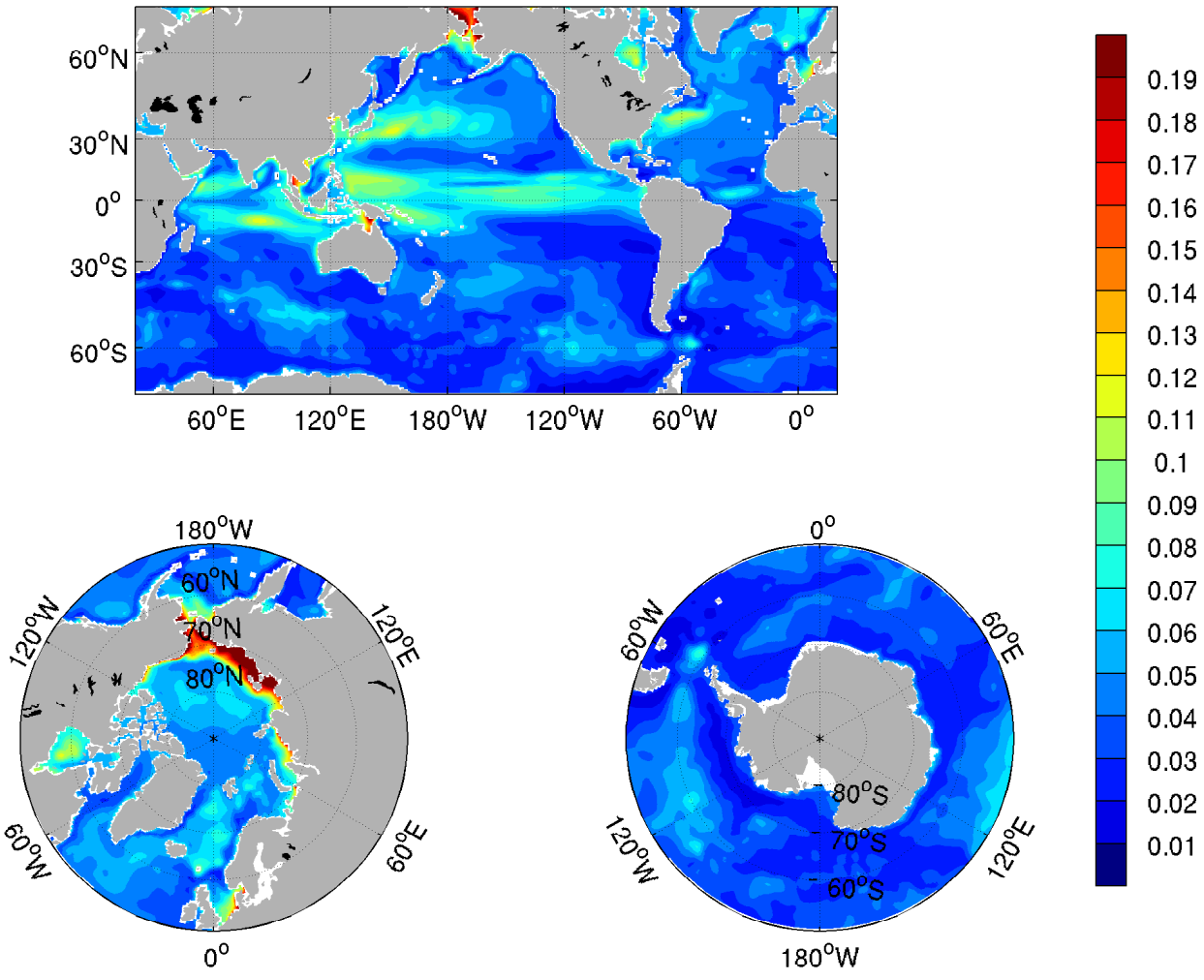

Figure : 1992-2011 standard deviation – sea surface height (INCLUDING ice, in m)

3D state variables

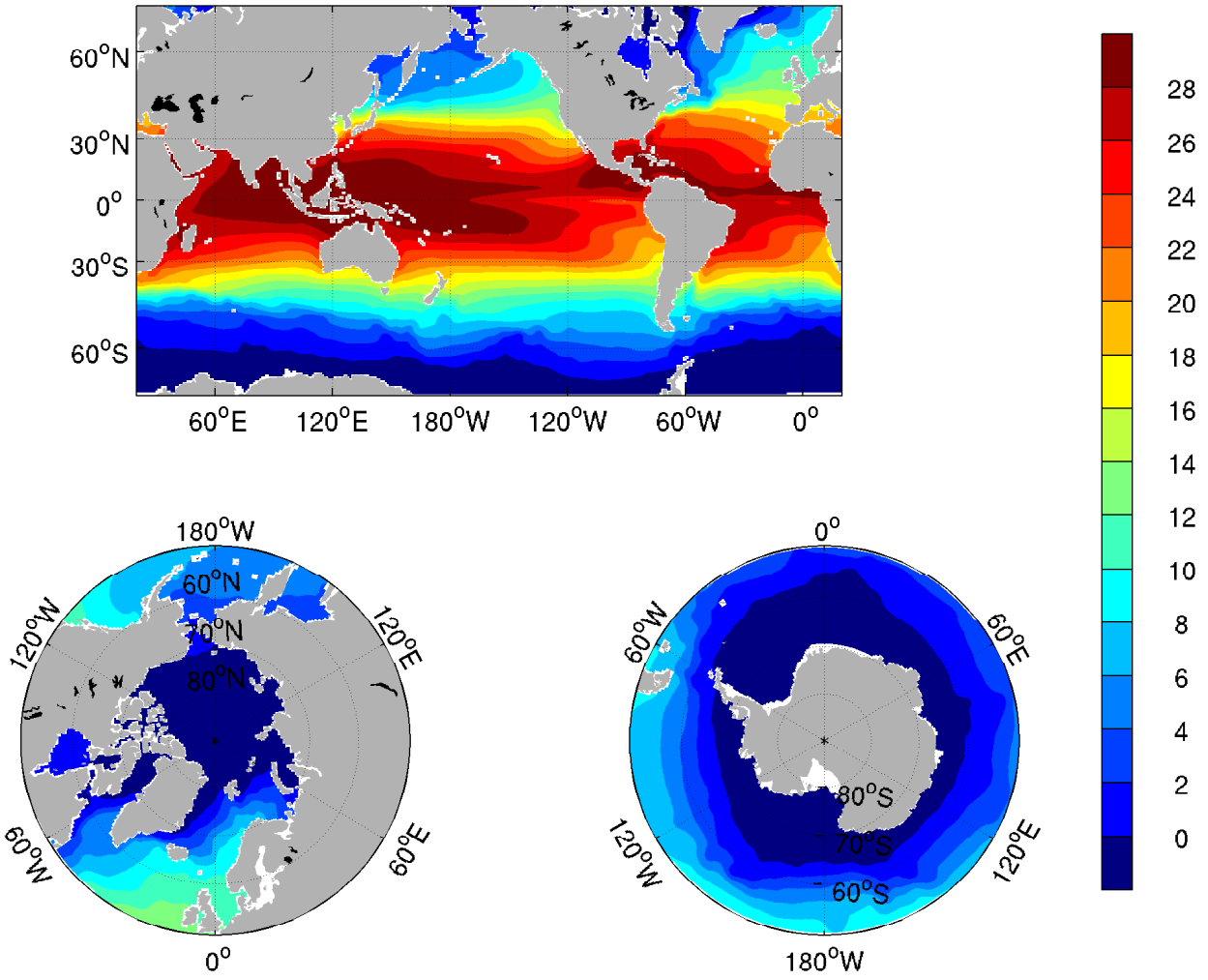

Figure : 1992-2011 mean – temperature (in degC) at 5m

3D state variables

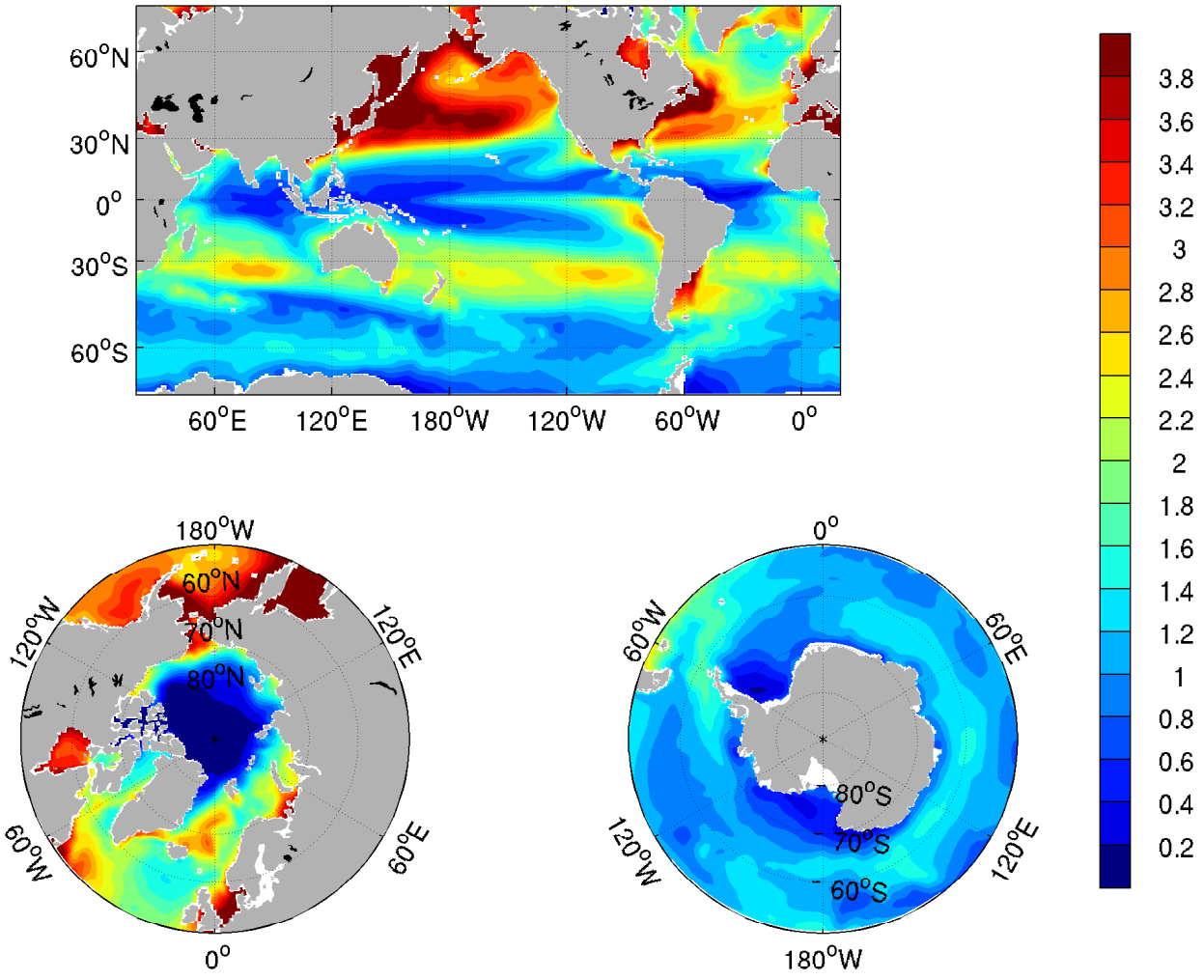

Figure : 1992-2011 standard deviation – temperature (in degC) at 5m

3D state variables

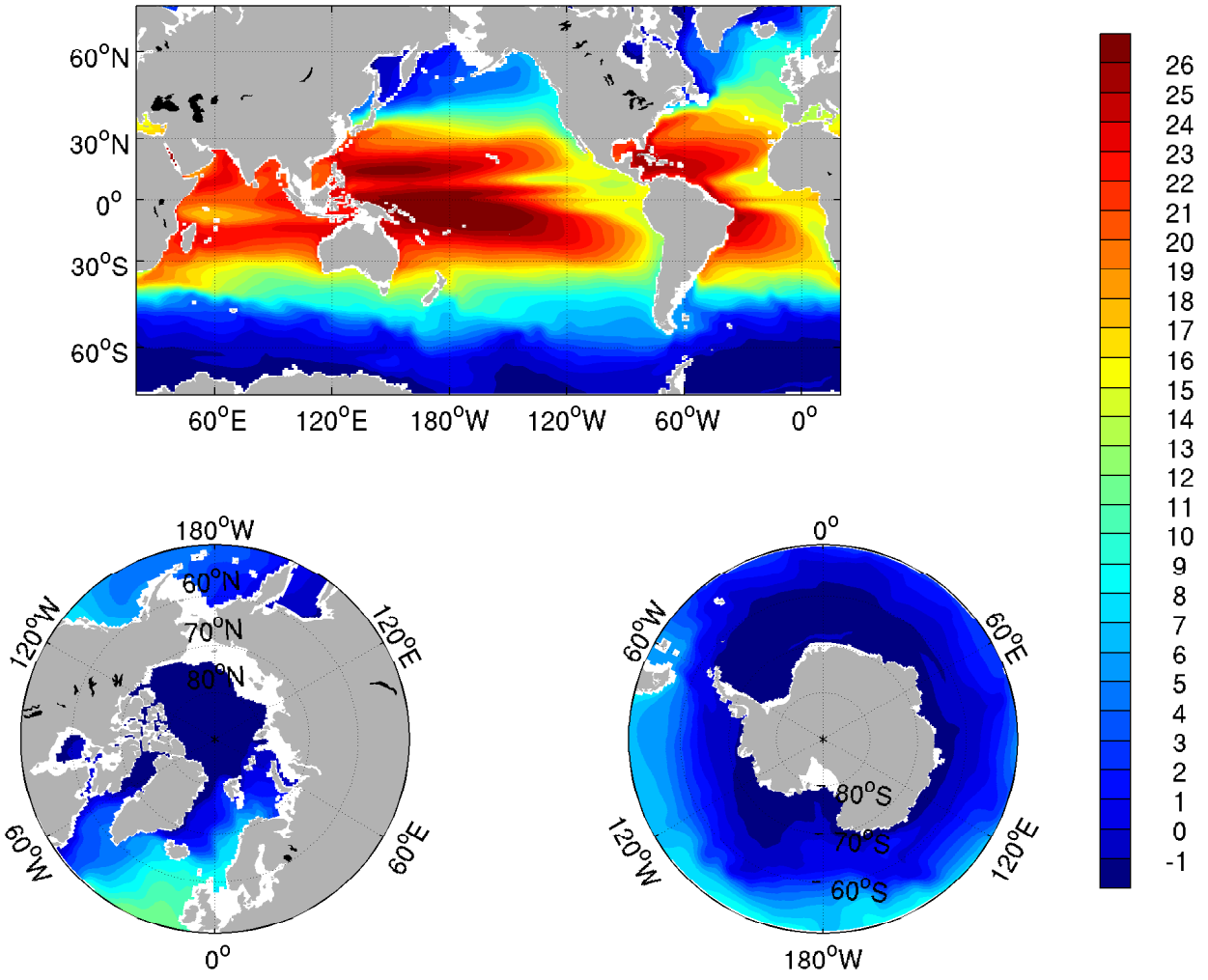

Figure : 1992-2011 mean – temperature (in degC) at 105m

3D state variables

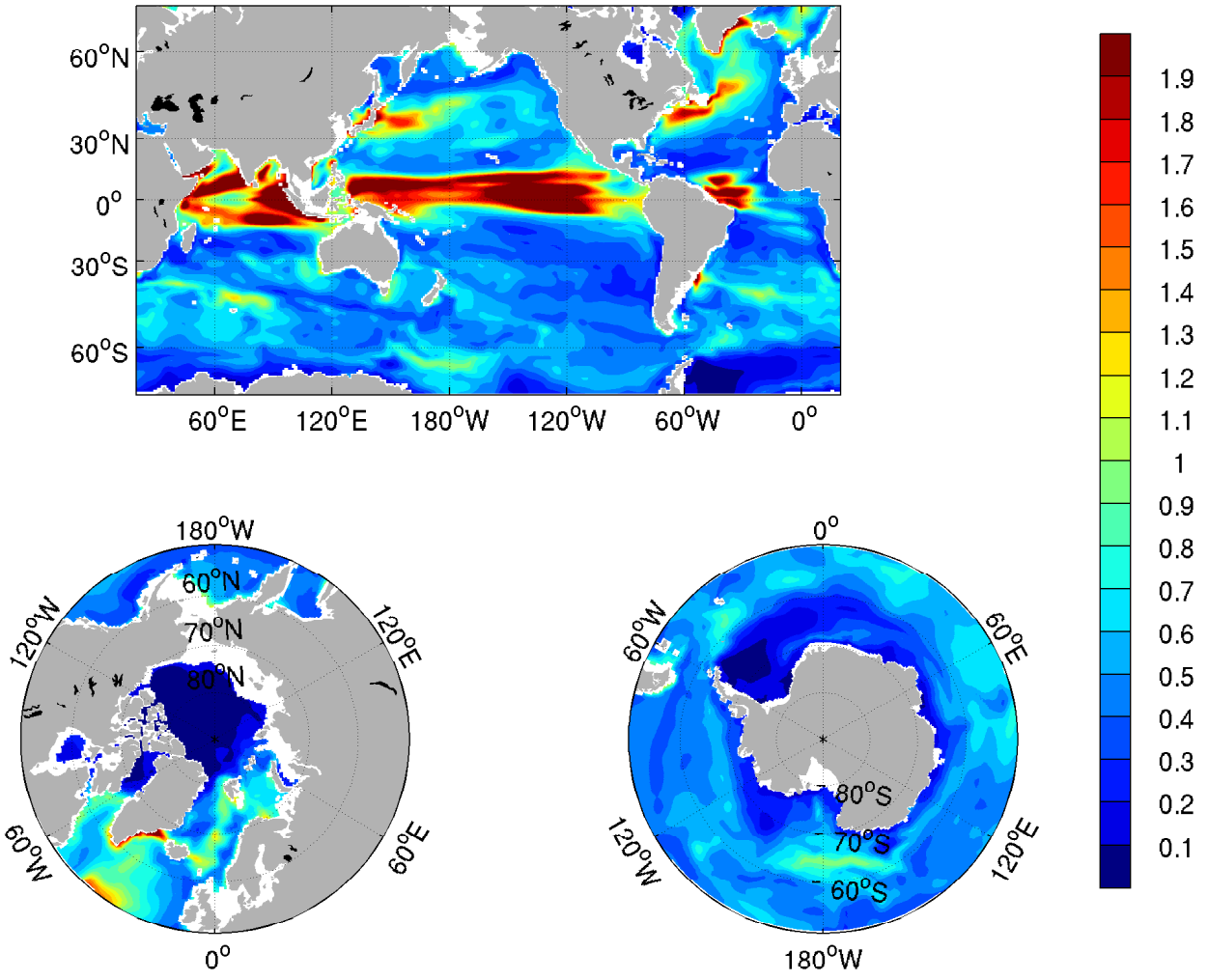

Figure : 1992-2011 standard deviation – temperature (in degC) at 105m

3D state variables

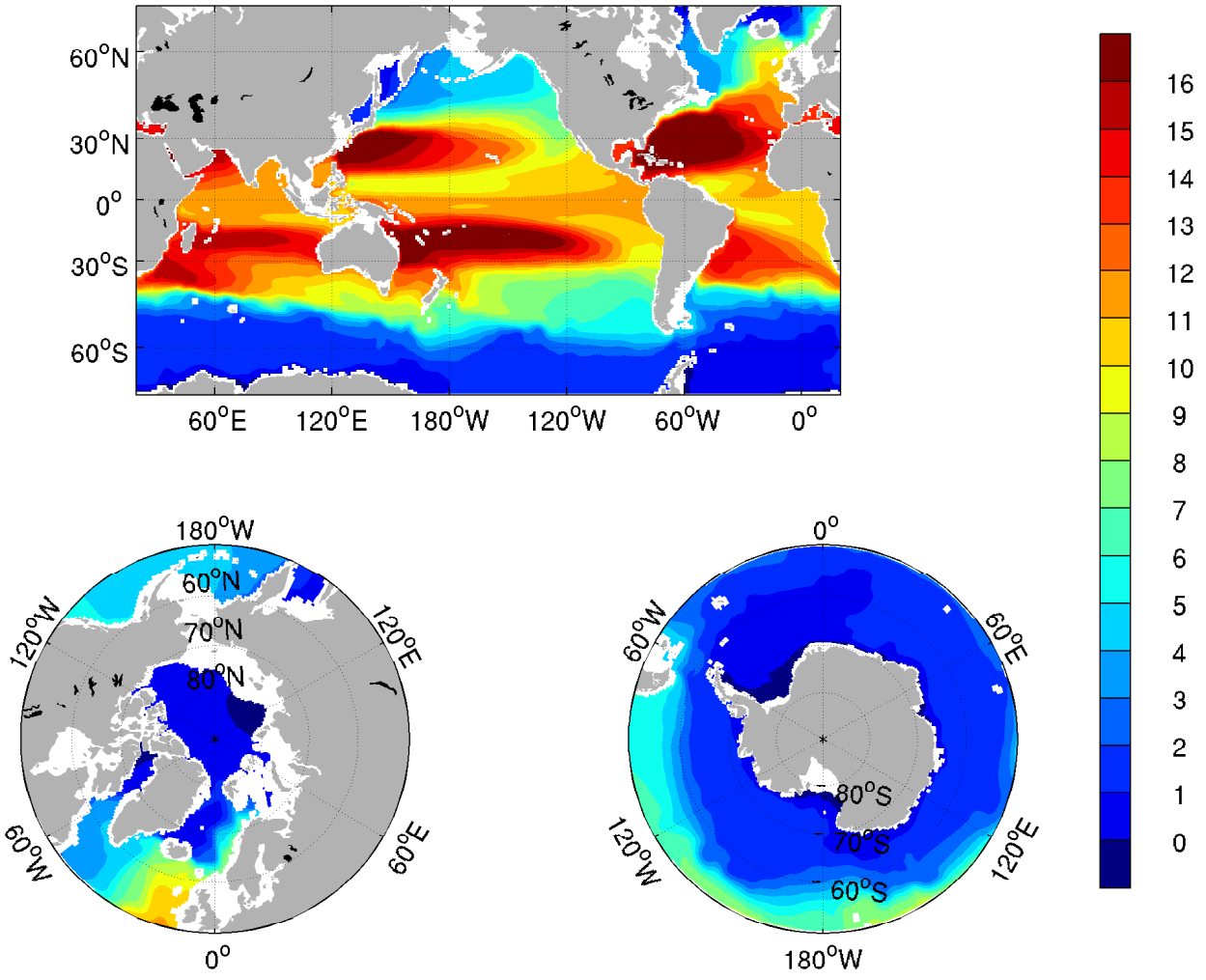

Figure : 1992-2011 mean – temperature (in degC) at 300m

3D state variables

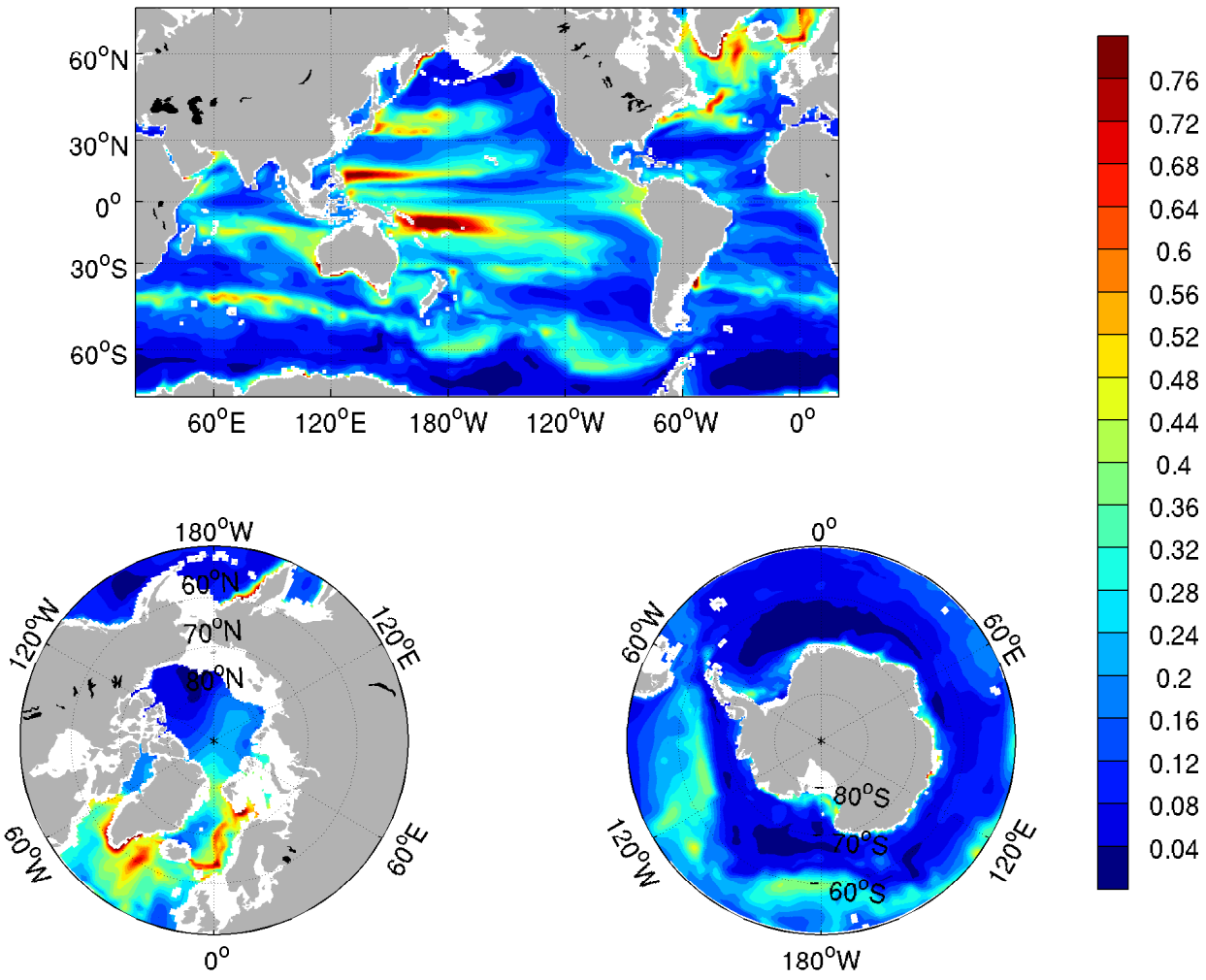

Figure : 1992-2011 standard deviation – temperature (in degC) at 300m

3D state variables

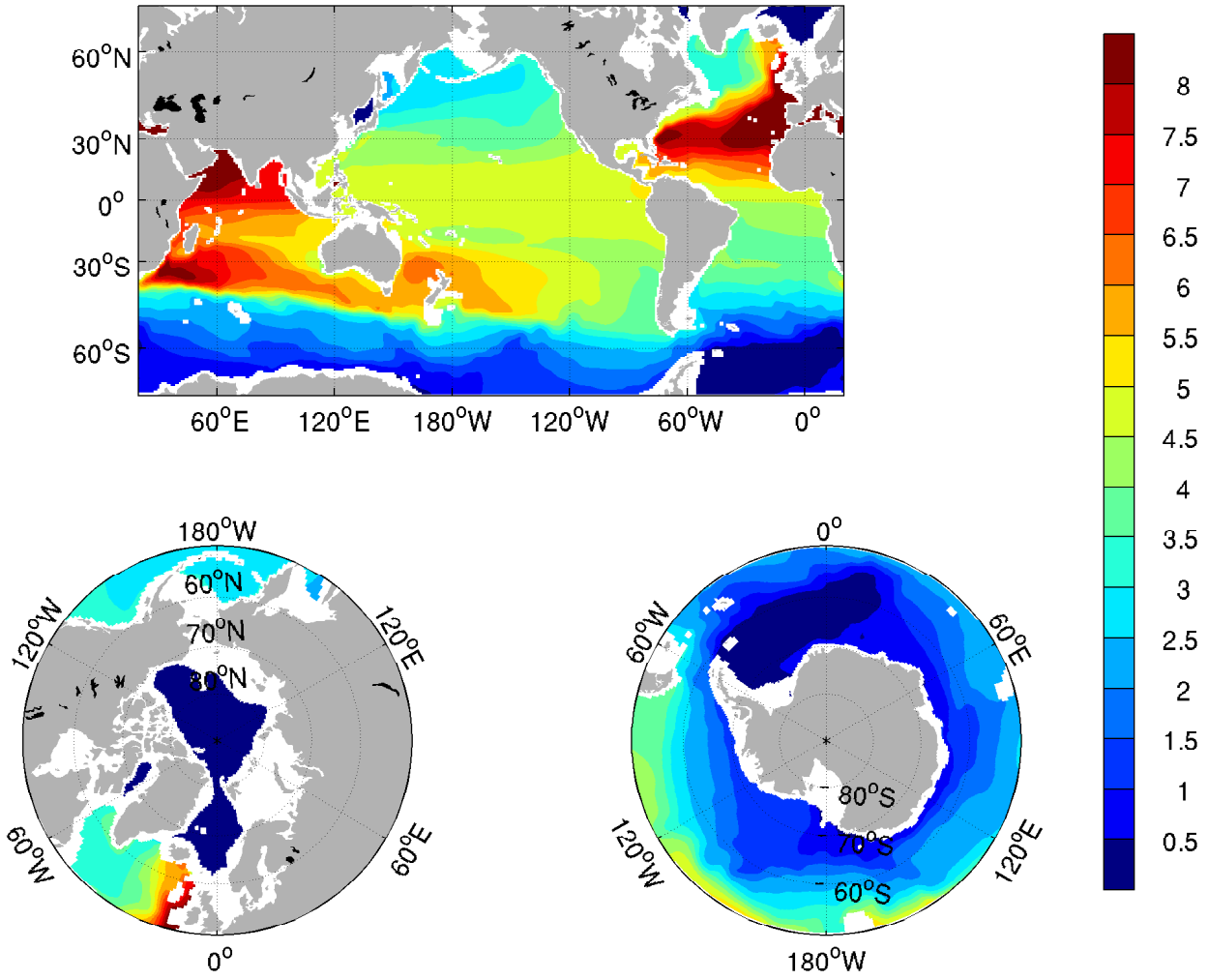

Figure : 1992-2011 mean – temperature (in degC) at 910m

3D state variables

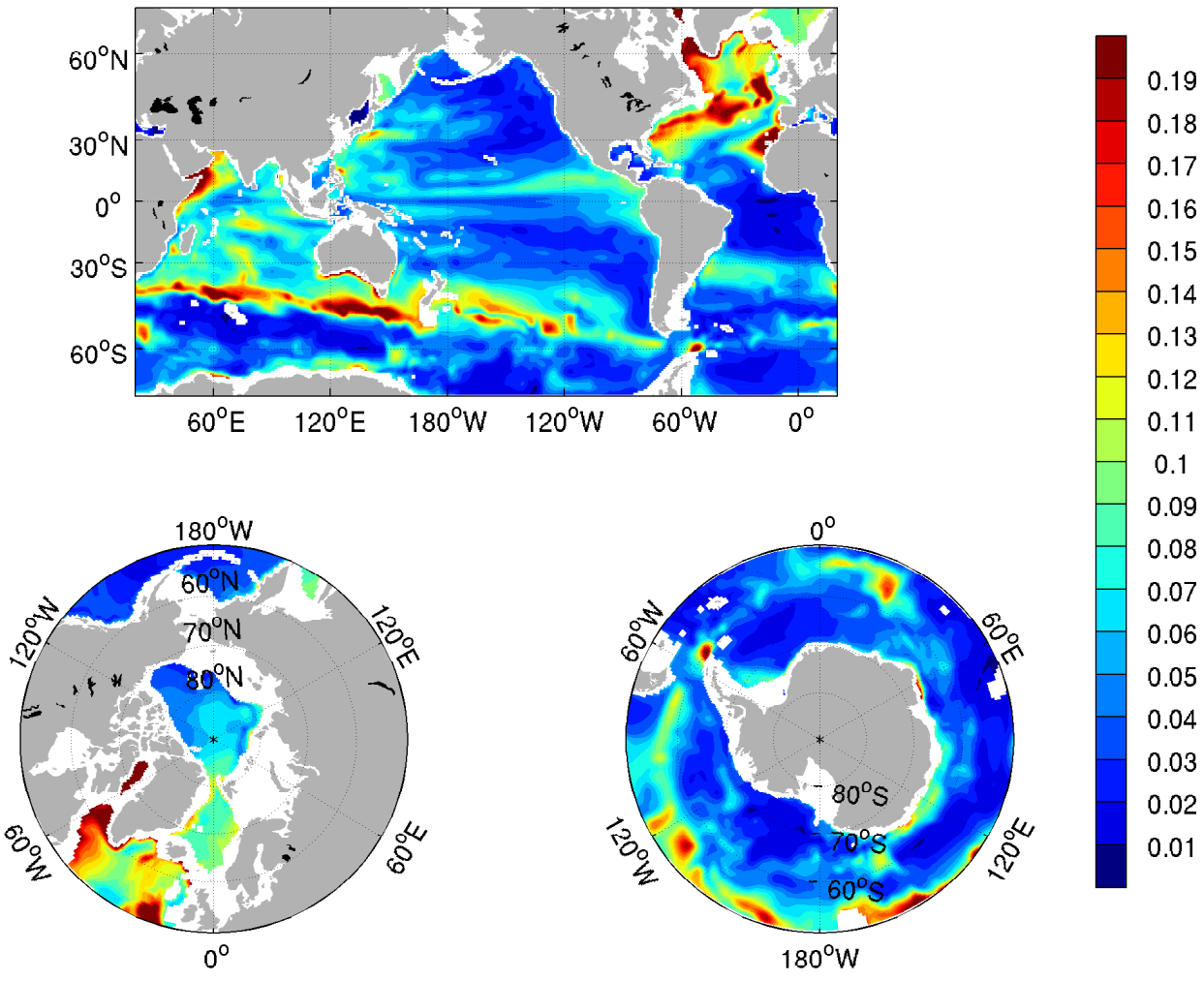

Figure : 1992-2011 standard deviation – temperature (in degC) at 910m

3D state variables

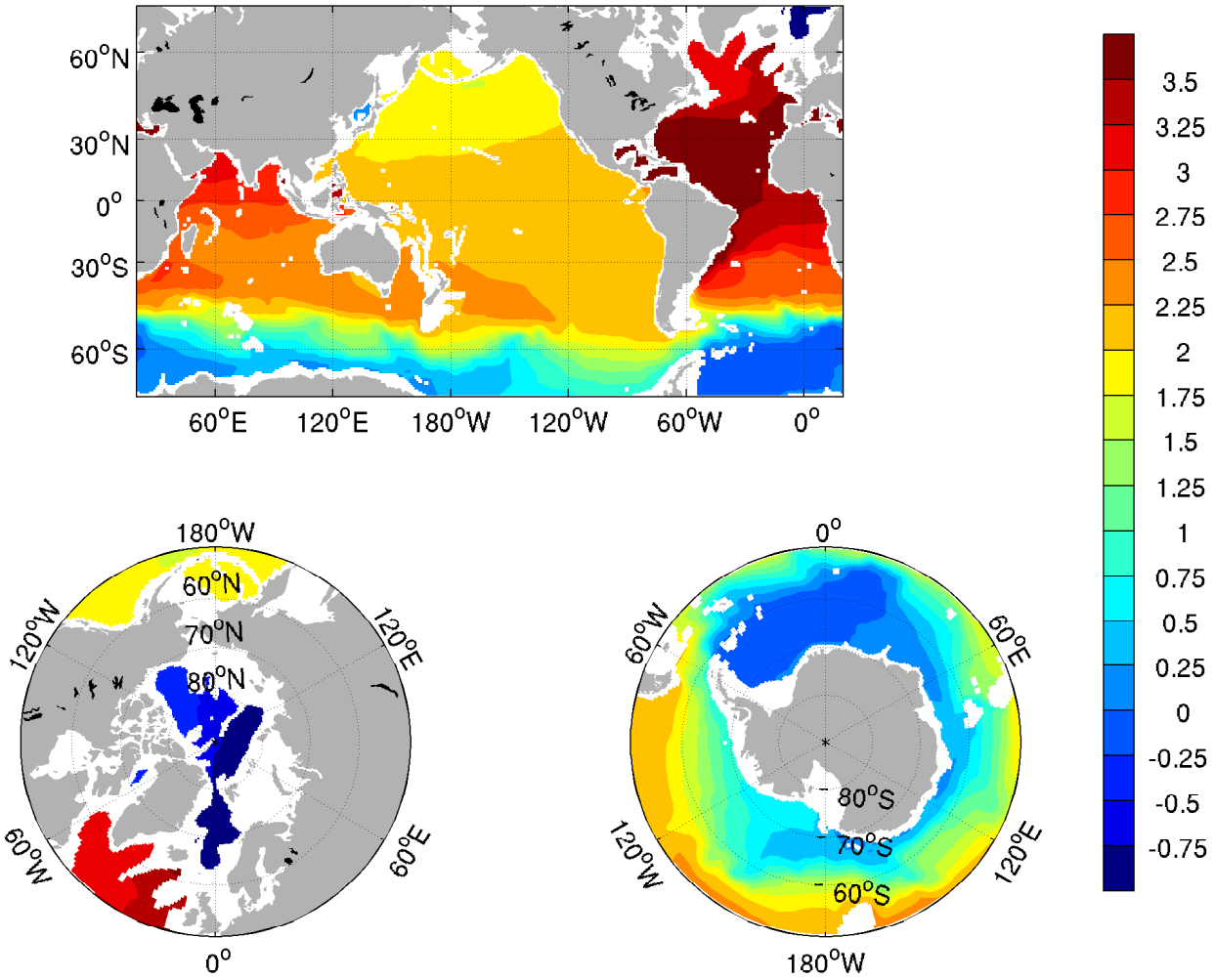

Figure : 1992-2011 mean – temperature (in degC) at 1914m

3D state variables

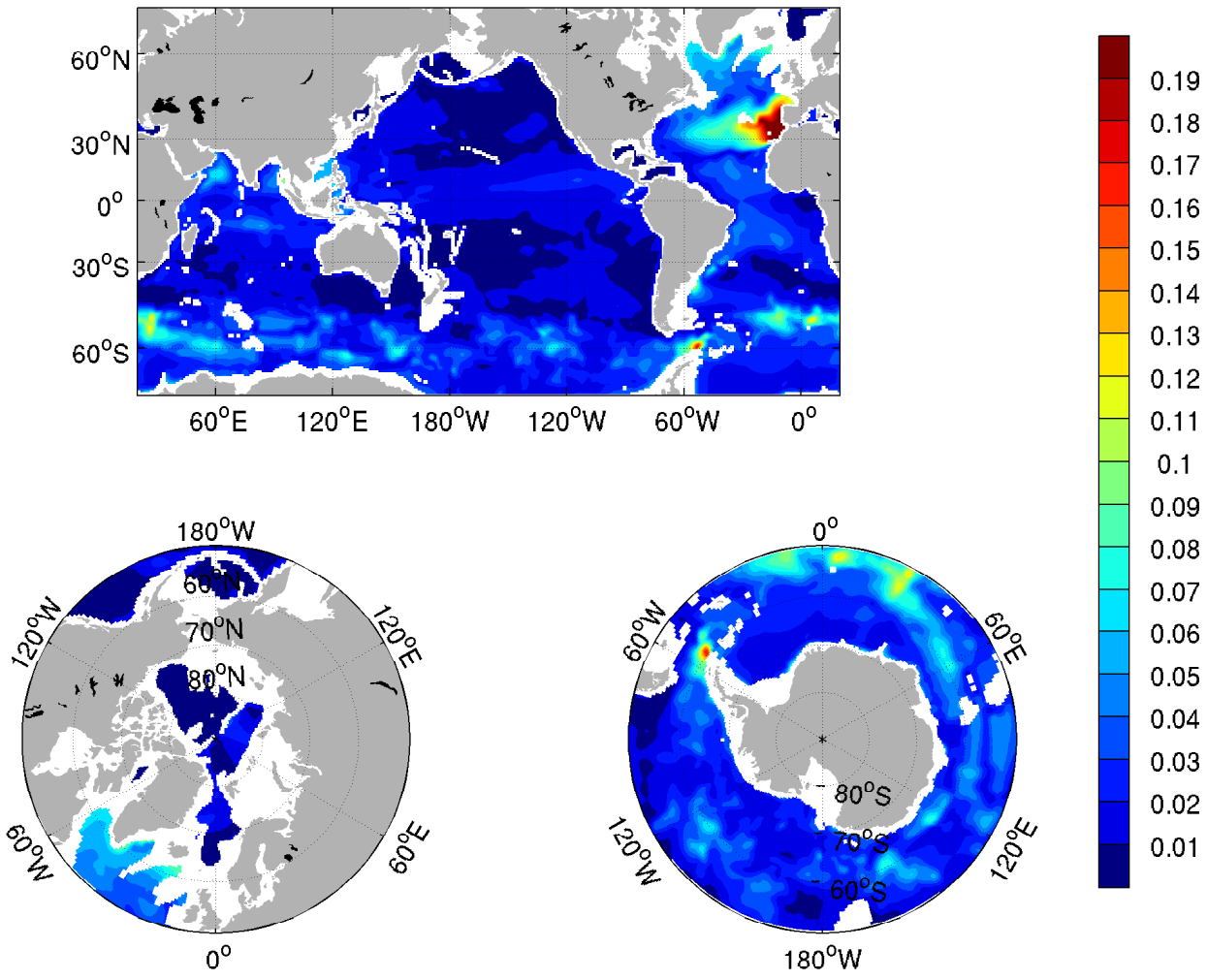

Figure : 1992-2011 standard deviation – temperature (in degC) at 1914m

3D state variables

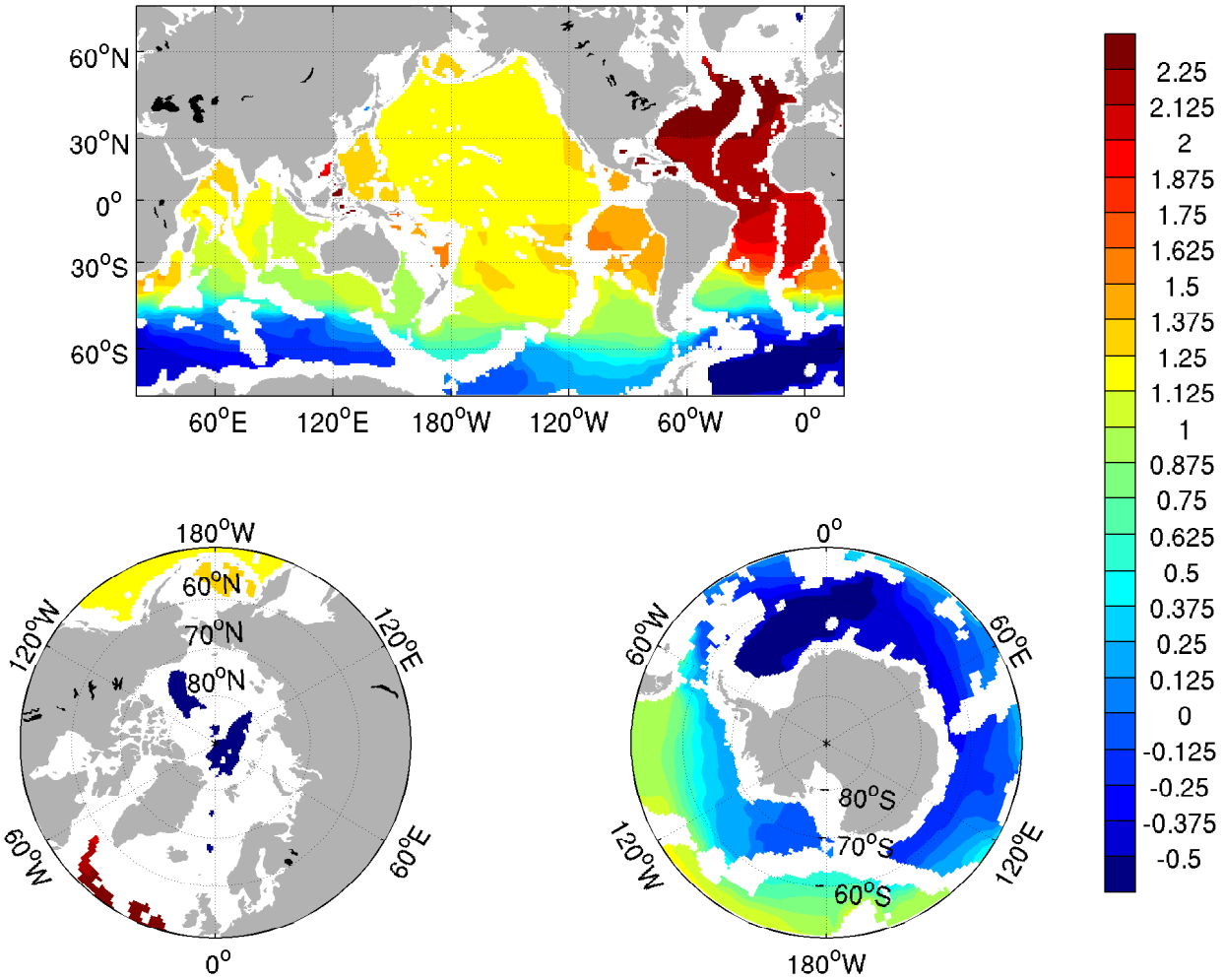

Figure : 1992-2011 mean – temperature (in degC) at 3581m

3D state variables

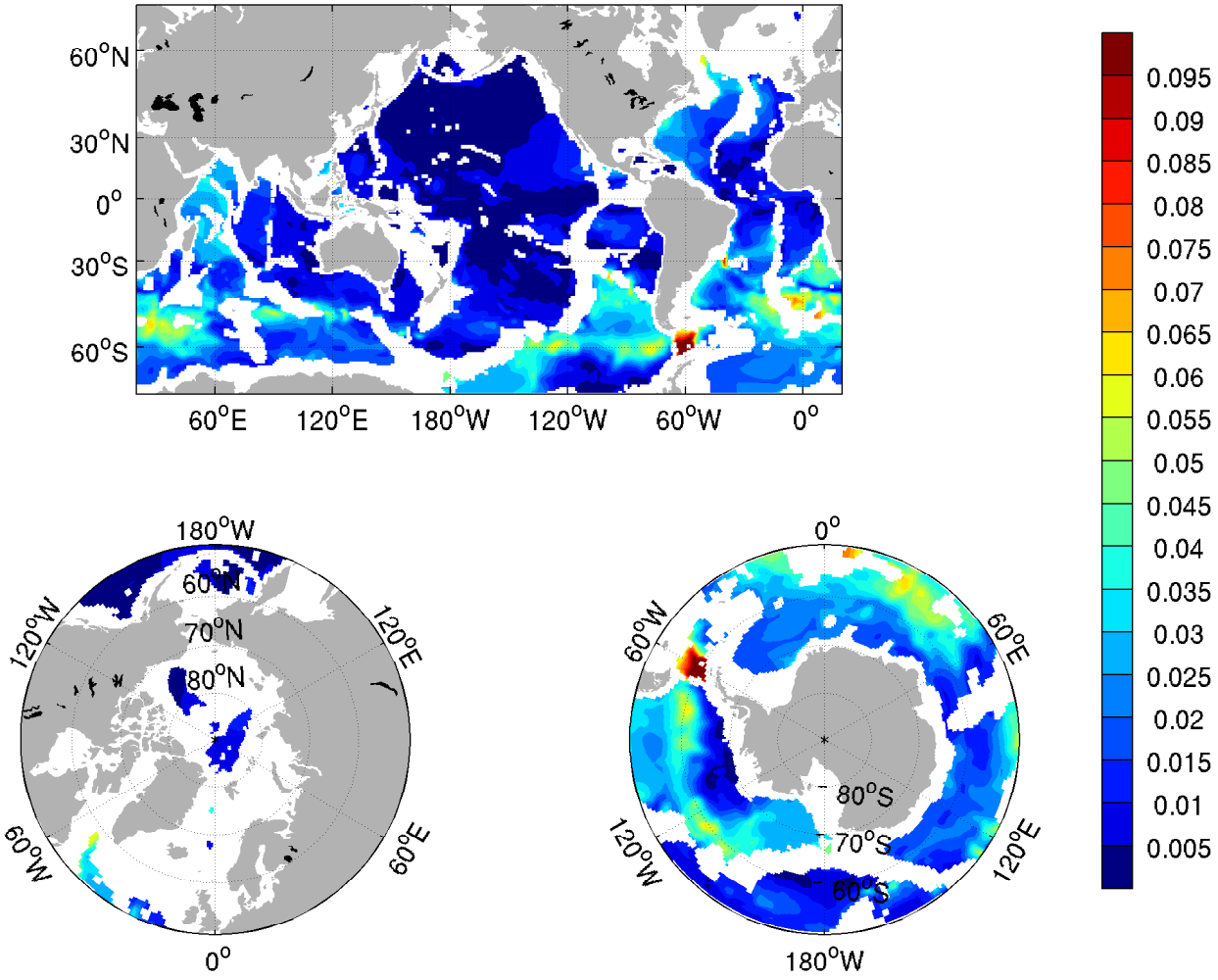

Figure : 1992-2011 standard deviation – temperature (in degC) at 3581m

3D state variables

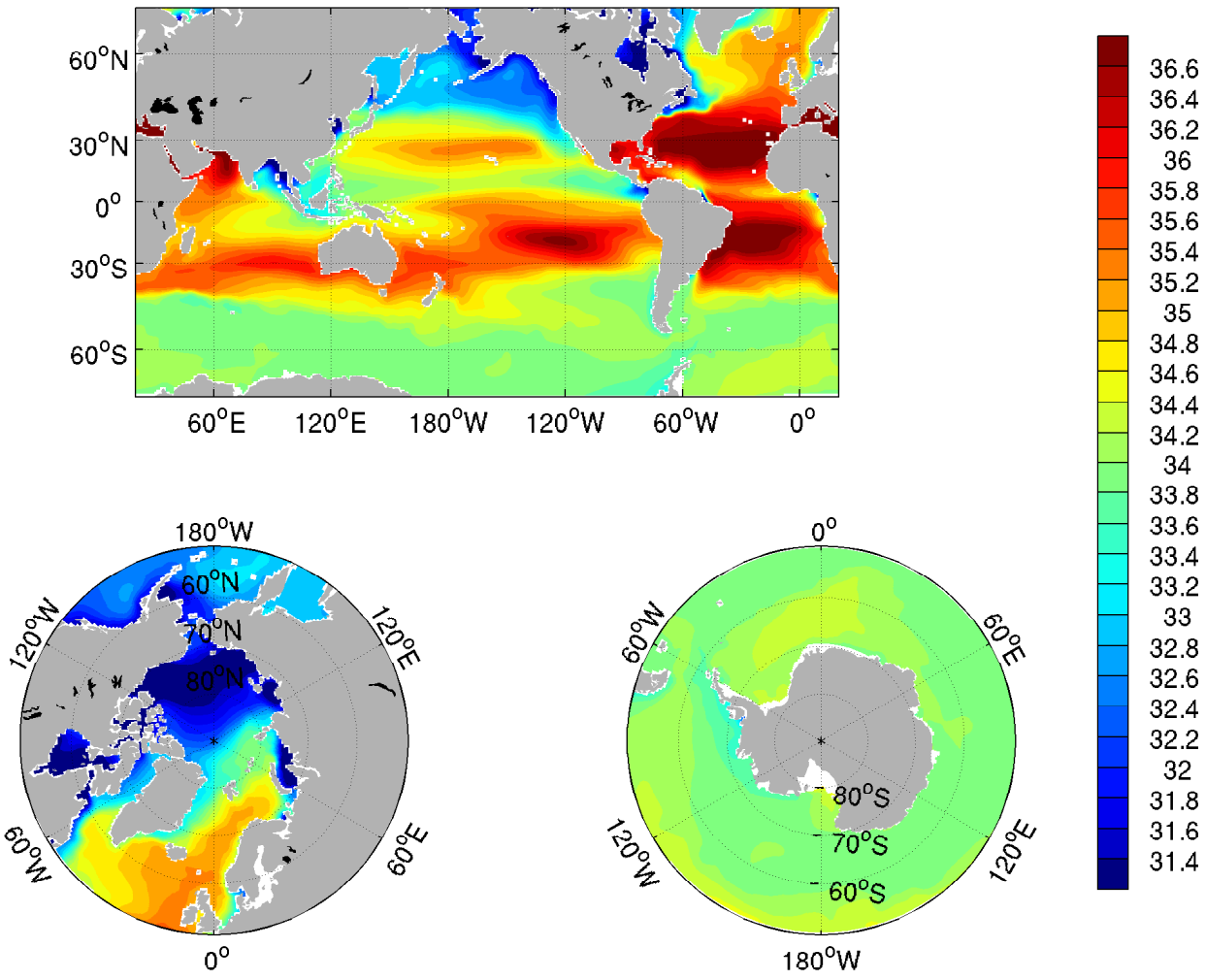

Figure : 1992-2011 mean – salinity (in psu) at 5m

3D state variables

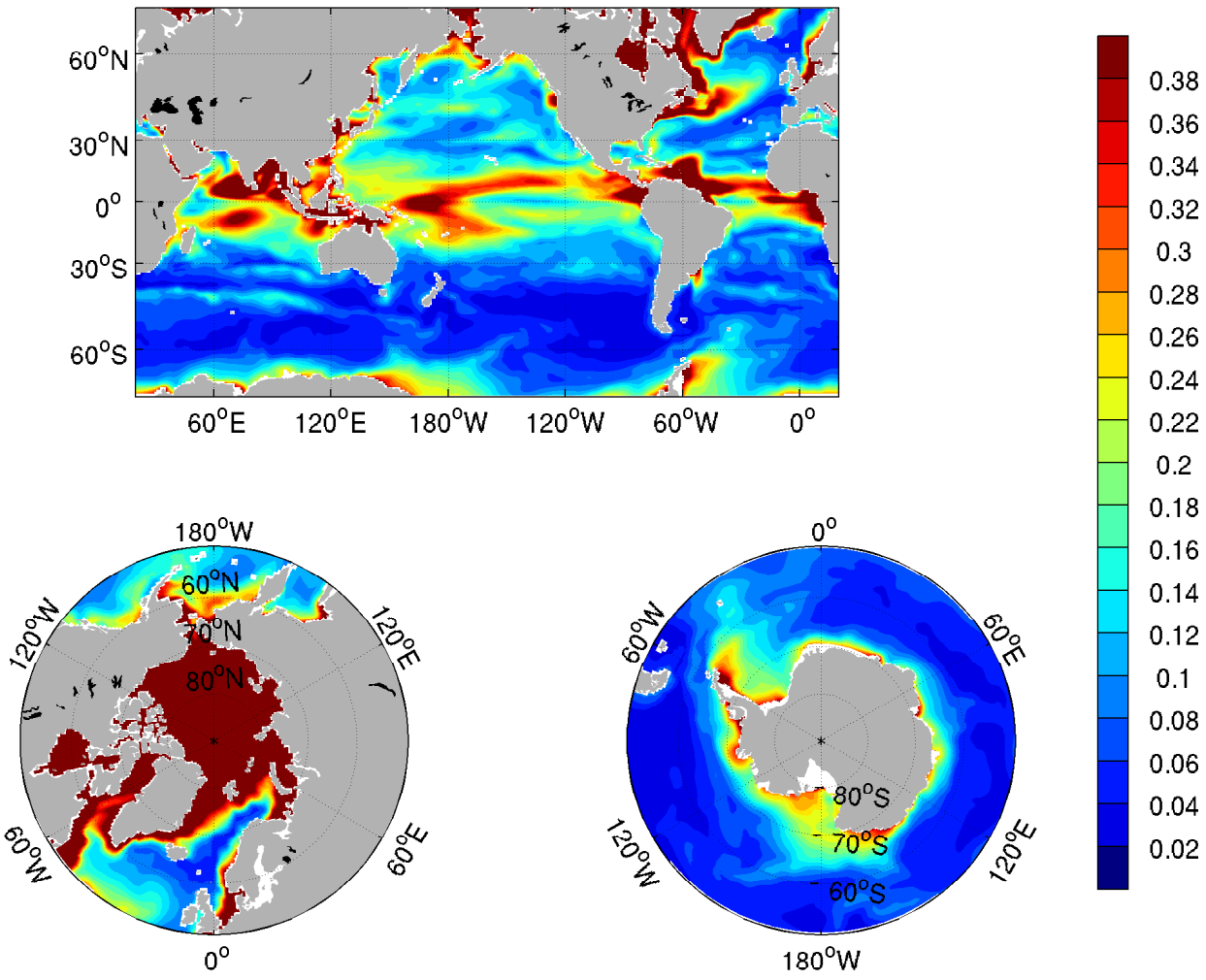

Figure : 1992-2011 standard deviation – salinity (in psu) at 5m

3D state variables

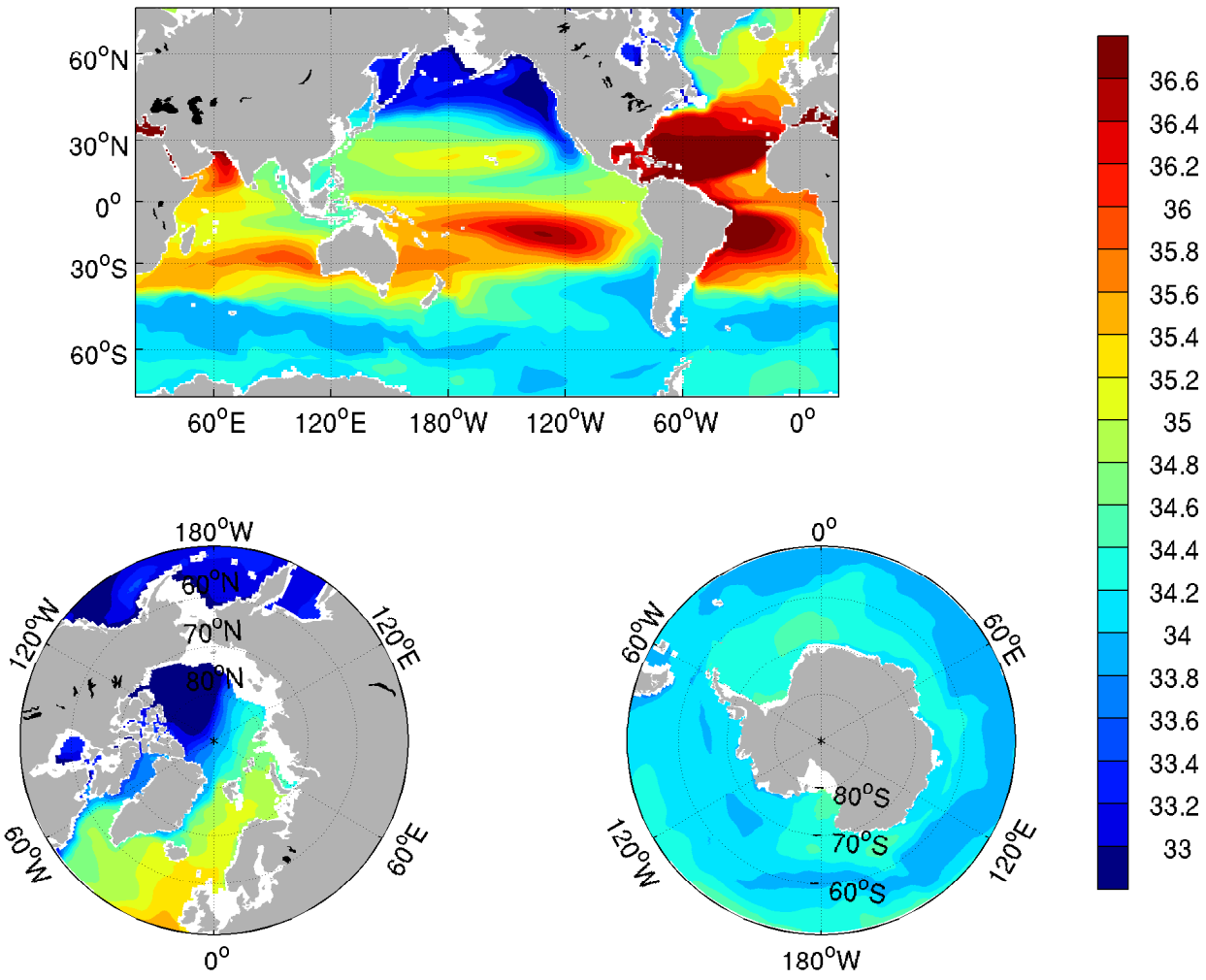

Figure : 1992-2011 mean – salinity (in psu) at 105m

3D state variables

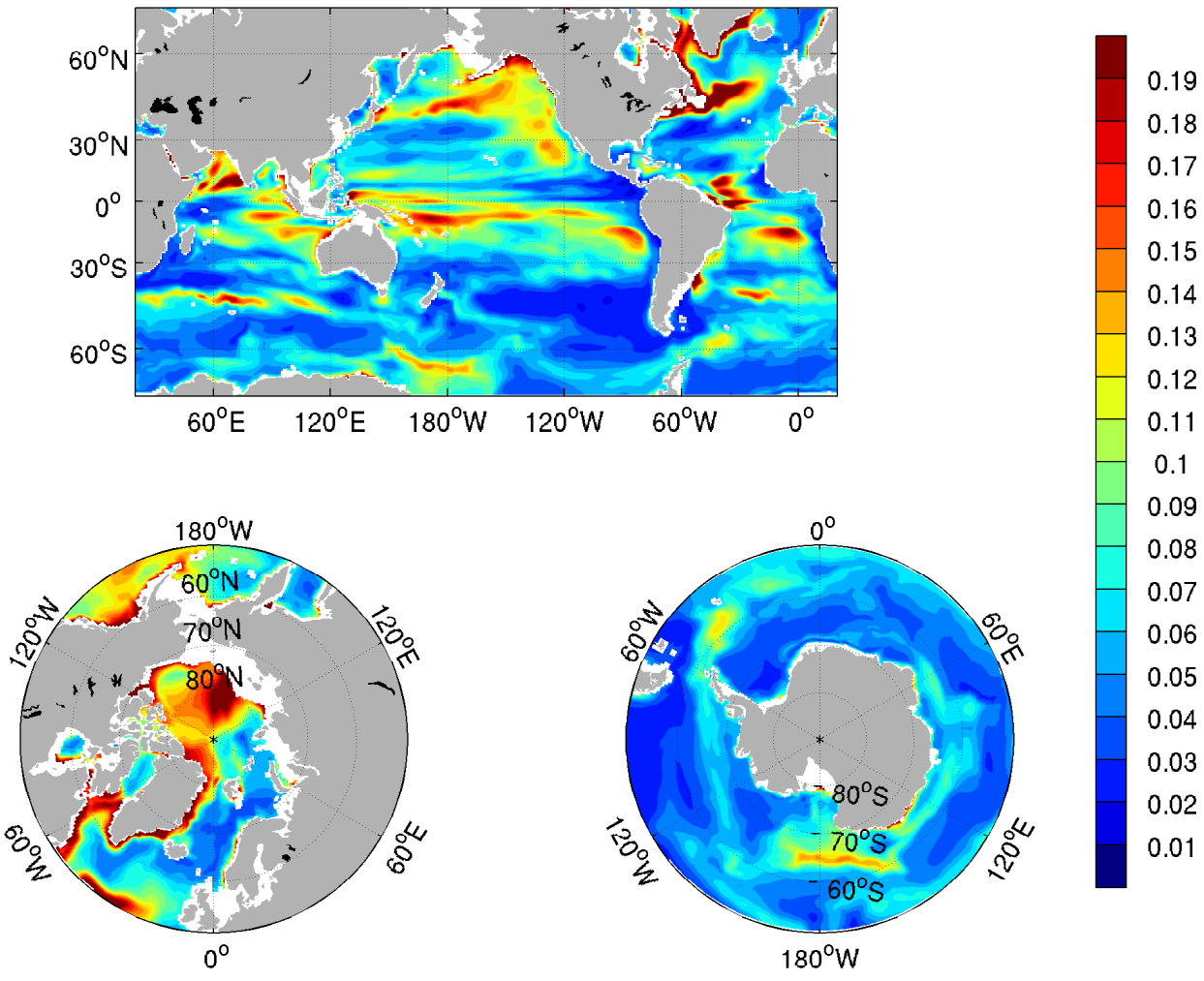

Figure : 1992-2011 standard deviation – salinity (in psu) at 105m

3D state variables

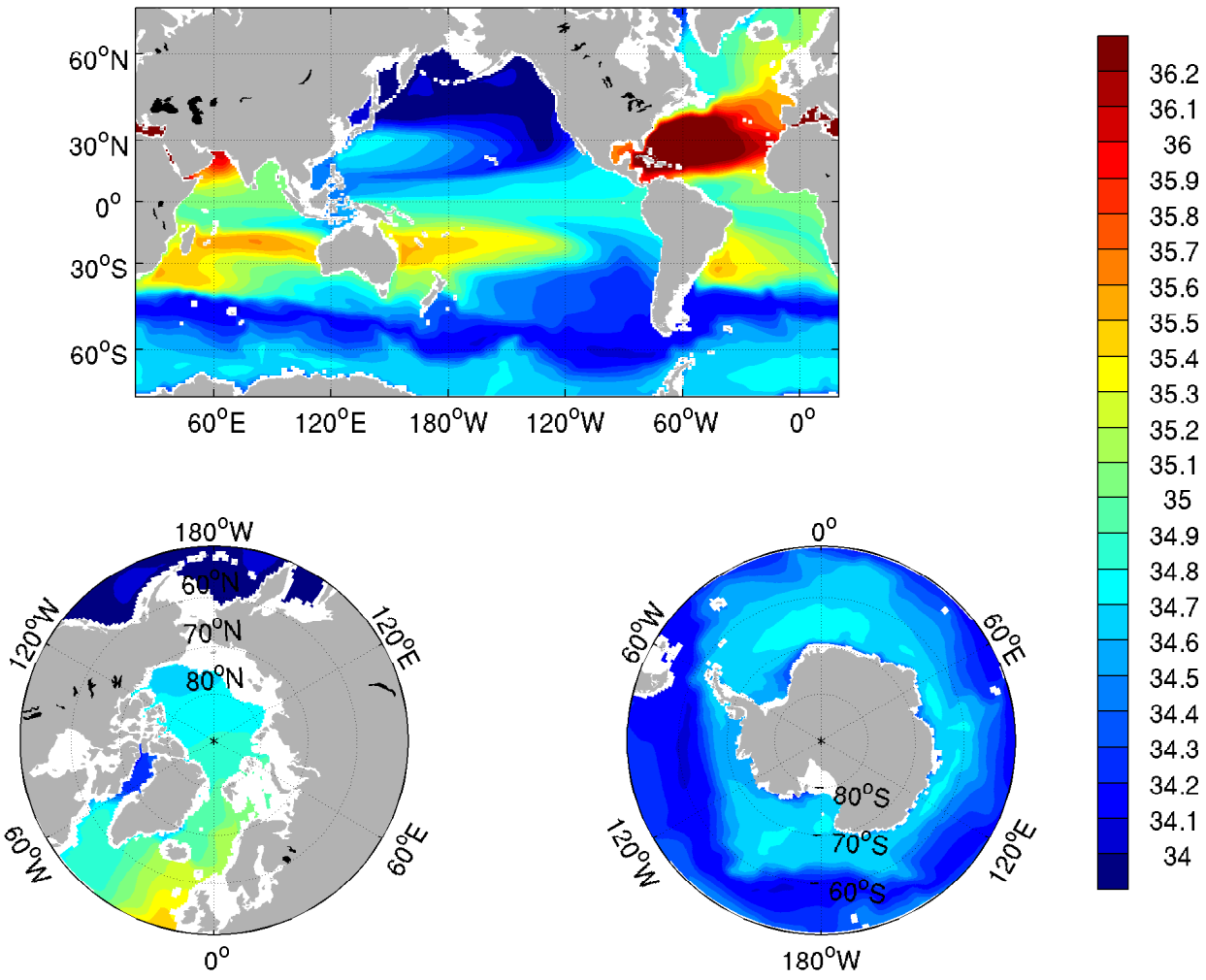

Figure : 1992-2011 mean – salinity (in psu) at 300m

3D state variables

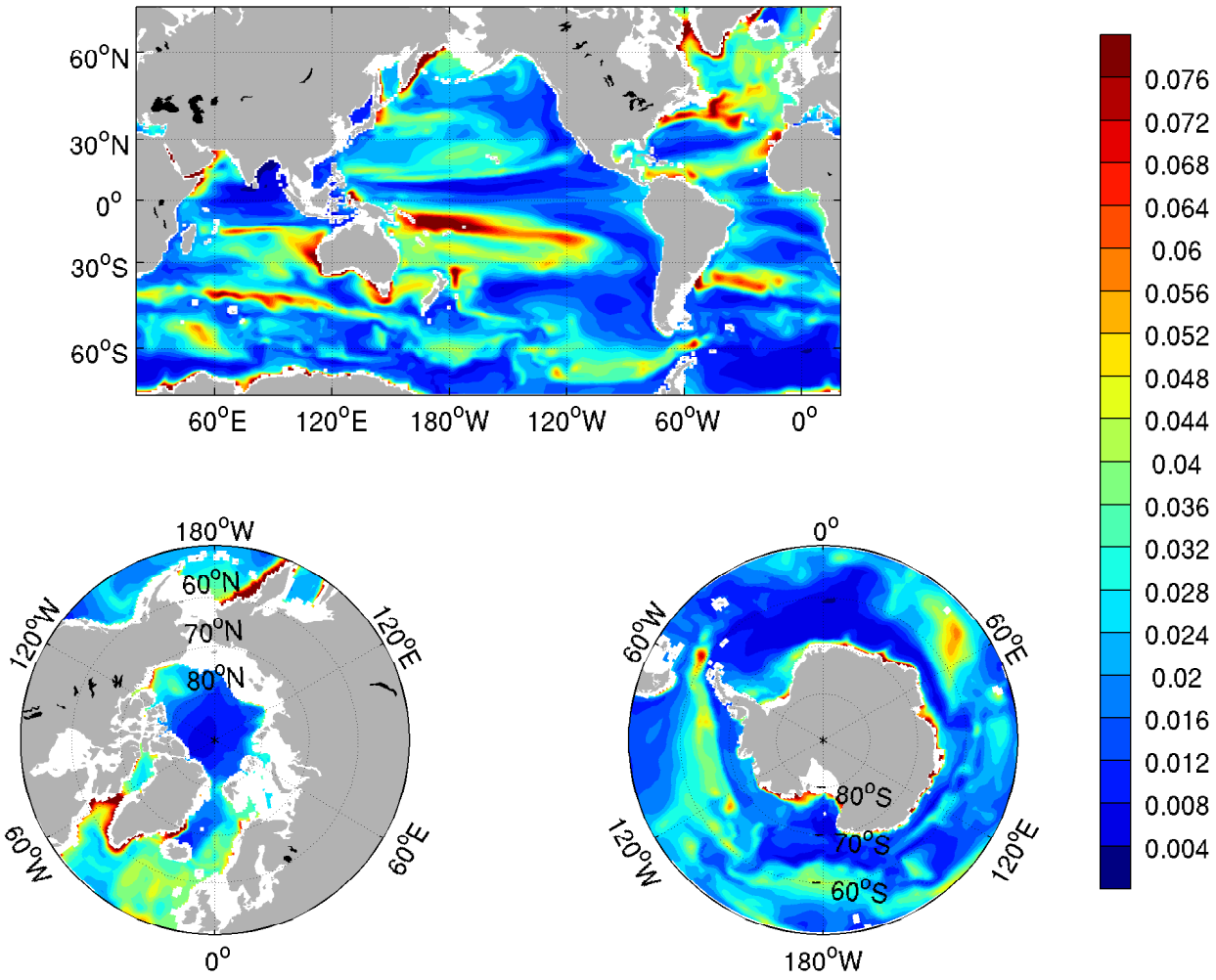

Figure : 1992-2011 standard deviation – salinity (in psu) at 300m

3D state variables

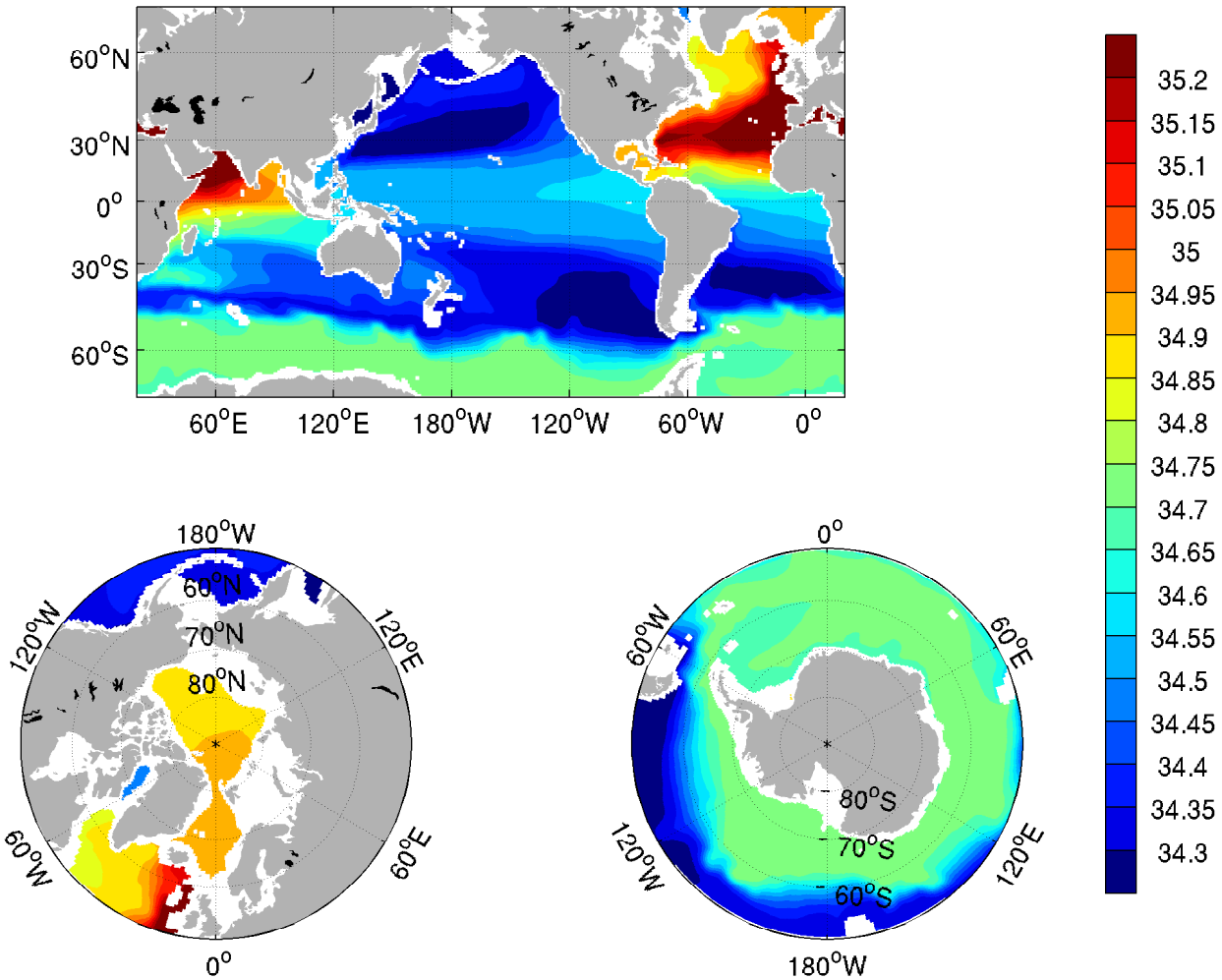

Figure : 1992-2011 mean – salinity (in psu) at 910m

3D state variables

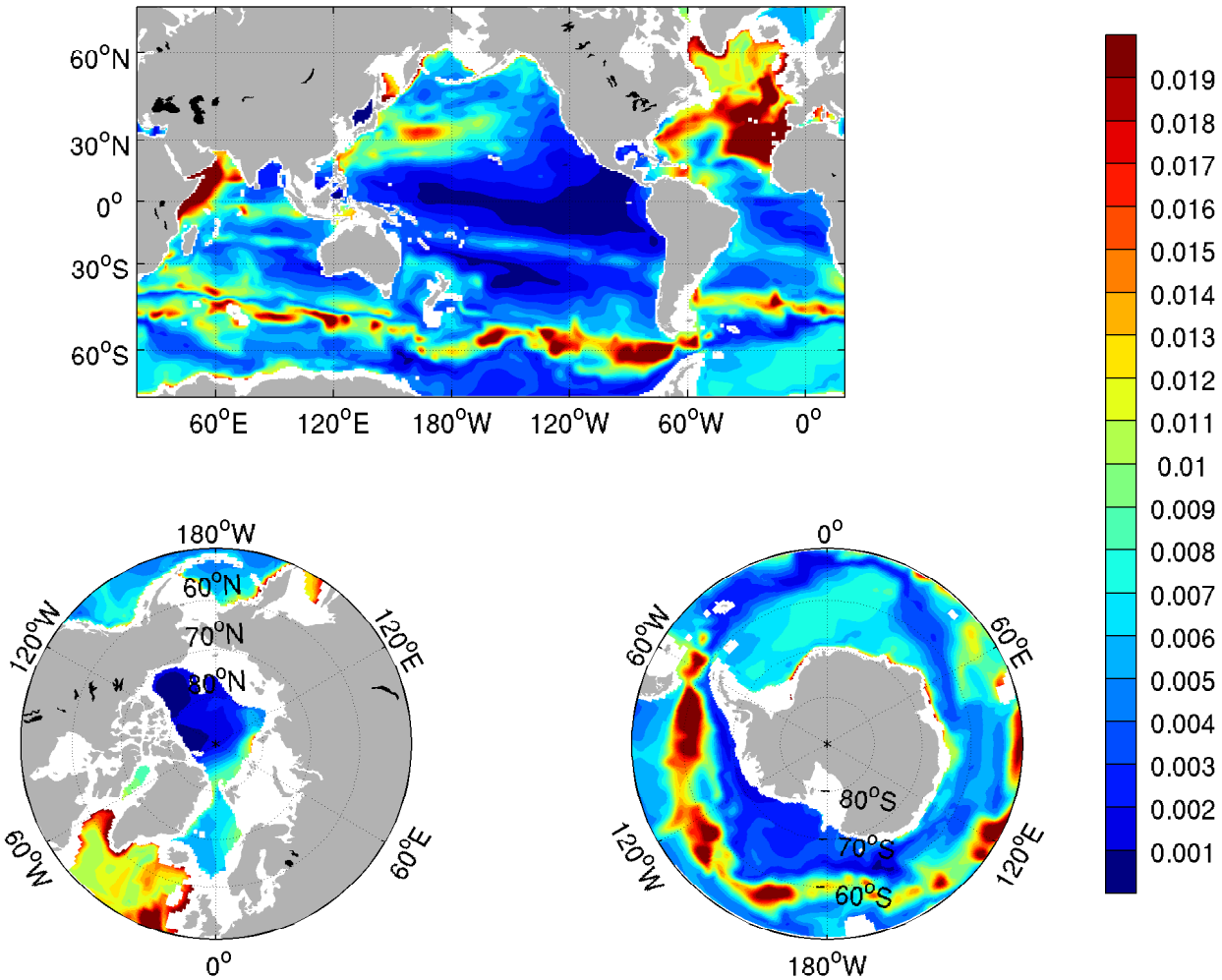

Figure : 1992-2011 standard deviation – salinity (in psu) at 910m

3D state variables

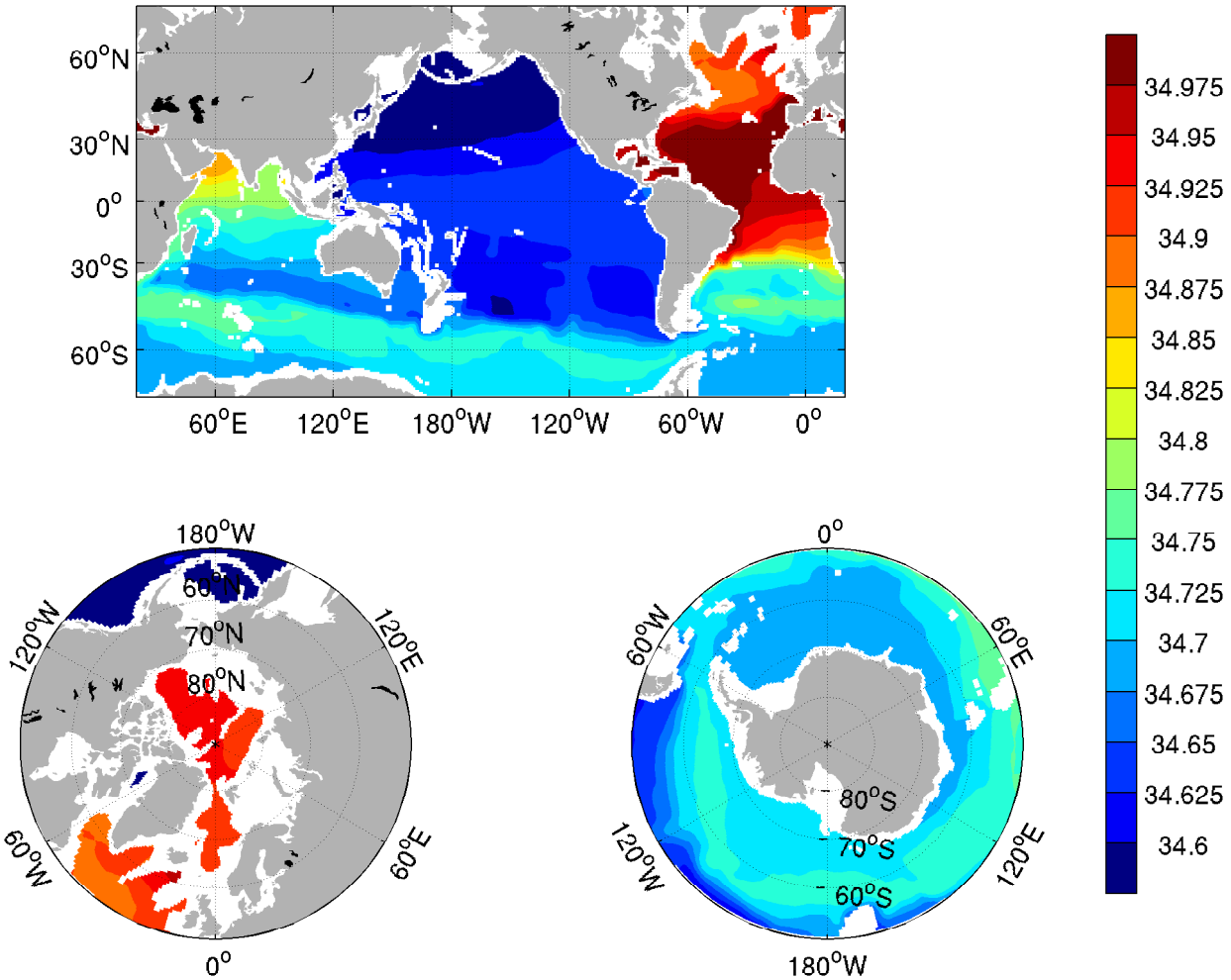

Figure : 1992-2011 mean – salinity (in psu) at 1914m

3D state variables

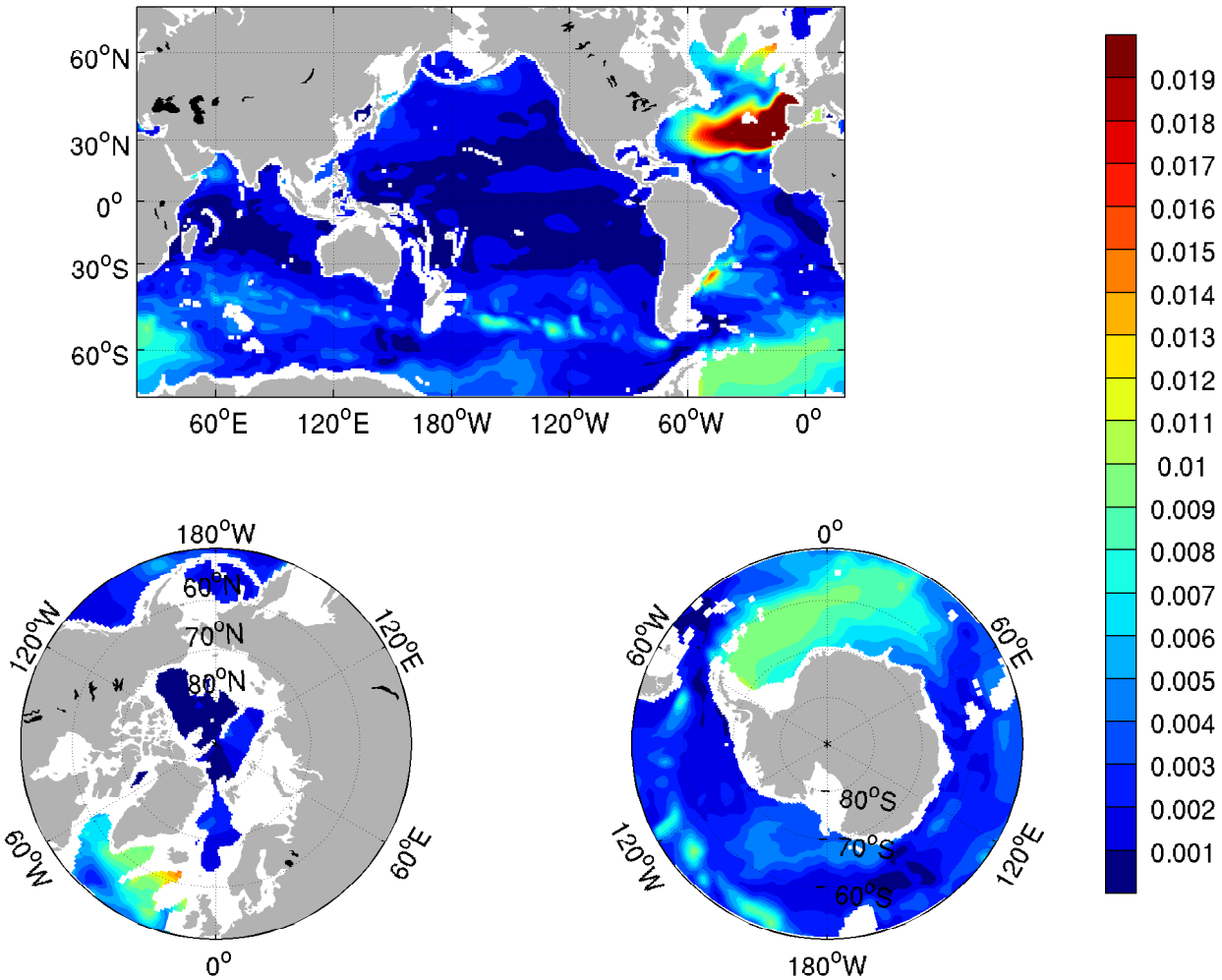

Figure : 1992-2011 standard deviation – salinity (in psu) at 1914m

3D state variables

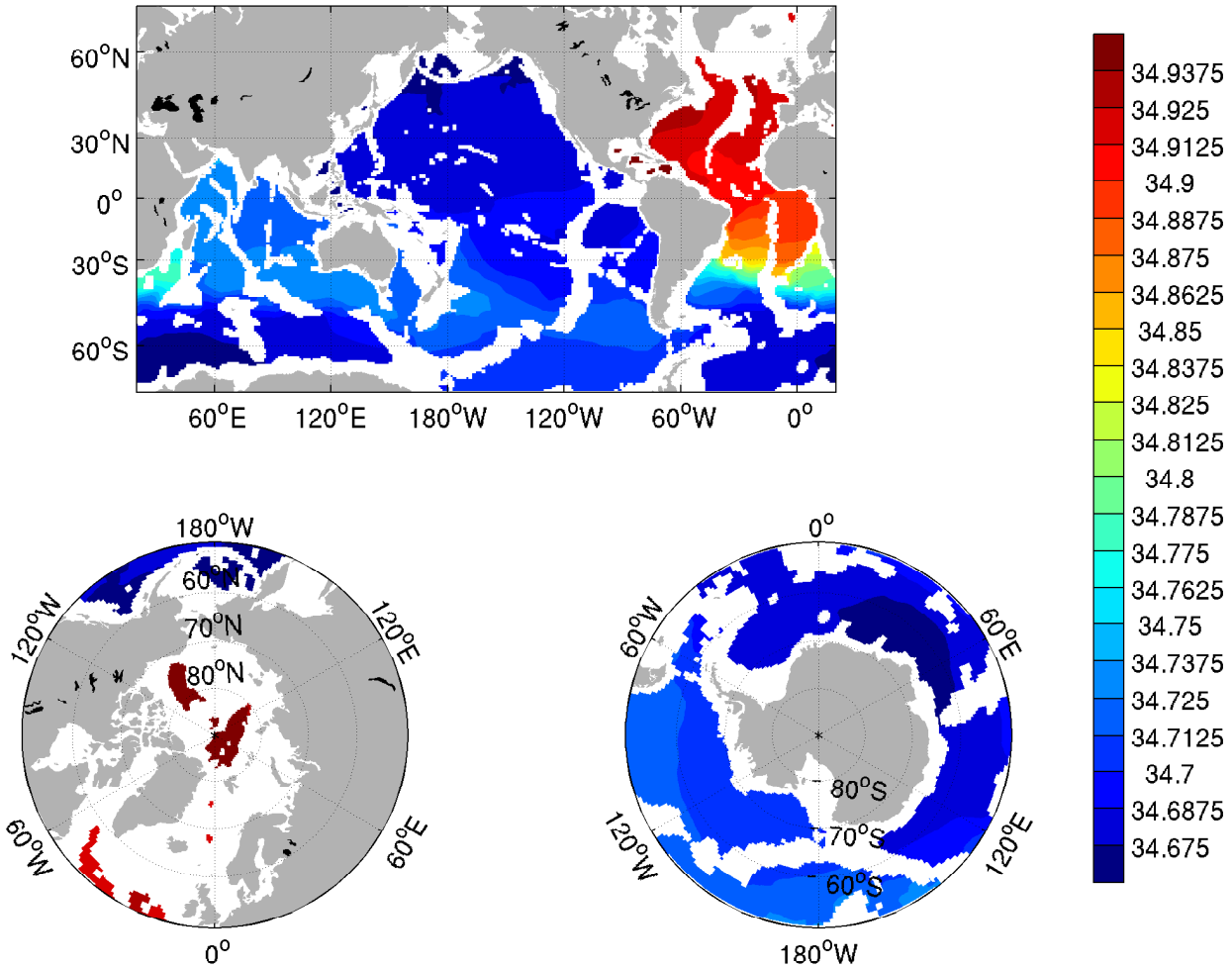

Figure : 1992-2011 mean – salinity (in psu) at 3581m

3D state variables

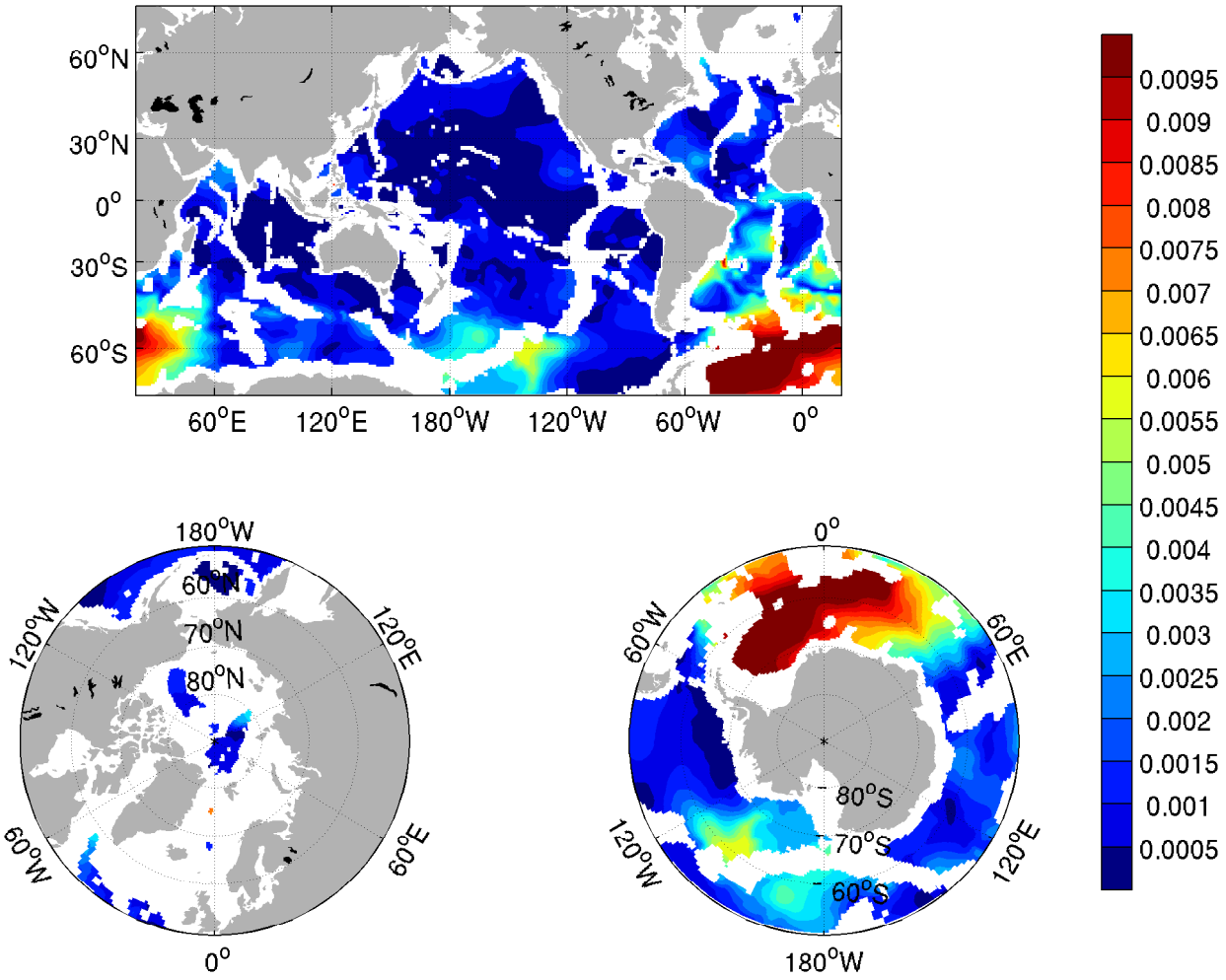

Figure : 1992-2011 standard deviation – salinity (in psu) at 3581m

3D state variables

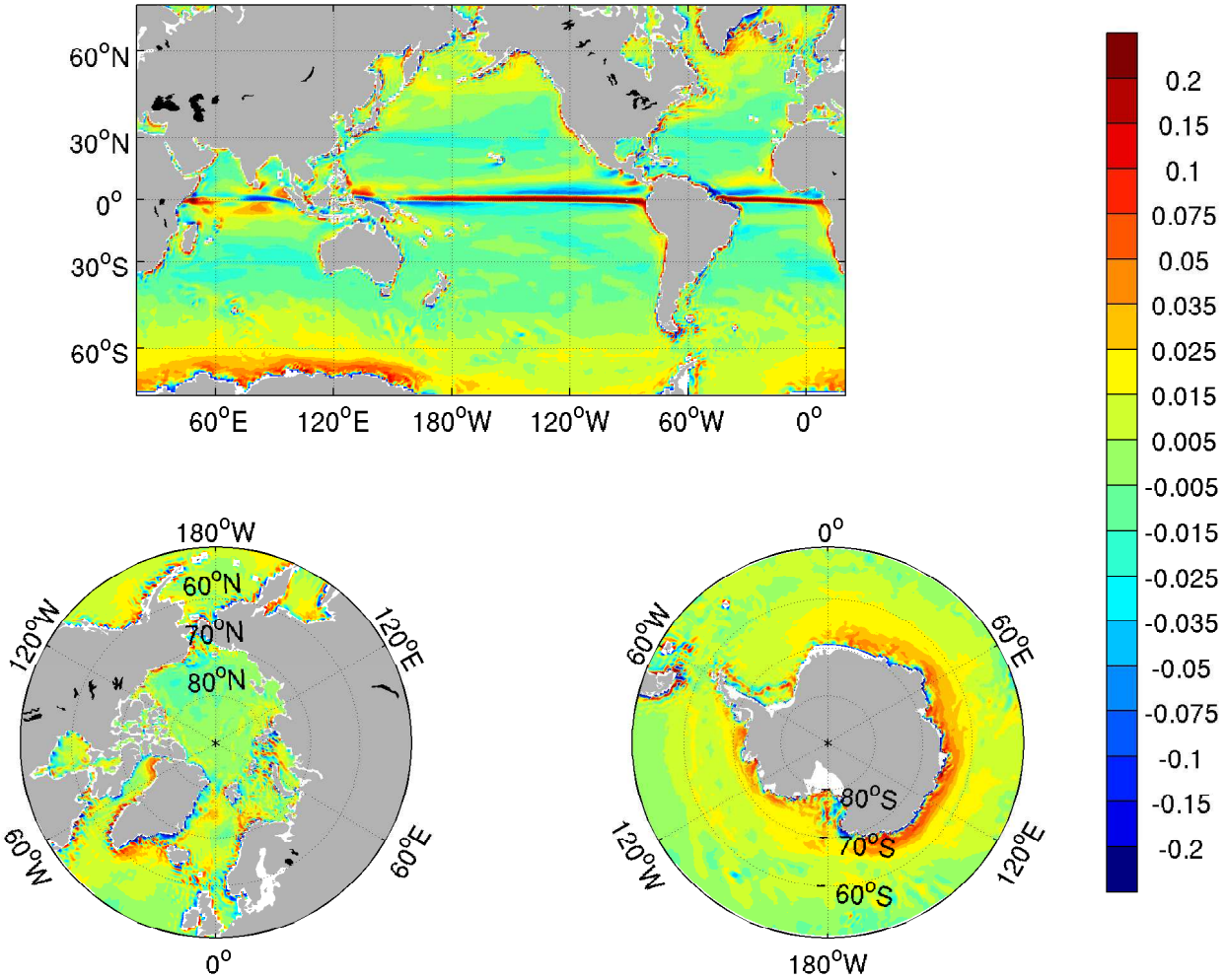

Figure : 1992-2011 mean – vertical velocity (in mm/year) at 15m

3D state variables

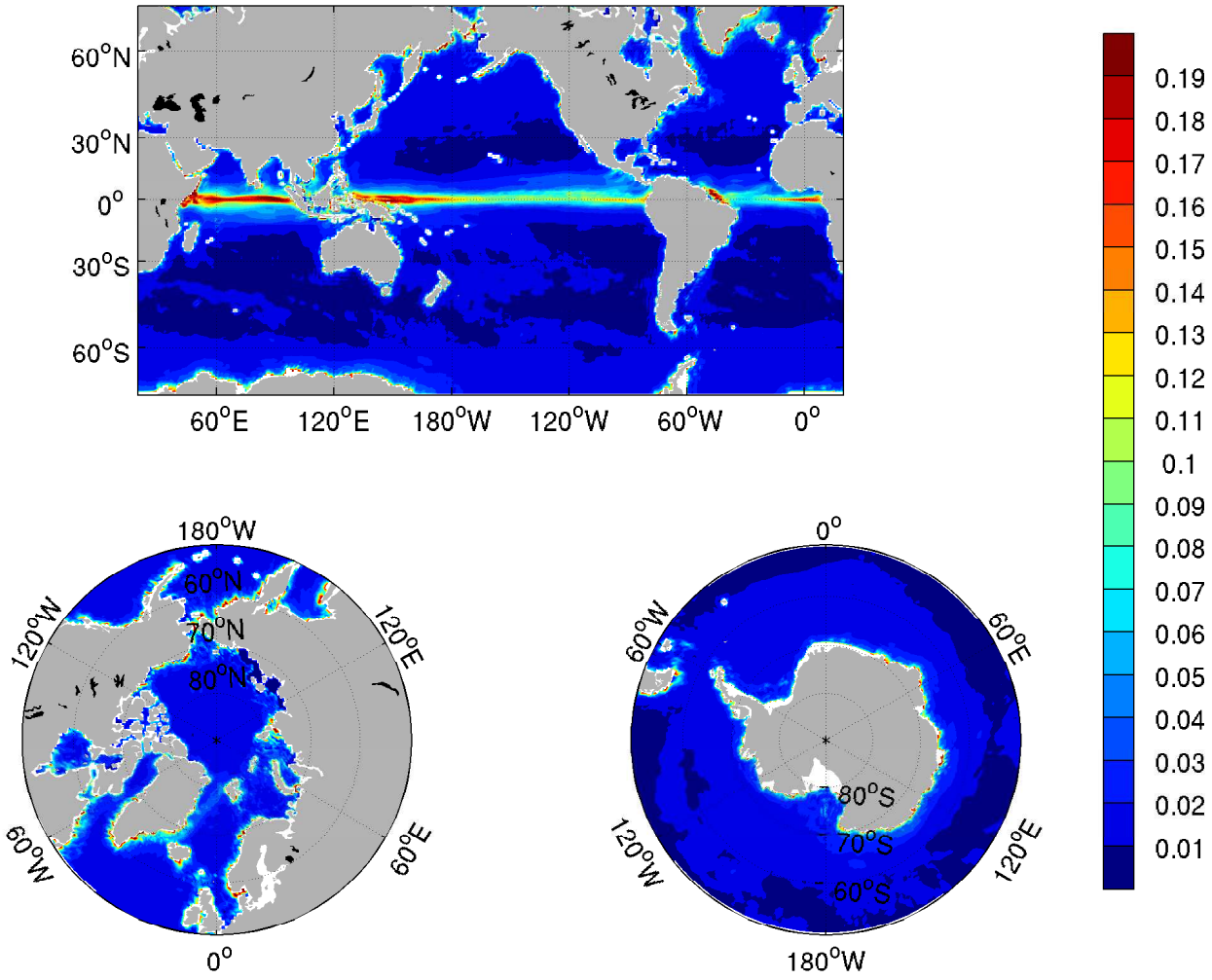

Figure : 1992-2011 standard deviation – vertical velocity (in mm/year) at 15m

3D state variables

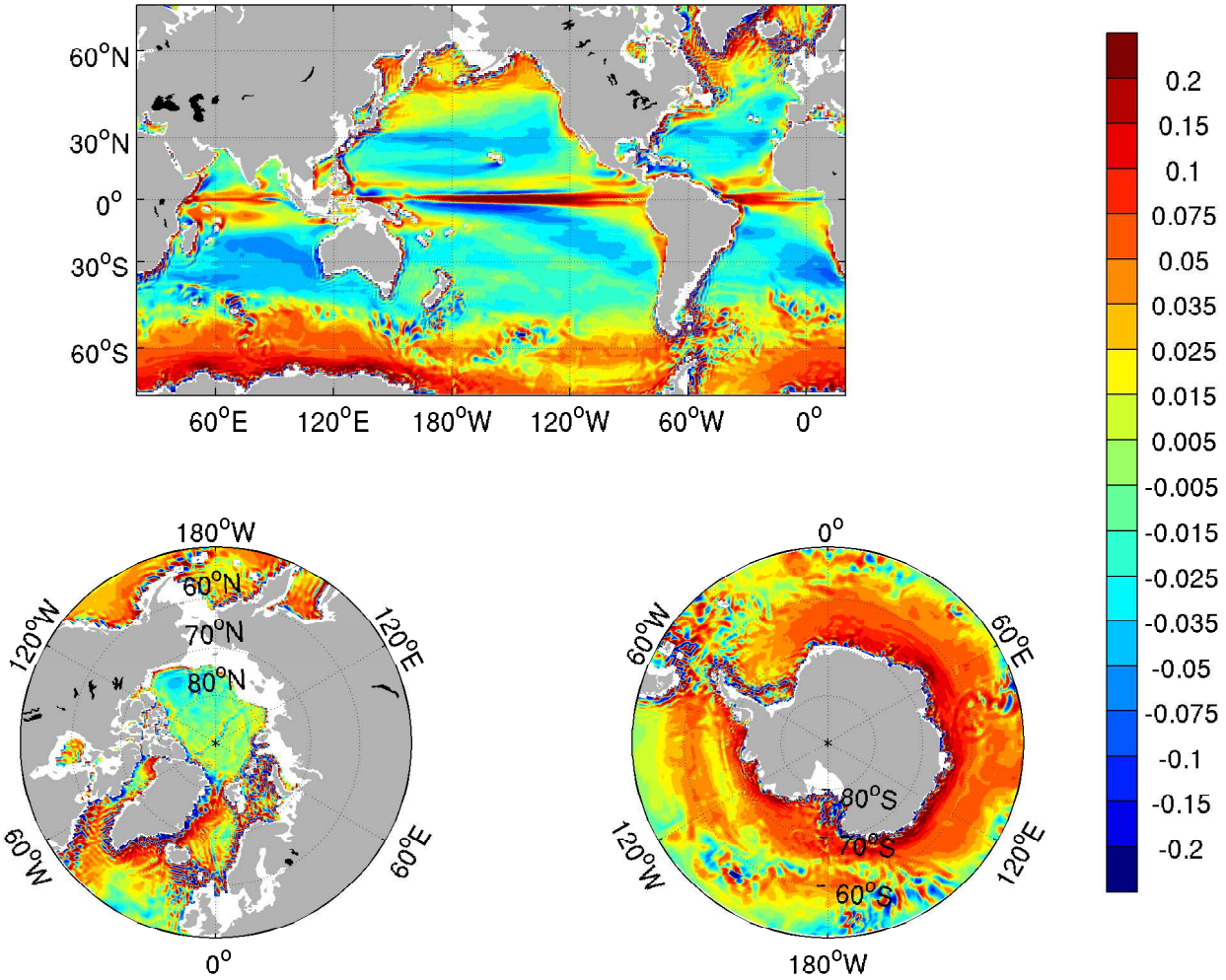

Figure : 1992-2011 mean – vertical velocity (in mm/year) at 105m

3D state variables

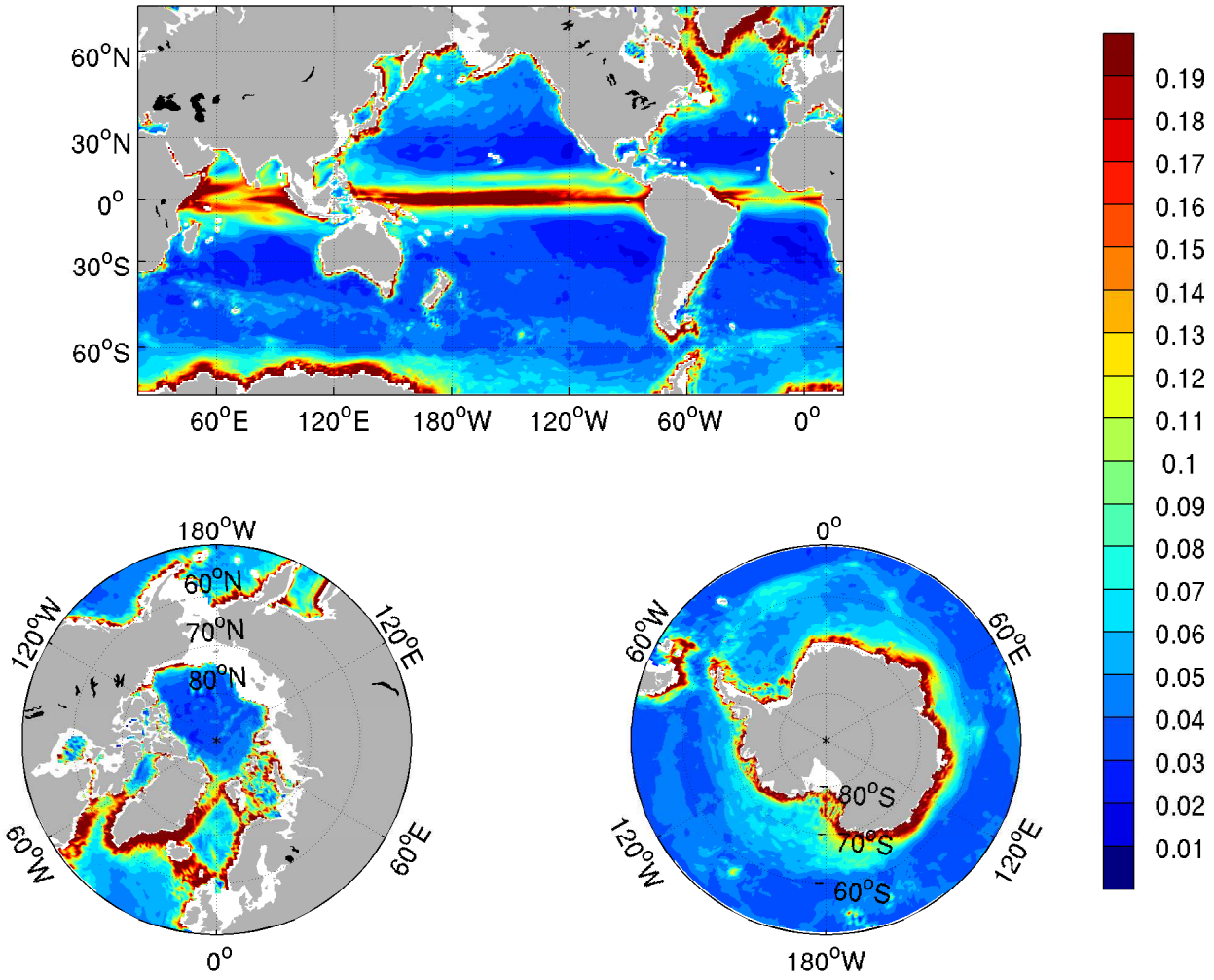

Figure : 1992-2011 standard deviation – vertical velocity (in mm/year) at 105m

3D state variables

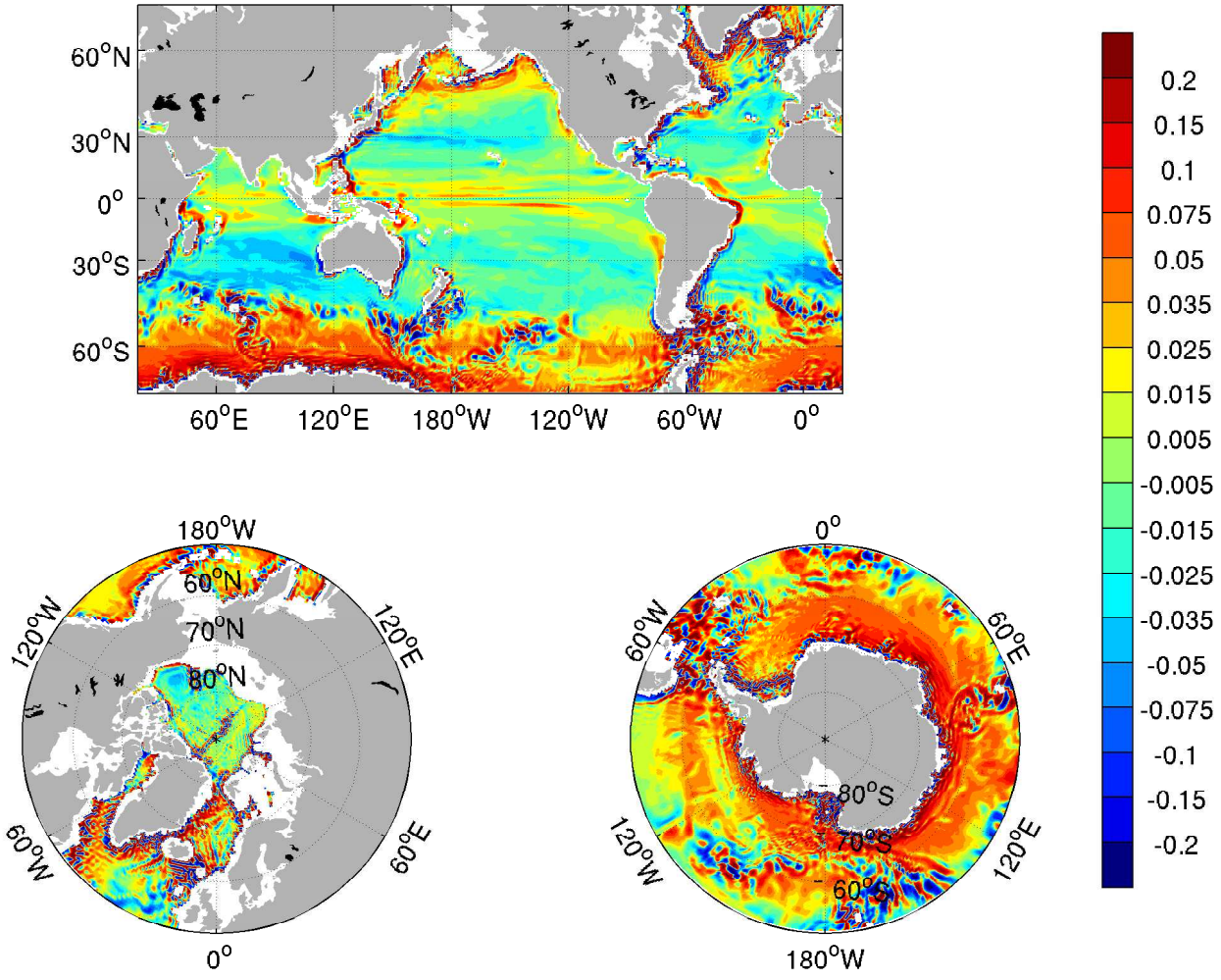

Figure : 1992-2011 mean – vertical velocity (in mm/year) at 300m

3D state variables

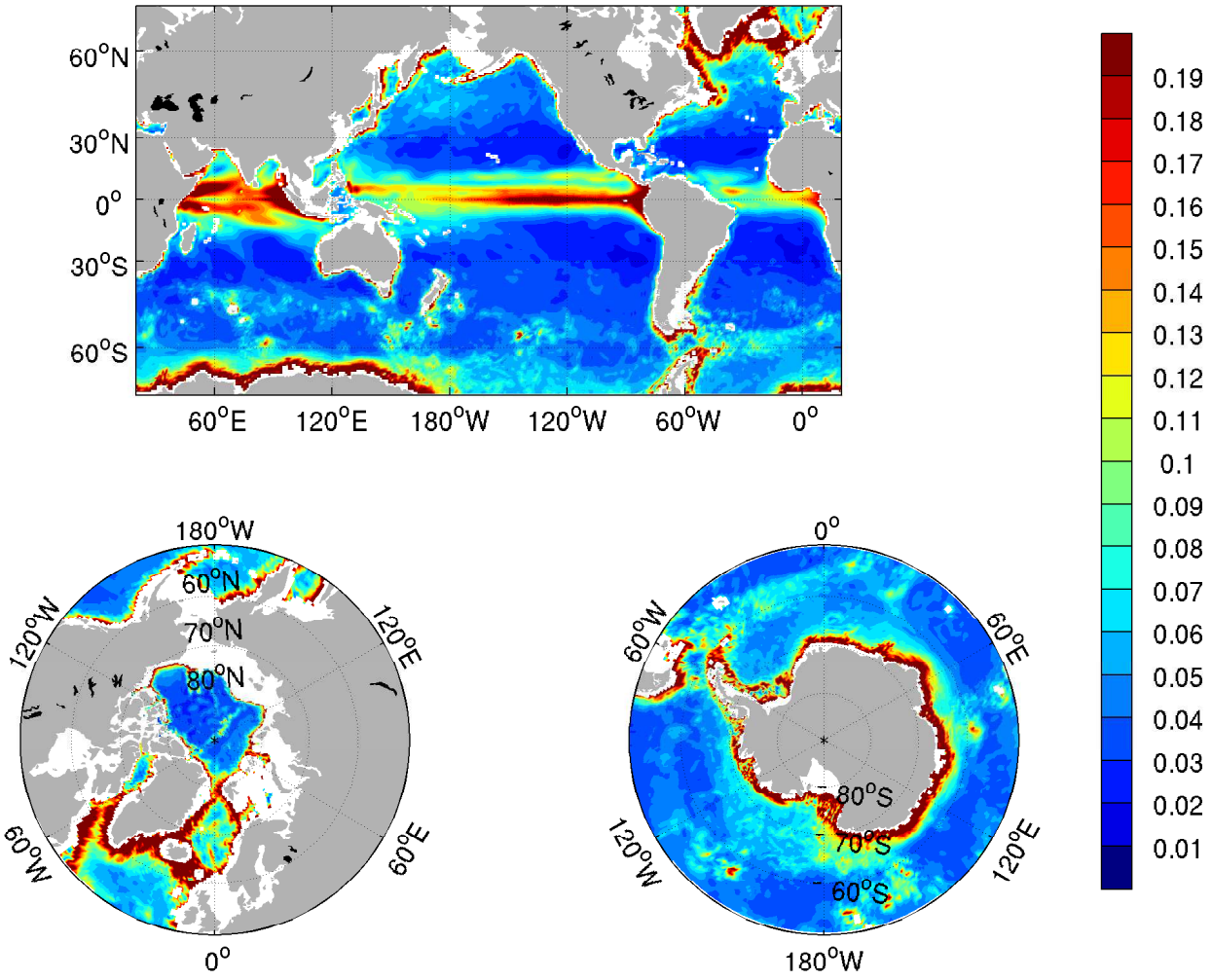

Figure : 1992-2011 standard deviation – vertical velocity (in mm/year) at 300m

3D state variables

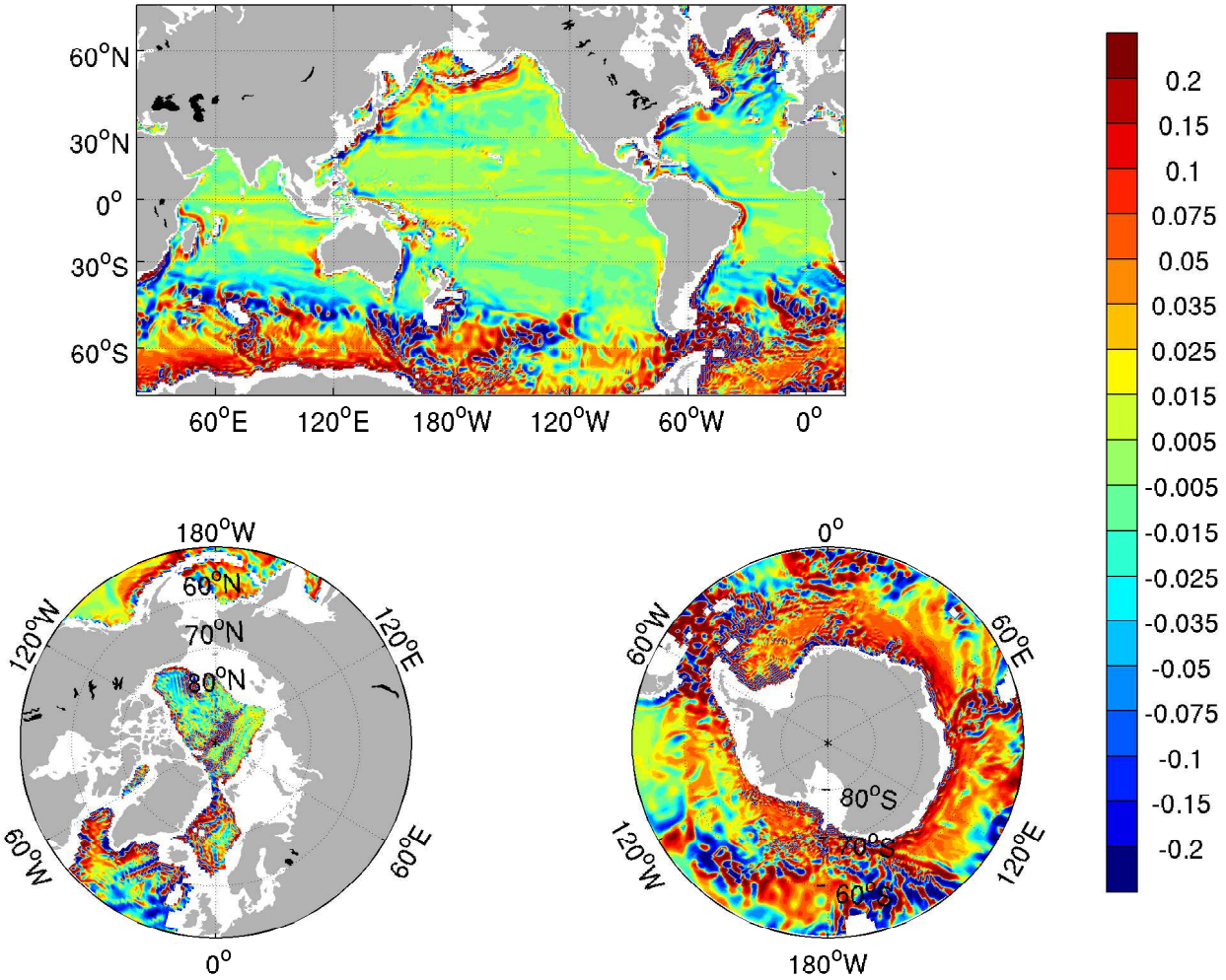

Figure : 1992-2011 mean – vertical velocity (in mm/year) at 910m

3D state variables

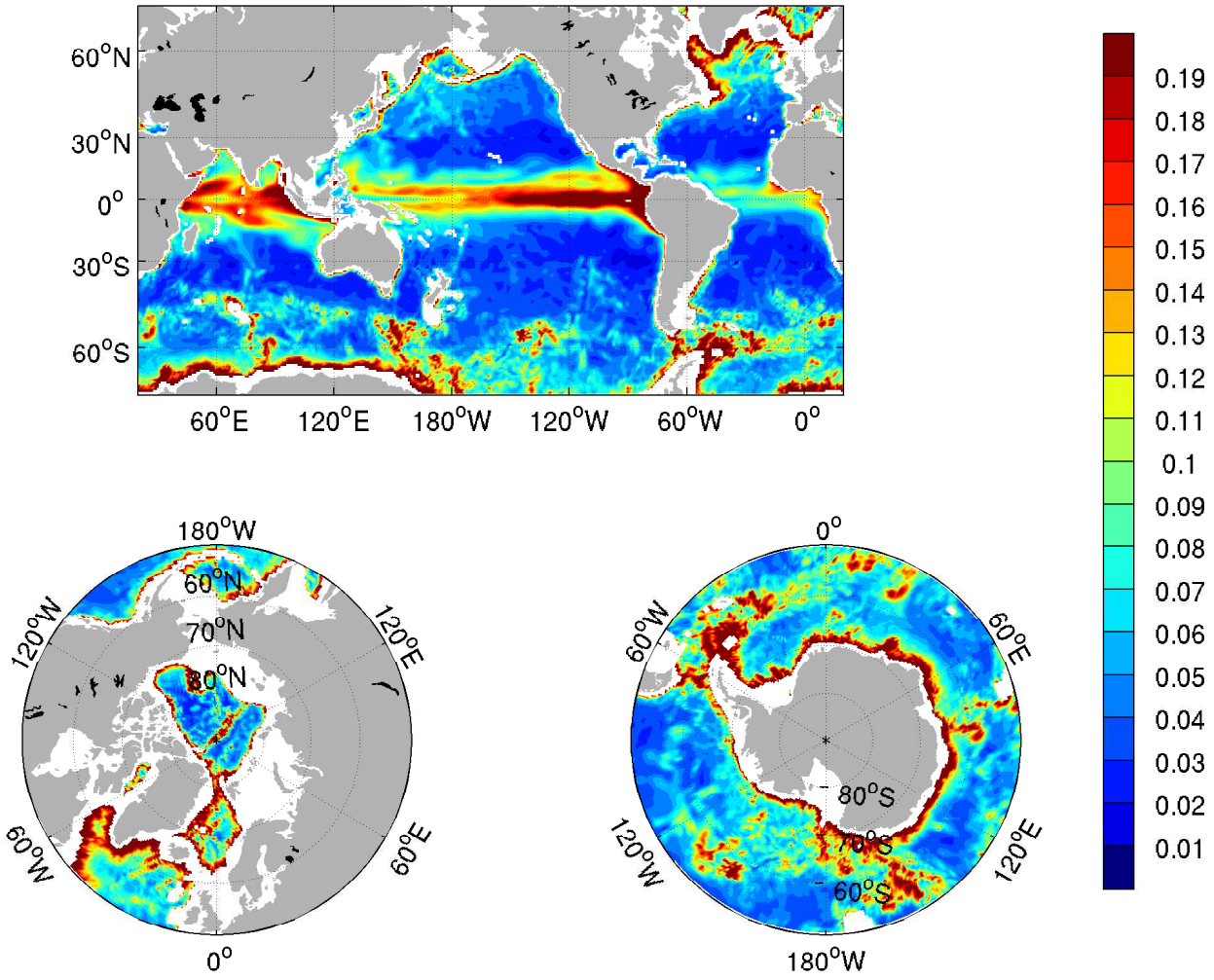

Figure : 1992-2011 standard deviation – vertical velocity (in mm/year) at 910m

3D state variables

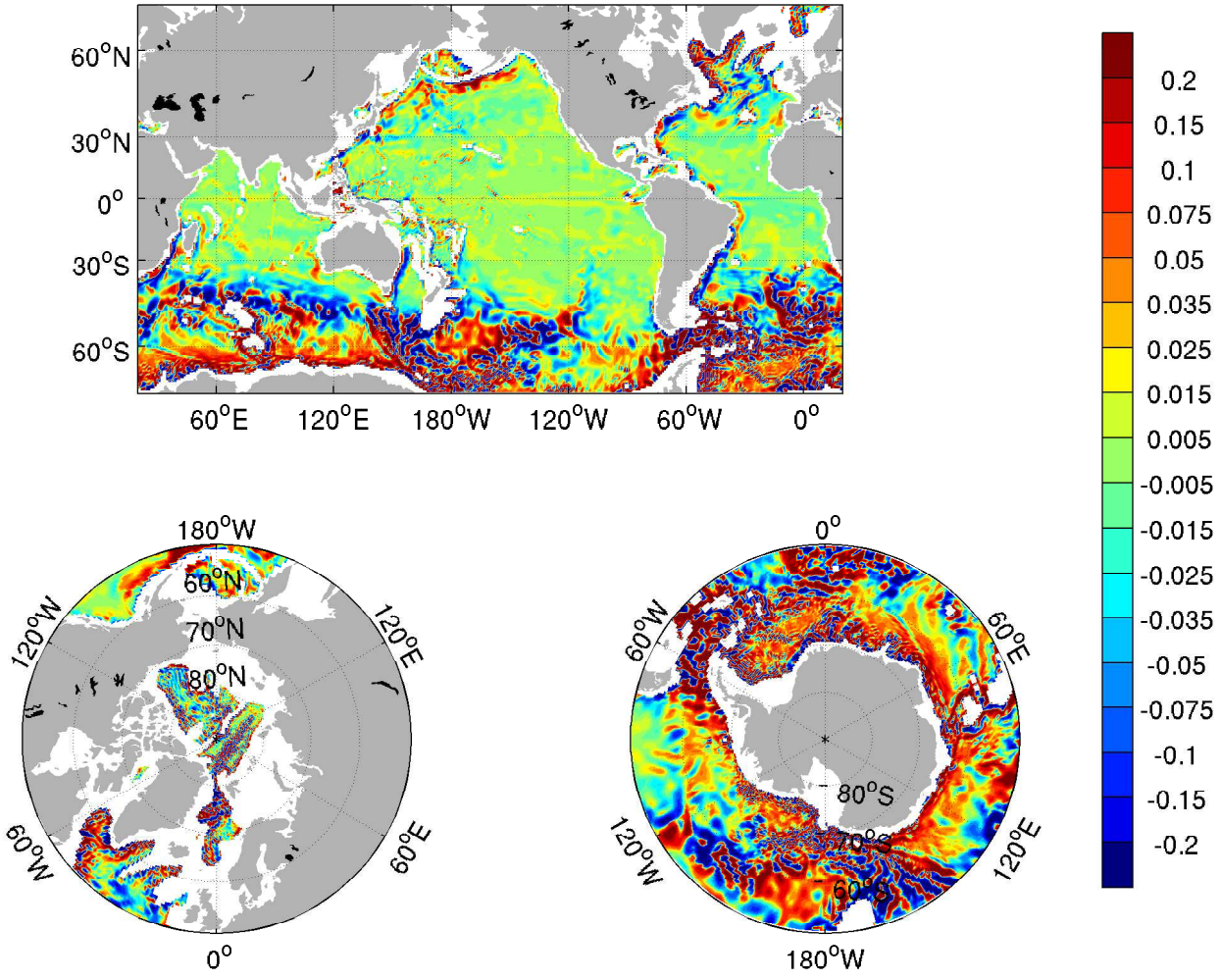

Figure : 1992-2011 mean – vertical velocity (in mm/year) at 1914m

3D state variables

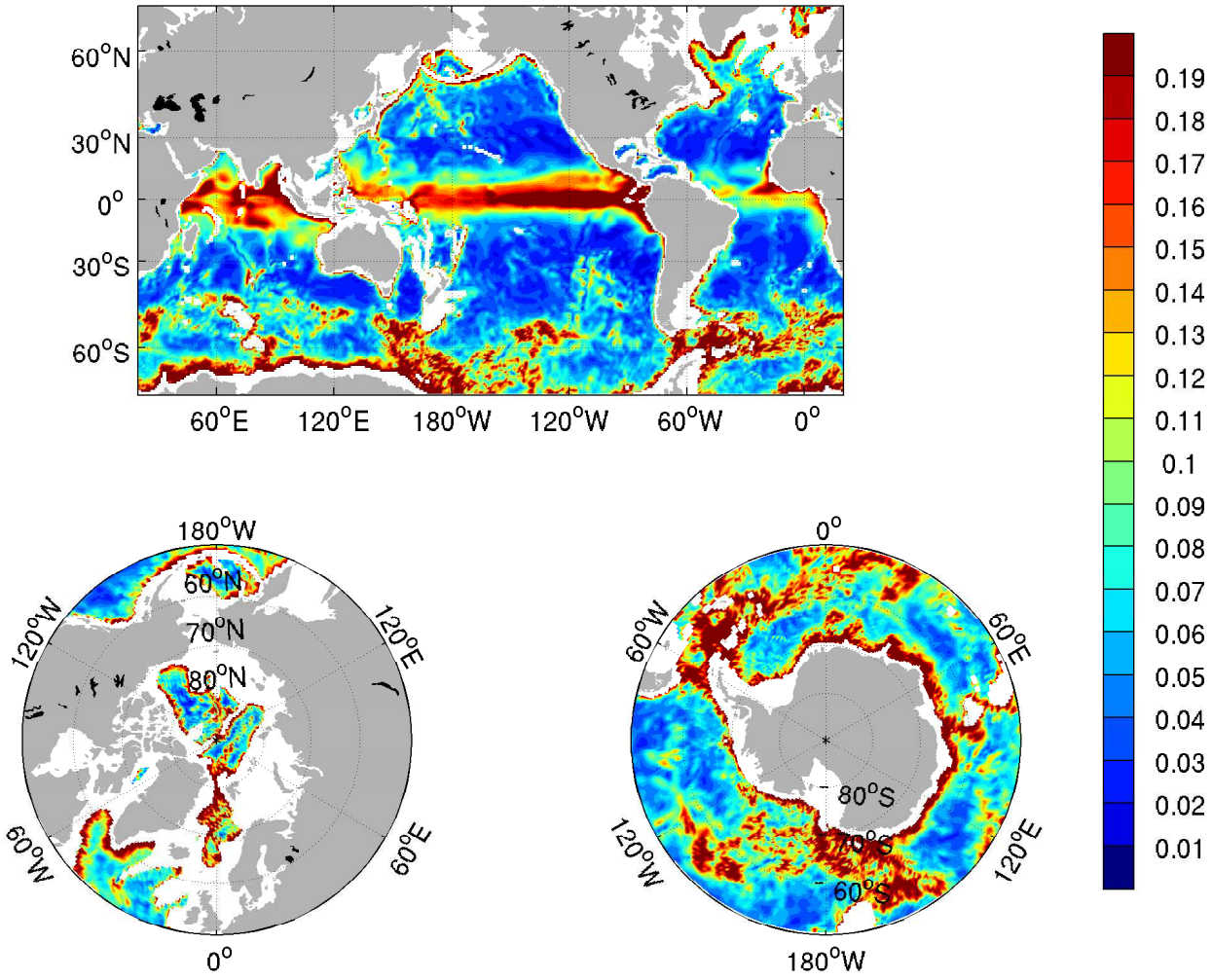

Figure : 1992-2011 standard deviation – vertical velocity (in mm/year) at 1914m

3D state variables

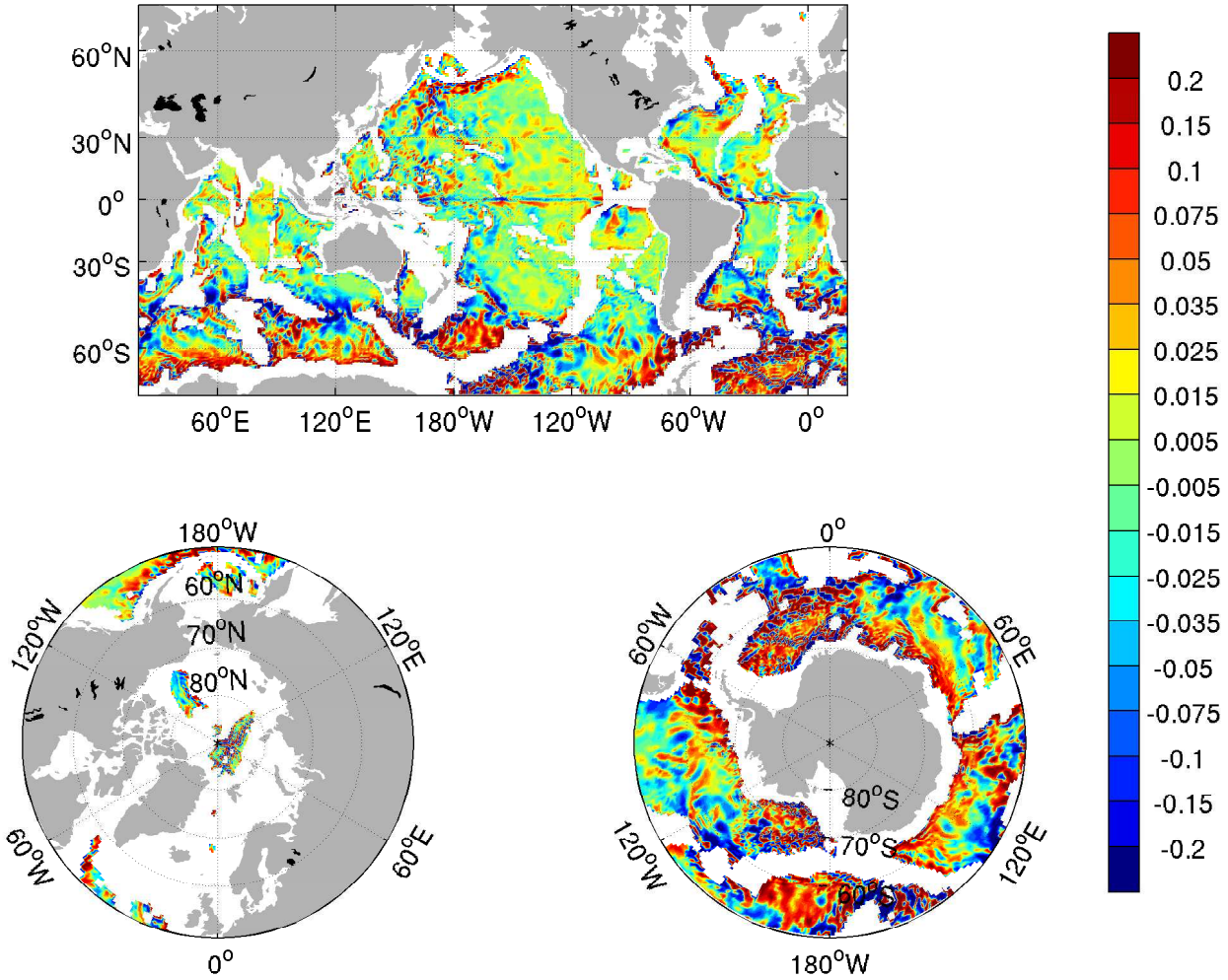

Figure : 1992-2011 mean – vertical velocity (in mm/year) at 3581m

3D state variables

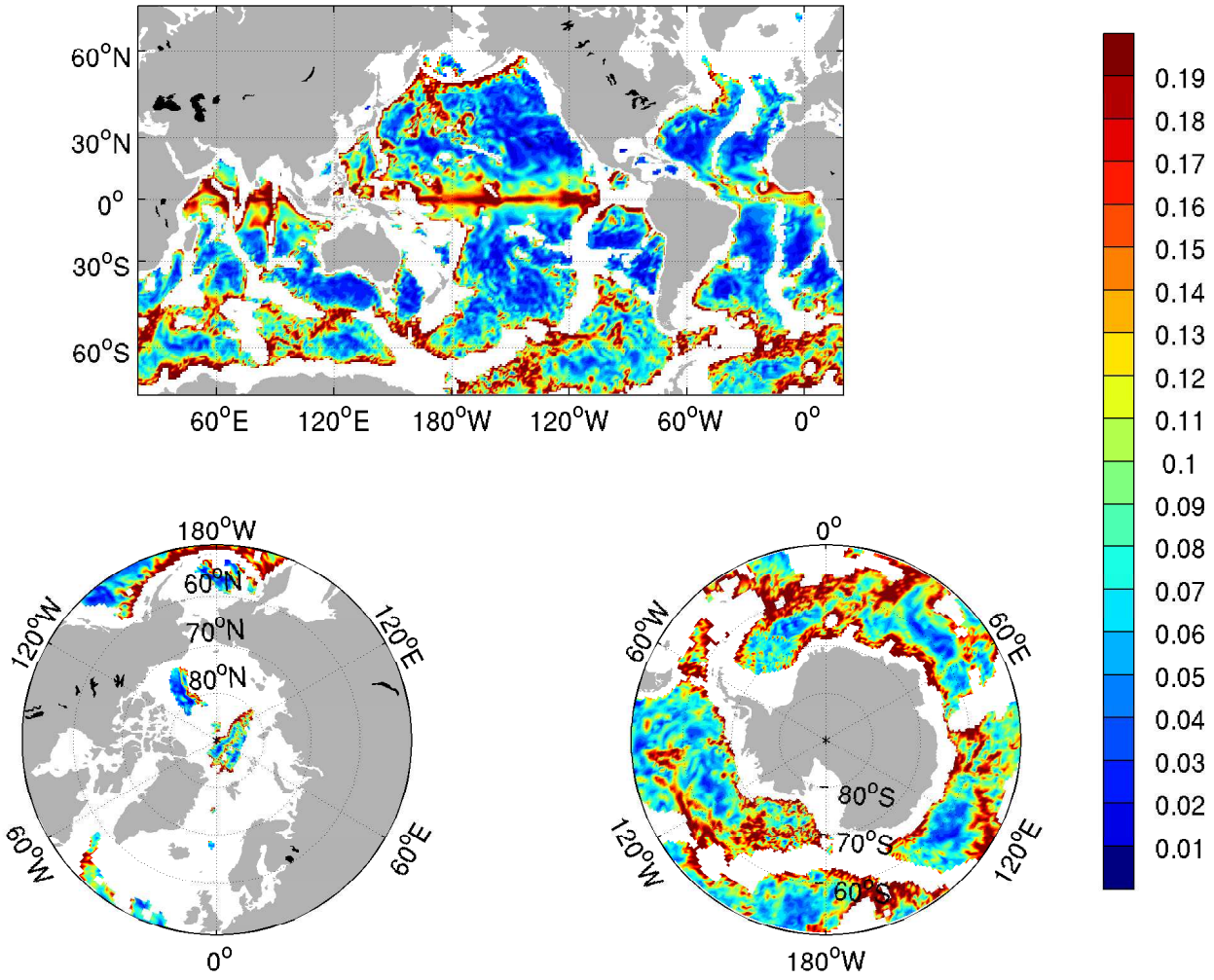

Figure : 1992-2011 standard deviation – vertical velocity (in mm/year) at 3581m

air-sea heat flux

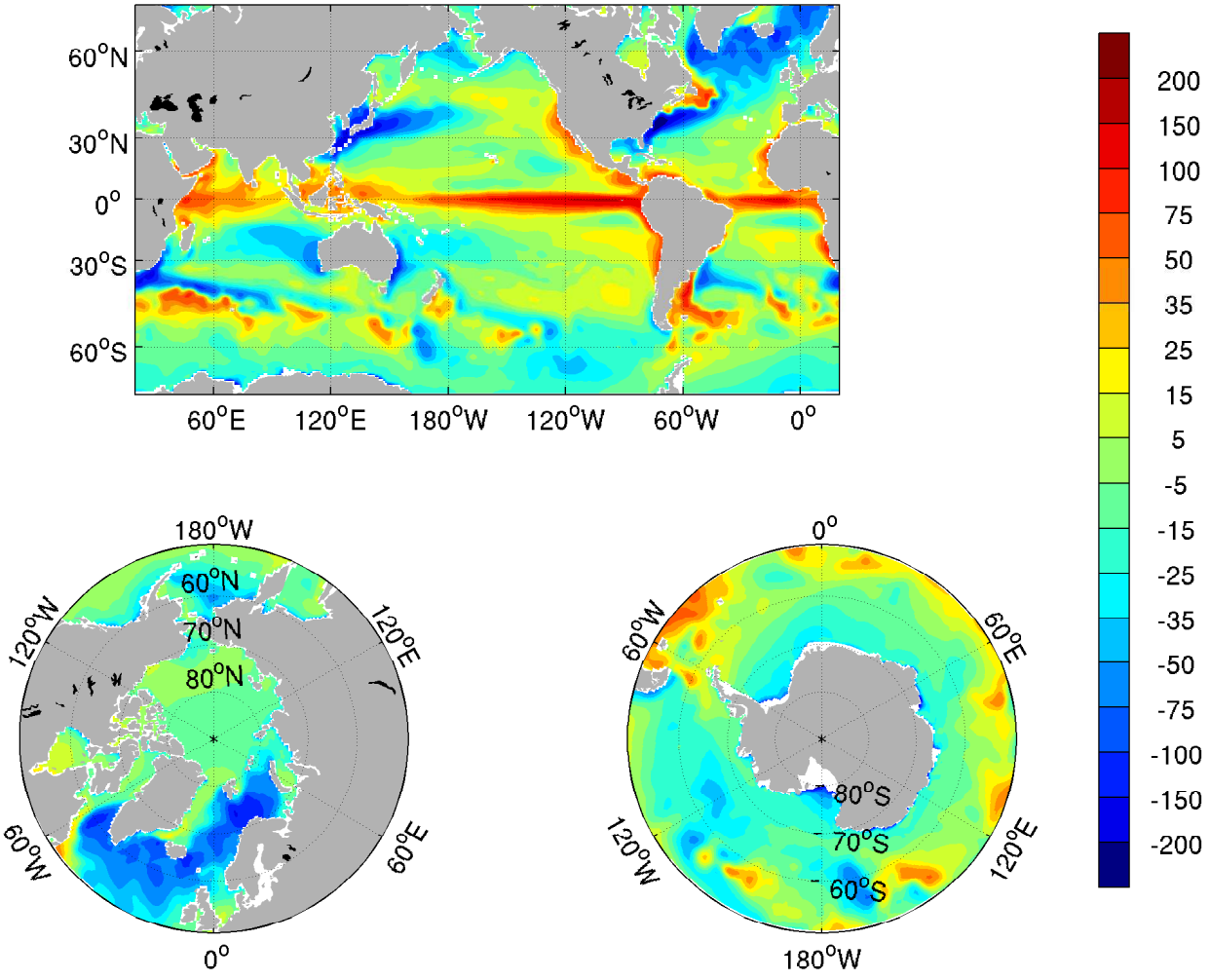

Figure : 1992-2011 mean – QNET to ocean+ice (W/m^2)

air-sea heat flux

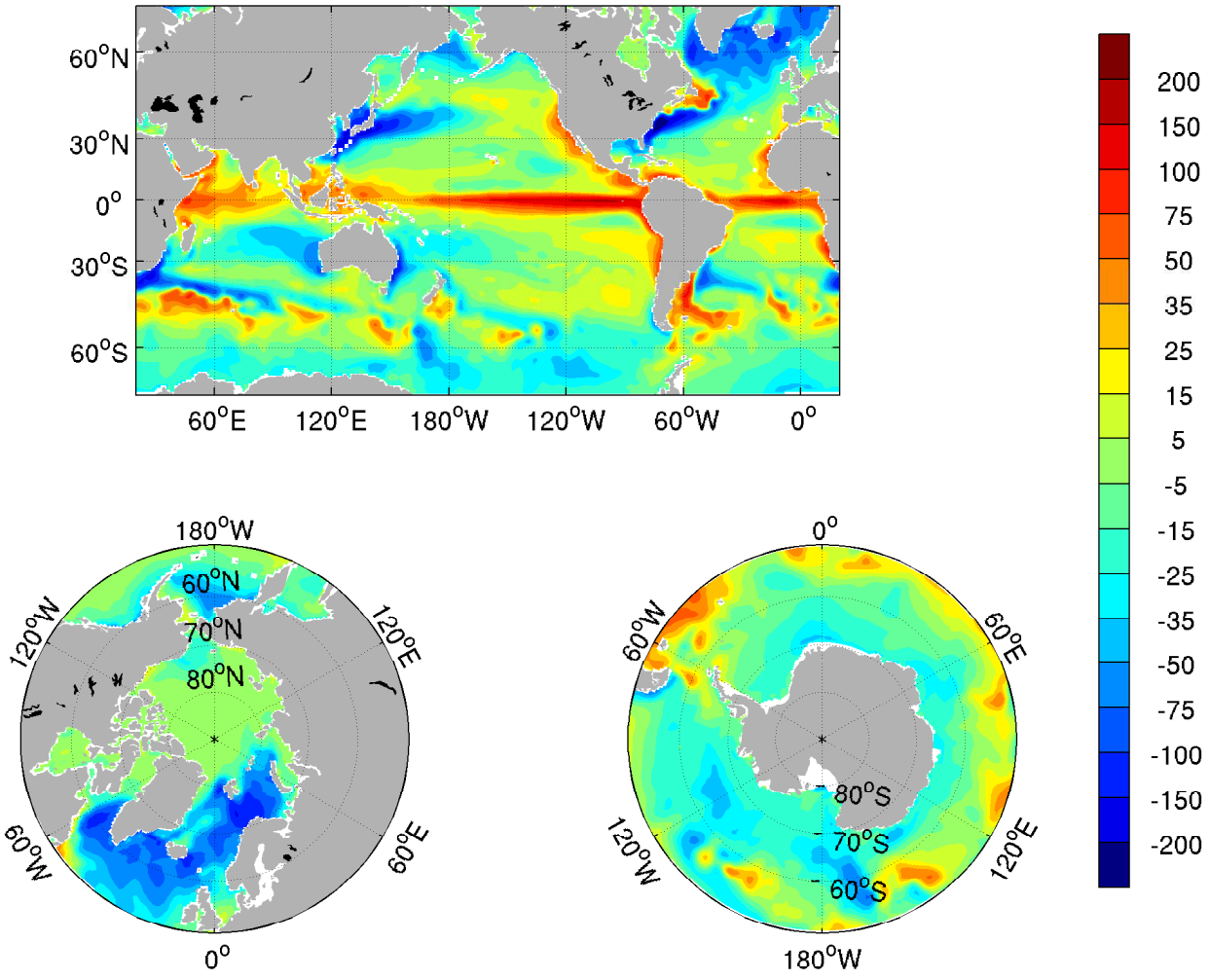

Figure : 1992-2011 mean – QNET to ocean (W/m^2)

air-sea heat flux

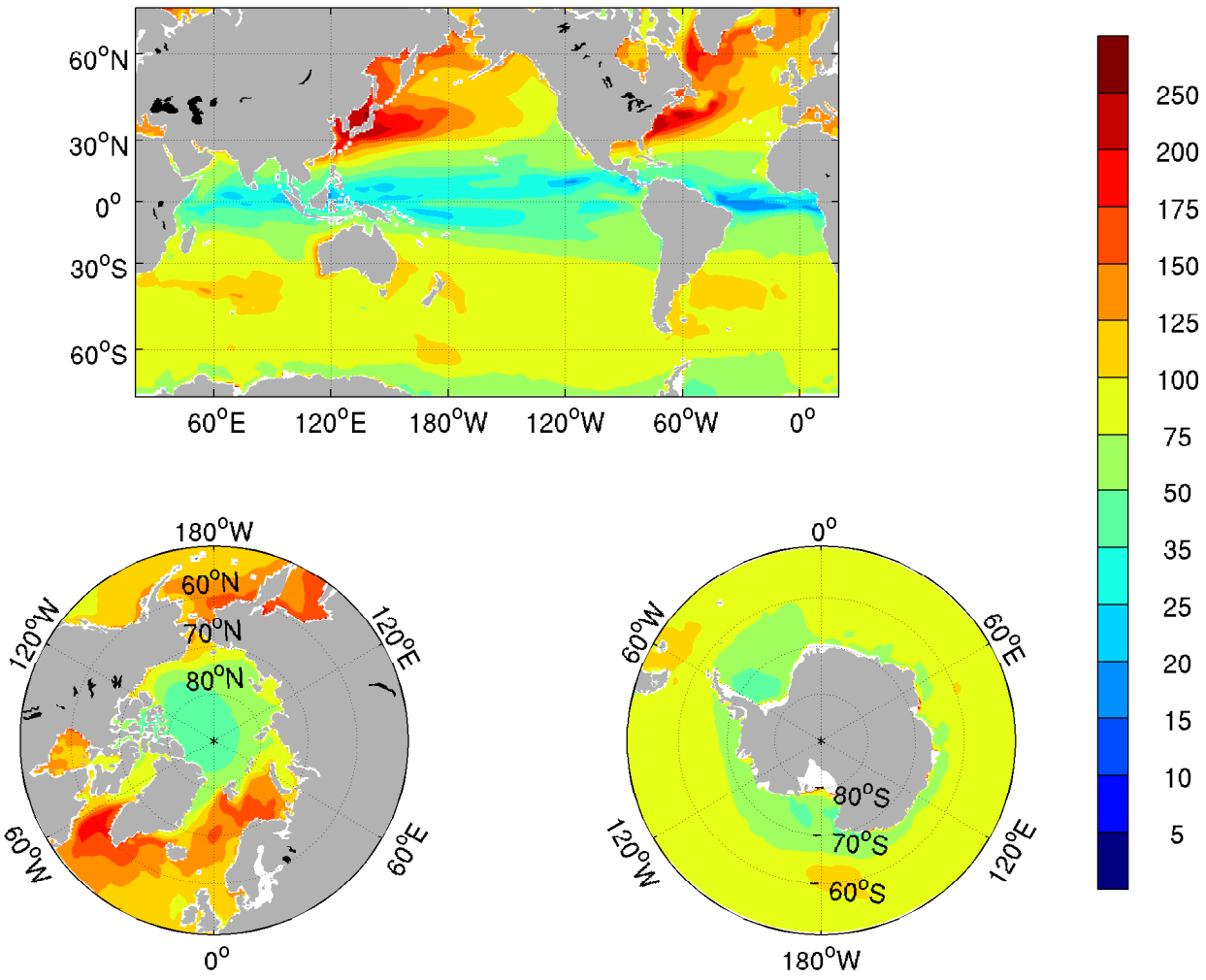

Figure : 1992-2011 standard deviation – QNET to ocean+ice (W/m^2)

air-sea heat flux

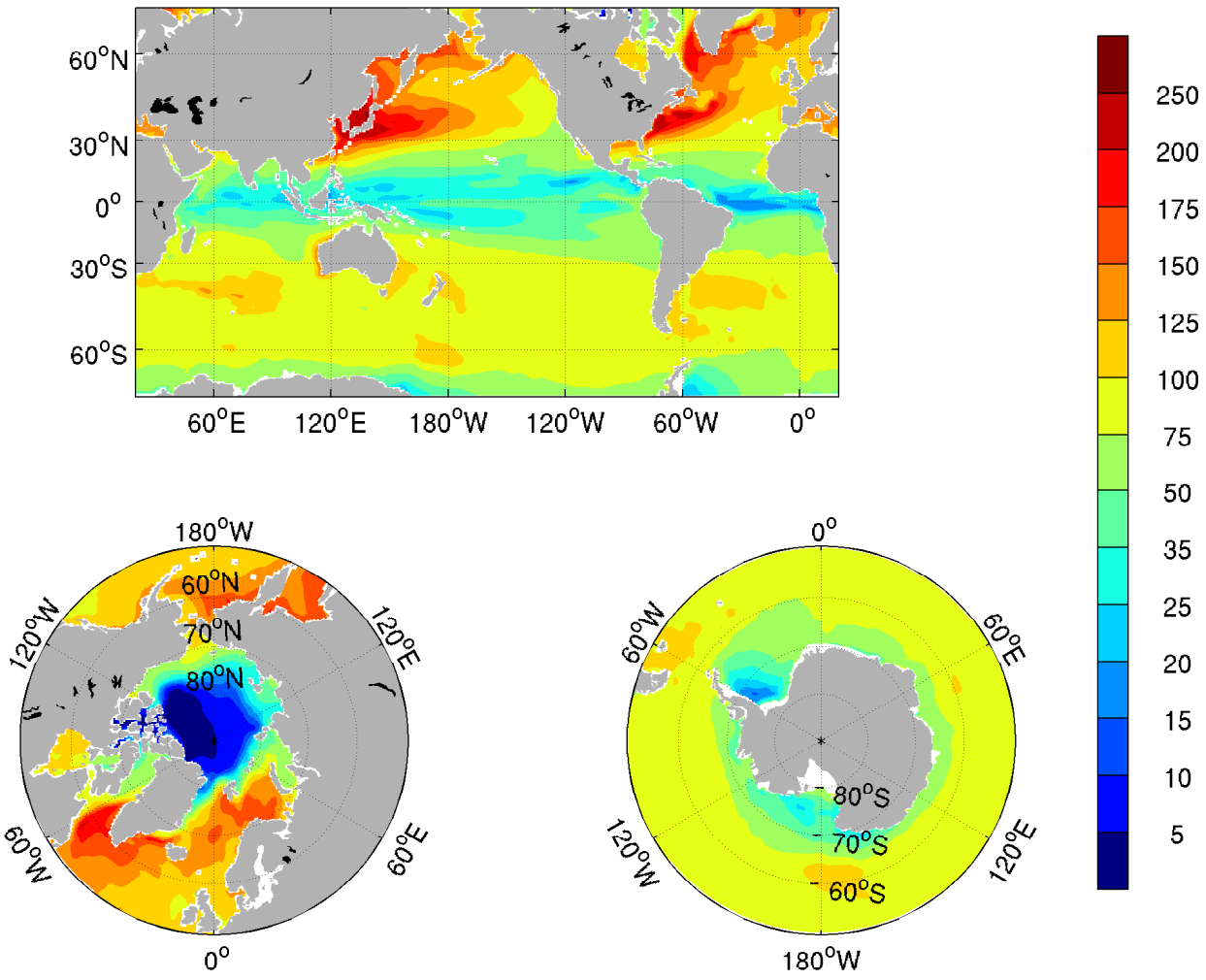

Figure : 1992-2011 standard deviation – QNET to ocean (W/m^2)

air-sea freshwater flux

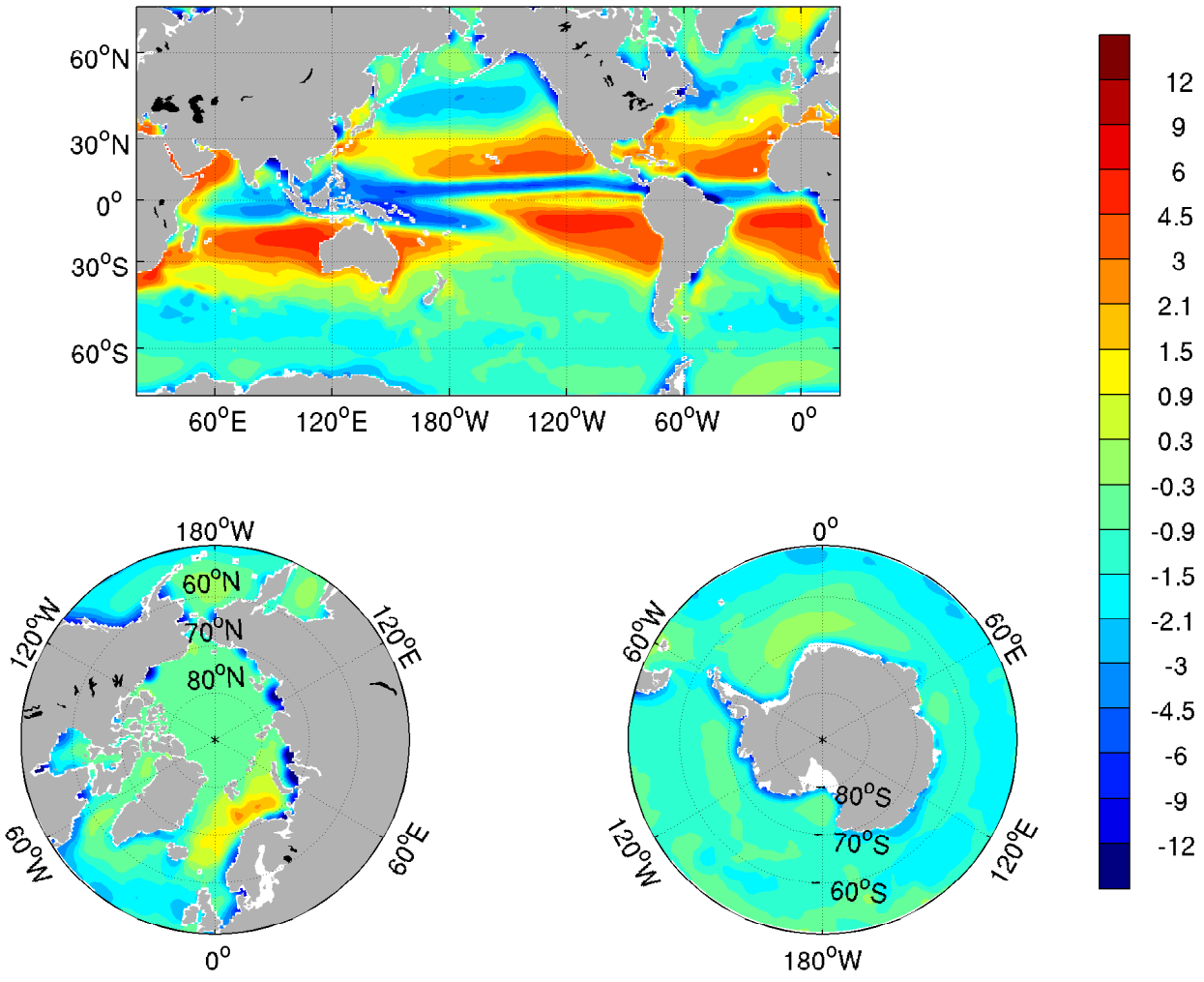

Figure : 1992-2011 mean – E-P-R from ocean+ice (mm/day)

air-sea freshwater flux

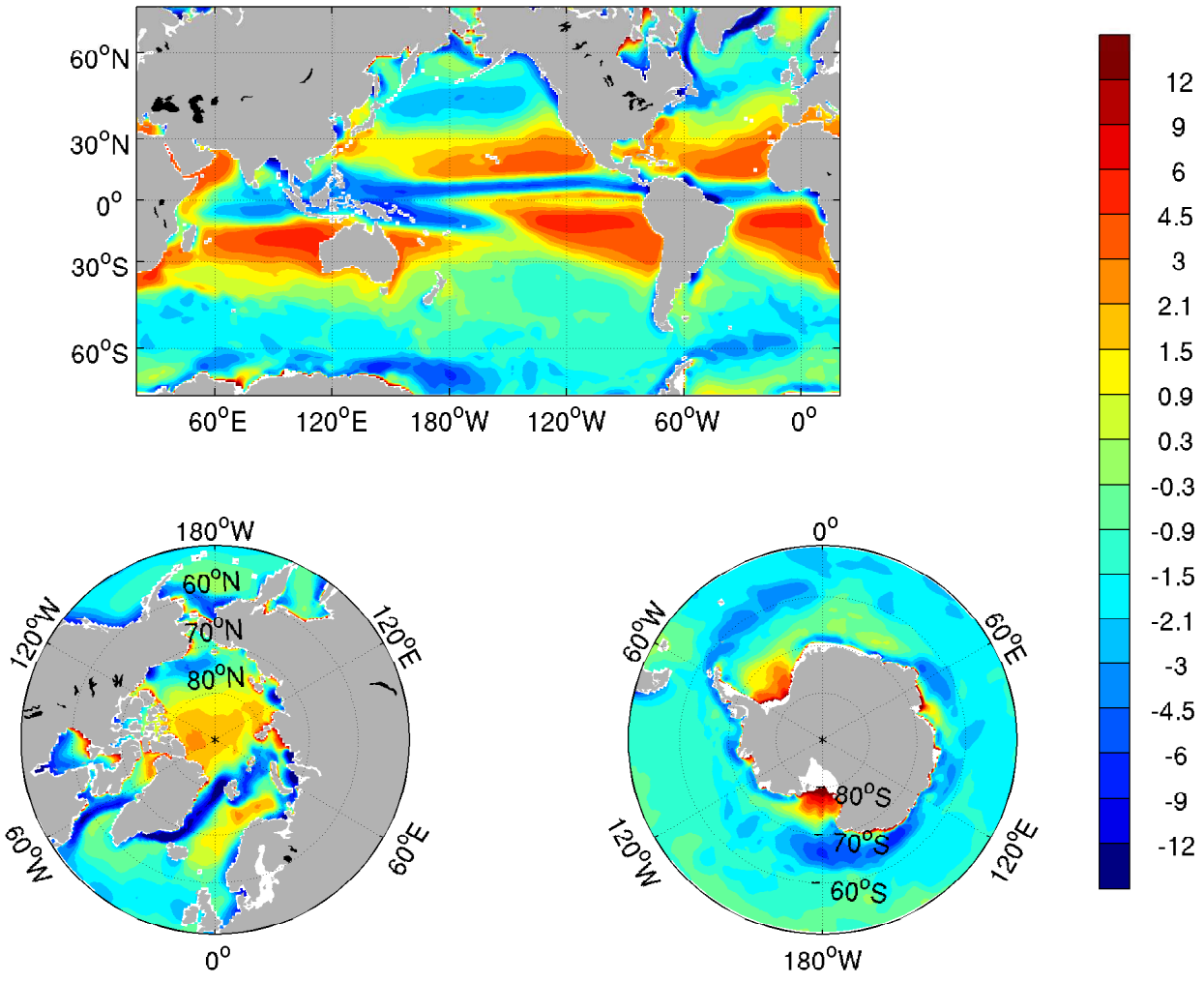

Figure : 1992-2011 mean – E-P-R from ocean (mm/day)

air-sea freshwater flux

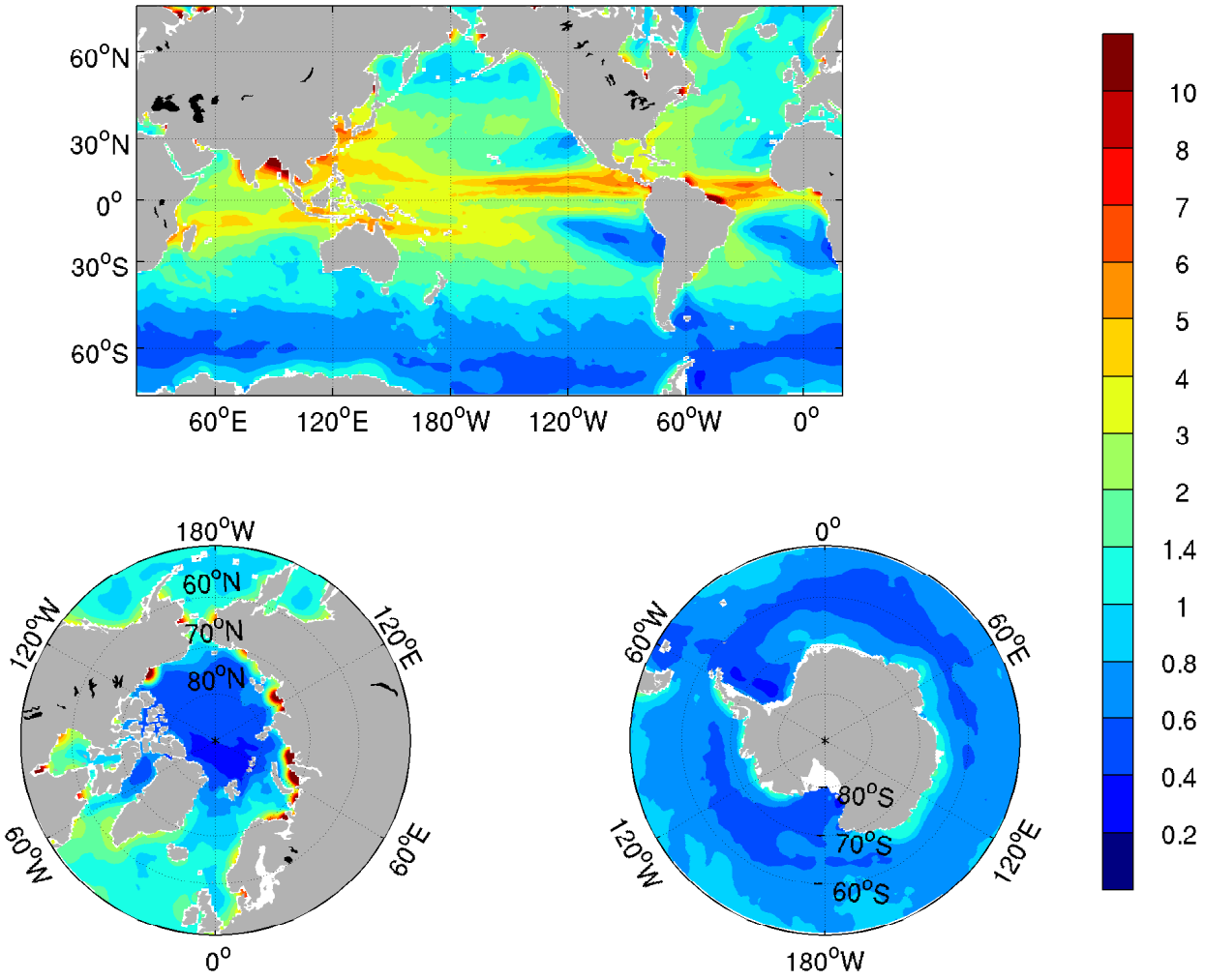

Figure : 1992-2011 standard deviation – E-P-R to ocean+ice (W/m^2)

air-sea freshwater flux

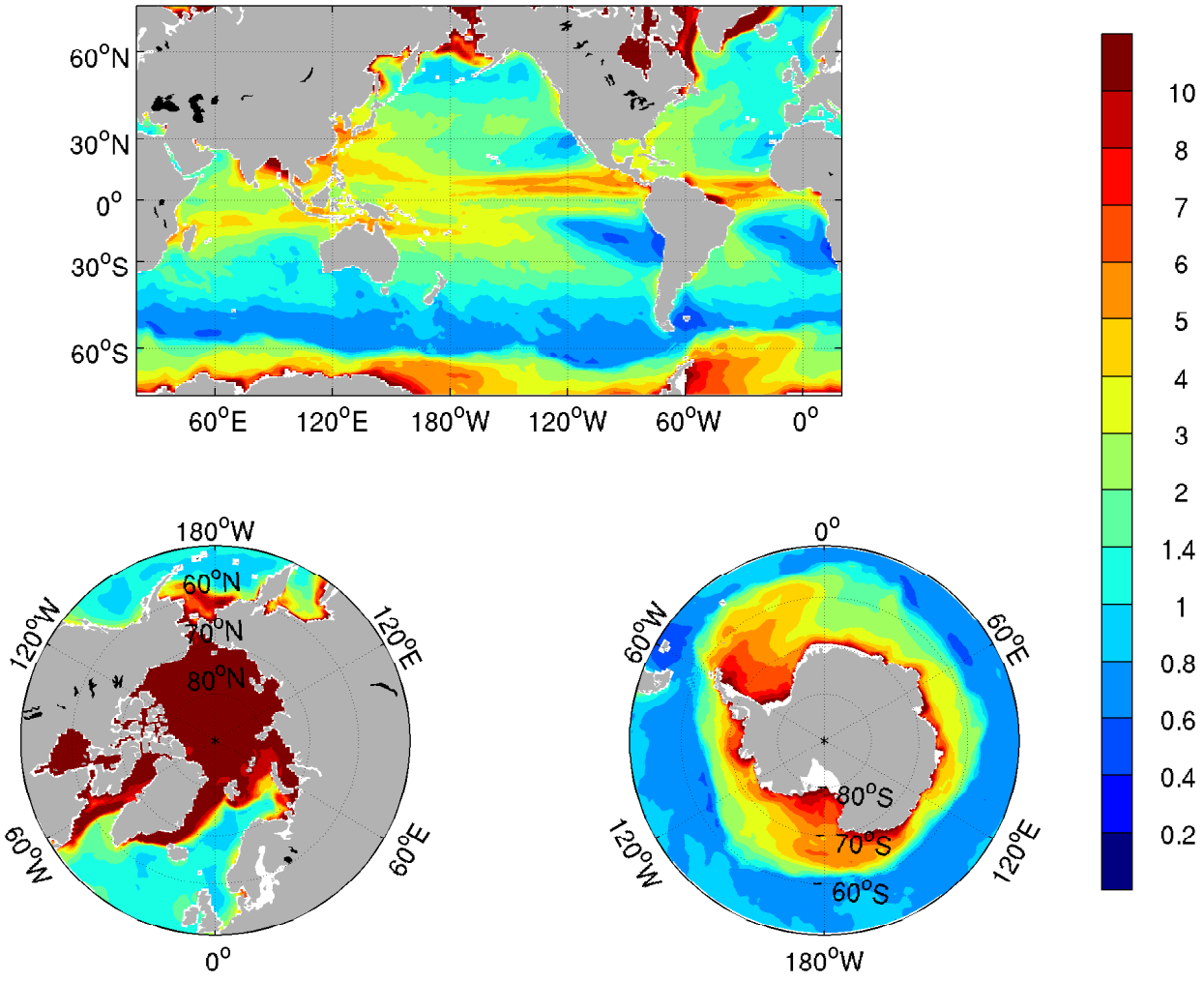

Figure : 1992-2011 standard deviation – E-P-R to ocean (W/m^2)

surface wind stress

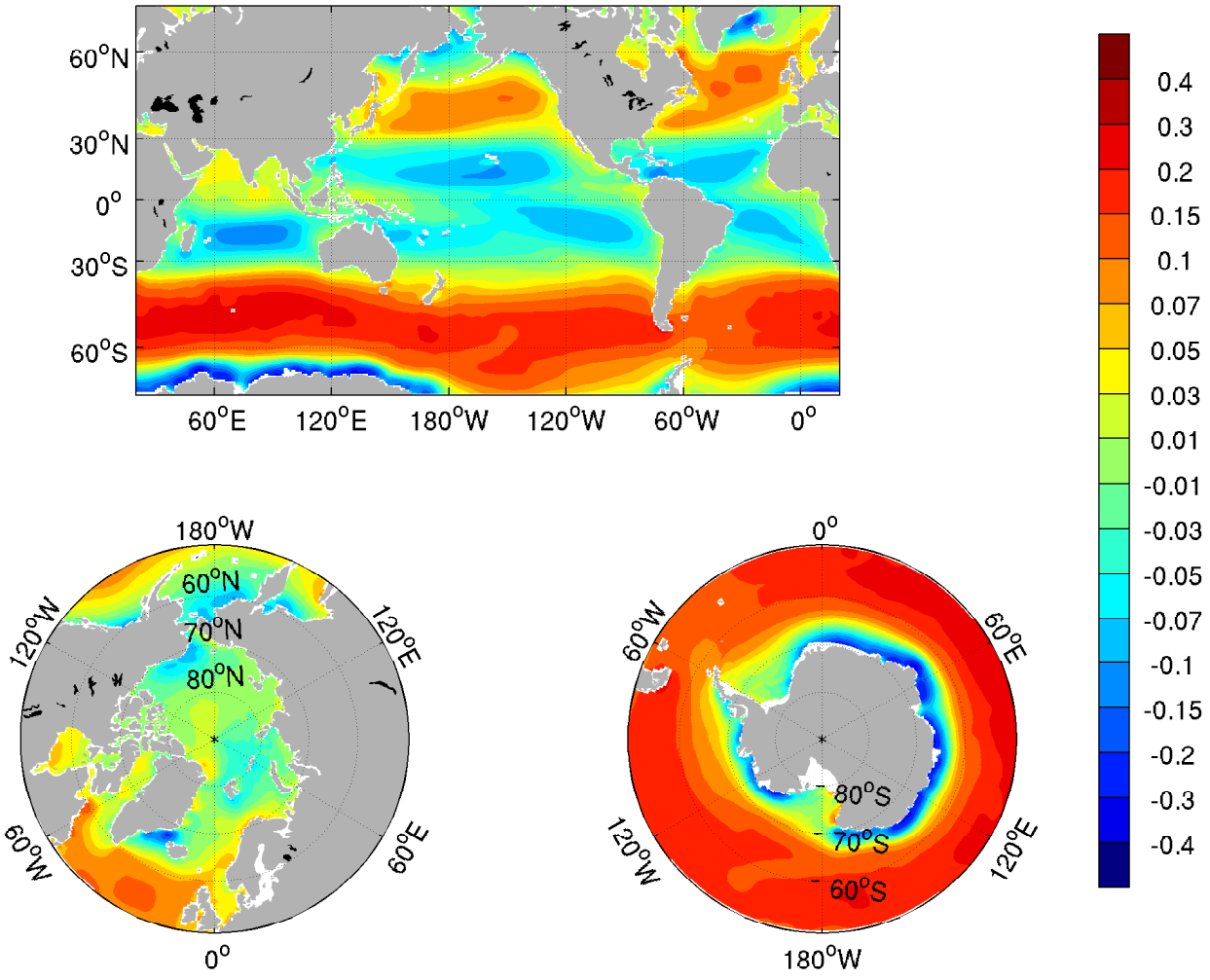

Figure : 1992-2011 mean – zonal wind stress (N/m^2)

surface wind stress

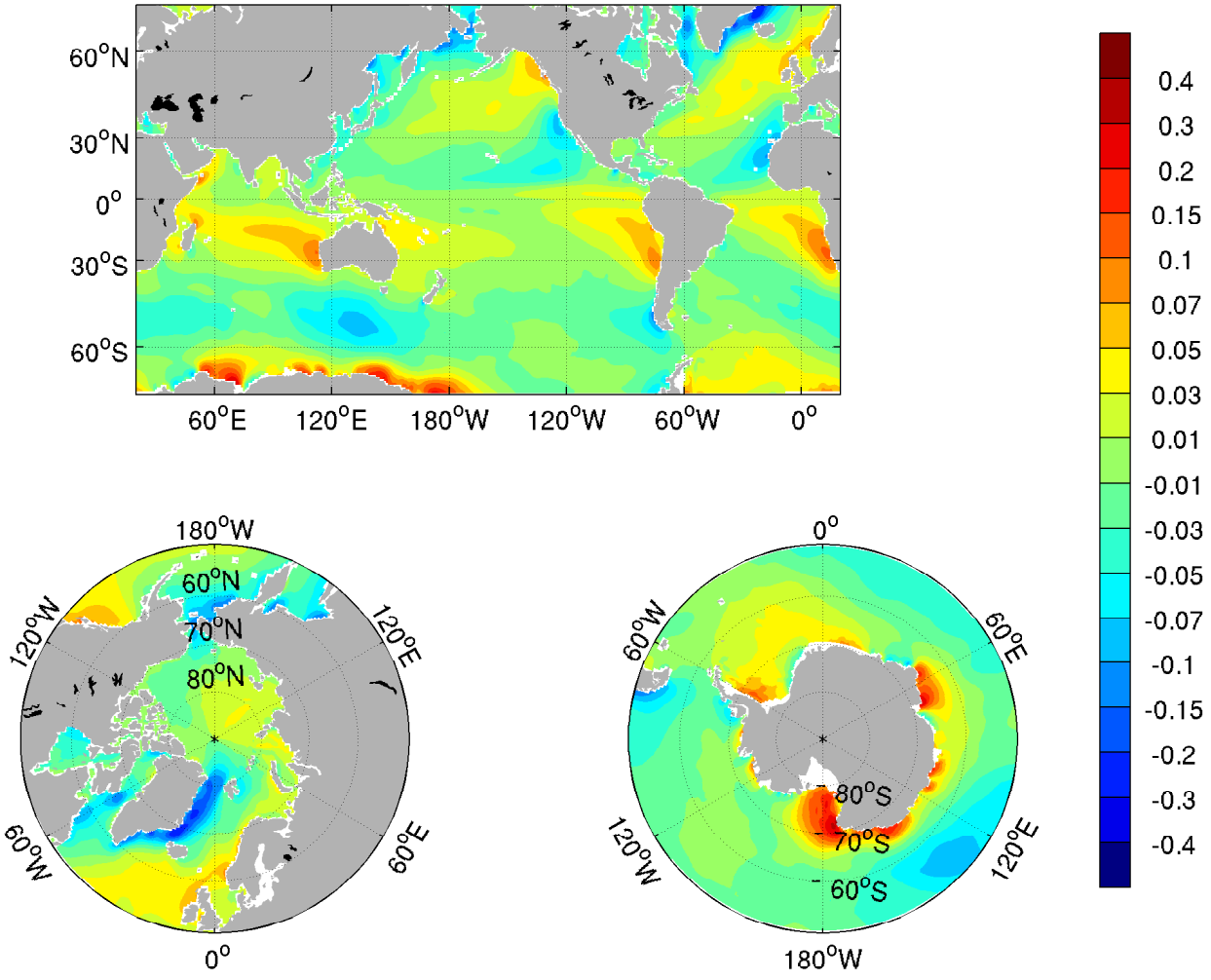

Figure : 1992-2011 mean – meridional wind stress (N/m^2)

surface wind stress

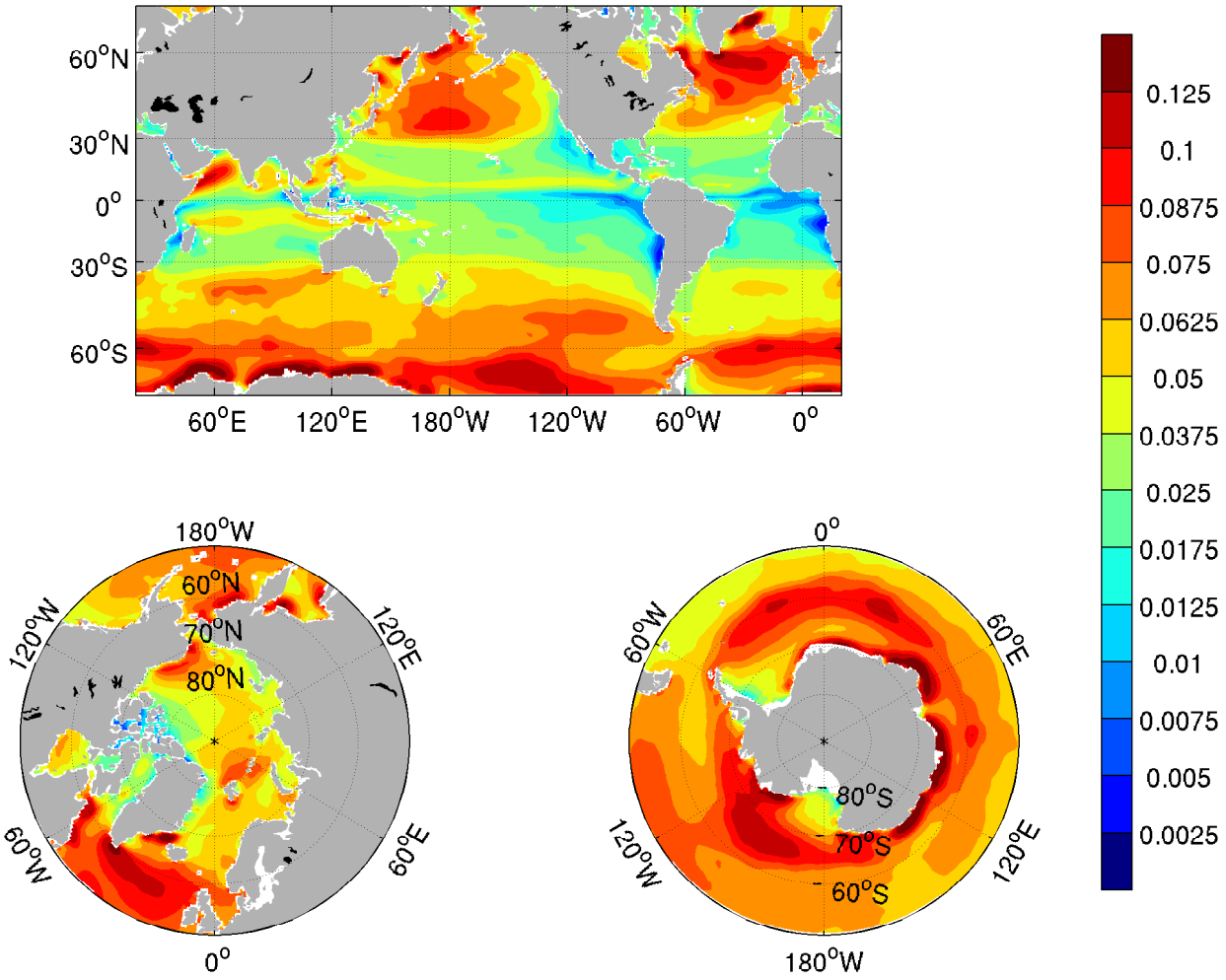

Figure : 1992-2011 standard deviation – tauZ (W/m^2)

surface wind stress

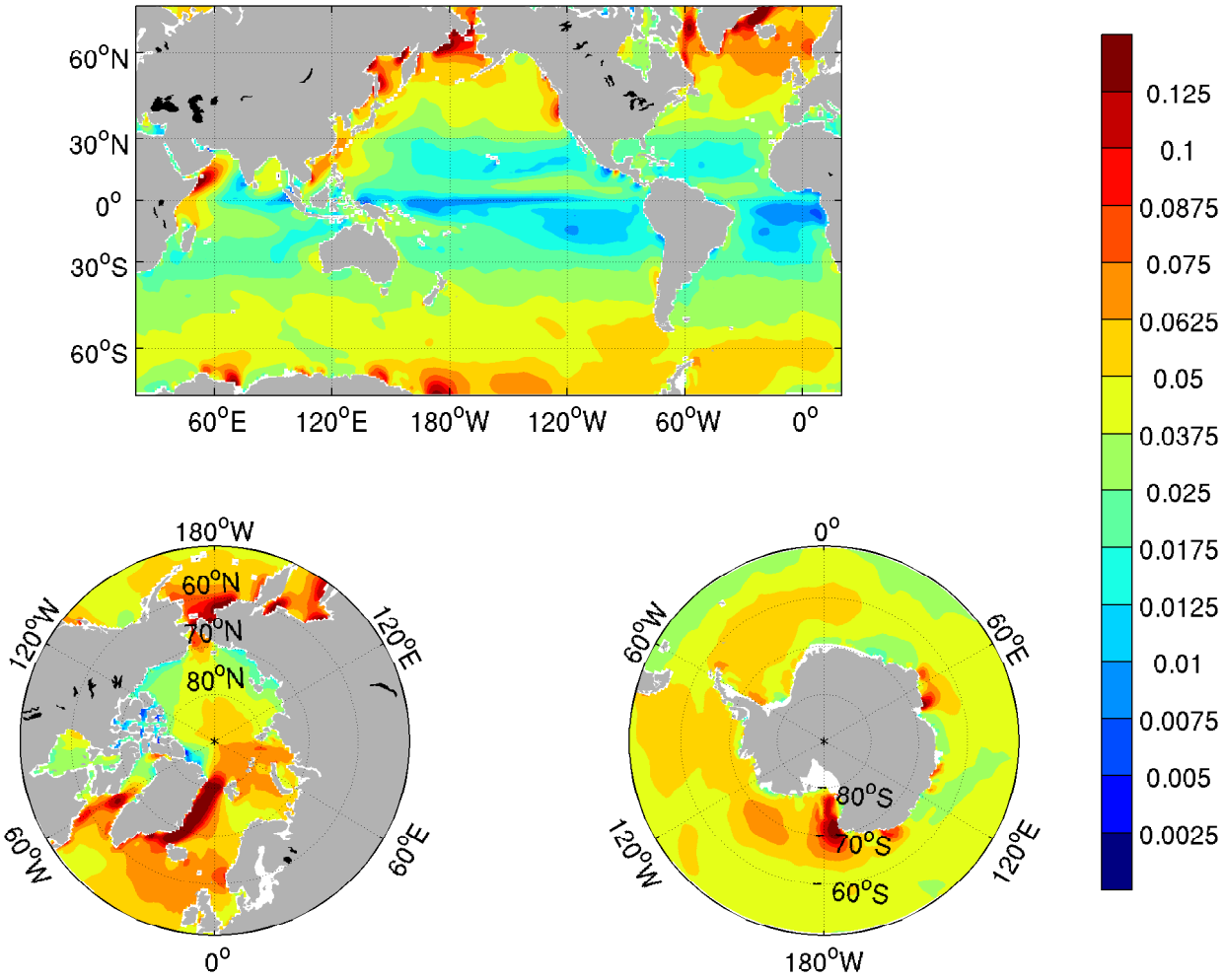

Figure : 1992-2011 standard deviation – tauM (W/m^2)

zonal mean tendencies

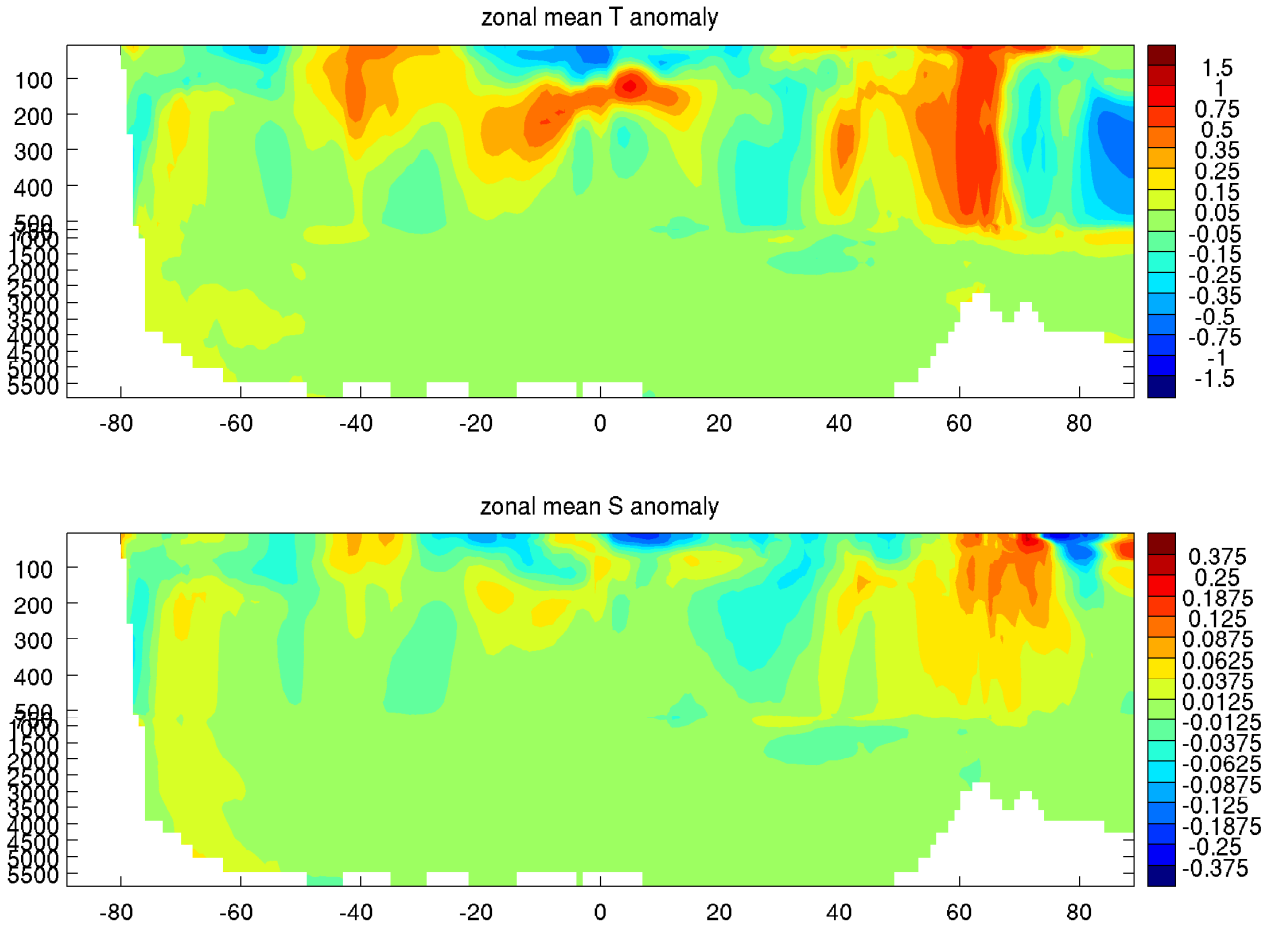

Figure : 1992-2011 , last year minus first year – zonal mean temperature (degC; top) and salinity (psu; bottom)

equatorial sections

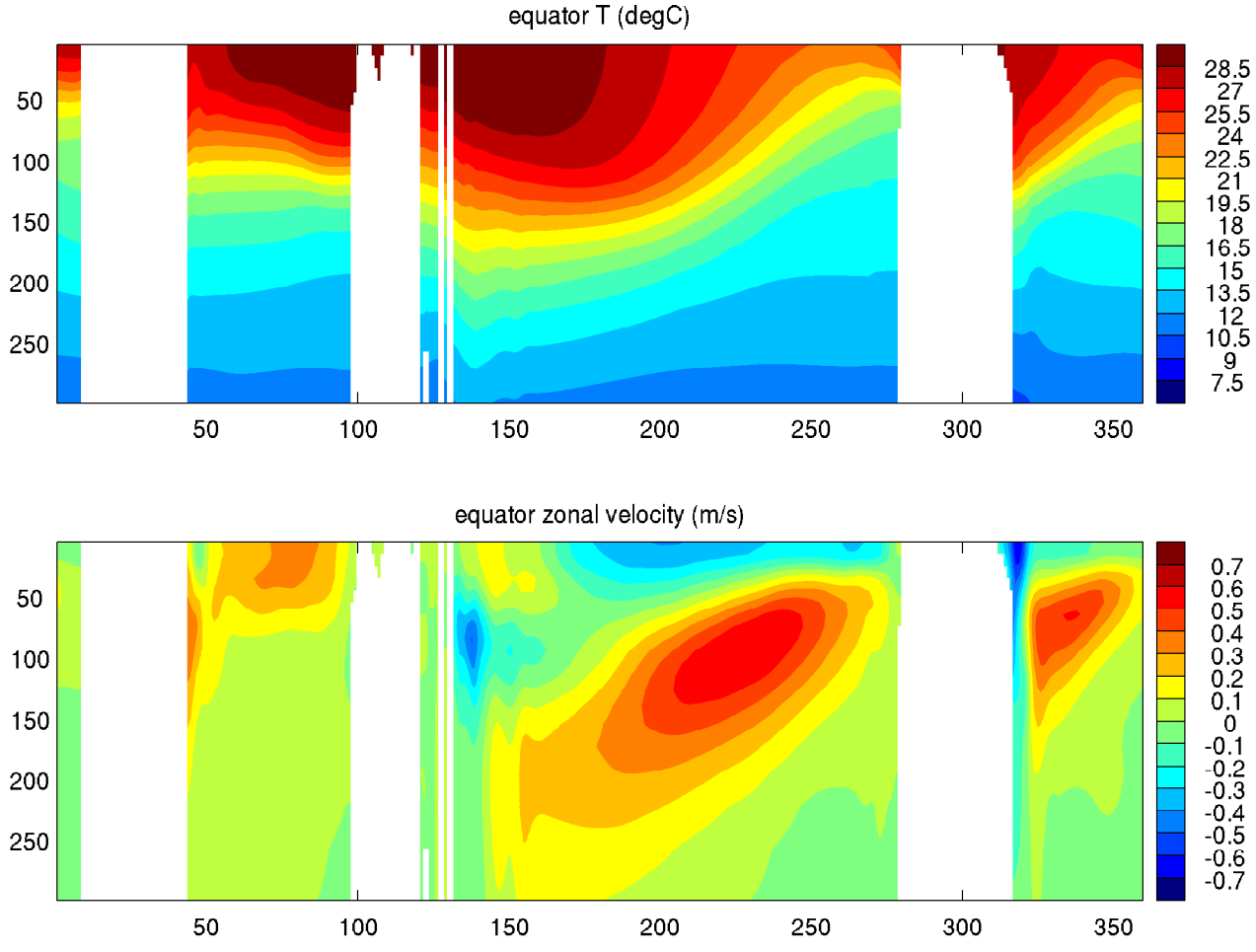

Figure : 1992-2011 mean – equator temperature (degC;top) and zonal velocity (m/s;bottom)

global mean properties

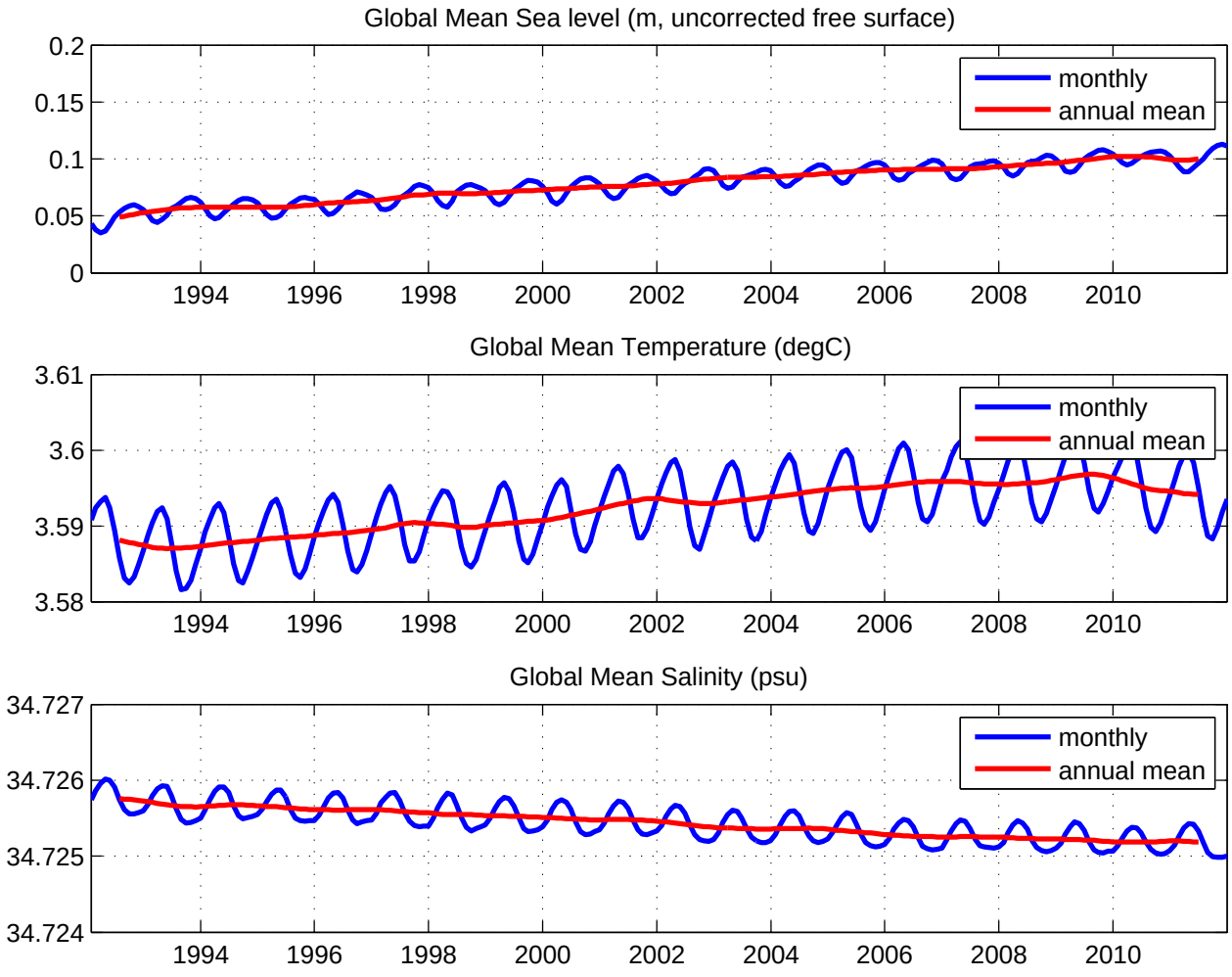

Figure : global mean T (degC; top) and S (psu; bottom)

global mean properties

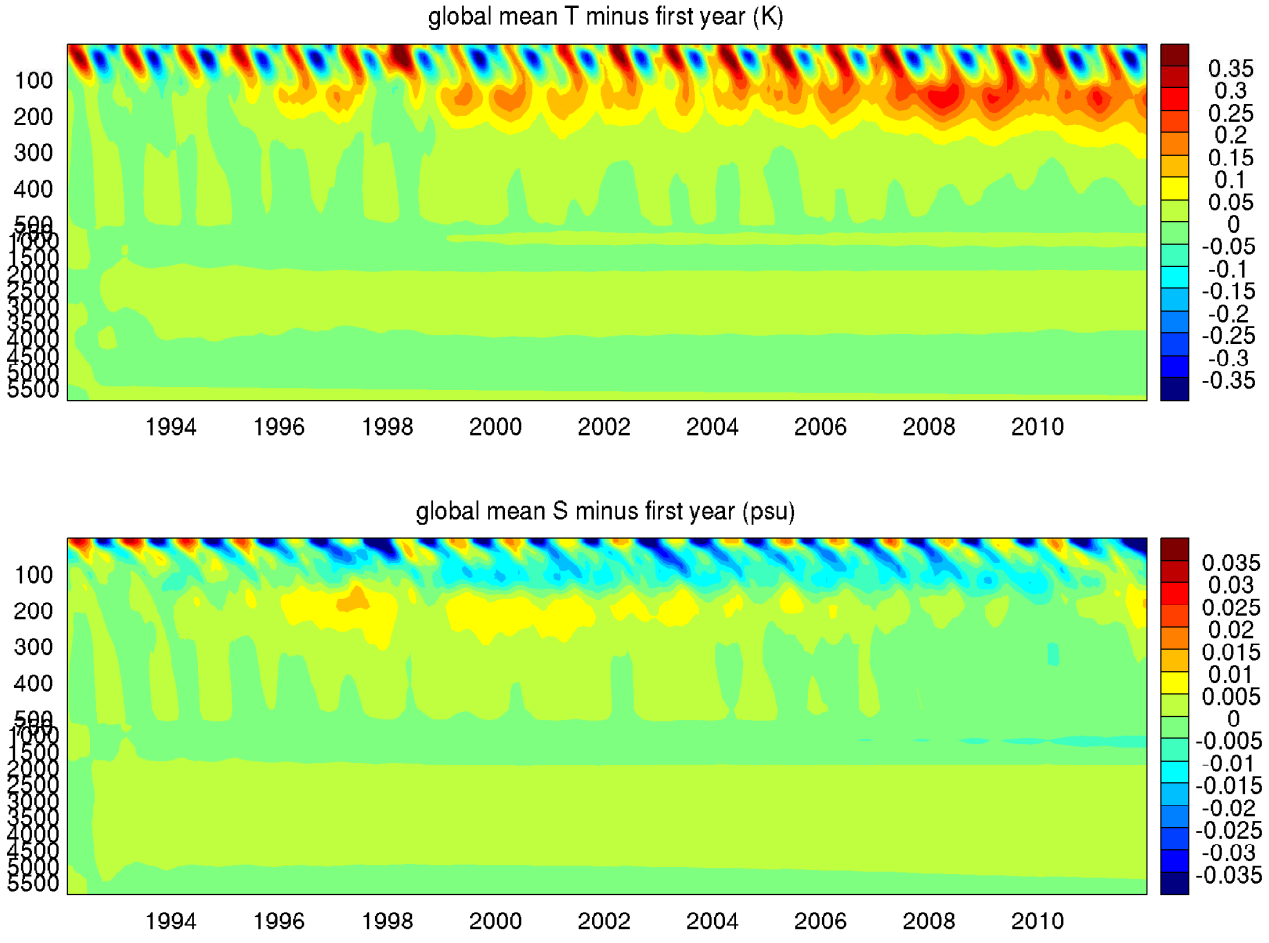

Figure : global mean temperature (K; top) and salinity (psu; bottom) minus first year

zonal mean properties

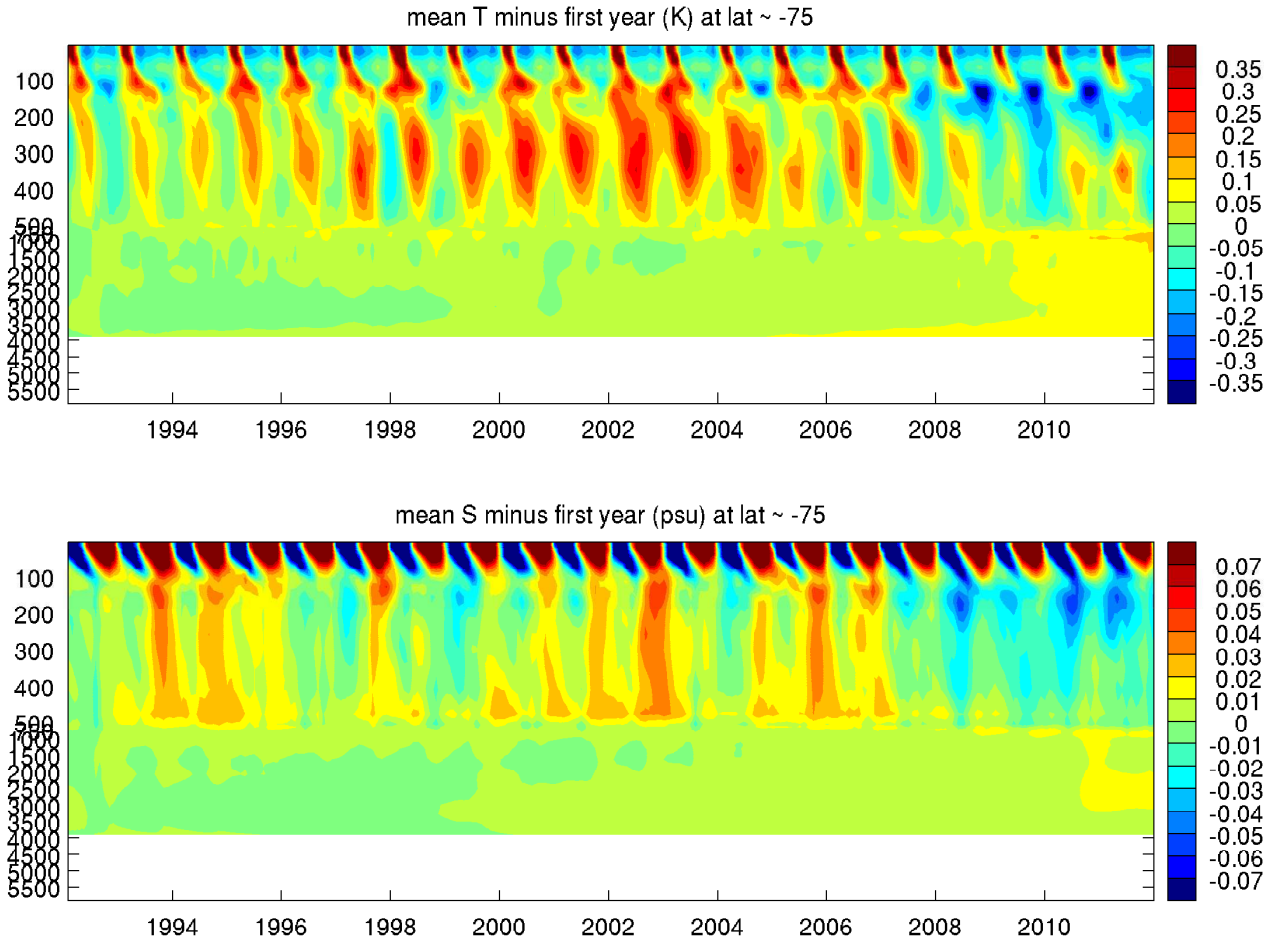

Figure : mean temperature (top; K) and salinity (bottom; psu) minus first year at lat $\approx$ -75

zonal mean properties

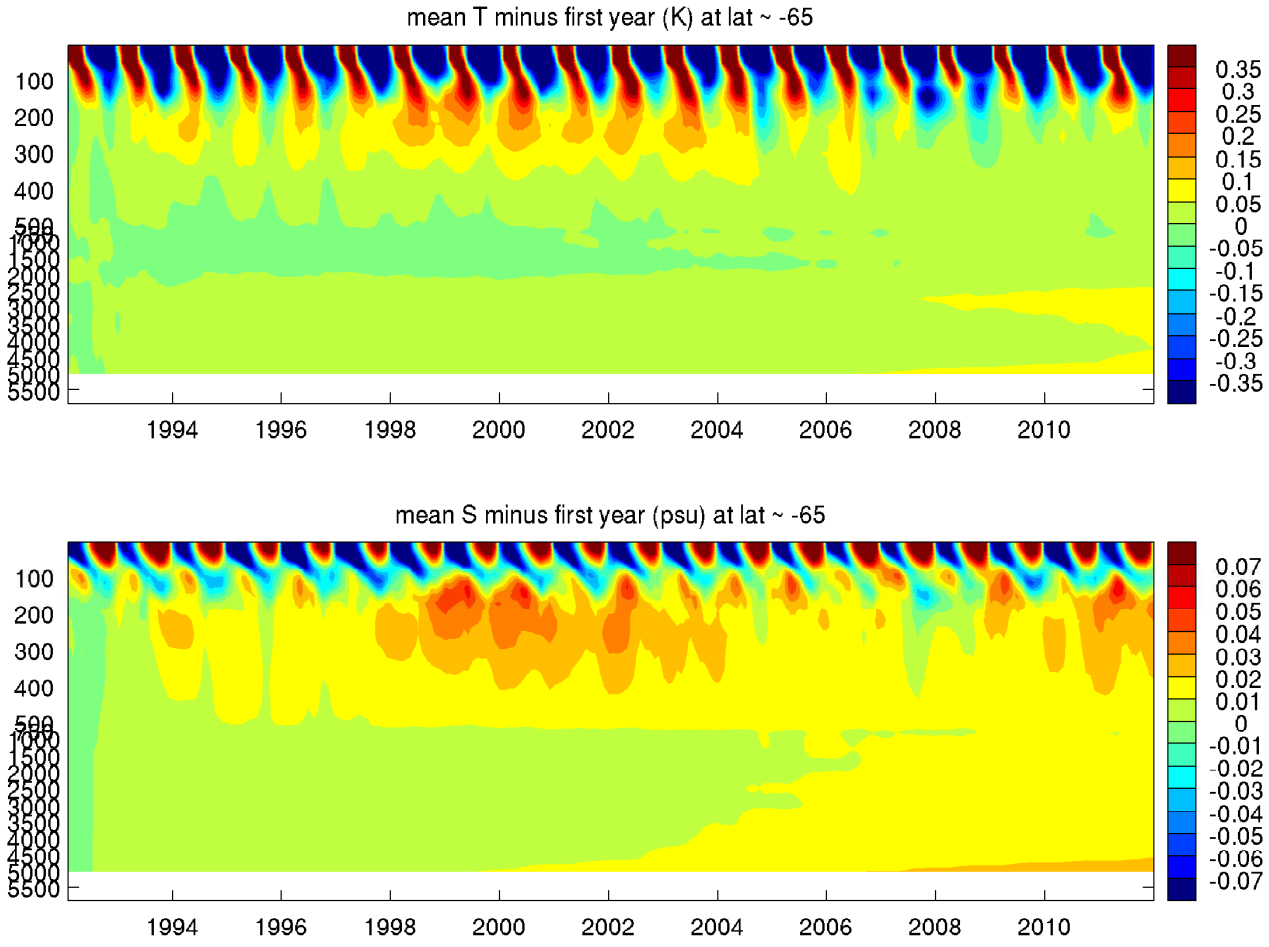

Figure : mean temperature (top; K) and salinity (bottom; psu) minus first year at lat $\approx$ -65

zonal mean properties

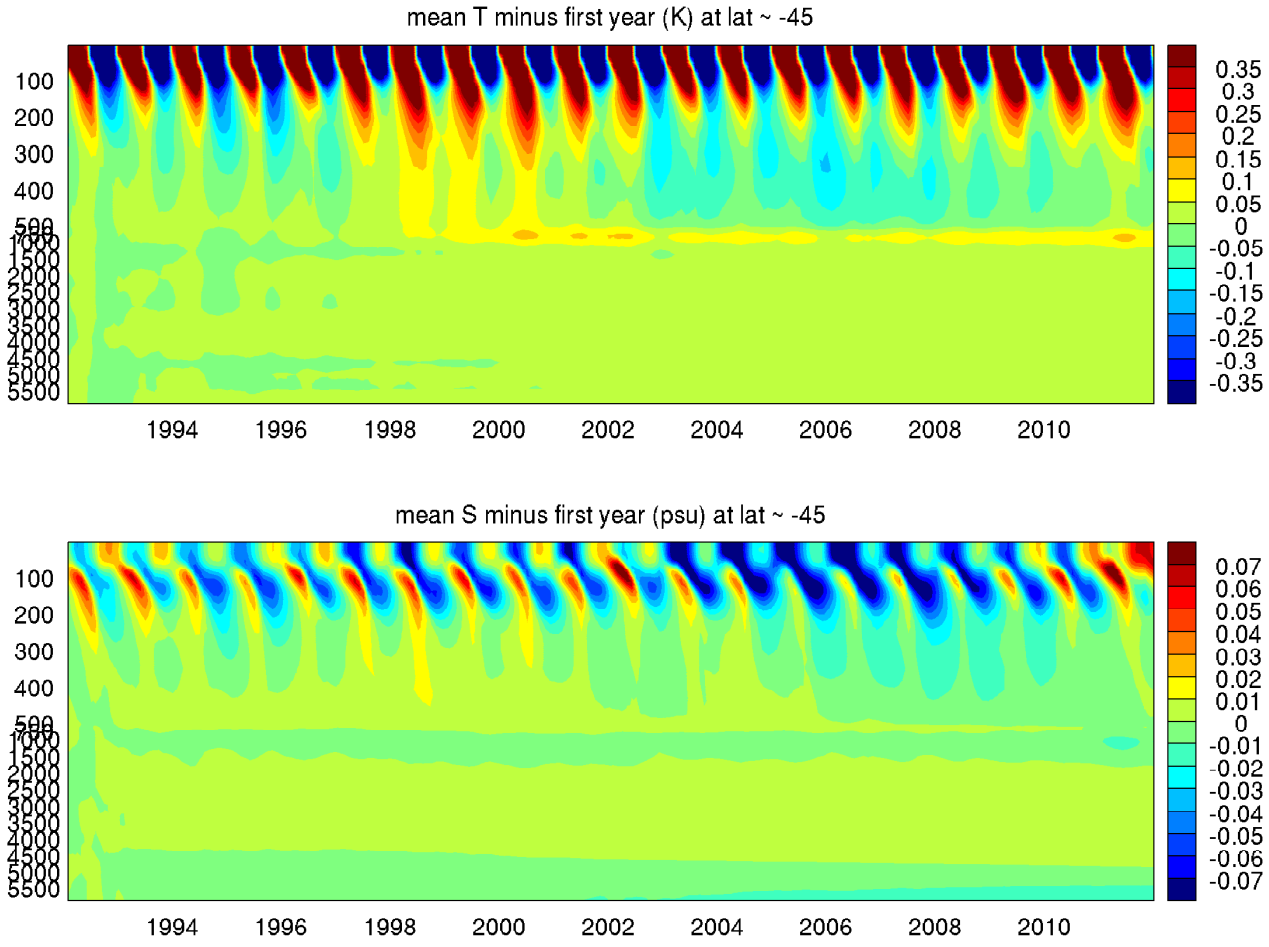

Figure : mean temperature (top; K) and salinity (bottom; psu) minus first year at lat $\approx$ -45

zonal mean properties

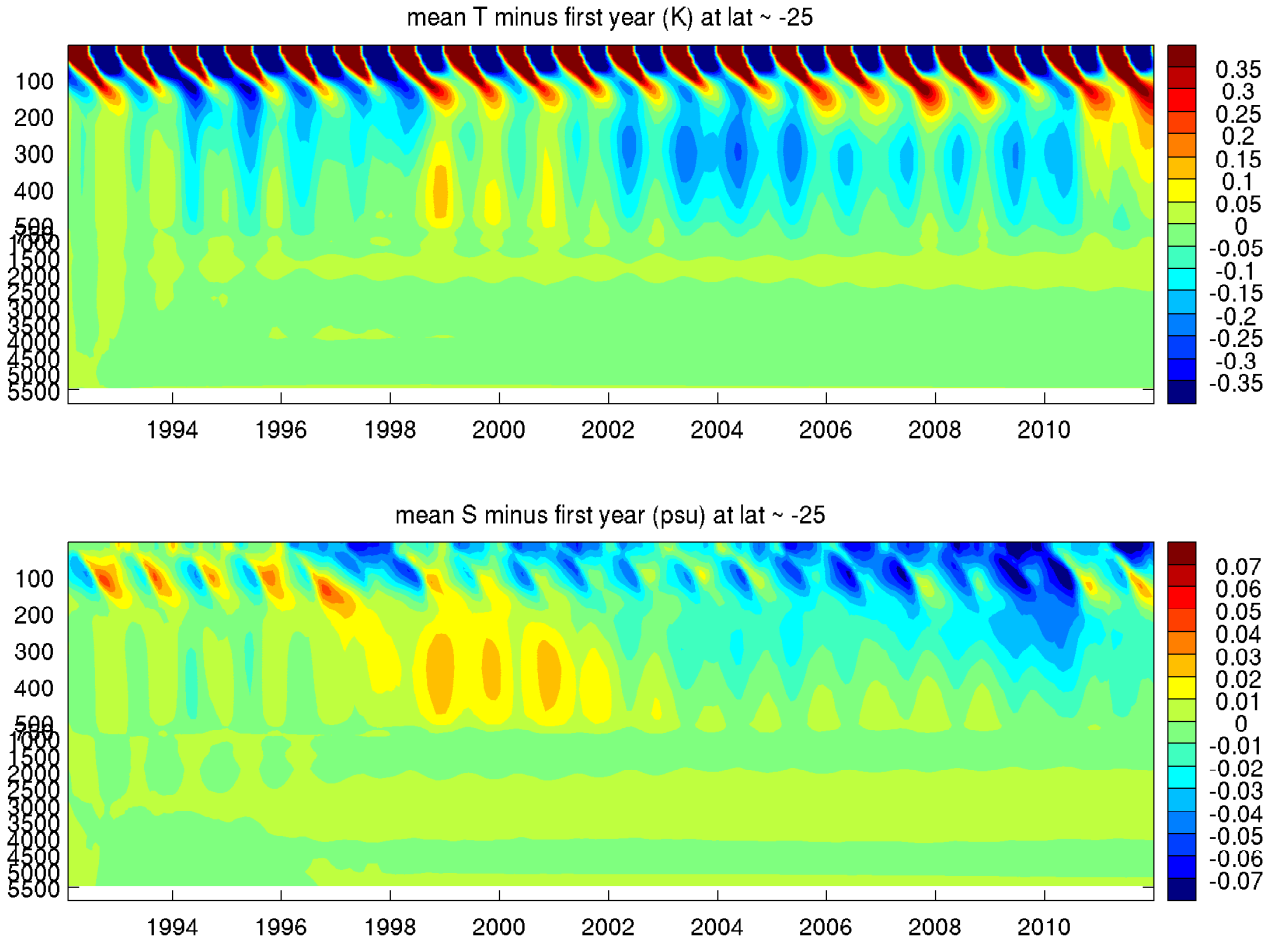

Figure : mean temperature (top; K) and salinity (bottom; psu) minus first year at lat $\approx$ -25

zonal mean properties

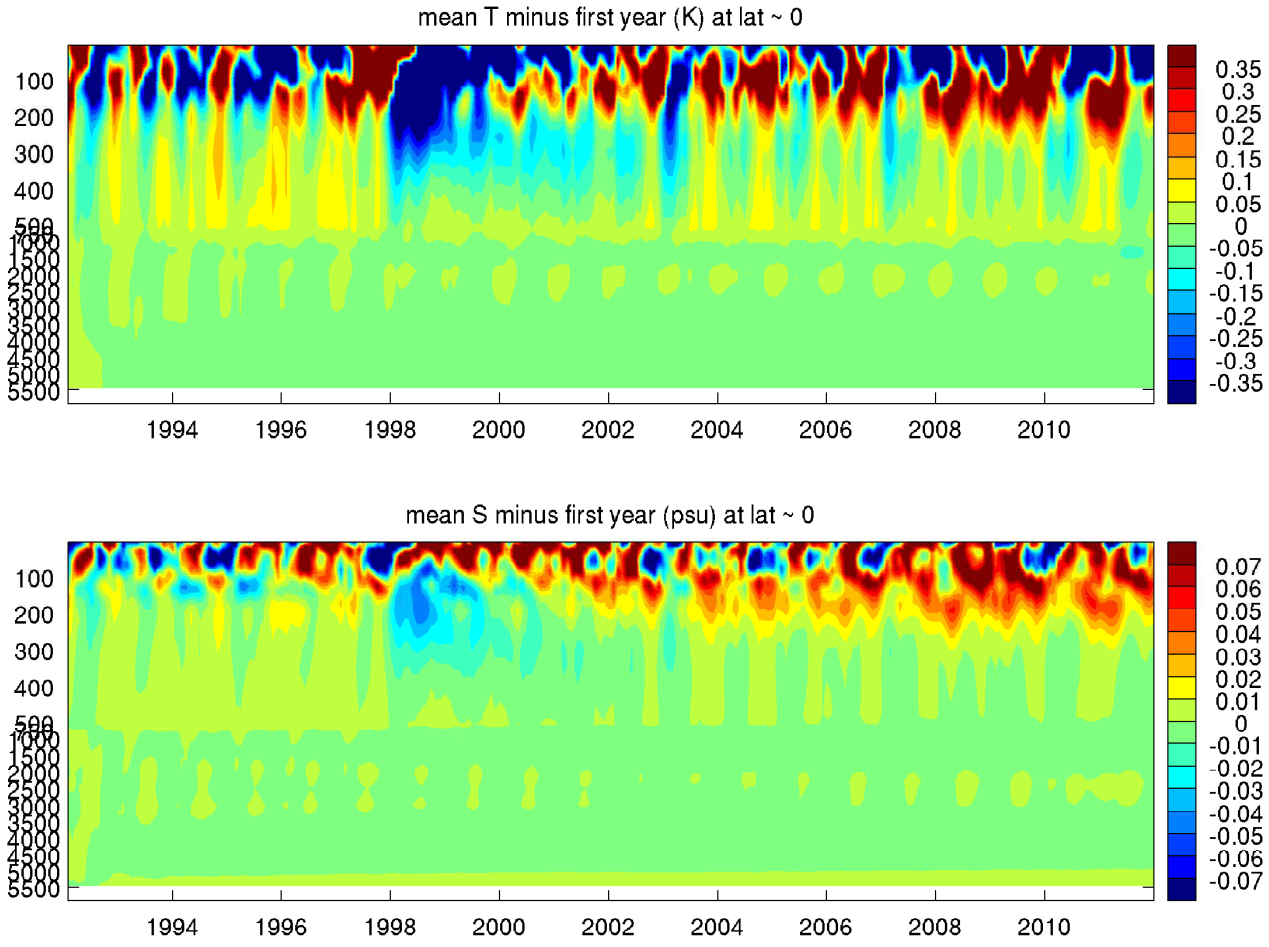

Figure : mean temperature (top; K) and salinity (bottom; psu) minus first year at lat ≈ 0

zonal mean properties

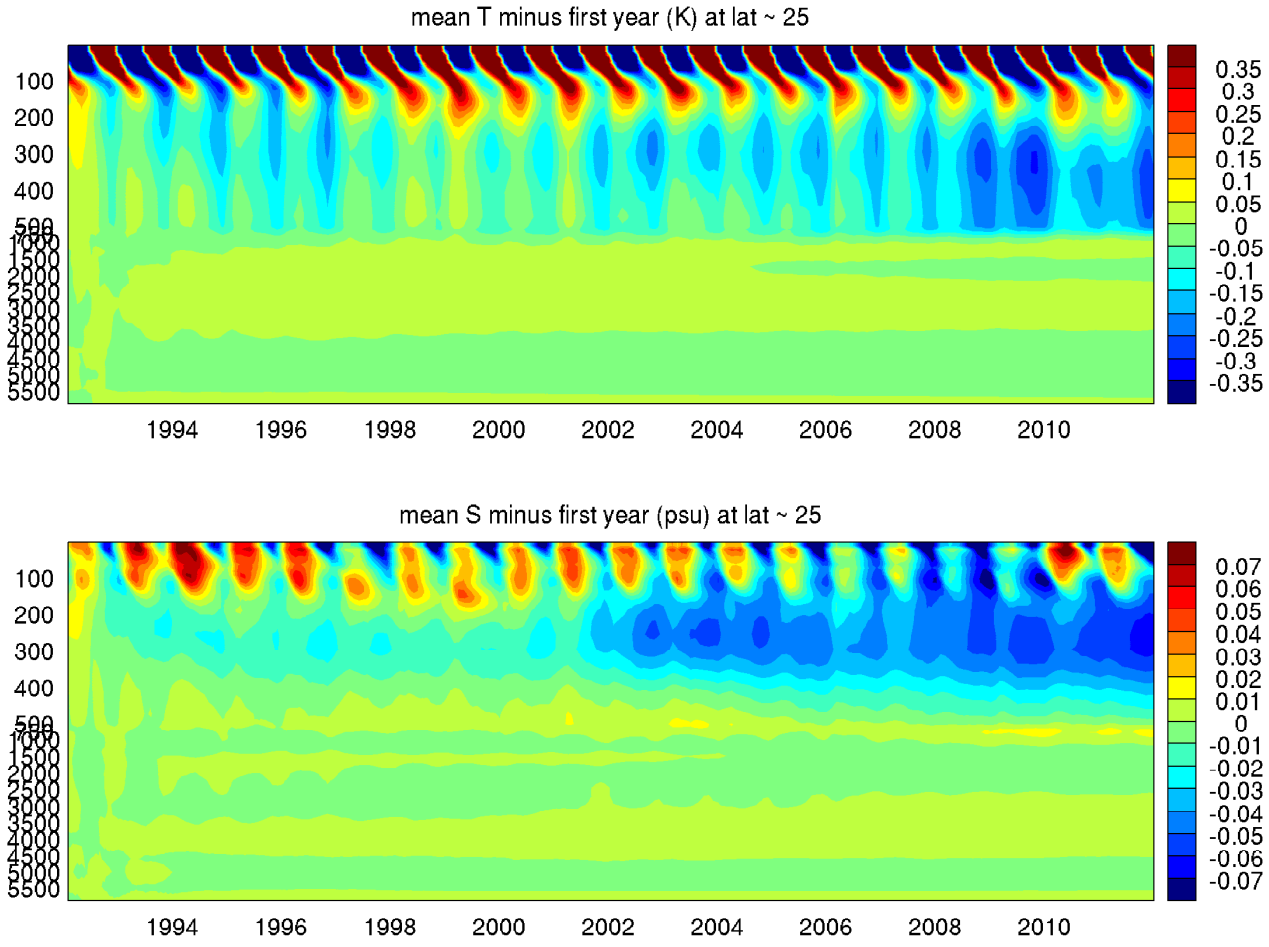

Figure : mean temperature (top; K) and salinity (bottom; psu) minus first year at lat $\approx$ 25

zonal mean properties

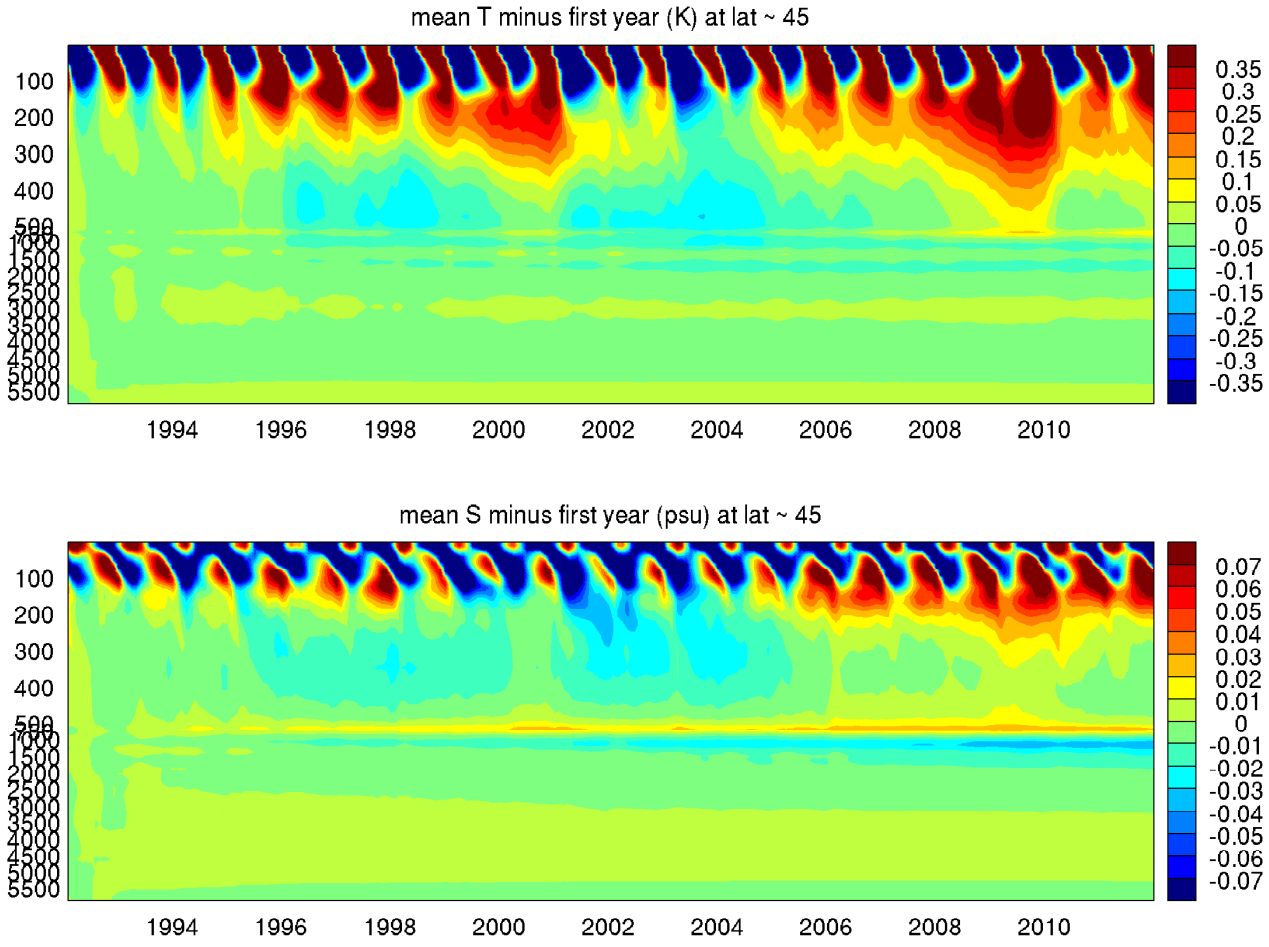

Figure : mean temperature (top; K) and salinity (bottom; psu) minus first year at lat $\approx$ 45

zonal mean properties

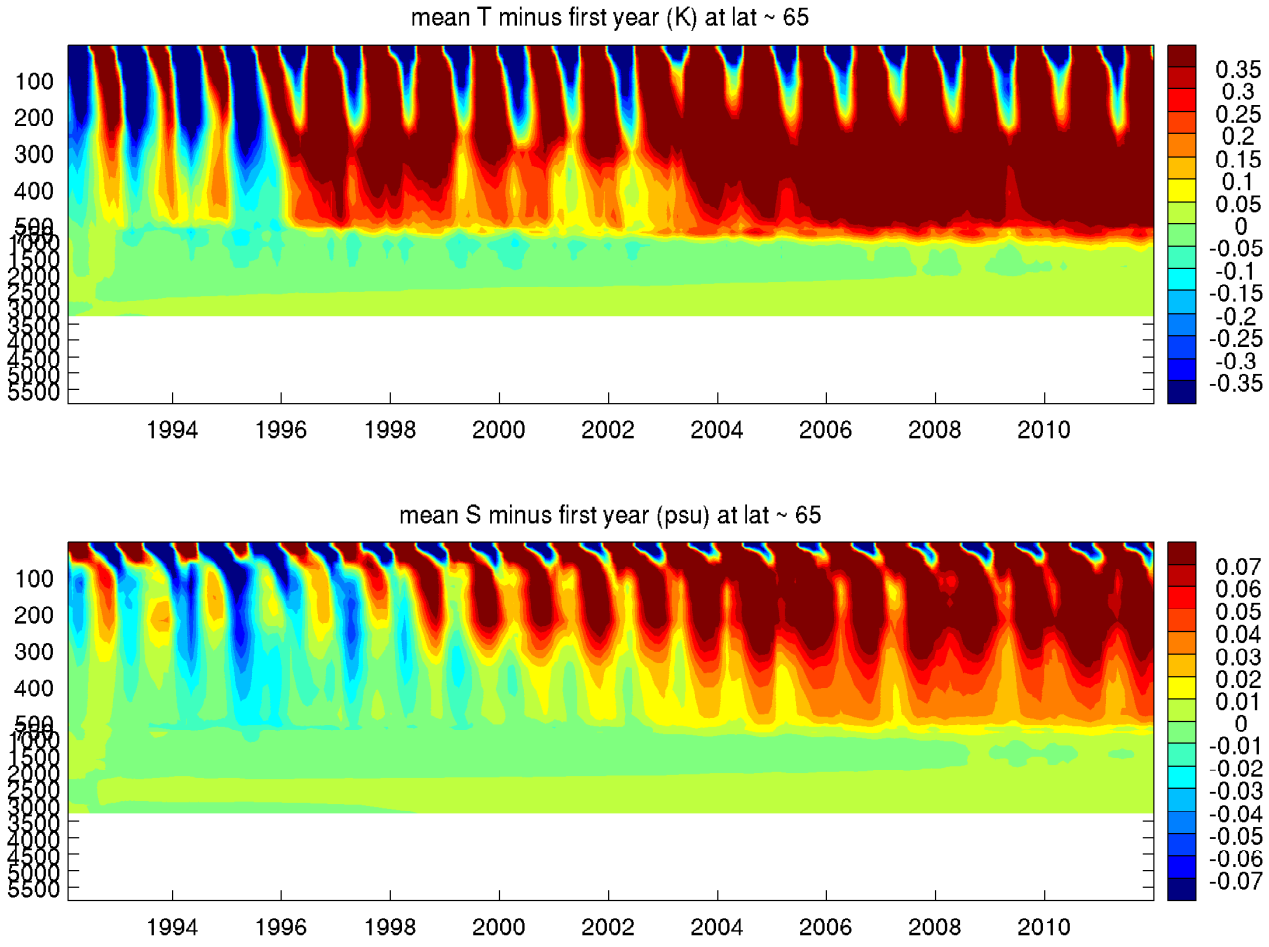

Figure : mean temperature (top; K) and salinity (bottom; psu) minus first year at lat $\approx$ 65

zonal mean properties

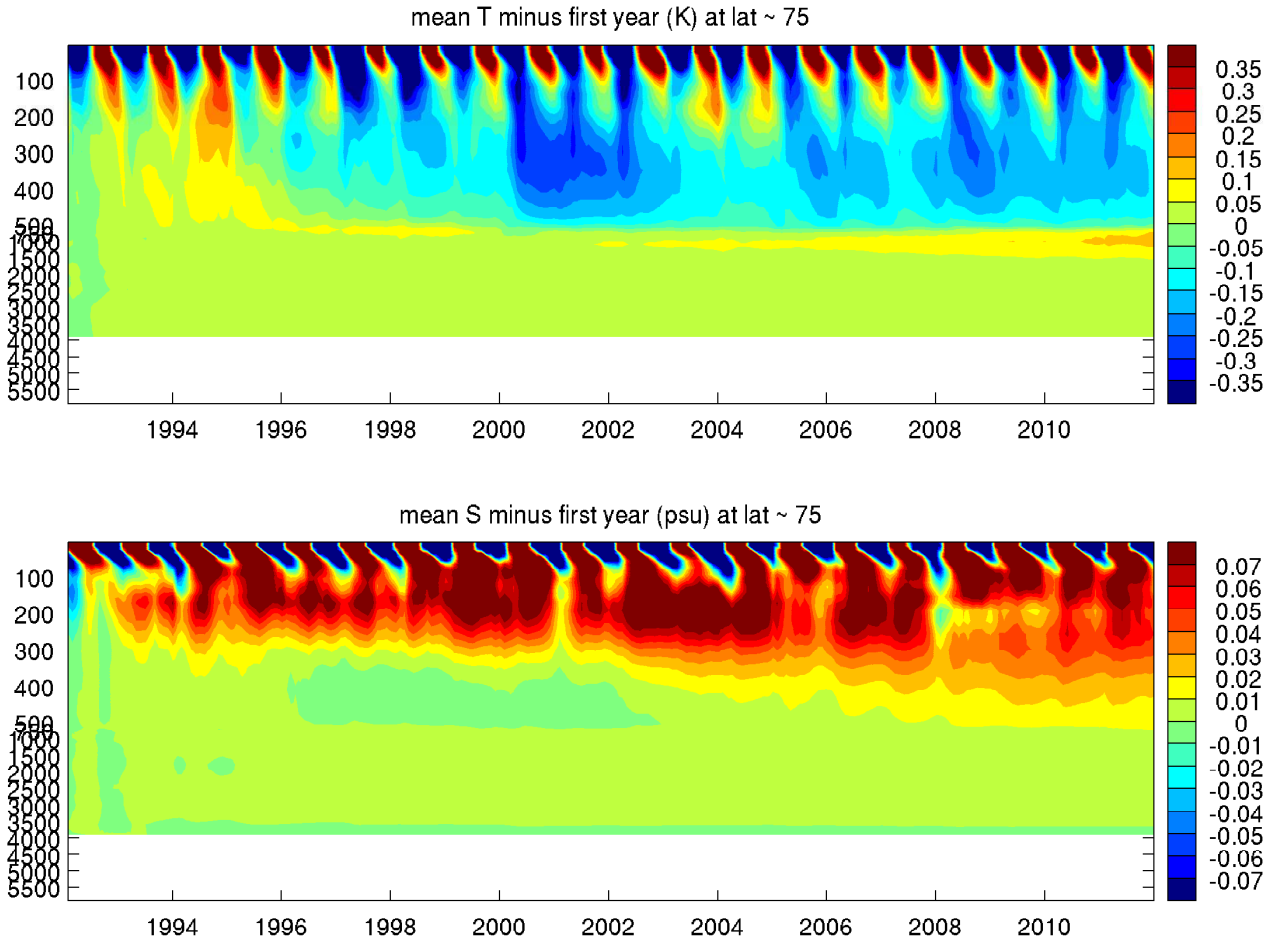

Figure : mean temperature (top; K) and salinity (bottom; psu) minus first year at lat $\approx$ 75

zonal mean properties (surface)

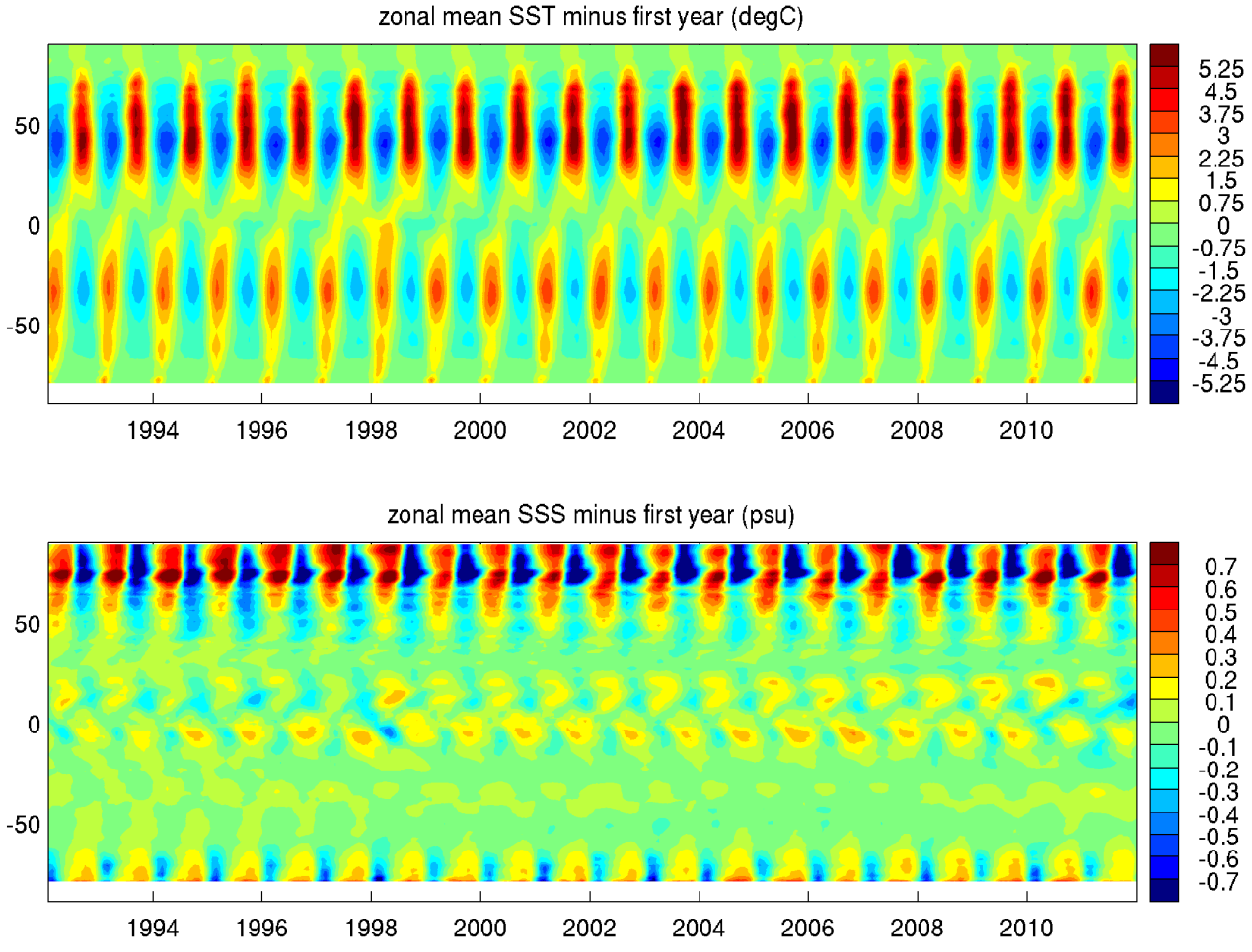

Figure : zonal mean temperature (degC; top) and salinity (psu; bottom) minus first year (psu) at 5m depth

zonal mean properties (surface)

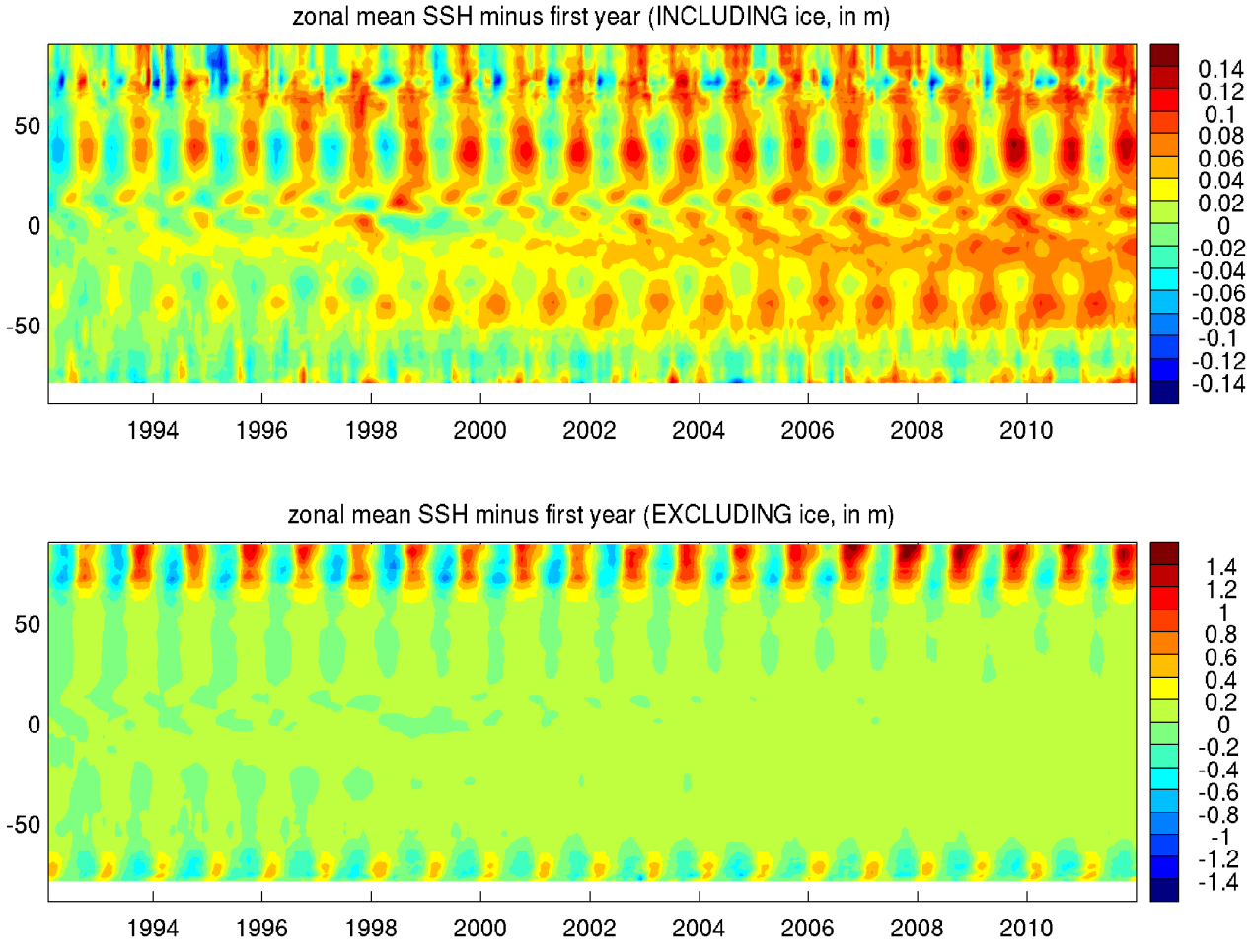

Figure : zonal mean SSH (m, uncorrected free surface) minus first year, including ice (top) and below ice (bottom)

zonal mean properties (surface)

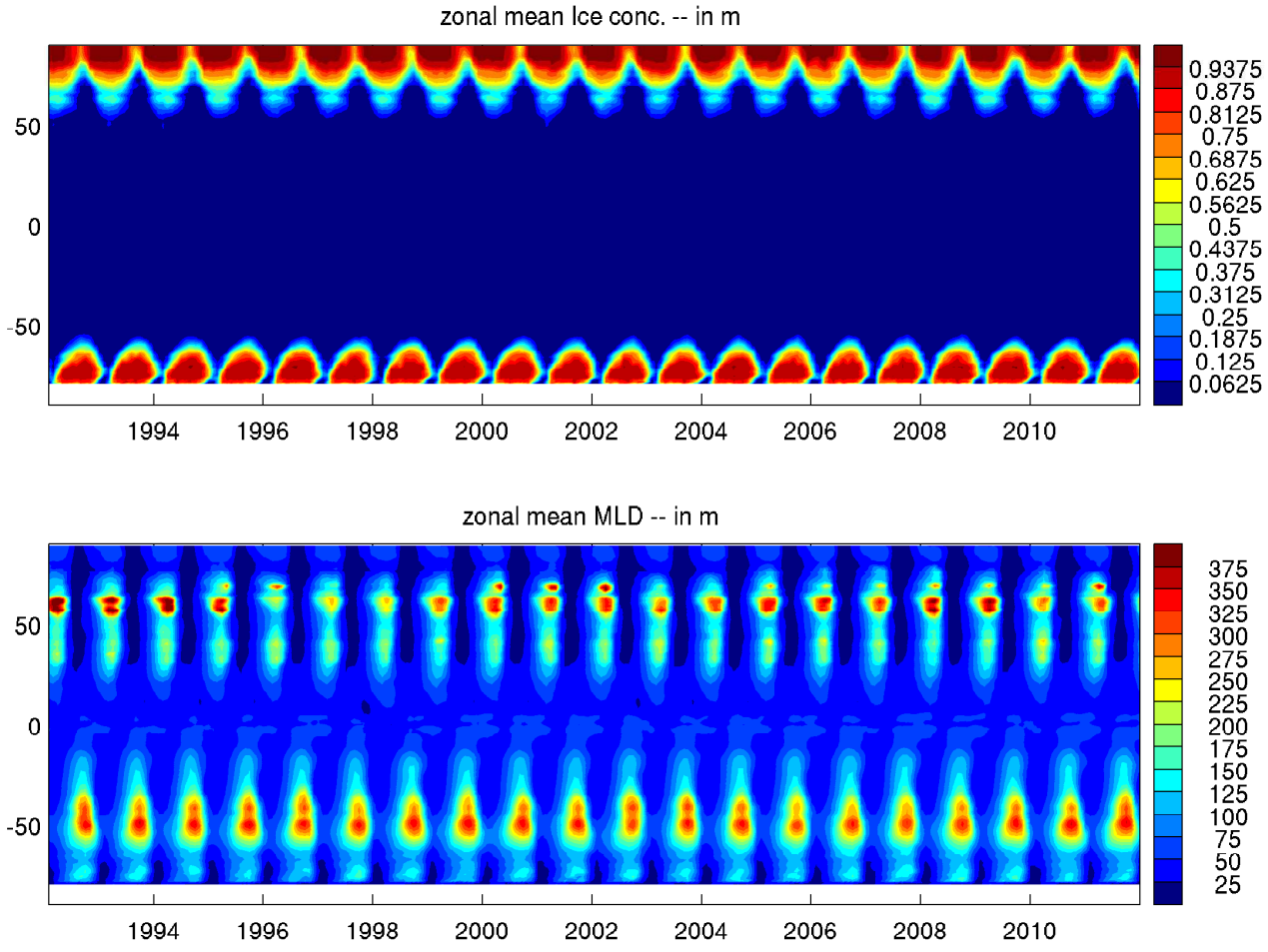

Figure : zonal mean ice concentration (no units) and mixed layer depth (m)

seaice time series

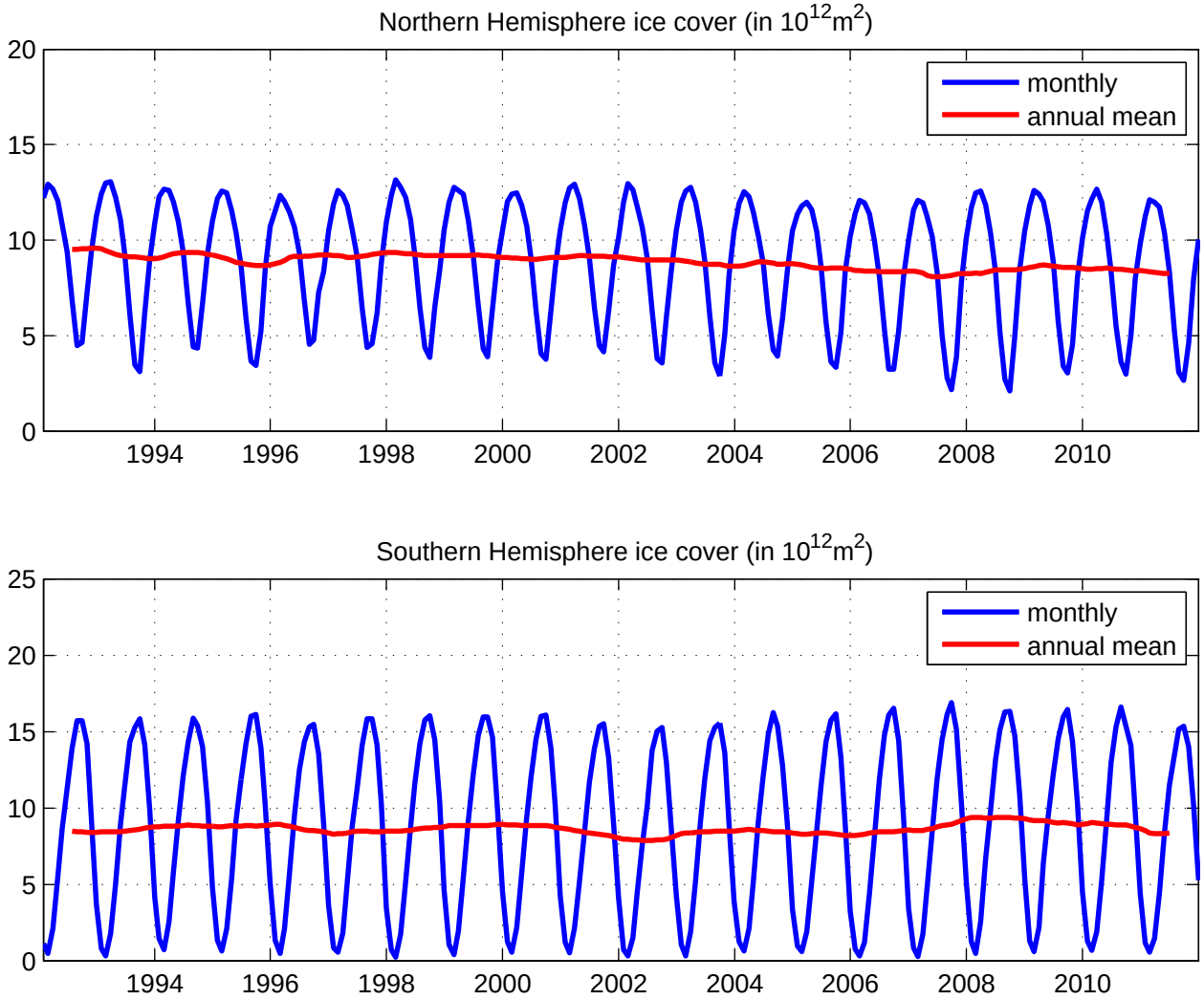

Figure : sea ice cover (in $10^{12}m^2$) in northern (top) and southern (bottom) hemisphere

seaice time series

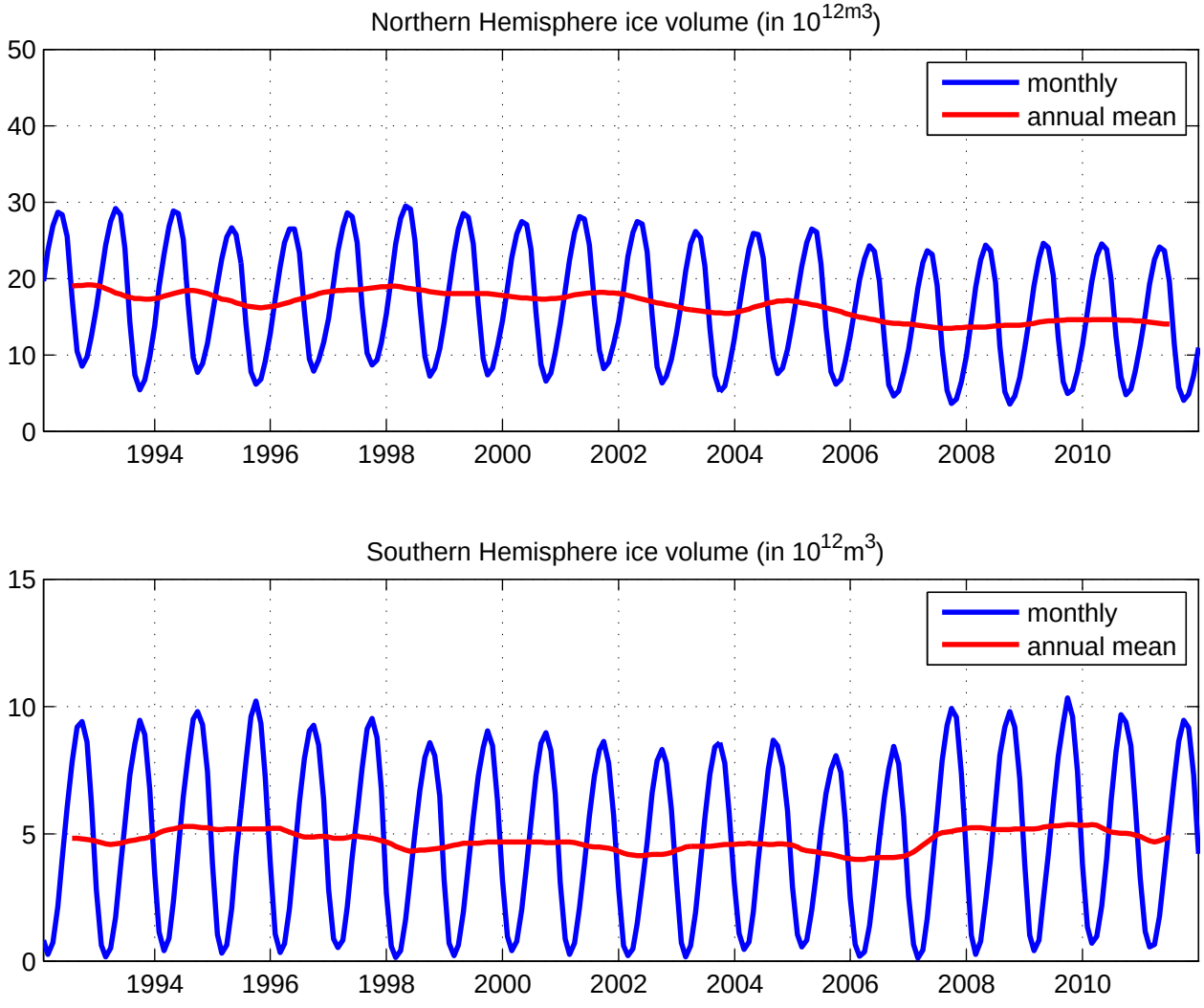

Figure : sea ice volume (in $10^{12}m^3$) in northern (top) and southern (bottom) hemisphere

seaice time series

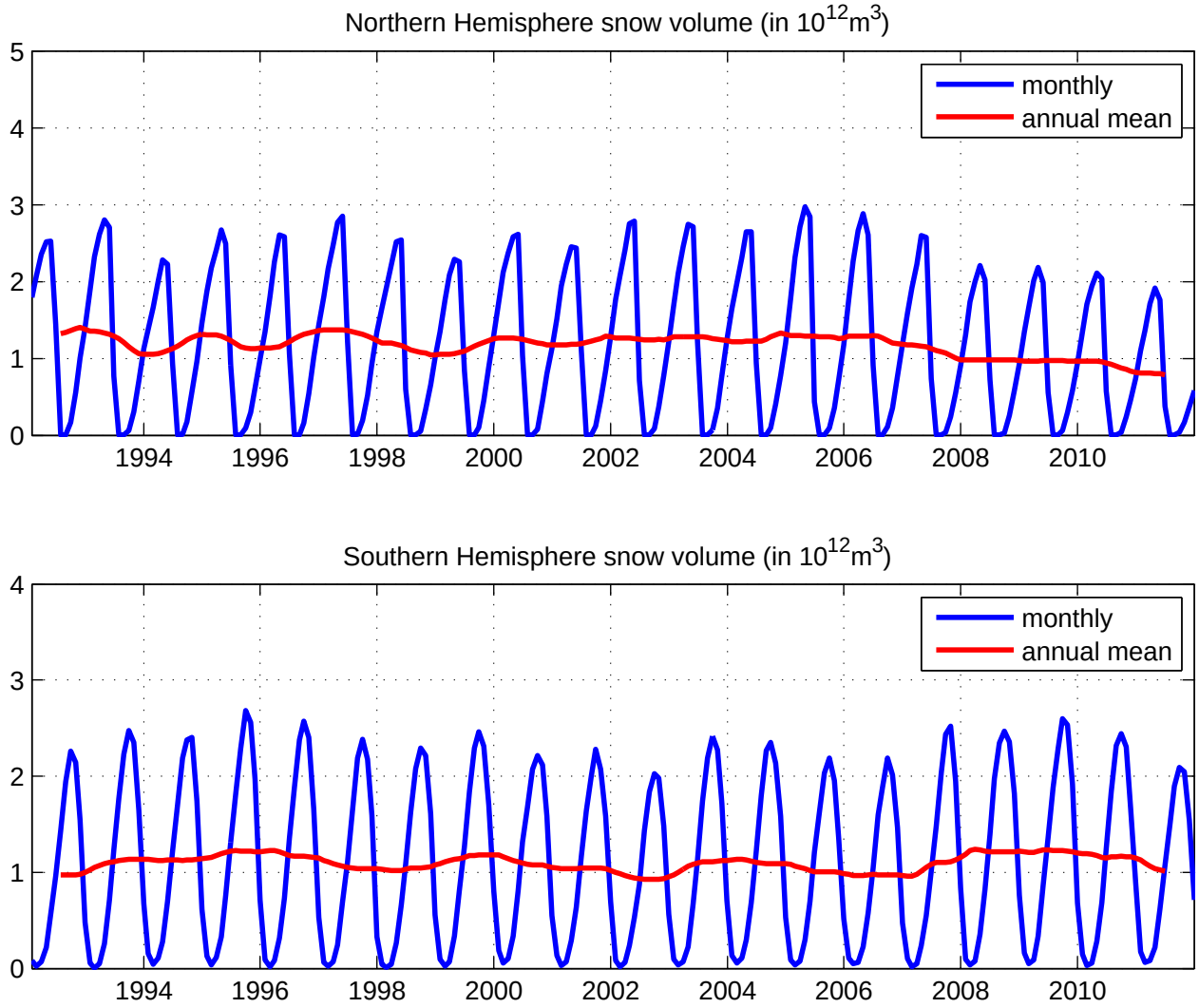

Figure : snow volume (in $10^{12}m^3$) in northern (top) and southern (bottom) hemisphere

seaice time series

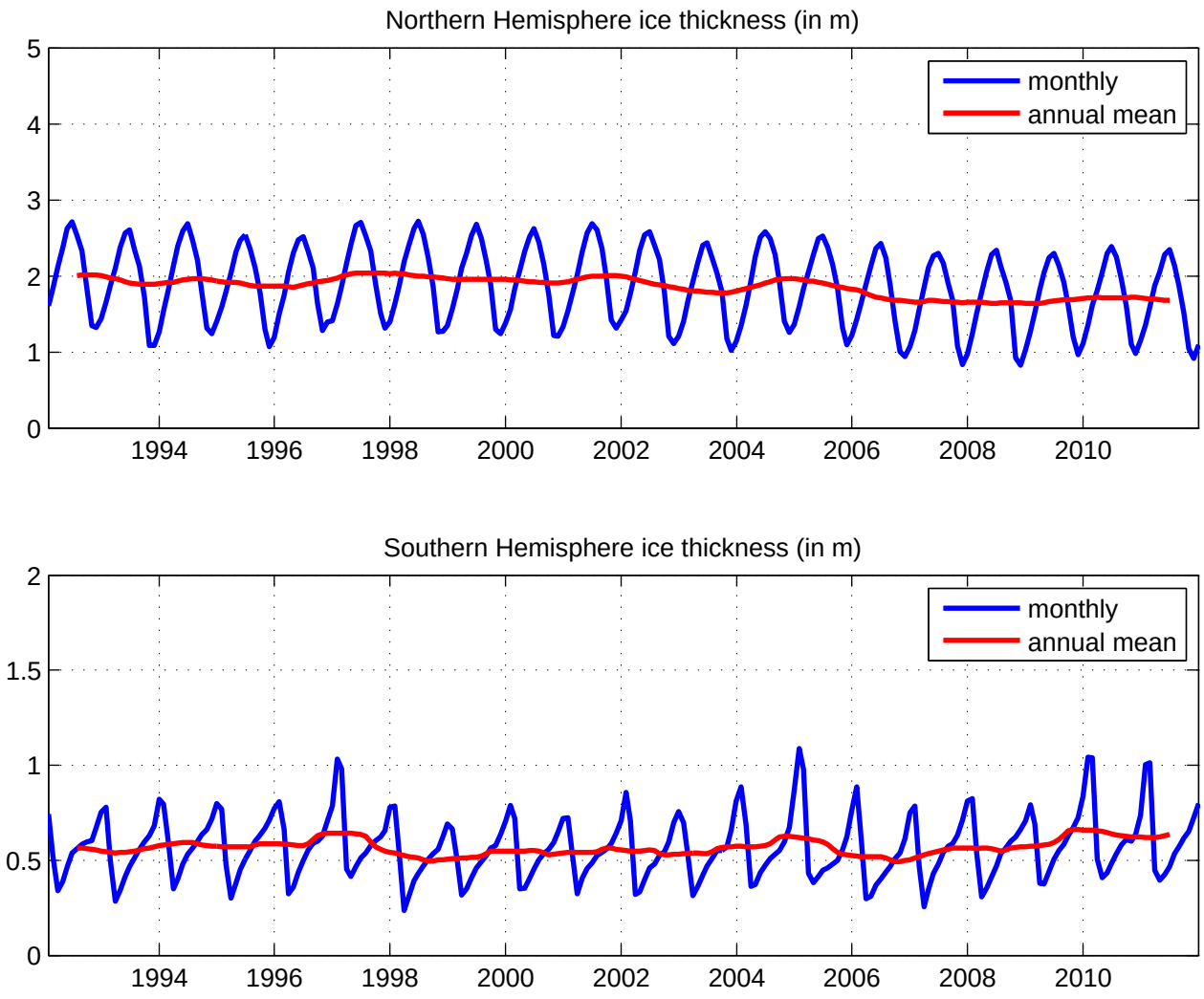

Figure : sea ice thickness (in m) in northern (top) and southern (bottom) hemisphere

seaice time series

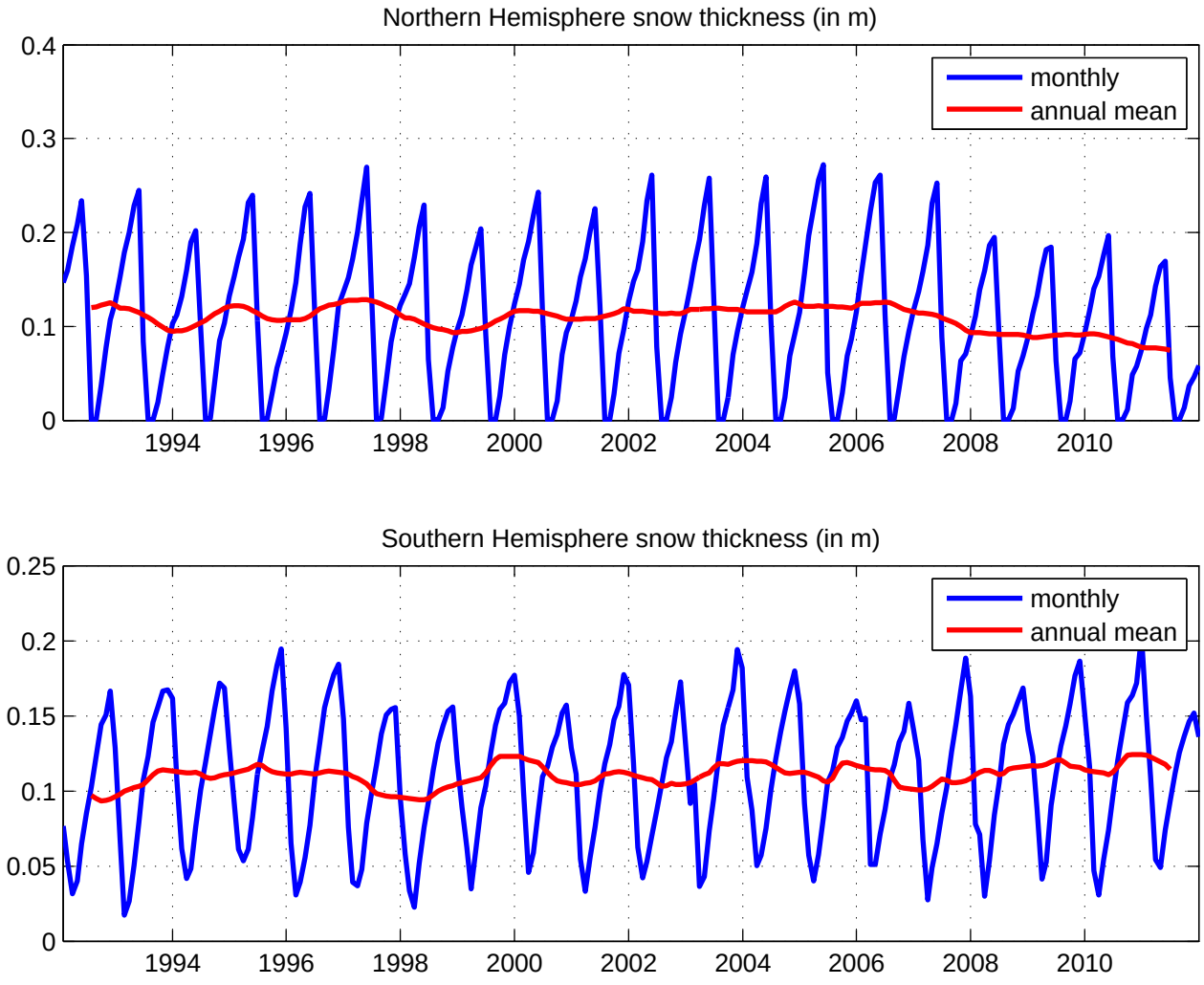

Figure : snow thickness (in m) in northern (top) and southern (bottom) hemisphere

mixed layer depth fields

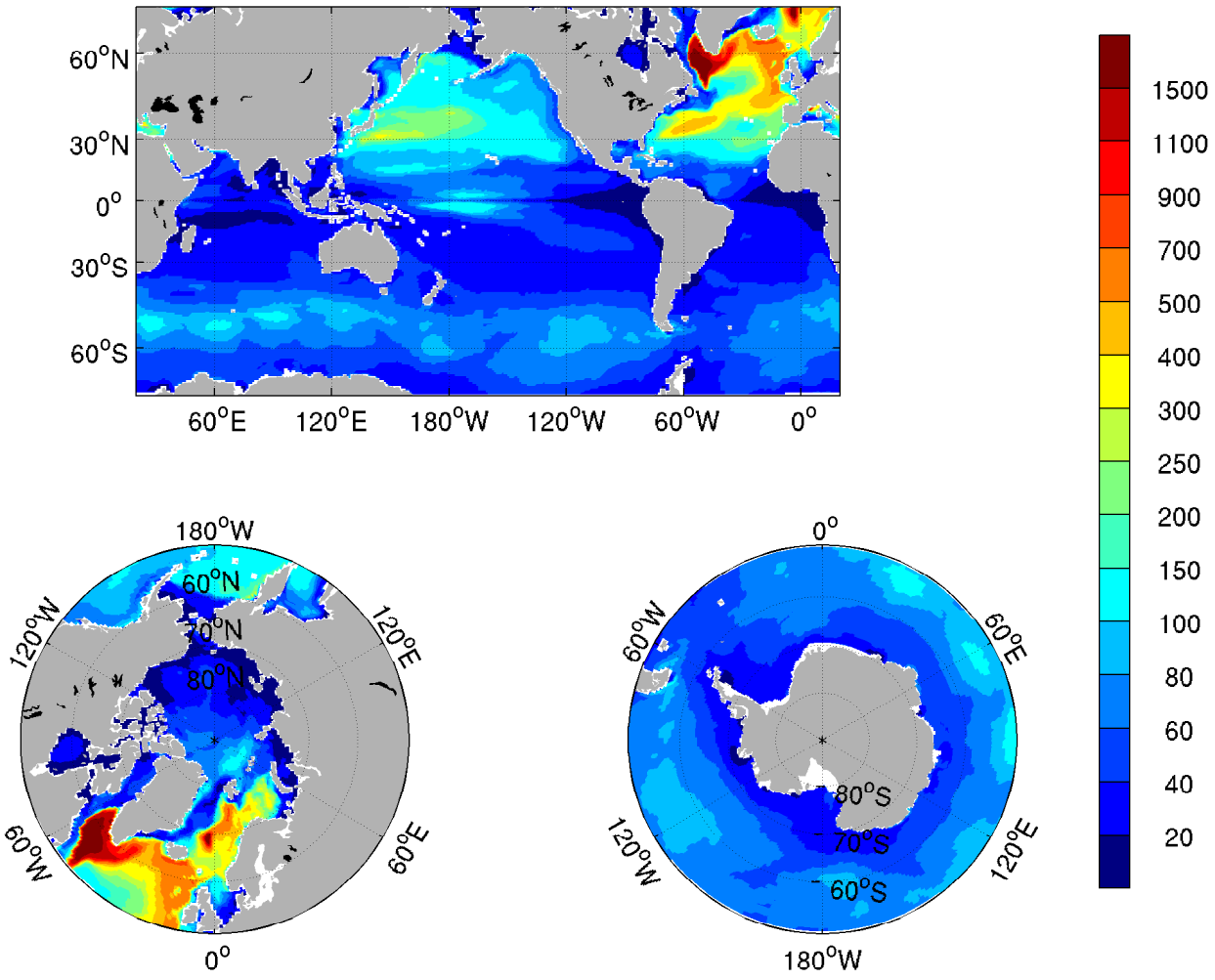

Figure : 1992-2011 March mean – mixed layer depth per Kara formula (m)

mixed layer depth fields

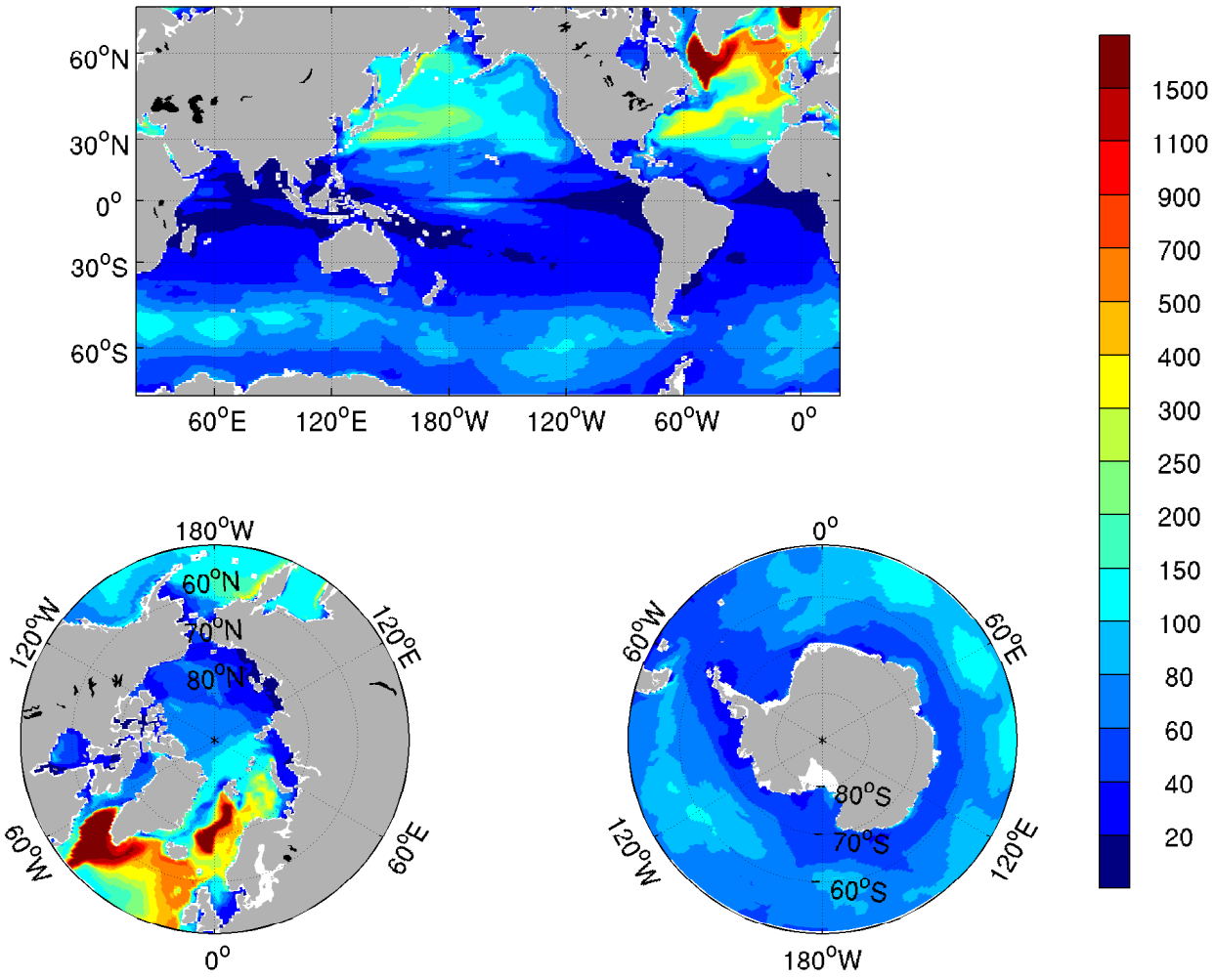

Figure : 1992-2011 March mean – mixed layer depth per Suga formula (m)

mixed layer depth fields

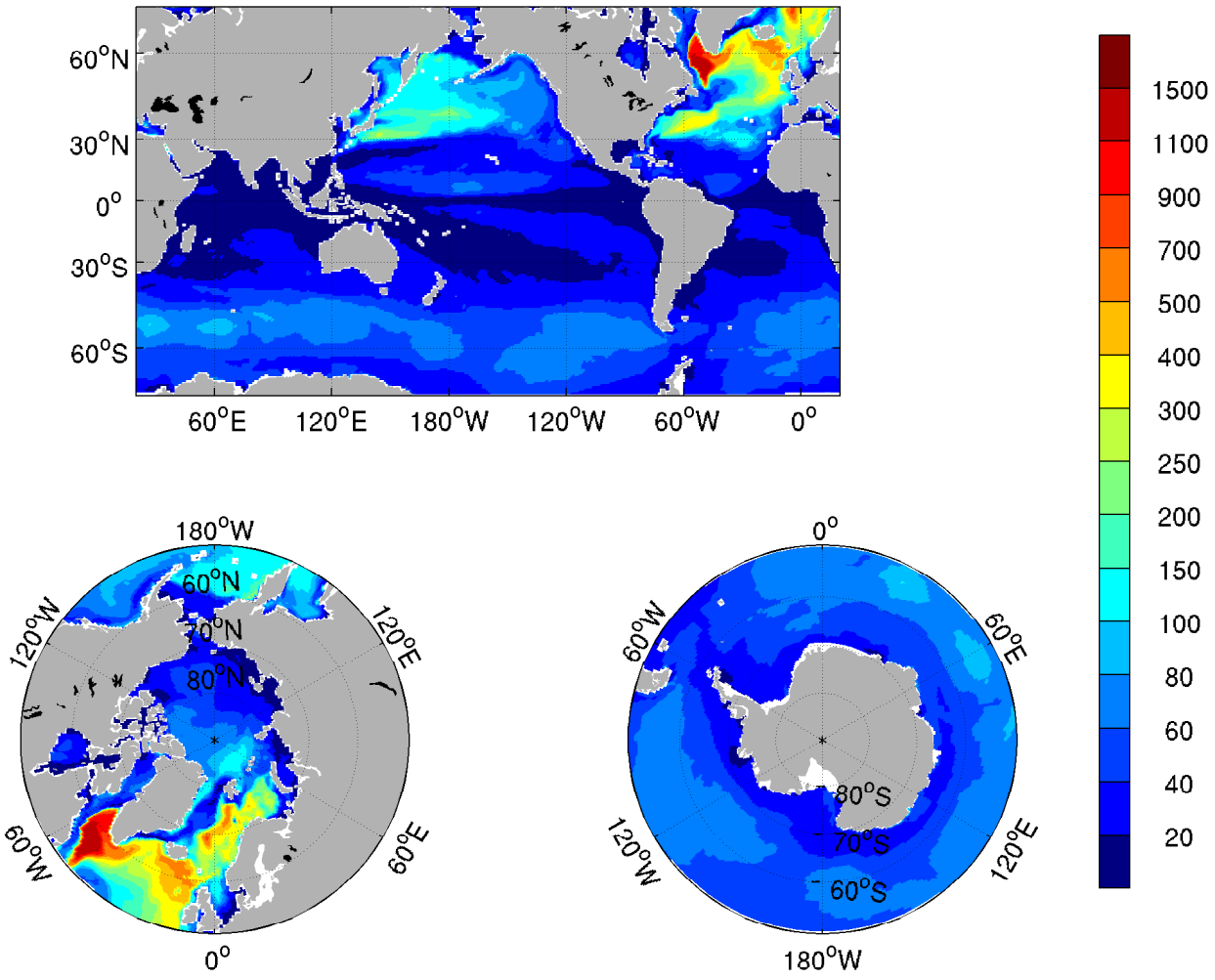

Figure : 1992-2011 March mean – mixed layer depth per Boyer M. formula (m)

mixed layer depth fields

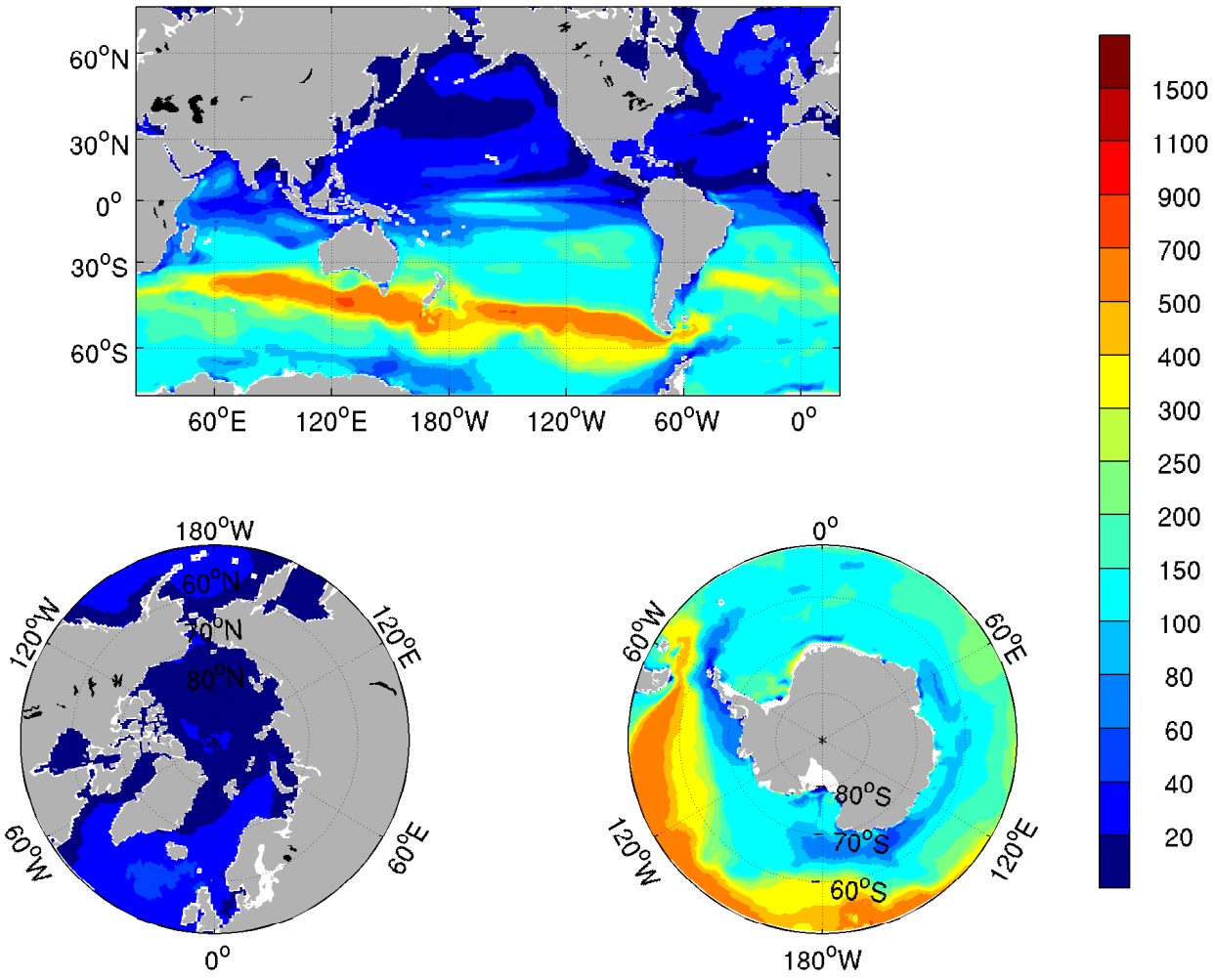

Figure : 1992-2011 September mean – mixed layer depth per Kara formula (m)

mixed layer depth fields

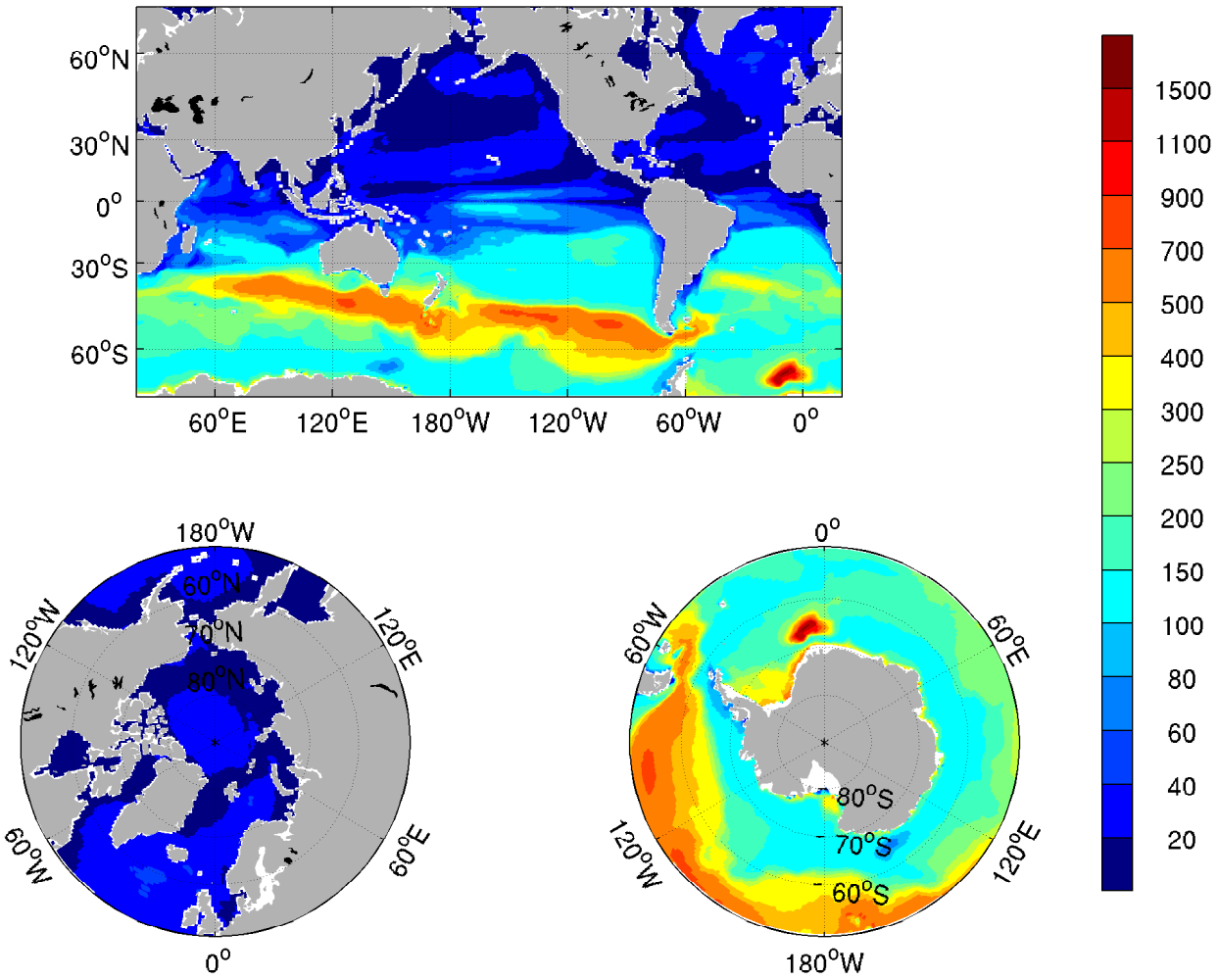

Figure : 1992-2011 September mean – mixed layer depth per Suga formula (m)

mixed layer depth fields

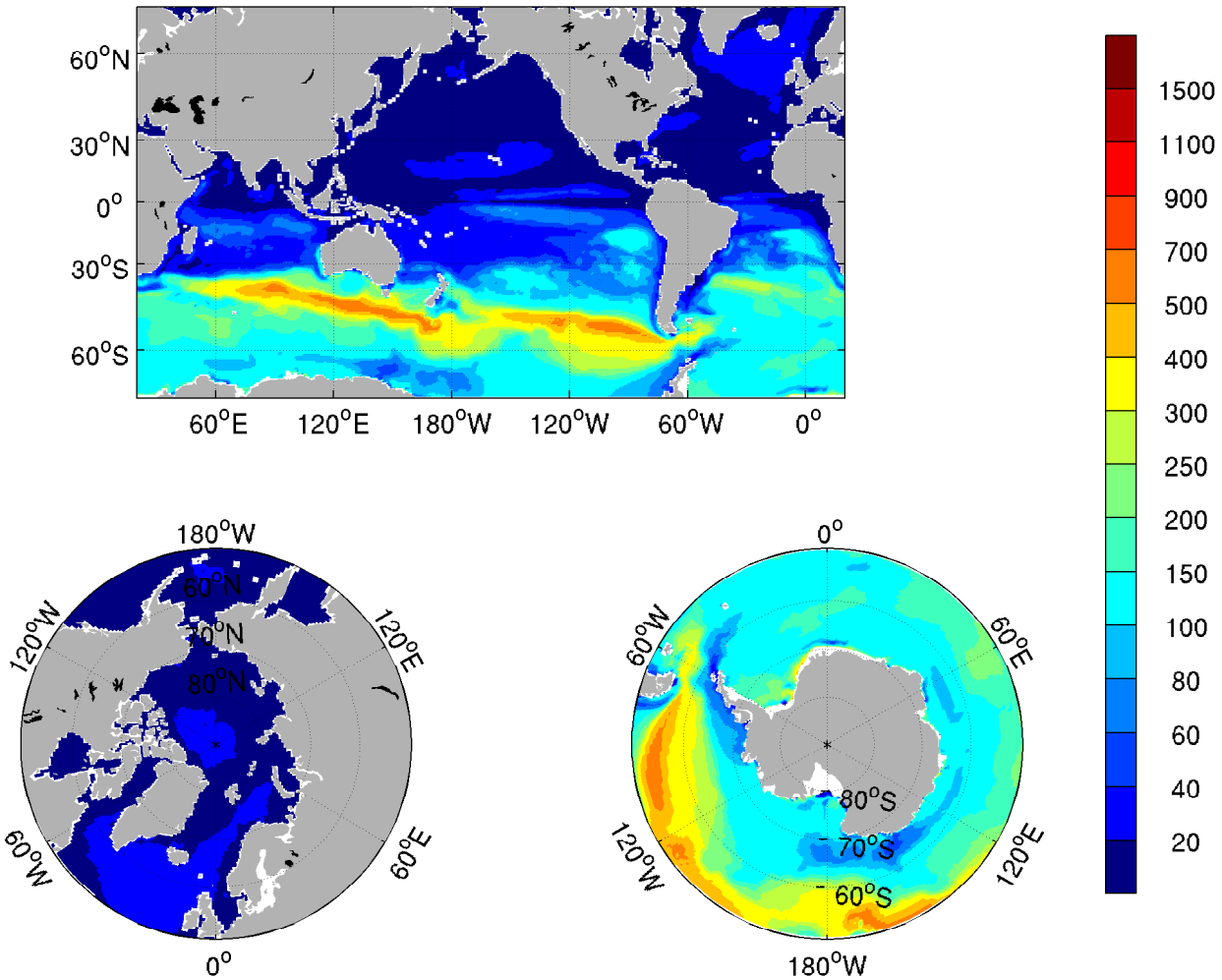

Figure : 1992-2011 September mean – mixed layer depth per Boyer M. formula (m)

budgets : volume, heat and salt (top to bottom)

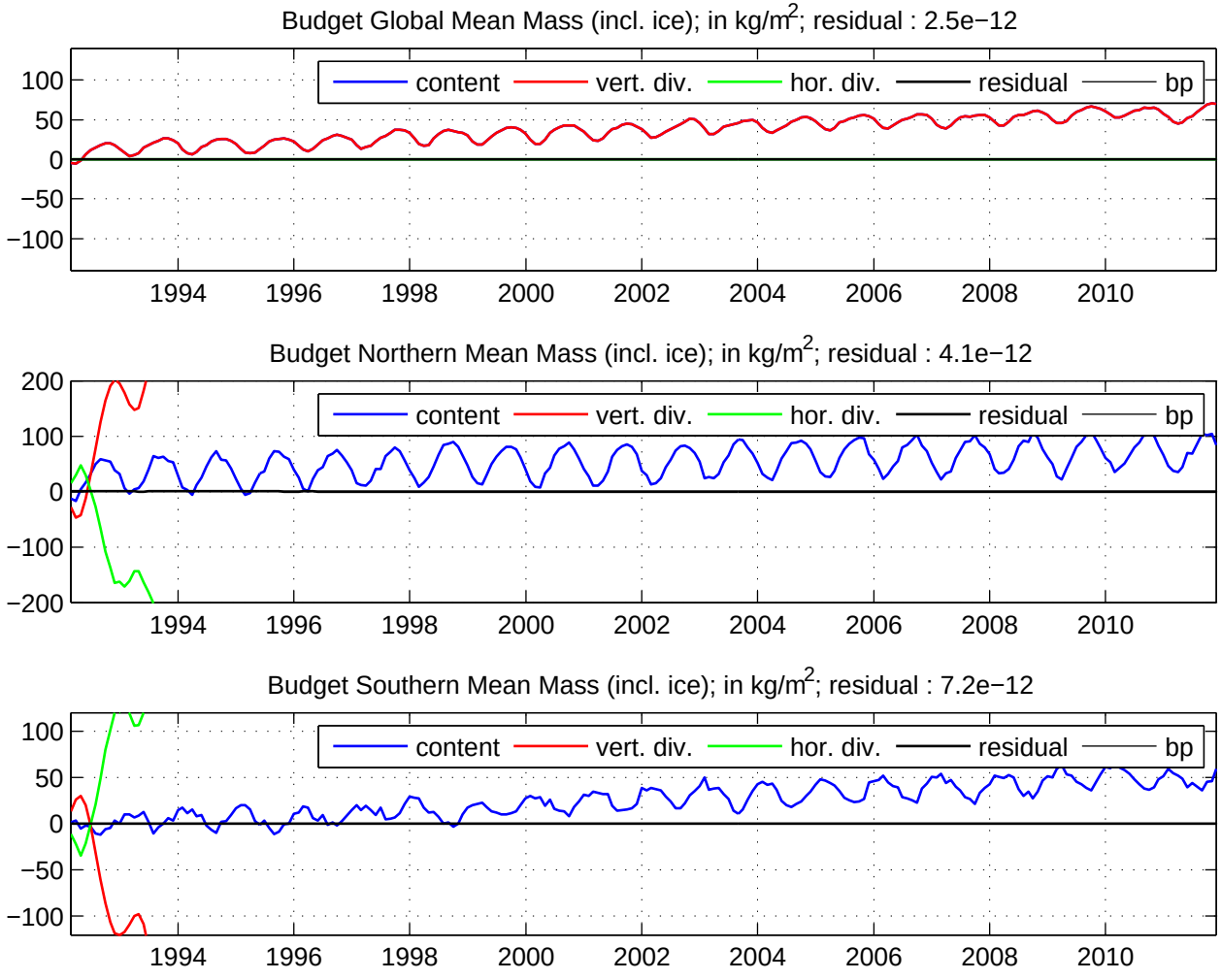

Figure : 1992-2011 global (upper) north (mid) and south (lower), mass budget (ocean+ice) in kg/m^2.

budgets : volume, heat and salt (top to bottom)

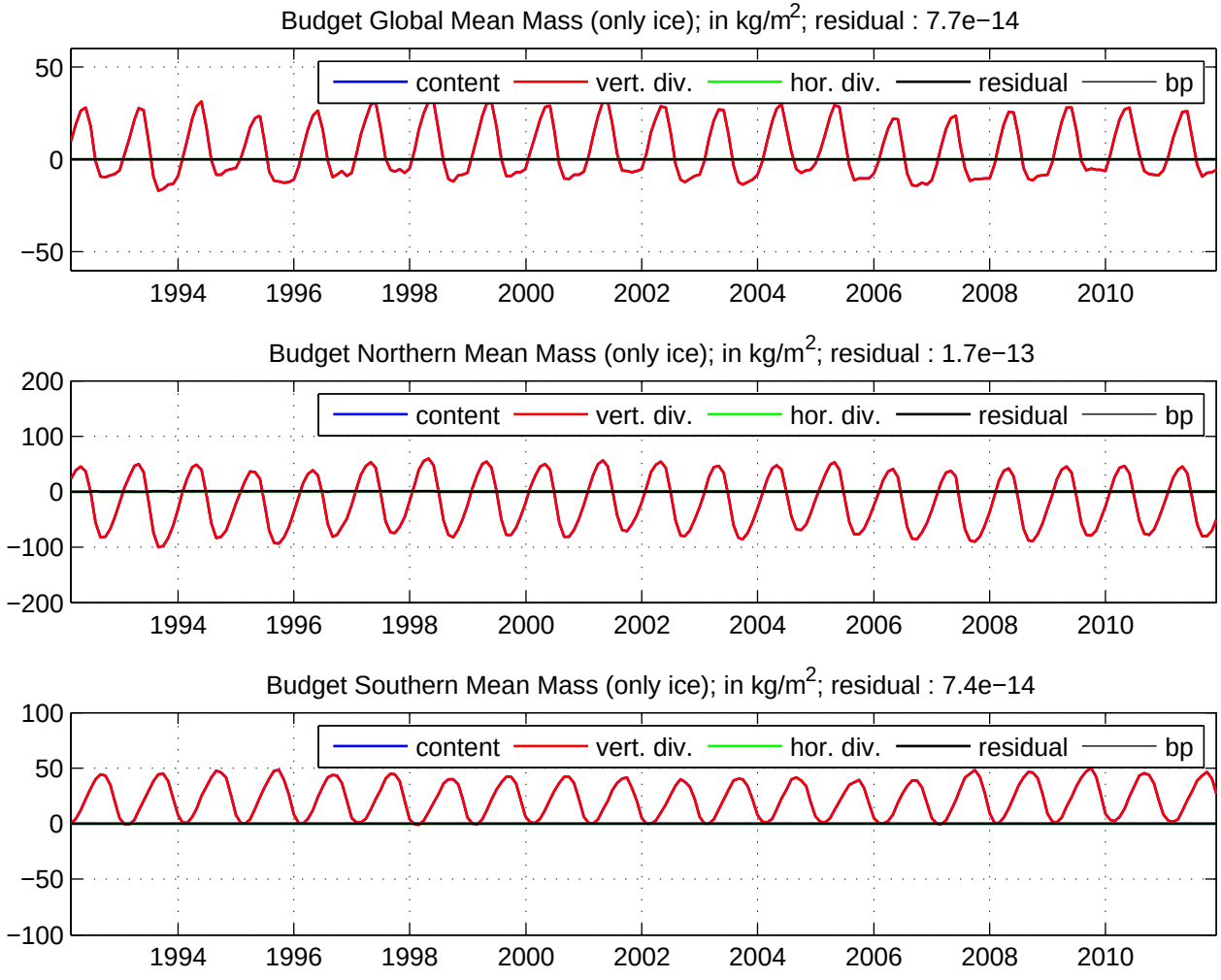

Figure : 1992-2011 global (upper) north (mid) and south (lower), mass budget (ice only) in kg/m^2.

budgets : volume, heat and salt (top to bottom)

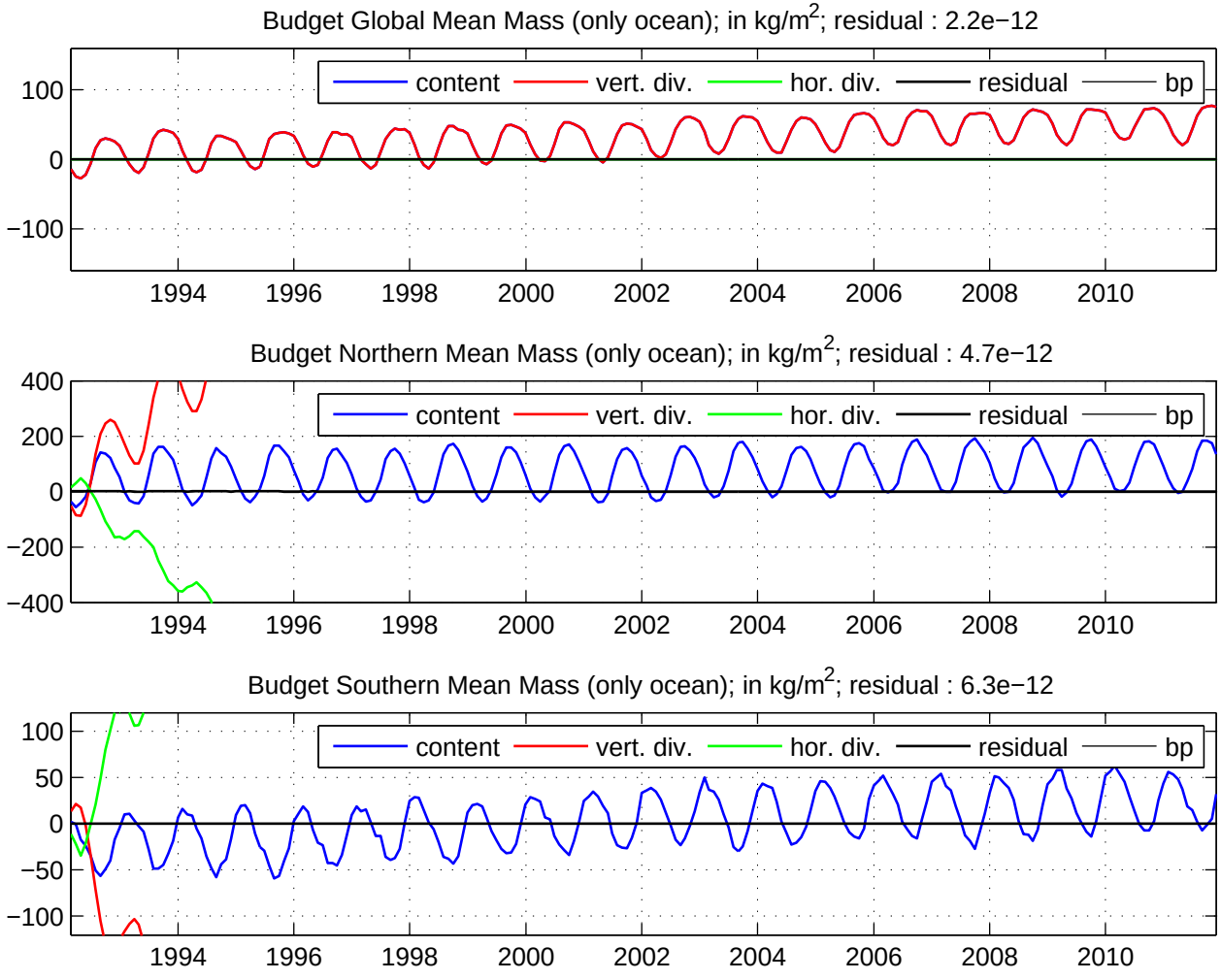

Figure : 1992-2011 global (upper) north (mid) and south (lower), mass budget (ocean only) in kg/m^2.

budgets : volume, heat and salt (top to bottom)

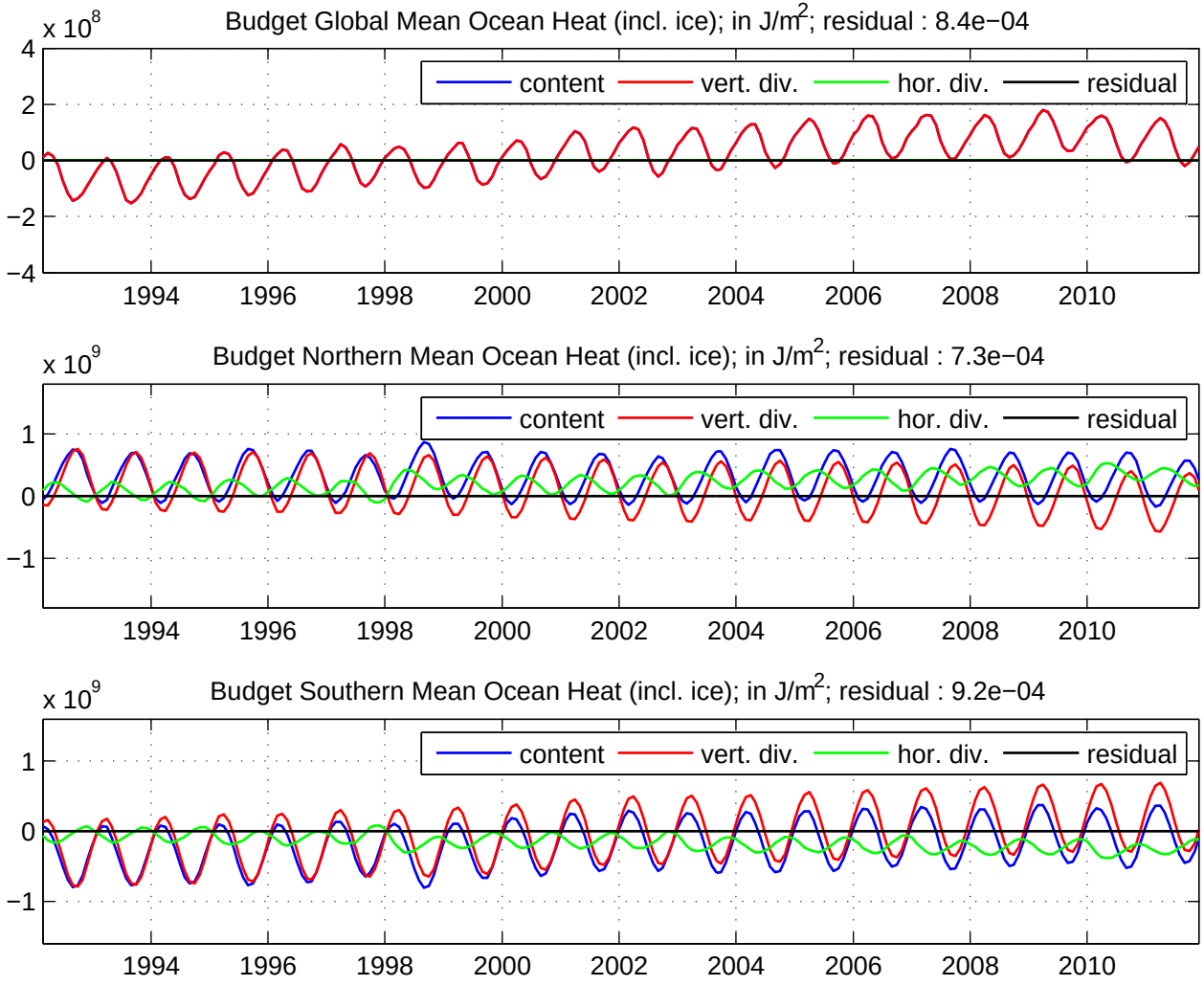

Figure : 1992-2011 global (upper) north (mid) and south (lower), heat budget (ocean+ice) in J/m^2.

budgets : volume, heat and salt (top to bottom)

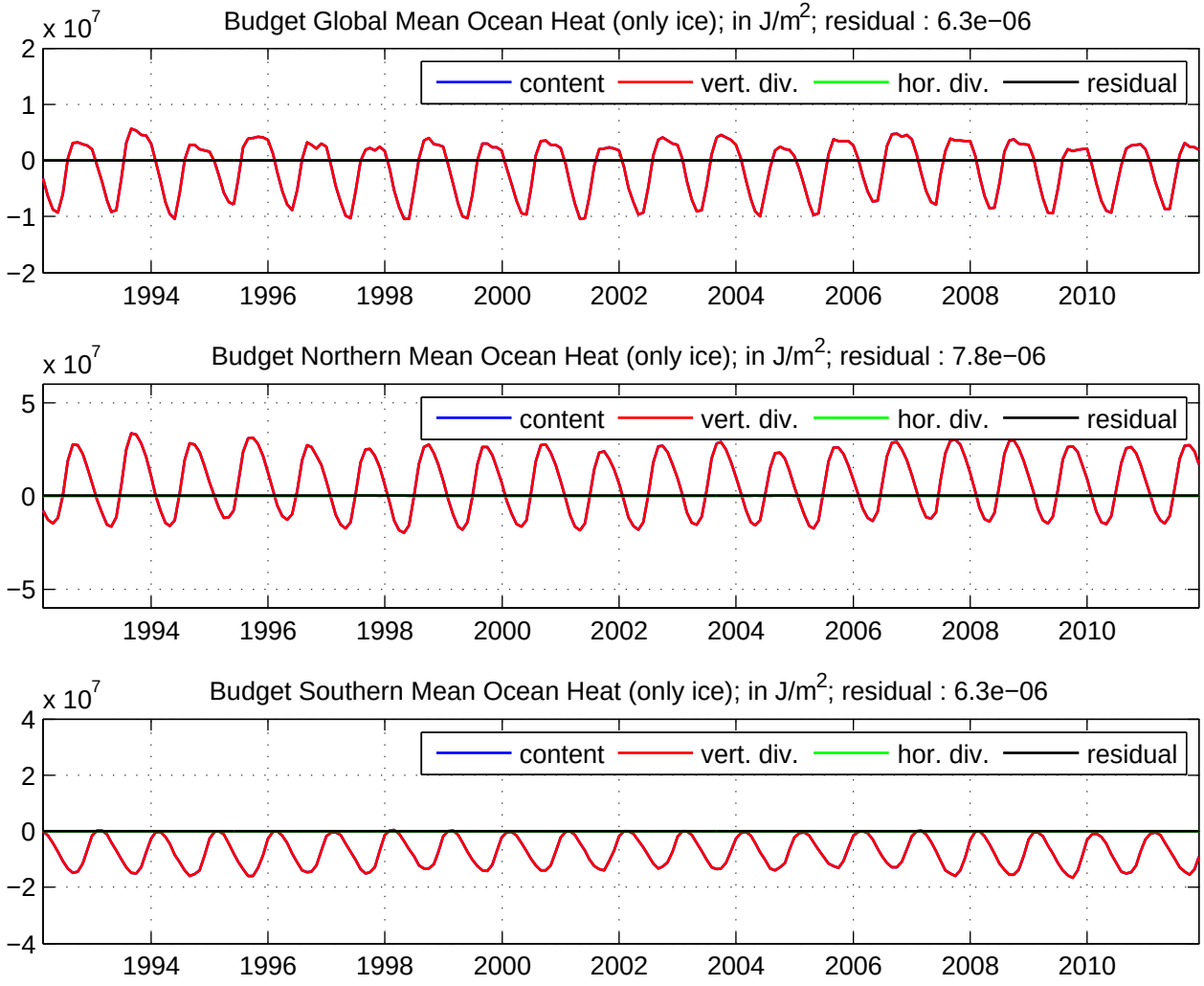

Figure : 1992-2011 global (upper) north (mid) and south (lower), heat budget (ice only) in J/m^2.

budgets : volume, heat and salt (top to bottom)

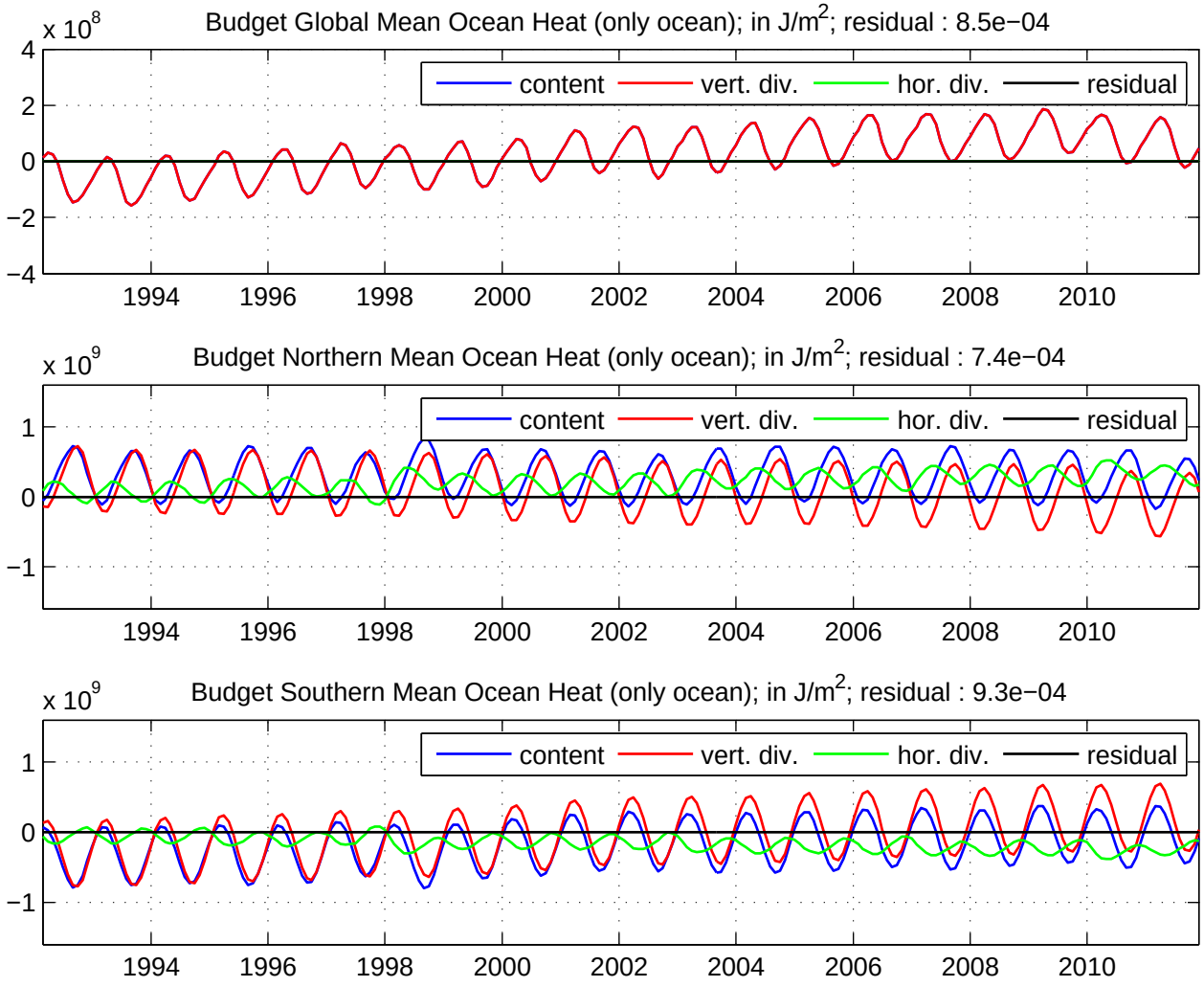

Figure : 1992-2011 global (upper) north (mid) and south (lower), heat budget (ocean only) in J/m^2.

budgets : volume, heat and salt (top to bottom)

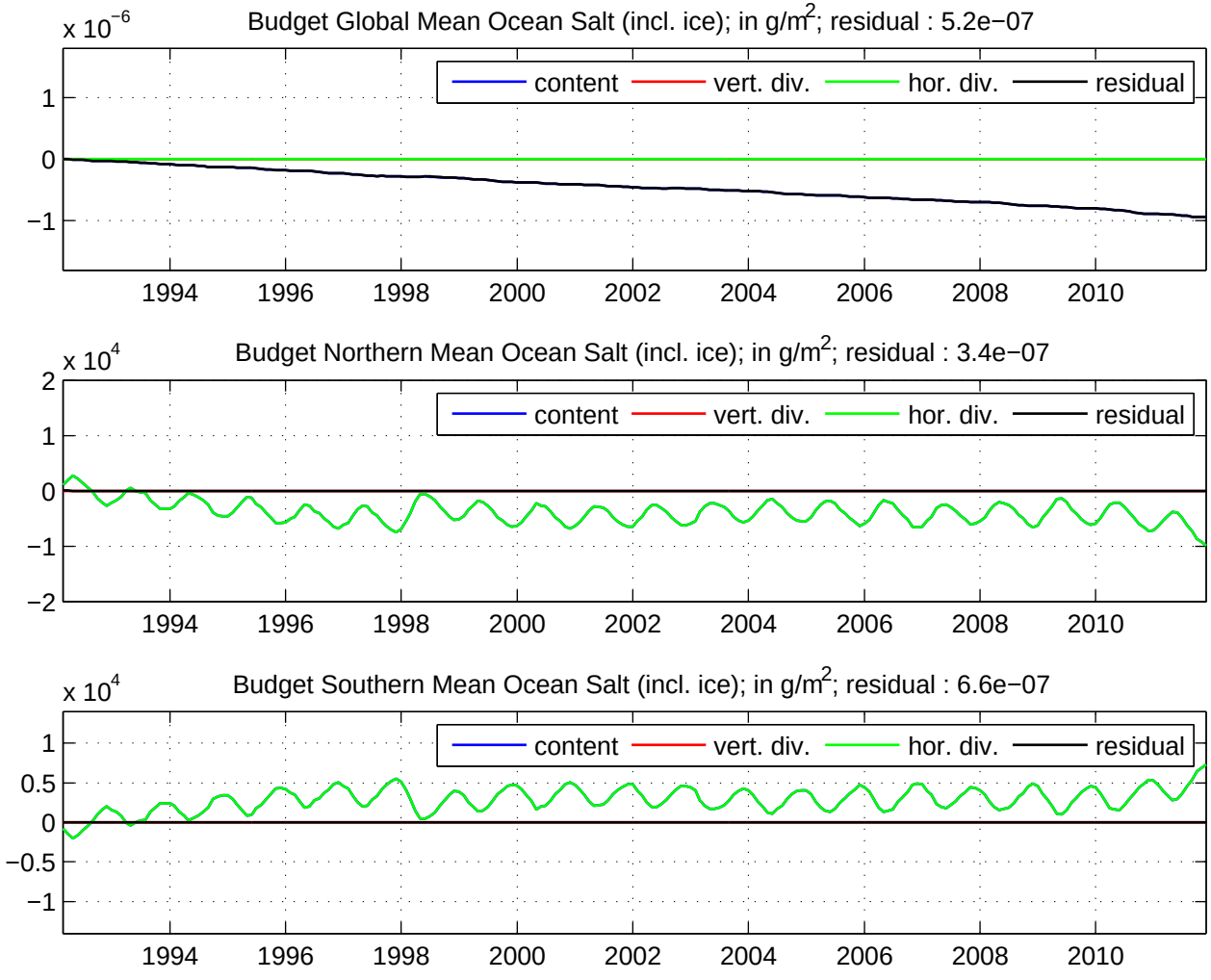

Figure : 1992-2011 global (upper) north (mid) and south (lower), salt budget (ocean+ice) in g/m^2.

budgets : volume, heat and salt (top to bottom)

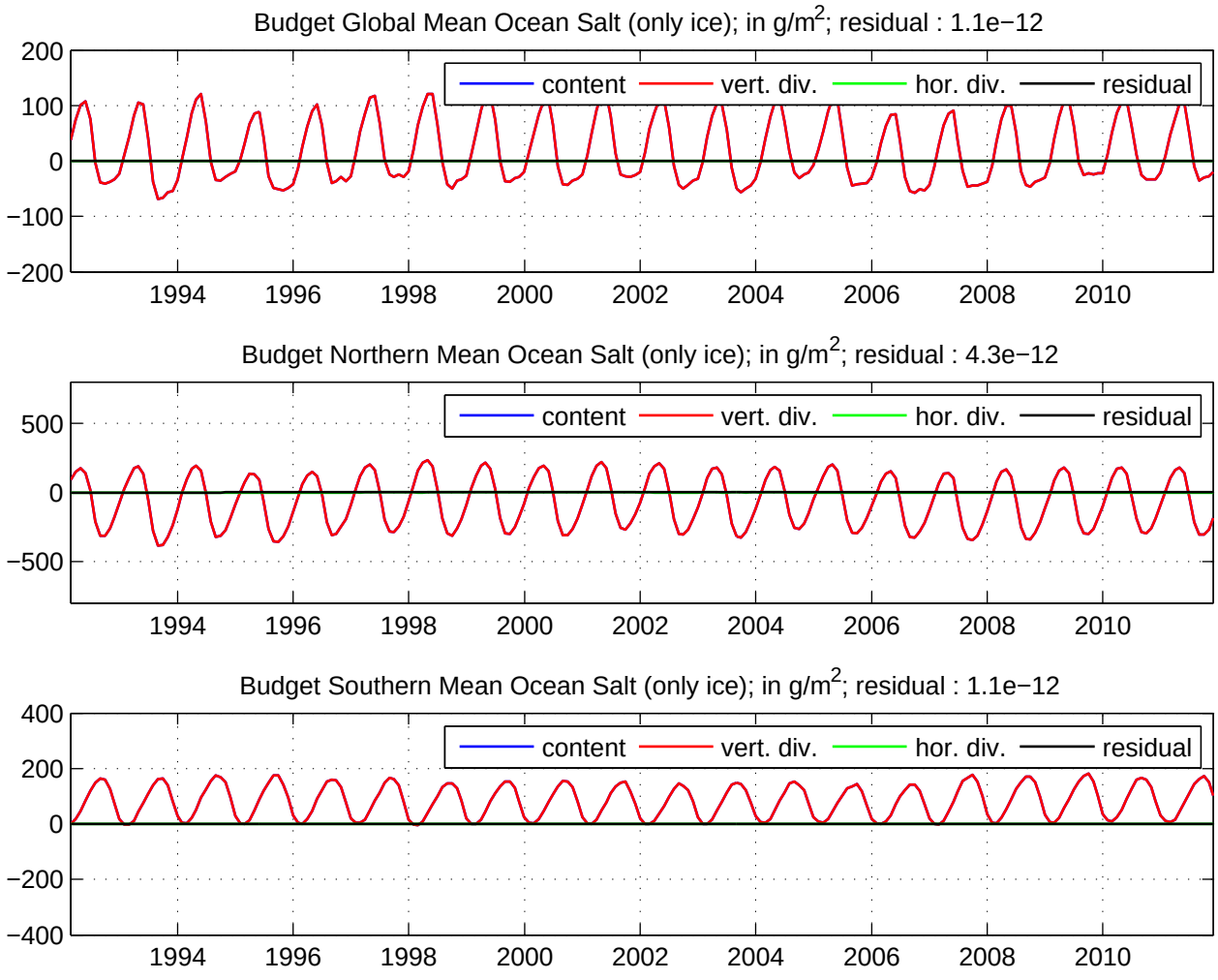

Figure : 1992-2011 global (upper) north (mid) and south (lower), salt budget (ice only) in g/m^2.

budgets : volume, heat and salt (top to bottom)

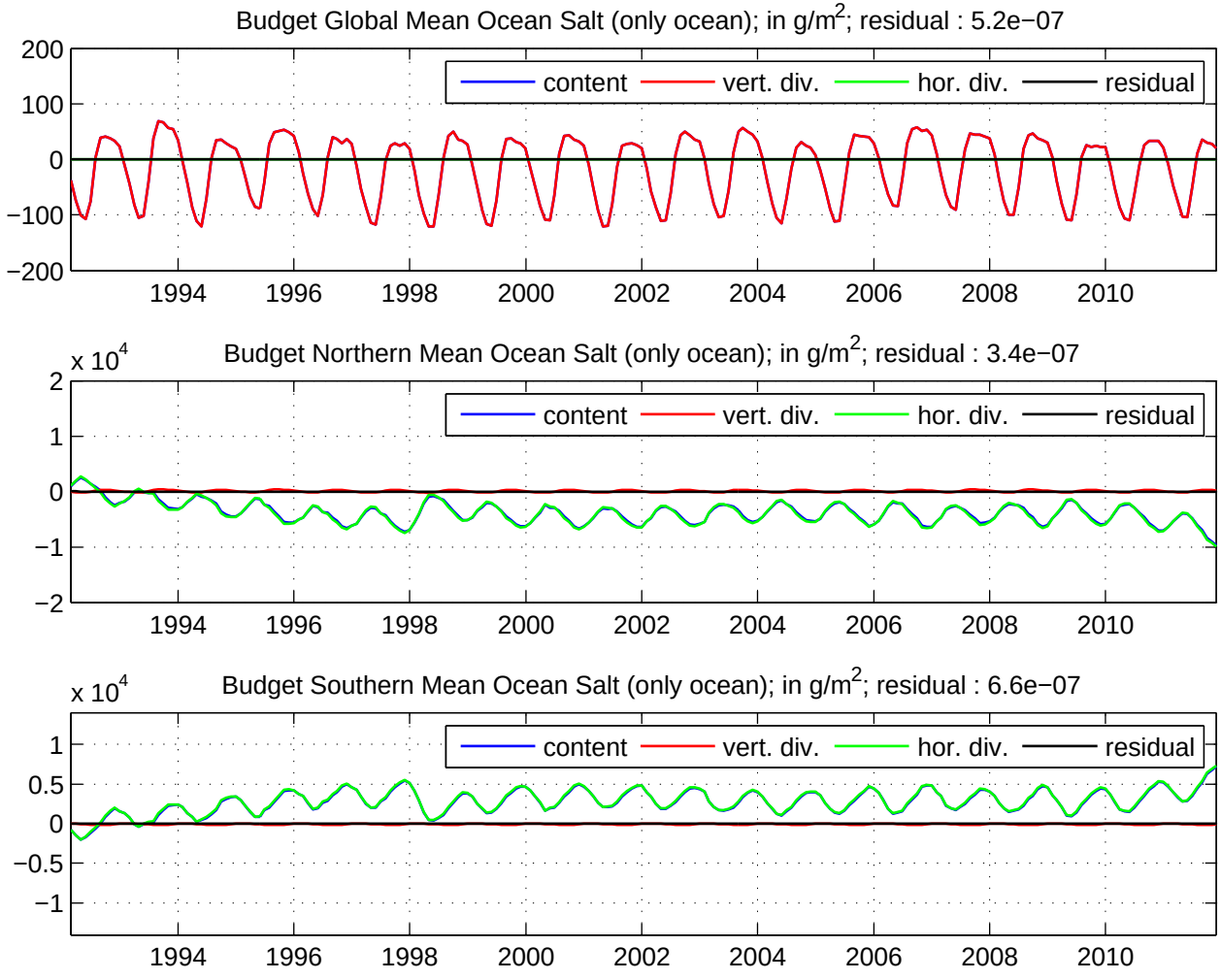

Figure : 1992-2011 global (upper) north (mid) and south (lower), salt budget (ocean only) in g/m^2.

budgets : volume, heat and salt (100m to bottom)

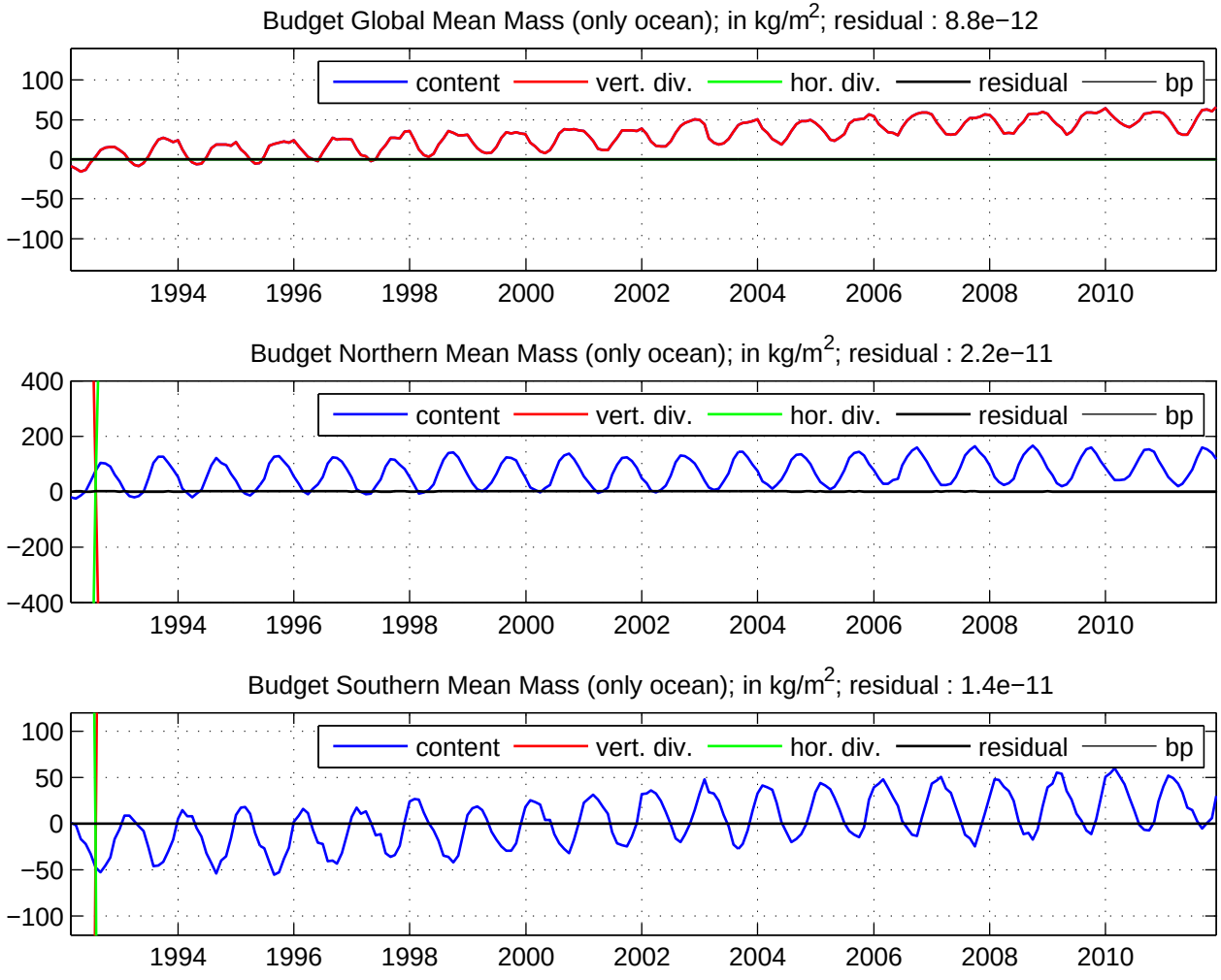

Figure : 1992-2011 global (upper) north (mid) and south (lower), mass budget (ocean only) in kg/m^2.

budgets : volume, heat and salt (100m to bottom)

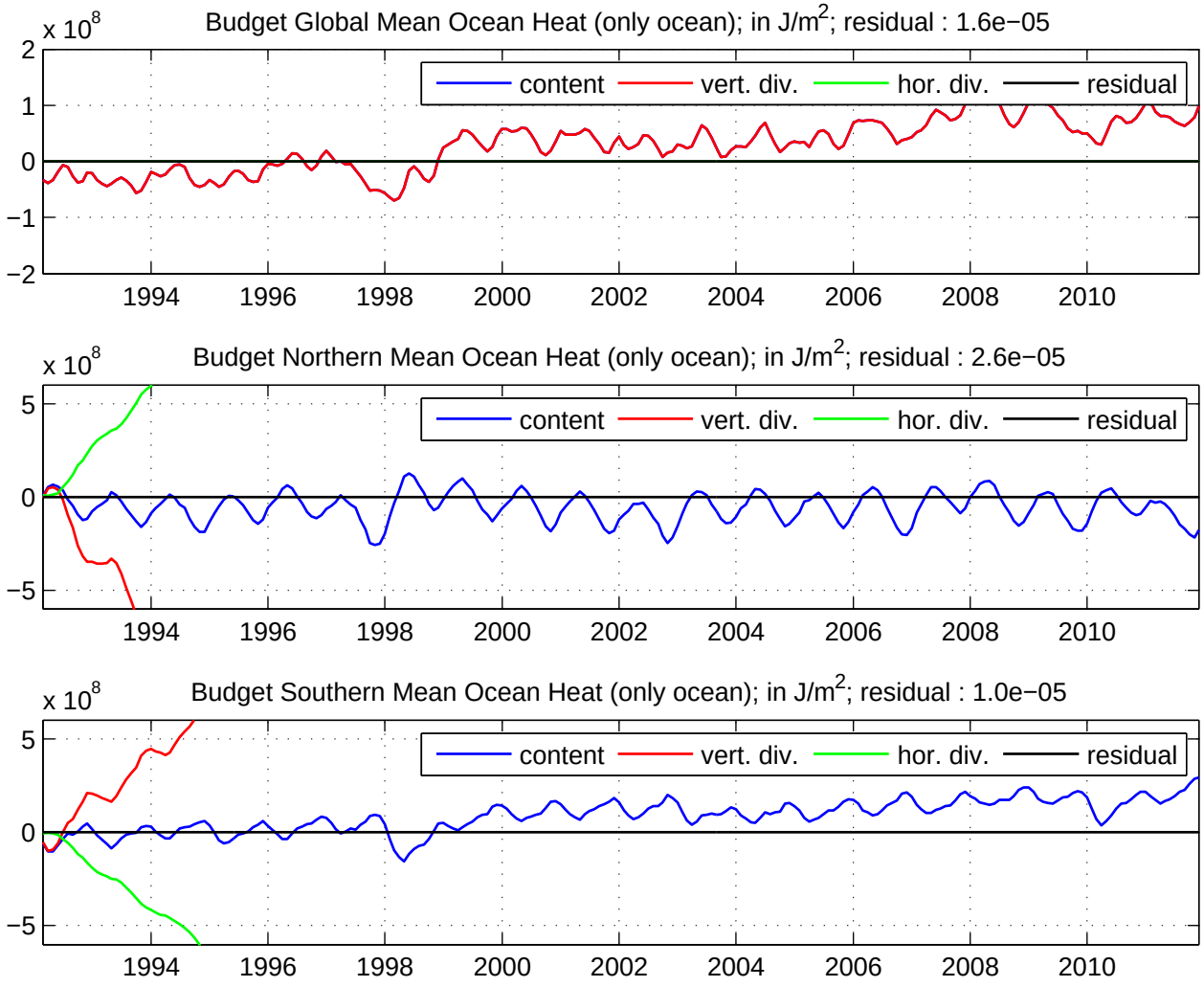

Figure : 1992-2011 global (upper) north (mid) and south (lower), heat budget (ocean only) in J/m^2.

budgets : volume, heat and salt (100m to bottom)

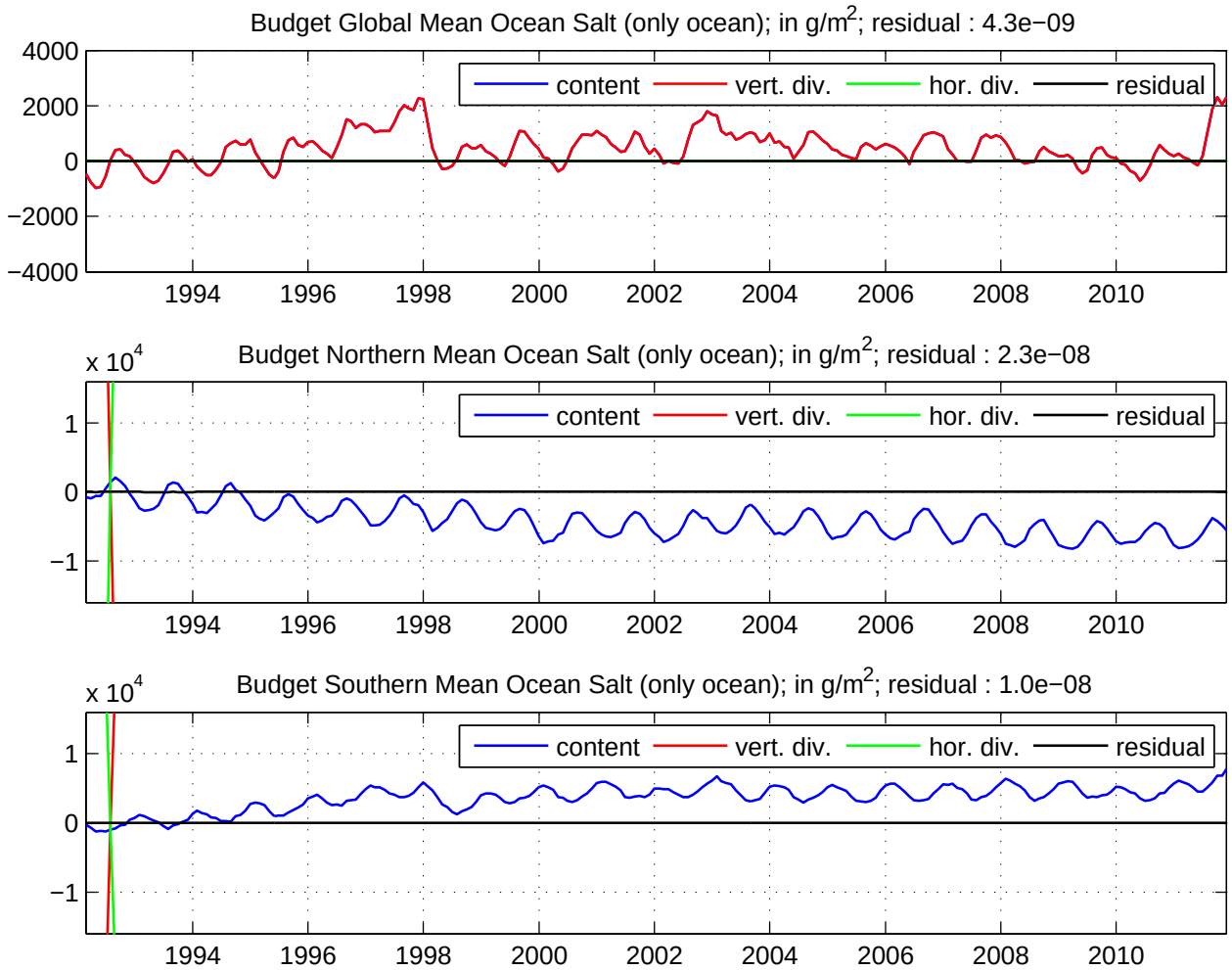

Figure : 1992-2011 global (upper) north (mid) and south (lower), salt budget (ocean only) in g/m^2.